DC AND AC CONDUCTION IN n-InP AND n-InSb IN MAGNETIC FIELDS AT VERY LOW TEMPERATURES

A thesis submitted for the degree of Doctor of
Philosophy of the University of London

by

Sayed Abboudy Ibrahim Omran Abboudy

(BSc, MSc)

Department of Physics

Royal Holloway and Bedford

New College

August 1988

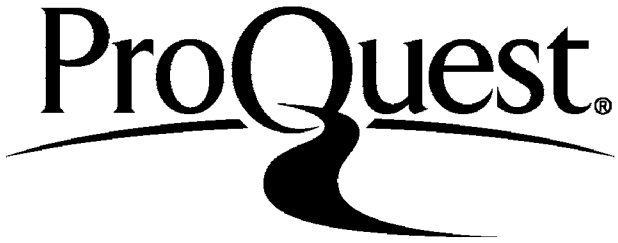

To My Wife, our Daughter Amal and My Family

ABSTRACT

Measurements of the longitudinal and transverse direct current (d.c.) magnetoresistance of n-type InP samples (carrier density from 5 $\times 10^{15}$ to 8 $\times 10^{15}$ cm^{-3}) and the alternating current (a.c.) conductivity of n-type InSb samples (carrier density from 6 $\times 10^{14}$ to 2 $\times 10^{15}$ cm^{-3}) have been made at temperatures T down to 0.04 K and in magnetic fields H up to 70 kG.

For H=0, the InP samples were nonmetallic. At low temperatures, the conductivity is due to nearest neighbour hopping (NNH) which is followed by variable range hopping (VRH) at lower T as described by the first and second terms in the expression; $\rho(T) = \rho_3(T)\exp(\varepsilon_3/k_BT) + \rho_0(T)\exp(T_0/T)^x$. In the NNH regime, it is necessary to plot ln (ρ/T) against T^{-1} and this yields values of the activation energy ε_3 much larger than the traditional ln ρ versus T^{-1} plots. In the VRH regime, Mott's law (x=1/4) is obeyed. Values of T_0 obtained by considering the temperature dependence of the pre-exponential factor are found to be much higher than if the temperature dependence of this factor is ignored. Good agreement between the theory and experiment is achieved in both NNH and VRH regions if an enhanced dielectric constant is used.

Magnetoresistance measurements in both the NNH and VRH regimes are analysed using the theories of Shklovskii and Efros (1984) and reasonable agreement is obtained. The anisotropy of the magnetoresistance in the NNH agrees closely with the expected H^2 dependence. In the VRH, $\ln(\rho(H)/\rho(0))$ varies as $T^{-3/4}$ and H^2 as expected for hopping with a constant density of states at the Fermi level.

The InSb samples are metallic-like in zero magnetic field. High magnetic fields are applied to shrink the donor wavefunctions (to induce the metal-insulator transition) and to locate the samples on the insulator side where the measurements are carried out. The d.c. resistivity was measured and at low temperatures was of a VRH type with $1/4 < x < 1/2$, and T_0 being magnetic field dependent. Reasonable agreement with the theory is found at high fields.

The real and imaginary parts of the a.c. conductivity were measured in the frequency range of 110-10^5 Hz.

The real part of conductivity σ was found to vary as ω^s where s is approaching 1 at low temperatures and high fields but decreasing as T increases. At the lowest temperatures σ was independent of T but at higher T the temperature dependence is stronger than the linear dependence predicted by the simple pair approximation theory. Data are interpreted in terms of multiple hopping of electrons which becomes important at high temperatures and/or low frequencies. The scaling formula; $\sigma(\omega,H,T)/\sigma(0,H,T) = f[A\tilde{\omega}/\tilde{\sigma}(0,H,T)]$ has been applied to discuss the results for the real part of the conductivity, where $\tilde{\omega}$ and $\tilde{\sigma}$ are normalized values and f is a universal function obtained by Summerfield (1985). The scaling parameter -$\log_{10}A$ is found to be 3.0 $\pm$ 0.2.

The relative dielectric constant, due to donors, calculated from the capacitive part was found to be a decreasing function as the frequency is increased and/or the temperature is lowered. At very low temperatures, depending on the magnetic field, however, a temperature-independent, but frequency-dependent behaviour is observed. The lowest temperature value of the dielectric constant was found to diverge as the magnetic field is reduced towards the metal-insulator threshold value.

ACKNOWLEDGEMENTS

I would like to record my sincere gratitude to Professor R. Mansfield and Dr. M.J. Lea who have supervised my studies at this college. Their insight, enthusiasm, active assistance and guidance have been a constant source of encouragement during the course of this work.

I am grateful to Dr. P. Fozooni for his interesting discussions and cooperation throughout this work. I would also like to thank Professor A.K. Jonscher for his suggestions and helpful discussions.

Thanks go to many other people in Physics Department, Physics computer centre and College computer center. In this respect I would especially like to thank Professor E.R. Dobbs, the head of the department for his support of this work. The technical assistance given by Mr. A.K. Betts and Mr. F. Greenough is also acknowledged.

Thanks also go to the family of the Egyptian Education Bureau (London) for several assistances and encouragement.

To my wife I owe my profound gratitude for her moral support and encouragement to finish this work.

Finally, I would like to acknowledge gratefully the scholarship granted to me by the University of Alexandria (Egypt). The financial support by the Overseas Research Students Award Scheme (UK) is also acknowledged.

Contents

Chapter 4 : DC Conduction in n-type InP

Chapter 5 : AC and DC Conduction in n-type InSb

CHAPTER 1
Introduction

Transport properties of semiconductor materials have been of considerable interest over the last thirty years from both experimental and theoretical points of view. The charge transport measurements in these systems provide some information about the different types of conduction mechanisms.

If a pure crystalline semiconductor is doped with the appropriate impurities, one can obtain crystals in which electronic energy states can be found in the energy gap of the crystal. Based on the impurity concentration, semiconducting materials can be divided into three groups. If the impurity concentration, N, is so small that

$$Na_B^{*3} \ll 1 \tag{1.1}$$

where a_B^* is the effective Bohr radius of an impurity atom, then the semiconductor is referred to as *lightly doped.* In this case the average separation between impurities much exceeds the characteristic wave function size, a_B^*. If $Na_B^{*3} \sim 1$, a semiconductor is called *moderately doped.* While for the case of $Na_B^{*3} \gg 1$, the semiconductor is described as *heavily doped.*

The well known examples of doped semiconductors which have been intensively studied are Ge and Si. The III-V compounds such as GaAs, InAs, InSb and InP have attracted the attention of many authors. The transport properties of these systems, in absence and presence of externally applied agents, such as pressure and magnetic field, have been dealt with both experimentally and theoretically (see, e.g., Mikoshiba 1963; Shklovskii 1973; Mott and Davis 1979; Biskupski and Dubios 1982; Tokumoto et al. 1980, 1982; Rosenbaum et al. 1983; Shklovskii and Efros 1984; Böttger and Bryksin 1985; Mansfield et al. 1985; Abboudy et al. 1987, 1988; Abdul-Gader et al. 1987; Mansfield et al. 1988).

The properties of electrons in the conduction band (or holes in the valence band) for a lightly doped semiconductor is well understood and theory agrees with experiment. The controversy arises when the temperature is so low that conduction

is by hopping. Exact conclusions about the actual mechanisms of conduction are not yet well established. The presence of a specimen at very low temperatures with a magnetic field as an external agent is recommended to shrink the donor wave functions and tune through the different types of conduction mechanisms. Other problems such as anisotropy, density of states at the Fermi level, metal-insulator (MI) transition, etc. are still not well established. The behaviour of the a.c. conductivity as a function of temperature, magnetic field and frequency is also needed to be closely investigated.

Shallow electronic energy states associated with impurity levels in semiconductors can be understood by means of a hydrogen model of the impurity (Yafet, Keyes and Adams 1956 (YKA)). In this case, one takes the wave functions and energy levels for various electronic impurity states the corresponding wave functions for a hydrogen atom in which the electron has a mass m^*, the effective mass of the electron in the crystal, and the nucleus has a charge e/ϵ, the normal protonic charge e decreased by the dielectric constant of the medium. Thus with the ground-state binding energy of the free hydrogen atom given by

$$R_y = \frac{m_0 e^2}{2\hbar^2} = 13.6 \qquad \mathbf{eV} \tag{1.2}$$

where m_0 and e are the rest mass of the free-electron and the electronic charge respectively; the effective Rydberg energy then can be expressed as

$$R_y^* = \frac{m^*}{m_0 \epsilon^2} R_y \tag{1.3}$$

material	m^*	ϵ	a_B^* (Å)	R_y^* (meV)
n-InSb	0.0145 m_0	17.6	645	0.65
n-InP	0.078 m_0	14	84	5.5
n-GaAs	0.066 m_0	12.6	100	5.67

Table 1.1

In the case of the III-V compounds, such as n-type InSb, where the effective mass m^* is small and the dielectric constant ϵ is large, then for a hydrogen-like

model of a donor centre the Rydberg constant R_y^* is small. Table 1.1 summarizes the values of m^*, ϵ, a_B^* and the corresponding R_y^* for some semiconductors.

Solution of the Schrödinger equation for a hydrogen-like atom shows that the wave function for the ground-state electron falls off exponentially from its hydrogen-like impurity centre as (Shklovskii and Efros 1984)

$$\psi(r) = \left(\pi a_B^{*3}\right)^{-1/2} \exp\left(-r/a_B^*\right) \tag{1.4}$$

where a_B^* is the effective Bohr radius which determines the characteristic dimensions of the wave function and is given by

$$a_B^* = \frac{m_0 \epsilon}{m^*} a_B \tag{1.5}$$

Here a_B is the Bohr radius for the free hydrogen atom and is given by $a_B = \hbar^2/m_0 e^2 = 0.53$ Å. Because of the large values of the dielectric constant and the small values of the effective mass, the Bohr radii in semiconductors turn out to be quite large. Hence, the wave functions associated with the donor impurity atoms extend over large distances throughout the host crystal. As a result, the wave functions may overlap strongly with each other unless the impurity concentration is so low that the isolation condition (1.1) is satisfied.

In the case of a finite concentration of similar impurities the single degenerate impurity level is replaced by an impurity band of finite width in energy. An electron localized near one of the impurity centres does not spread in time over other centres constituting the band. The wave function remains localized, and wave functions of electrons of neighbouring impurity atoms are almost identical with the wave functions of free atoms. The electrons are said to be trapped by their individual donor sites and become localized in the associated discrete energy states. These states lie below the delocalized conduction band at a distance equal to the effective Rydberg constant. Electrons occupying these states can only participate in conduction if an appropriate energy is supplied to excite them into the conduction band where they can behave freely as free electrons in a crystal band.

In n-type semiconductor, decreasing the temperature, T, leads to freeze-out of electrons from the conduction band to their donors, and the conductivity, σ, decreases exponentially as T is lowered. The temperature dependence of the direct current (d.c.) conductivity in this case is given by (Mott and Towse 1961)

$$\sigma = \sigma_1 \exp\left(-\varepsilon_1 / k_B T\right) \tag{1.6}$$

where the pre-exponential factor σ_1 depends on the type of the material under investigation and the external agents, ε_1 is the activation energy for the donor sites of the order of R_y^* and k_B is the Boltzmann constant.

The freeze-out of conduction electrons with decreasing the temperature leads to a situation in which the main contribution to the electrical conductivity comes from electrons that hop directly between impurities without being excited to the conduction band. This mechanism is well known as "*hopping conduction*" and is important at low temperatures. The nature of this process can be understood by considering the fact that random fluctuations in the potential of the charged impurity atoms create significant differences between the energies of the discrete energy levels of the isolated donor sites (Madelung 1978). Systems in which the crystalline potential fluctuates so that it is no longer periodic are described as "*disordered*" materials. For electron to hop from an occupied to an empty site (due to compensation) a phonon has to be absorbed (or emitted). If the hopping takes place between the adjacent isolated localized states near the Fermi energy, then the process is known as "*thermally activated phonon – assisted*" hopping conduction (Mott and Towse 1961). Since the electron hops are associated with a weak overlap of wave function tails from neighbouring donors, the hopping mechanism of conduction then corresponds to a very low mobility. However, at low temperatures, hopping conduction wins in the competition with band conduction. It has been found that a conductivity of this type, which is known, frequently, as "*nearest neighbour hopping*" conduction, is of the form (Miller and Abrahams 1960)

$$\sigma = \sigma_3 \exp\left(-\varepsilon_3 / k_B T\right) \tag{1.7}$$

where the pre-exponential factor σ_3 depends on the material under investigation and the temperature (though weakly) and ε_3 is the activation energy which arises due to the dispersion of impurity levels and is less than ε_1. ε_3, indeed, is a function of impurity concentration. For weakly doped semiconductors, the activation energy ε_3 was obtained by considering ionized donors (energy levels placed above the Fermi level) in the vicinity of negatively charged acceptors (Shklovskii and Efros 1970; Shklovskii 1973). The Coulomb interaction between a donor and an acceptor raises the energy level of the donor relative to the level of an isolated donor by an amount of the order of $e^2/\epsilon r_D = E_{coul}$, where r_D is the average intermajority distance. Thus one can write

$$\varepsilon_3 = const.\frac{e^2}{\epsilon r_D} \tag{1.8}$$

This formula is assumed to be valid for any compensation ratio $K = N_A/N_D$ but the constant, indeed, depends on K (Efros et al. 1972, Shklovskii and Efros 1971, 1984). For high impurity concentration, the neighbouring hops might affect each other and become correlated (Knotek and Pollak 1974). The effect of this correlation would reduce ε_3 below its theoretical value. Different mechanisms were also proposed to account for the lower values of the activation energy ε_3 (see, e.g., Shklovskii and Efros 1984, Mansfield et al. 1988). The pre-exponential factor in equation (1.7) is given by

$$\sigma_3 = \sigma_{03} \exp\left(-\alpha_1/N^{1/3}a_B^*\right) \tag{1.9}$$

which represents the concentration dependence of the conductivity in the nearest neighbour hopping regime. The parameter α_1 in the above equation has been calculated by percolation theory (Shklovskii and Efros 1984); $\alpha_1 = 1.73$.

At sufficiently low temperatures, hopping between nearest neighbours might become more difficult than hops between remote sites. This, indeed, can be understood as follows. As the temperature is reduced, then the number and energy of the available phonons will decrease. In this case, the typical resistance between neighbouring impurities may become larger than those connecting some remote

impurities whose energy levels happen to be very close to the Fermi level. Hence, carriers will prefer to hop to larger distances to find vacant impurity which is energetically closer than the nearest neighbour ones. In this case, the average hopping length varies with the temperature and grows as $T^{-1/4}$ (Shklovskii and Efros 1984). According to the original work of Mott (1968), provided that there is a nonvanishing density of states at the Fermi level, the temperature dependence of the conductivity with no external field present exhibits a universal behaviour

$$\sigma = \sigma_0 \exp\left[-\left(\frac{T_0}{T}\right)^{1/4}\right] \tag{1.10}$$

which is well known as Mott's $T^{-1/4}$-law. Conduction of this type is generally described as *variable range hopping* (VRH). The pre-exponential factor in the above equation, σ_0, depends, among many other factors, on the density of states at the Fermi level, $g(\mu)$ and the temperature, T (Madelung 1978) and the parameter T_0 is model dependent and for the present case is given by an expression of the form

$$T_0 = \frac{\beta'}{k_B g(\mu) a_B^{*3}} \tag{1.11}$$

where β' is a numerical factor. The derivative $d(\ln \rho)/d(k_B T)^{-1}$ may be called the activation energy at a given temperature. From Mott's law it follows that this activation energy monotonically decreases with the temperature as $T^{3/4}$. For this reason, conductivity obeying Mott's law is sometimes referred to as conductivity with decreasing activation energy.

Although the Mott's $T^{-1/4}$-law has been verified by many authors (see, e.g., Mott 1974; Mott and Davis 1979; Benzaquen et al. 1985) its validity still receives a lot of controversy. The basic arguments come from some assumptions used in the theoretical derivation of this law as the energy independence of the density of localized states near the Fermi level and the neglection of the correlation effects between electrons that execute hops. If the density of states near the Fermi level is not constant, then the temperature dependence of the conductivity in the VRH regime is, indeed, different from that suggested by Mott (see, e.g., Efros and Shklovskii 1975; Efros 1976; Efros et al. 1979; Mott and Davis 1979). For a

density of states varying as

$$g(\varepsilon) = g_0 \varepsilon^p \tag{1.12}$$

where g_0 is some constant, p is a numerical factor (≥ 0) and the energy ε is measured from the Fermi level, the conductivity is given by (Efros and Shklovskii 1975, Efros 1976)

$$\sigma = \sigma_0 \exp\left[-\left(\frac{T_0}{T}\right)^x\right] \tag{1.13}$$

with the exponent $x = p+1/p+4$ and T_0 depends on the energy distribution of the density of states $g(\varepsilon)$. Efros and Shklovskii (1975) have pointed out that, due to Coulomb interaction, the density of localized states is diminished in the immediate vicinity of the Fermi level. The resultant minimum is called the Coulomb gap. Because of this Coulomb gap, VRH conduction thus obeys the above finding (1.13) with p=2 and x=1/2. Accordingly, equation (1.13) takes the form

$$\sigma = \sigma_0 \exp\left[-\left(\frac{T_0}{T}\right)^{1/2}\right] \tag{1.14}$$

Conductivity of such behaviour is also reported by many authors (see, e.g., Emel'yanenko et al. 1973; Zabrodskii 1977; Finlayson and Mason 1986).

The above arguments were restricted only to the case of hopping in the absence of external agents. The different types of conduction mechanisms can also be examined if one applies a magnetic field. This field will shrink the wave functions of the donor sites and consequently the temperature dependence of the conductivity will change (see, e.g.; Mikoshiba 1963; Shklovsii 1973, 1977; Suprapto and Butcher 1975; Tokumoto et al. 1980, 1982; Shklovskii and Efros 1984). The calculations given by these authors show that the magnetic field dependence of the resistivity in the nearest neighbour hopping regime for a weak field is given by

$$\rho_3(H) = \rho_3(0) \exp\left(t \frac{a_B^3 e^2 H^2}{N c^2 \hbar^2}\right) \tag{1.15}$$

where the parameter t is given by $t = 0.036$ (Shklovskii 1974). In a large magnetic field, the dependence becomes

$$\rho_3 \sim \exp(const. \frac{q E_H^{1/4} H^{1/2}}{N^{1/2}}) \tag{1.16}$$

where q =0.92 and E_H is the ground state ionization energy in a magnetic field. Shklovskii (1977) has shown that the anisotropy in the resistivity in this region is given by

$$\frac{\rho_\perp - \rho_\parallel}{\rho_\perp} \sim H^2 \tag{1.17}$$

for the weak field case, and

$$\frac{\rho_\perp}{\rho_\parallel} \sim H^{3/2} \tag{1.18}$$

for the strong field case.

In the VRH regime, in a weak field and for a constant density of states at the Fermi level, the resistivity varies as

$$\ln\left(\frac{\rho(H)}{\rho(0)}\right) \sim t_1 H^2 \left[\frac{T_0}{T}\right]^{3/4} \tag{1.19}$$

where t_1 is a constant (t_1 = 0.0025). For an arbitrary power-law dependence of the density of states on energy, the resistivity reads

$$\ln\left(\frac{\rho(H)}{\rho(0)}\right) \sim t_2 H^2 \left[\frac{T_0}{T}\right]^{3/2} \tag{1.20}$$

where t_2 is another constant ($\approx$ 0.0015).

The conductivity in the VRH regime for the case of large magnetic field, indeed, can be described by equation (1.13), but the parameters σ_0, T_0 and the exponent x depend on the energy dependence of the density of states at the Fermi level and the type of donor wave function used. Strictly speaking, the exponent x takes values in the range of 1/4 to 2/3 depending on the type of the wave function.

In the above argument we confined ourselves to the case of lightly doped semiconductors, in which the majority impurity concentration is assumed to be low enough that the wave functions of electrons of neighbouring impurity atoms are localized (and are practically identical with the wave functions of free atoms). However, as the carrier concentration increases, the overlap between the adjacent wave functions of the impurity centres increases. When the concentration increases so that the isolation condition (1.1) is no longer valid, then the discrete energy levels will eventually be transferred into a broad band of Bolch type energy states,

i.e. delocalized. In this case, the electrons can move freely in this band and the conductivity becomes of metallic-like type, i.e., it tends to a finite value in the limit of $T \rightarrow 0$ (Mott and Davis 1979). The energy gap between this impurity band and the conduction band decreases with increasing impurity concentration and at some concentration the two bands merge. Therefore, even in the limit $T \rightarrow 0$, the conduction band contains free electrons.

Now, one can say that by changing the doping level, a metal-insulator (MI) transition can be induced. This has already been observed in some semiconductors such as Ge and Si (Allen and Adkins 1972; Mott and Davis 1979; Rosenbaum et al. 1980, 1983; Newman and Holcomb 1983; Hirsch and Holcomb 1987). Mott (1949, 1967) was the first to show that the MI transition occurs at a critical concentration N^c at which the properties of a semiconductor changes abruptly. According to Mott's calculations, at MI transition one has

$$N^{c1/3} a_B^* = 0.25 \tag{1.21}$$

which is well known as the Mott criterion. Accordingly, the average distance between the impurity centres at which MI transition occurs is $2.5 a_B^*$. This criterion has been proved to be valid for a wide range of semiconductors with equation (1.21) replaced by (Edwards and Sienko 1978)

$$N^{c1/3} a_B^* = 0.26 \pm 0.05 \tag{1.22}$$

In addition to the above described band and hopping mechanisms of conduction, semiconductors with low compensation ($K < 0.2$) display another activated mechanism which manifests itself in a limited range of concentrations near the Mott transition (Mott 1982). This mechanism contributes one more term of the form

$$\sigma_2 = \sigma_{02} \exp\left(-\frac{\varepsilon_2}{k_B T}\right) \tag{1.23}$$

to the temperature dependence of the conductivity. This mechanism works in the intermediate temperature range between the band and the hopping conductivity regimes. The origin of the ε_2 conduction has been studied by many authors (see,

e.g., Nishimura 1965; Yamanouchi 1965; Biskupskii et al. 1980, 1984). It is believed that the mechanism of ε_2 conductivity is connected with the motion of electrons over singly filled neutral donors.

Although, changing the doping level of the impurities proved to be quite good and successful tool to induce the MI transition in some semiconductors, such as Ge and Si, however it is, practically, difficult to be employed in certain types of semiconductors such as n-InSb. In n-InSb, the donor concentration at which MI transition occurs is estimated by Mott's criterion to be $\sim 6.5 \times 10^{13}$ cm^{-3}. This, indeed, is less than the concentration of the purest sample available. In these materials, however, the MI transition can be achieved by varying the spatial extent of the wave functions of the donor impurity centres. This can be performed by applying certain external agents such as pressure (Fritzsche 1962) or a magnetic field (YKA). The advantages of these methods are that the compensation ratio and the doping level are kept constants and consequently the disorder is unchanged. In a metallic-like material such as n-InSb, the magnetic-field-induced MI transition has been used successfully by many authors (see, e.g., Mansfield et al. 1985; Abdul-Gader et al. 1987). It has been reported by these authors that the MI transition in these materials occurs at a particular threshold value of the magnetic field which, indeed, depends on the concentration of the carriers.

So far we were concerned with the d.c. conduction in doped semiconductors, i.e., the conductivity at zero frequency. One of the major features of the hopping conduction in disordered systems is the strong increase of the real part of the alternating current (a.c.) conductivity, $\sigma(\omega)$, with increasing the frequency, ω. The investigation of the temperature and frequency dependence of the a.c. conductivity has been dealt with by many authors (Pollak and Geballe 1961 (PG); Pollak 1971; Böttger and Bryksin 1976; Butcher and Hayden 1977; Baranovskii and Uzakov 1981; Efros 1981). In a.c. conduction, it is only necessary to transfer an electron between a pair of states. This is, indeed, a main distinguishing feature over the d.c. conduction which requires a continuous percolation path between the electrodes so as the current can flow. This suggests the approach of pair approximation which is

normally adopted in calculation of the a.c. loss. The transition between the sites is suggested to be due to phonon-assisted hopping, and the main contribution to the conductivity comes from pairs with transition frequency of the order of ω, i.e., pairs at a separation

$$r_\omega = \frac{a}{2}\ln(\nu_{ph}/\omega) \tag{1.24}$$

where a is the localization length and ν_{ph} is a frequency of the order of a phonon frequency ($\sim 10^{12}$ Hz). According to the original work of PG the frequency dependence of the a.c. conductivity can be written as

$$\sigma(\omega) \sim \omega \ln^4(\nu_{ph}/\omega) \tag{1.25}$$

or simply

$$\sigma(\omega) \sim \omega r_\omega^4 \tag{1.26}$$

It has generally been accepted to describe the experimental data of the a.c. conductivity by a dependence of the form

$$\sigma(\omega) \sim \omega^s \tag{1.27}$$

where the exponent s is in general smaller than unity. From equation (1.27), one finds

$$s = d\ln\sigma/d\ln\omega = 1 - 4/\ln(\nu_{ph}/\omega) \tag{1.28}$$

This gives a value of ~ 0.8 for the exponent s at normal frequency of about 10^4 Hz with $\nu_{ph} \sim 10^{12}$ Hz. As far as the temperature dependence of the a.c. conductivity is concerned, it is found theoretically that the conductivity, indeed, varies only weakly with the temperature. This can be written as

$$\sigma(\omega) \sim \omega \ln^4(\nu_{ph}/\omega) g_0^2 k_B T \tag{1.29}$$

where g_0 is the density of states at the Fermi level. It has been pointed out by Pollak (1971) and subsequently by Efros (1981) (see also Efros and Shklovskii 1985) that at low temperatures and due to intersite correlation between electrons on neighbouring sites, then the above equation reads

$$\sigma(\omega) \sim \omega \ln^3(\nu_{ph}/\omega) g_0^2 \tag{1.30}$$

which shows that the conductivity becomes temperature independent and the frequency dependence as expressed by s in this case is given by

$$s = 1 - 3/\ln(\nu_{ph}/\omega) \tag{1.31}$$

The failure of the pair approximation theory to account for the d.c. limit of the conductivity, (ω=0), led Summerfield and Butcher (1982) to investigate the effect of the external network on the pair under consideration. The results of these calculations led to the extended pair approximation theory (EPA). In a recent work by Summerfield (1985), the extended pair approximation theory (developed by Butcher and Summerfield (1981) and Summerfield and Butcher (1982)), has been used to scale the a.c. conductivity into its d.c. limit. Summerfield has obtained a formula of the form

$$\frac{\sigma(\omega,T)}{\sigma(0,T)} = f\left(\frac{A\tilde{\omega}}{\tilde{\sigma}(0,T)}\right) \tag{1.32}$$

where $\tilde{\omega}$ and $\tilde{\sigma}$ are the angular frequency and conductivity in reduced units (Summerfield 1985). The parameter A involved in the above equation depends on the site statistics. The function $f(x')$ is believed to be universal and approximated by (Summerfield 1985)

$$f(x') = 1 + x'^{0.725} \tag{1.33}$$

Summerfield scaling formula has been used to interpret the experimental data of some disordered materials including Si, Ge and GaAs. The universality of Summerfield scaling formula is inferred from the similarity in the shape of the resulting curves. It is interesting to examine this scaling formula for some other semiconductors such as InSb.

Basic ideas related to the Dielectric Behaviour:

Maxwell's equation defining the current I in terms of d.c. conductivity and of displacement current in the frequency domain can be written as (Jonscher 1983)

$$I(\omega) = \sigma_0 E(\omega) + i\omega D(\omega) \tag{1.34}$$

where E is the electric field, ω is the angular frequency and $D(\omega)$ is the dielectric induction given by

$$D = \epsilon_0 E + P \tag{1.35}$$

where ϵ_0 is the permittivity of free space and P is the polarization

$$P = \epsilon_0 \chi E$$

Thus, one can write

$$D = \epsilon_0(1 + \chi)E = \epsilon E \tag{1.36}$$

where the term $(1 + \chi)$ is known as the relative permittivity or the dielectric constant of the material and ϵ is the dielectric permittivity. The quantity χ is the dielectric susceptibility represented by a complex form as

$$\chi = \chi_1 - i\chi_2 \tag{1.37}$$

Hence,

$$I(\omega) = \left[\sigma_0 + \omega\epsilon_0\chi_2(\omega) + i\omega\epsilon_0(1 + \chi_1(\omega))\right] E(\omega) \tag{1.38}$$

This expression, indeed, shows that the dielectric medium can be represented by a parallel combination of frequency-dependent conductance ($G \sim \sigma_0 + \omega\epsilon_0\chi_2(\omega)$) and a capacitance ($C \sim \omega\epsilon_0[1 + \chi_1(\omega)]$). Therefore, one can write for the admittance

$$Y(\omega) = G(\omega) + i\omega C(\omega) \tag{1.39}$$

In the present work we have used the magnetic field to induce the MI transition in n-InSb samples with carrier concentration in the range of 5 $\times 10^{14}$ cm^{-3} to 2 $\times 10^{15}$ cm^{-3}. Measurements of the a.c. conductivity (in the frequency range of 110 to 10^5 Hz) as well as the d.c. limit were carried out in magnetic fields greater than the threshold value suggested by Ishida and Otsuka (1977) and up to 70 kG over a temperature range down to 0.04 K. We have also measured the d.c. limit in the same range of fields. Measurements of both the longitudinal and transverse d.c. magnetoresistance of n-InP samples of carrier concentration in the range of 5.7 $\times 10^{14}$ cm^{-3} to 7.8 $\times 10^{15}$ cm^{-3} in fields from 0 kG up to 70

kG are also carried out. The results of both the d.c. and a.c. conductivity will be discussed in the light of the above theoretical background.

In chapter 2, a brief account of the behaviour of an electron in a magnetic field is given. The theory of hopping conduction in the absence and presence of a magnetic field is discussed in both the nearest neighbour and variable range hopping regimes. The temperature and frequency dependence of the a.c. conductivity is also reviewed. An outline of the extended pair approximation theory and scaling formula as well as some aspects related to the metal-insulator transition in doped semiconductors are also given in this chapter.

The details of the experimental techniques used in both the d.c. and a.c. measurements are given in chapter 3.

In chapter 4 the results of the d.c. conductivity of n-InP samples are discussed.

Chapter 5 is devoted to discuss the experimental results of the a.c. and d.c. conductivity of the n-InSb samples.

Conclusions are given in chapter 6.

CHAPTER 2
THEORY

2.1 Introduction:

The transport properties of a semiconducting material under certain conditions can be very dependent on external influences such as a magnetic field. Measurement of magnetoresistance is considered a common tool in the field of semiconductor physics. The magnetoresistance may be large or small depending on band structure of the material and the strength of the field.

Motion of a free electron of mass m_0 in a magnetic field H has been studied by many authors (see, e. g., Ziman 1972). It has been found that this motion can be resolved into two components: the motion along the field direction (z-direction, say) and that in a plane perpendicular to H. The magnetic field does not change the longitudinal component, while the motion in the plane perpendicular to it is similar to the motion of a linear harmonic oscillator, the energy spectrum of which is given by $(n' + 1/2)\hbar\omega_c$, where ω_c is the cyclotron frequency, $\omega_c = eH/m_0c$ and $n' = 0, 1, 2, \ldots$ Thus, the energy of the electron in a magnetic field can be written as

$$\varepsilon' = (n' + 1/2)\hbar\omega_c + \frac{p_z^2}{2m_0} \tag{2.1}$$

where p_z^2 is the momentum in the z-direction. Equation (2.1) is the sum of a translational energy along the magnetic field, together with the quantized energy of the cyclotron motion. This can be represented by a family of quadratic parabolae shifted relative to one another along the energy scale by the value of $\hbar\omega_c$, (Landau levels). Taking into account the electron spin, the total energy then becomes

$$\varepsilon = (n' + 1/2)\hbar\omega_c + \frac{p_z^2}{2m_0} + m_s g\mu_B H \tag{2.2}$$

where m_s is the z-component of the spin angular momentum $= \pm\ 1/2$, the parameter g is the Landé splitting factor and μ_B is the Bohr magneton.

In $\underline{k}$-space, the orbital area in a plane transverse to H is quantized and

given by (Ziman 1972)

$$A_{n'} = \frac{2\pi eH}{\hbar c}(n' + 1/2) \tag{2.3}$$

Then, when the magnetic field increases, the orbit in real space which corresponds to the reciprocal of the orbit in $\underline{k}$-space shrinks.

Motion of electrons in crystals in magnetic fields is generally complicated. However, if the crystal potential is neglected, the electrons in the conduction band (Bloch electrons) can be considered as free electrons with an effective mass m^*. Hence, the electron energy should be quantized in the band in accordance with equation (2.2) with m_0 replaced by m^*. Thus the quasi-continuous energy spectrum in the band becomes discrete in presence of the magnetic field. This leads to a redistribution of electrons among the allowed Landau levels up to the Fermi energy μ defined by

$$\int_{-\infty}^{\infty} g(\varepsilon) f(\varepsilon) d\varepsilon = n \tag{2.4}$$

where $g(\varepsilon)$ is the density of states function in presence of magnetic field. For the energy spectrum of (2.1) it is given by (Brandt and Chudinov 1975) as

$$g(\varepsilon) = \frac{\hbar\omega_c m^{*3/2}}{\sqrt{2}\pi^2\hbar^3} \sum_{n'} \left[\varepsilon - \left(n' + \frac{1}{2}\right)\hbar\omega_c\right]^{-1/2} \tag{2.5}$$

$f(\varepsilon)$ is the Fermi-Dirac distribution function given by

$$f(\varepsilon) = \frac{1}{1 + \exp(\frac{\varepsilon - \mu}{k_B T})} \tag{2.6}$$

and n is the density of electrons in the band. From equations (2.4), (2.5) and (2.6), the total electron density in the presence of a magnetic field can be expressed in the form

$$n = \left(\frac{m^{*3} k_B T \omega_c^2}{2\pi^4\hbar^4}\right)^{1/2} \sum_{n'} F_{-1/2}(\mu^*) \tag{2.7}$$

where

$$\mu^* = \frac{\mu - (n' + 1/2)\hbar\omega_c}{k_B T} \tag{2.8}$$

and $F_{1/2}(\mu^*)$ is a member of the family of Fermi-Dirac integrals (see Blakemore 1974) given by

$$F_j(\mu^*) = \int_0^{\infty} \frac{t^j dt}{1 + \exp(t - \mu^*)} \tag{2.9}$$

2.2 A hydrogen-like impurity atom in a Magnetic Field:

The simple picture given above for the behaviour of free electrons in a magnetic field is still applicable for the case of bound electrons provided that the field is the dominant contributor to the energy of the electrons. Yafet, Keyes and Adams (1956) (YKA); were the first to study the effect of a strong magnetic field on the energy levels and wave function of a hydrogen-like impurity state in a semiconductor. They take as the wave functions and energy levels for various electronic impurity states the corresponding wave function for a hydrogen atom in which the mass of the electron is m^* and the charge of the nucleus is e/ϵ, where ϵ is the dielectric constant of the material. The ratio of the zero point energy, $\hbar\omega_c/2$, to the Rydberg constant R_y in such hydrogen-like states depends strongly on the effective mass m^* and the dielectric constant ϵ. For materials with very small effective mass and very high dielectric constant, this ratio can exceed unity. YKA presented their calculations in terms of a parameter γ which is given by

$$\gamma = \frac{\hbar\omega_c}{2R_y} \tag{2.10}$$

For small magnetic fields, ($\gamma \ll 1$), the perturbation effects of this weak external field lead to the ordinary magnetic splitting of the hydrogen atomic energy levels (Powell and Crasemann 1965). As γ approaches unity, the magnetic forces have a larger and larger effect on the electronic wave function and they tend to compress the atom in the transverse dimension, but along the direction of the field there is much smaller compression. For very strong magnetic fields, $\gamma \gg 1$, the field dominates the internal Coulomb attraction of the hydrogen core. Thus the Coulomb binding energy can be treated as a perturbation in the magnetic field. This can be explained in the framework of the previous discussion of an electron in a magnetic field. In very strong field region, where $\gamma \gg 1$, the motion parallel to the field will be slightly altered. However, the orbit in a plane perpendicular to the field will shrink as H increases so that the atom would progressively, become ovoid, barrel- and cigar-shaped for very strong fields. The result of this procedure is that the electron spends more time closer to the nucleus and hence the ionization

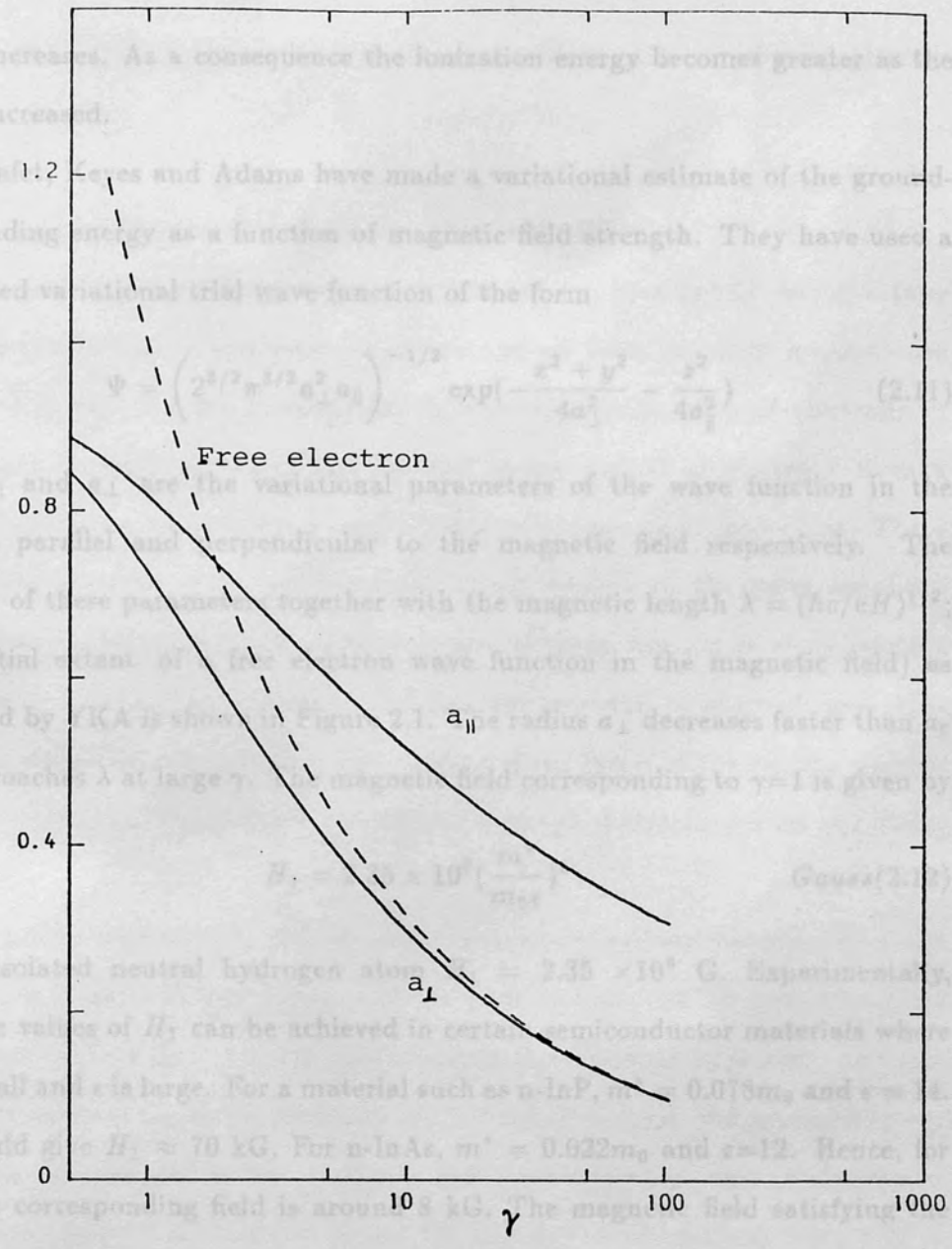

Figure 2.1

The spatial extents of the free electron wave function together with the donor wave function of the type used by Yafet, Keyes and Adams, in units of the effective Bohr radius as a function of the dimensionless parameter γ.

energy increases. As a consequence the ionization energy becomes greater as the field is increased.

Yafet, Keyes and Adams have made a variational estimate of the ground-state binding energy as a function of magnetic field strength. They have used a normalized variational trial wave function of the form

$$\Psi = \left(2^{3/2}\pi^{3/2}a_{\perp}^{2}a_{\parallel}\right)^{-1/2} \exp\left(-\frac{x^2+y^2}{4a_{\perp}^{2}} - \frac{z^2}{4a_{\parallel}^{2}}\right) \qquad (2.11)$$

where $a_{\parallel}$ and $a_{\perp}$ are the variational parameters of the wave function in the direction parallel and perpendicular to the magnetic field respectively. The variation of these parameters together with the magnetic length $\lambda = (\hbar c/eH)^{1/2}$; (the spatial extent of a free electron wave function in the magnetic field) as calculated by YKA is shown in Figure 2.1. The radius $a_{\perp}$ decreases faster than $a_{\parallel}$ and approaches λ at large γ. The magnetic field corresponding to γ=1 is given by

$$H_1 = 2.35 \times 10^{9}\left(\frac{m^*}{m_0\epsilon}\right)^{2} \qquad Gauss(2.12)$$

For an isolated neutral hydrogen atom $H_1 = 2.35 \times 10^9$ G. Experimentally, accessible values of H_1 can be achieved in certain semiconductor materials where m^* is small and ϵ is large. For a material such as n-InP, $m^* = 0.078m_0$ and $\epsilon = 14$. This would give $H_1 \approx 70$ kG. For n-InAs, $m^* = 0.022m_0$ and ϵ=12. Hence, for γ=1, the corresponding field is around 8 kG. The magnetic field satisfying the condition of $\gamma = 1$ could be even lower for materials such as n-InSb (less than 2 kG). There are several other materials (such as n-GaAs) for which the magnetic field at which $\gamma = 1$ is sufficiently low and hence the condition $\gamma \gg 1$ can be attained easily.

YKA have concluded that the effect of a strong magnetic field on an isolated hydrogen-like impurity atoms in semiconductors can be observed as a decrease in the free charge carriers in the conduction band. This phenomenon, which is known as the magnetic freeze-out, can be explained in terms of the increase in the ionization energy of the impurity atom as the magnetic field is increased. The YKA model should apply provided that the spacing between neighbouring

impurity atoms (r_D) is not less than ten times the effective Bohr radius a_B^* (Putley 1966).

2.3 Hopping Conduction In Zero Magnetic Field:

At relatively high temperatures the conduction in a lightly doped n-type semiconductor is due to electrons which are ejected from impurity levels to the conduction band. As the temperature is lowered, the number of electrons in the conduction band decreases rapidly and jumps (hops) of electrons from a neutral (full) donor to an ionized (empty) donor become more important. These jumps occur because of an exponentially small overlap of the wave functions of neighbouring impurity sites. The presence of compensation is an important parameter in this hopping process. The random potential of charged impurities leads to slight differences between the energies of the levels of the various donors, and the absorption of phonons is necessary for jumps of electrons from one donor to another.

Hopping conduction in semiconductor materials has been discussed by many authors (see Shklovskii and Efros 1984 for review) (SE). Miller and Abrahams (1960) have tackled this problem by proposing the following approach. Starting with electron wave functions localized on individual donors, the probability γ_{ij} that an electron located at site i hops to site j with the emission or absorption of a phonon can be calculated. Thus the number of transitions from i to j can be deduced. In the absence of an external electric field, an equal number of electrons undergo the reverse transition . In a weak electric field, the forward and backward transitions are not the same, i. e., no detailed balance and the current is proportional to the field. This yields a resistance R_{ij} of a given transition. Hence the whole problem can be reduced to calculating the resistivity of an equivalent random network of resistors in which each pair of sites is connected by a resistor R_{ij} .

Following Shklovskii and Efros (1984) (SE), let us consider two donors i and j with coordinates $\mathbf{r_i}$ and $\mathbf{r_j}$, sharing one electron, i.e., one of the two donors

is neutral (full) and the other donor is ionized (empty). Assume that the ground-state wave function of an isolated donor is represented by $\Psi(\mathbf{r}-\mathbf{r}_i) \equiv \Psi(\mathbf{r})$ which satisfies $(H_0+U)\psi = E\psi$ where H_0 is the electron Hamiltonian in the host crystal and $U = -e^2/\epsilon \mid \mathbf{r}-\mathbf{r_i} \mid$. If the distance between the two donors $r_{ij} = \mid \mathbf{r_i}-\mathbf{r_j} \mid$ is much larger than the characteristic wave function size, a, then the overlap of functions Ψ_i and Ψ_j will be weak. The interaction between the electron and both donors produces a splitting of the degenerate state. The split-state wave functions represent a symmetric and antisymmetric combination of the atomic functions, hence

$$\Psi_{1,2} = \frac{\Psi_i \pm \Psi_j}{2^{1/2}(1 \pm \int \Psi_i^* \Psi_j d\mathbf{r})^{1/2}} \tag{2.13}$$

Evaluation of the energy of states 1 and 2 with the Hamiltonian

$$H = H_0 - \frac{e^2}{\epsilon \mid \mathbf{r}-\mathbf{r}_i \mid} - \frac{e^2}{\epsilon \mid \mathbf{r}-\mathbf{r}_j \mid} \tag{2.14}$$

gives (SE)

$$E_{2,1} = -E_0 - \frac{e^2}{\epsilon r_{ij}} \pm I_{ij} \tag{2.15}$$

where -E_0 is the energy level of an isolated donor, and I_{ij} is the energy overlap integral given by (SE)

$$I_{ij} = \int \Psi_i^* \Psi_j \frac{e^2}{\epsilon \mid \mathbf{r}-\mathbf{r}_j \mid} d\mathbf{r} - \int \Psi_i^* \Psi_j d\mathbf{r}' \int \frac{e^2 \mid \Psi_i \mid^2}{\epsilon \mid \mathbf{r}-\mathbf{r}_j \mid} d\mathbf{r} \tag{2.16}$$

For a hydrogen-like function of the form $\Psi(\mathbf{r}) = uF(\mathbf{r})$ where u is a periodic function having the period of the lattice and $F(\mathbf{r})$ is of the form $F(r) = (\pi a^3)^{-1/2} \exp(-r/a)$ the overlap integral (2.16) becomes

$$I_{ij} = \frac{2}{3}\left[\frac{e^2}{\epsilon a}\right]\left[\frac{r_{ij}}{a}\right] \exp\left[\frac{-r_{ij}}{a}\right] \tag{2.17}$$

In lightly doped semiconductors, for every pair of donors the following inequality should hold

$$\Delta_i^j \gg I_{ij} \tag{2.18}$$

where

$$\Delta_i^j = w(r_j) - w(r_i) \tag{2.19}$$

and $w(r)$ is potential energy between the electron and the charged impurities surrounding the donor at r. If the potential energy $w(r)$ is included in the Hamiltonian, then by performing a variational calculation with the function

$$\Psi = A_i\Psi_i + A_j\Psi_j \tag{2.20}$$

Miller and Abrahams (1960) show that when the inequality (2.18) is satisfied, the wave functions of the two lowest states are of the form

$$\Psi_i' = \Psi_i + \frac{I_{ij}}{\Delta_i^j}\Psi_j \tag{2.20a}$$

$$\Psi_j' = \Psi_j - \frac{I_{ij}}{\Delta_i^j}\Psi_i \tag{2.20b}$$

The transition of electron from state Ψ_i' to Ψ_j' implies a transfer of a charge $-e$ over a distance r_{ij}. Obviously, this transition yields a current.

Shklovskii and Efros have shown that the transition probability $i \rightarrow j$ with absorption of one phonon is given by

$$\gamma_{ij} = \gamma_{ij}^0 \exp(-2r_{ij}/a) N(\Delta_i^j) \tag{2.21}$$

where

$$\gamma_{ij}^0 = \frac{E_1^2 \Delta_i^j}{\pi d v_s^5 \hbar^4} \left(\frac{2e^2}{3\epsilon a}\right)^2 \frac{r_{ij}}{a^2} \left[1 + \left(\frac{\Delta_i^j a}{2\hbar v_s}\right)^2\right]^{-4} \tag{2.22}$$

$$N(\Delta_i^j) = \left[\exp\left(\frac{\Delta_i^j}{k_B T}\right) - 1\right]^{-1} \tag{2.23}$$

and

d = density,

v_s = longitudinal velocity of sound,

E_1 = deformation-potential constant.

Assume that $n_i = (0,1)$ is the donor occupation number of the $i-$th donor. The transition i to j occurs only if i is full and j is empty, i. e., when $n_i = 1$ and $n_j = 0$. Therefore, the number of electrons which jump from i to j per unit time is given by

$$\Gamma_{ij} = < \gamma_{ij} n_i (1 - n_j) > \tag{2.24}$$

where <> denotes an average. To evaluate Γ_{ij}, SE have introduced some simplifications. With the assumption that site occupation numbers and energies do not fluctuate in time, but remain equal to their average value, then the number of transitions per unit time can be written as

$$\Gamma_{ij} = \gamma_{ij}^0 \exp(-2r_{ij}/a) N(\varepsilon_j - \varepsilon_i) f_i (1 - f_j) \tag{2.25}$$

where f_i is the average occupation number $\equiv < n_i >$ and the phonon energy absorbed in the transition $i \rightarrow j$ is taken to be $\Delta_i^j = \varepsilon_j - \varepsilon_i$

For the reverse transition from j to i one has

$$\Gamma_{ji} = \gamma_{ij}^0 \exp\left(-2r_{ij}/a\right) \left[N(\varepsilon_j - \varepsilon_i) + 1\right] f_j (1 - f_i) \tag{2.26}$$

Thus the current between the donors i and j is given by

$$J_{ij} = -e(\Gamma_{ij} - \Gamma_{ji}) \tag{2.27}$$

In zero electric field, there will be a detailed balance between the transitions $i \rightarrow j$ and $j \rightarrow i$, thus $\Gamma_{ij} = \Gamma_{ji} = \Gamma_{ij}^0$, and therefore $J_{ij} = 0$. If an external electric field E is introduced, it will redistribute electrons over donors, create corrections δf_i to f_i, and affect the donor-level energies ε_i and ε_j, then the balance will be destroyed. In this case one can write

$$f_i(E) = f_i^0 + \delta f_i = \left[1 + \frac{1}{2} \exp\left(\frac{\varepsilon_i^0 - \delta\mu_i - \mu}{k_B T}\right)\right]^{-1} \tag{2.28}$$

and

$$\varepsilon_i = \varepsilon_i^0 + \delta\varepsilon_i$$

where f_i^0 is the value of the function f_i in the equilibrium and ε_i^0 is the average energy on site i at $E = 0$. $\delta\varepsilon_i$ can be written as (SE)

$$\delta\varepsilon_i = e\mathbf{E}.\mathbf{r}_i + \frac{e^2}{\epsilon} \sum_{k \neq i}^{don} \frac{\delta f_k}{\mid r_i - r_k \mid} \tag{2.29}$$

The first term in the above equation represents the direct action of the external field E, while the second one describes the variation in the Coulomb potential

due to a redistribution of electrons. Now, to calculate the conductivity, one has to consider the case of a closed circuit in which the electric field is so small that the corrections $\delta\mu_i$ and $\delta\varepsilon_i$ are small compared to k_BT, then one can proceed expansions of the functions f_i, f_j and $N(\varepsilon_i - \varepsilon_j)$. This yields a current of the form

$$J_{ij} = \frac{e\Gamma^0_{ij}}{k_BT}\Big[\delta\mu_j + \delta\varepsilon_j - (\delta\mu_i + \delta\varepsilon_i)\Big] \tag{2.30}$$

the parameter Γ^0_{ij} here is the frequency of transitions $i \rightarrow j$ and $j \rightarrow i$ at equilibrium. The above equation can be rewritten in the form

$$J_{ij} = R^{-1}_{ij}(U_i - U_j) \tag{2.31}$$

with

$$R_{ij} = \frac{k_BT}{e^2\Gamma^0_{ij}} \tag{2.32}$$

and

$$-eU_i = \delta\varepsilon_i + \delta\mu_i = e\mathbf{E}.\mathbf{r}_i + \delta\mu_i + \frac{e^2}{\epsilon}\sum_{k\neq i}^{don}\frac{\delta f_k}{\mid r_i - r_k \mid} \tag{2.33}$$

The quantity $-eU_i$ is considered as a local electrochemical potential on donor i, counted from the electron chemical potential μ. The difference $(U_i - U_j)$ is regarded as a voltage drop on the transition $i \rightarrow j$ and R_{ij} as the resistance of this transition. Now, for a real system having many donors, one can calculate the total current through the sample as the sum of all currents piercing any cross-section. Thus the hopping conductivity problem can be reduced to that of calculating the conductivity of a random network in which the resistance (2.32) connects each pair of donors.

At very low temperatures the parameter Γ^0_{ij} can be written as (SE)

$$\Gamma^0_{ij} = \gamma^0_{ij}\exp\Big(-2r_{ij}/a\Big)\exp\Big(-\varepsilon_{ij}/k_BT\Big) \tag{2.34}$$

where

$$\varepsilon_{ij} = 1/2[\mid \varepsilon_i - \varepsilon_j \mid + \mid \varepsilon_i - \mu \mid + \mid \varepsilon_j - \mu \mid] \tag{2.35}$$

Then equation (2.32) becomes

$$R_{ij} = R^0_{ij}\exp(\xi_{ij}) \tag{2.36}$$

where

$$R_{ij}^{0} = \frac{k_B T}{e^2 \gamma_{ij}^{0}} \tag{2.36a}$$

and

$$\xi_{ij} = \frac{2r_{ij}}{a} + \frac{\varepsilon_{ij}}{k_B T} \tag{2.37}$$

The resistance network (2.36) represents an exponentially wide spectrum of resistance R_{ij}. Evaluation of such resistance has been tackled by many authors using the percolation theory (see for example Ambegaokar, Halperin and Langer 1971(AHL); Pollak 1972; Shklovskii and Efros 1971). In this approach, one assumes that the random sites are chaotically distributed points in space with N being the average number of sites per unit volume. Consider that ξ_{ij} is some function of r_{ij} which connects sites i and j. According to the percolation theory, sites i and j will be considered bonded if, for some number ξ,

$$\xi_{ij} \leq \xi \tag{2.38}$$

If two sites are connected (bonded) directly or via other bonded sites, they belong to the same cluster. Thus, one has to find a percolation threshold ξ_c, that is, the lower bound of the parameter ξ which still permits an infinite cluster to be formed. In another words, one can use the bonding criterion

$$r_{ij} \leq r$$

which can be satisfied if site j is within a sphere of radius r about site i. Consequently, spheres of radius r are constructed about all sites, and one has to find the lowest value $r = r_c$ which allows for an endless chain of sites in which each site lies inside the sphere constructed about the preceeding site.

To evaluate the resistivity of a network of connected sites the percolation threshold ξ_c or percolation radius r_c has to be evaluated. The percolation radius r_c depends solely on the site concentration N. Now, assume that the mean number of bonds per site within the radius r is $B = \frac{4}{3}\pi N r^3$. Thus r_c can be expressed in terms of the dimensionless threshold parameter B_c as

$$B_c = \frac{4}{3}\pi N r_c^3 \tag{2.39}$$

where $B_c = 2.7$, (Pike and Seager 1974). Hence,

$$r_c = 0.865 N^{-1/3}$$

and

$$\xi_c = \frac{2r_c}{a} + \frac{\varepsilon_{ij}}{k_B T} \tag{2.40}$$

This would give a resistivity of the form

$$\rho = \rho_{03} \exp\left(\alpha_1 / N^{1/3} a\right) \exp\left(\varepsilon_{ij}/k_B T\right) = \rho_3 \exp\left(\varepsilon_{ij}/k_B T\right) \tag{2.41}$$

where the parameter α_1 in the above equation is found theoretically to be

$$\alpha_1 = 1.73 \tag{2.42}$$

The experimental concentration dependence of the resistivity has been studied by many authors (see, e.g., Emel'yanenko et al.1973, Eddols 1966, Kahlert et al. 1976, and Lemoine et al. 1976). These authors find α_1 for n-GaAs ranging from 1.7 to 1.9. A value of 1.9 ± 0.2 has been found by Emel'yanenko et al. (1975) for n-InP. The temperature dependence of ρ obtained by these authors in the hopping region was rather weak and the value of the activation energy $\varepsilon_3 \equiv \varepsilon_{ij}$ was around 0.3 meV. As the pre-exponential factor in equation (2.41) depends on the temperature, better agreement between theory and experiment is expected if one plots ln (ρ/T) versus $1/T$.

It should be pointed out that equation (2.41) is applicable only to the case of lightly doped materials with isotropic hydrogenic wave functions decaying at large distances as exp $(-r/a)$.

2.4 Hopping Conduction In a Magnetic Field:

Nearest-neighbour hopping conduction will also occur in a magnetic field. A magnetic field H shrinks the wave functions of the donors which leads to a reduction in the overlap integral. Shklovskii (1974) has considered an isolated hydrogen-like atom located at the centre of a cylindrical coordinate system (ρ', ϕ, z) in which the z axis is directed along the magnetic field H. For a relatively weak

field in which the inequality $\lambda \gg a$ holds, Shklovskii has pointed out that the wave function Ψ falls according to the law

$$\Psi \propto \exp\left[-\left(\frac{r}{a} + \frac{\rho'^2 ra}{24\lambda^4}\right)\right] \tag{2.43}$$

where λ is the magnetic length and is given by

$$\lambda = \left[\frac{c\hbar}{eH}\right]^{1/2} \tag{2.44}$$

$$r = (x^2 + y^2 + z^2)^{1/2}, \rho' = (x^2 + y^2)^{1/2}$$

As the exponent ξ is given by

$$\xi_{ij} = \frac{2r_{ij}}{a} + \frac{(x_{ij}^2 + y_{ij}^2)ar_{ij}}{12\lambda^4} \tag{2.45}$$

[N.B.: the temperature dependence term in equation (2.37) is neglected here as we are considering the concentration dependence] thus, for the case of weak field one can show that the threshold parameter ξ_c is given by

$$\xi_c = \frac{\alpha_1}{N^{1/3}a} + \frac{B_c a}{24\pi N\lambda^4} \tag{2.45a}$$

The first term coincides with the value of ξ_c for $H = 0$, while the second term describes a correction due to the magnetic field which gives rise to an exponential magnetic field dependence of the form

$$\rho_3(H) = \rho_3(0)\exp(t\frac{ae^2H^2}{Nc^2\hbar^2}) \tag{2.46}$$

where $t = B_c/24\pi = 0.036$ (Shklovskii 1974).

In a weak magnetic field, hopping occurs over distances of the order of $N^{-1/3}$, just as in the absence of the field. Thus, equation (2.46) is valid provided $\lambda \gg a$ and $\lambda^2/a \gg N^{-1/3}$ which can be satisfied only in lightly doped semiconductors, where $N\ a^3 \ll 1$, and for weak fields. The field H_c defining the limit of the weak field region is determined by the condition $\lambda \gg a/(N\ a^3)^{1/6}$ which gives

$$H_c = \frac{N^{1/3}c\hbar}{ae} \tag{2.47}$$

In a large magnetic field such that $a_H \gg \lambda$, and for a donor wave function of the form (Hasegawa and Howard 1961 (HH); Shklovskii 1972; Shklovskii and Efros 1984)

$$\Psi = (2\pi\lambda^2 a_H)^{-1/2} \exp\left[-\frac{x^2+y^2}{4\lambda^2} - \frac{|z|}{a_H}\right] \tag{2.48}$$

where

$$a_H = \hbar/(2m^* E_H)^{1/2} \tag{2.49}$$

is the characteristic length of the wave-function decay in the direction of the magnetic field, and E_H is ground state ionization energy in a magnetic field, in this case Shklovskii and Efros (1984) have shown that the percolation parameter ξ has the form

$$\xi_{ij} = \frac{2\,|\,z_{ij}\,|}{a_H} + \frac{x_{ij}^2 + y_{ij}^2}{2\lambda^2} \tag{2.50}$$

The surface of constant ξ_{ij} now consists of two truncated paraboloids having a common base and a common axis of revolution directed along the magnetic field. In this case, the threshold parameter ξ_c is given by

$$\xi_c = \frac{B_c^{1/2}}{(\pi N a_H \lambda^2)^{1/2}} \tag{2.51}$$

Thus the resistivity takes the form

$$\rho = \rho_{03} \exp\left(\frac{B_c^{1/2}}{(\pi N a_H \lambda^2)^{1/2}}\right) \exp\left(\varepsilon_{ij}/k_B T\right) \tag{2.52}$$

Thus the magnetic field dependence of the resistivity can be written in the form

$$\begin{aligned} \rho_3 &= \rho_{03} \exp\left(\frac{q}{(N a_H \lambda^2)^{1/2}}\right) \\ &= \rho_{03} \exp\left(\frac{q 2^{1/4} m^{*1/4} e^{1/2} E_H^{1/4} H^{1/2}}{c^{1/2} \hbar N^{1/2}}\right) \end{aligned} \tag{2.53}$$

where $q = (B_c/\pi)^{1/2} = 0.92$ for $B_c = 2.7$.

Shklovskii and Efros (1984) have pointed out that equations (2.46) and (2.53) are applicable for fields $H < H' \equiv 2H_c$ and $H > H'' \equiv 6H_c$ respectively. The anisotropy of hopping conduction has been dealt with by Shklovskii (1977).

Shklovskii proposed that the anisotropy in a magnetic field is given by

$$\begin{aligned} \frac{\rho_{xx}}{\rho_{zz}} &= \frac{\rho_{\perp}}{\rho_{\parallel}} \\ &= \left[\frac{<|\, z_{ij} \,|>}{<|\, x_{ij} \,|>}\right]^2 \end{aligned} \tag{2.54}$$

In a weak magnetic field this gives (Shklovskii 1977)

$$\begin{aligned} \frac{\rho_{\perp}(H) - \rho_{\parallel}(H)}{\rho_{\perp}(H)} &= \frac{\alpha^2}{48}\left[\frac{H}{H_c}\right]^2 \\ &\approx \left[\frac{H}{4H_c}\right]^2 \end{aligned} \tag{2.55}$$

and in strong field case:

$$\frac{\rho_{\perp}}{\rho_{\parallel}} \approx 0.11\left[\frac{H}{H_c}\right]^{3/2} \tag{2.56}$$

2.5 Variable-Range Hopping in zero Magnetic Field:

At sufficiently low temperatures, Mott (1967,1969) has observed that the conductivity decreases less rapidly than expected by equation (2.41) for an activated hopping process. Following the spirit of Mott's calculations and because of the factor exp (ε_{ij}/k_BT) in equation (2.41) at very low temperatures only resistances having a small value of ε_i will contribute to the conduction. The electrons therefore will hop to remote sites which are not necessarily the nearest neighbours to reduce the energy necessary for the transition. Hence only energies ε_i and ε_j lying close to the Fermi level will be involved. In this case, the characteristic hopping length increases on lowering the temperature according to (SE)

$$\bar{r} \approx a(T_0/T)^{1/4} \tag{2.57}$$

hence the name variable range hopping (VRH). Mott was the first to give a qualitative derivation of the temperature dependence of the conductivity in this regime in zero magnetic field.

If the density of states at the Fermi level is given by

$$g(\varepsilon) = g_0\varepsilon^p \tag{2.58}$$

then the number of available states within a radius r and with energy between 0 and Δ is given by

$$\begin{aligned} &\frac{4\pi}{3}r^3 \int_0^{\Delta} g(\varepsilon)d\varepsilon \\ &\qquad = \frac{4\pi}{3}r^3 \int_0^{\Delta} g_0 \varepsilon^p d\varepsilon \\ &\qquad = \frac{4\pi}{3}r^3 \frac{g_0 \Delta^{p+1}}{p+1} \\ &\qquad = B_c \end{aligned} \tag{2.59}$$

According to (2.36), the resistivity ρ can be written as

$$\rho \propto \exp -\left(\frac{2r}{a} + \frac{\Delta}{k_B T}\right) \tag{2.60}$$

hence using r from equation (2.59) and minimizing the exponent to find the optimum hopping energy one gets

$$\rho \propto \exp -\left(\frac{T_0}{T}\right)^x \tag{2.61}$$

where $x = p + 1/p + 4$.

Thus for a constant density of states at the Fermi level, $p = 0$, $x = 1/4$, $T_0 = S_1(g_0 a^3 k_B)^{-1}$, $S_1 = 49$.

The original theory of VRH assumed a constant density of states at the Fermi level. Subsequently it was suggested that, because of electron-electron interaction, a gap appears in the one-electron excitation spectrum and this results in the density of states dropping to a minimum, Pollak (1970), or zero, Efros and Shklovskii (1975). An expression similar to (2.58) has been derived with $p = 2$. This gives a resistivity of the form (2.61) but with $x = 1/2$ and $T_0 = S_2(g_0^{1/3} a k_B)^{-1}, S_2 = 10$. Efros et al. (1979) have shown by computer simulation that when a screened Coulomb interaction in the form of $U(r) = \frac{e^2}{\epsilon r}\exp(-r/r_s)$ is used the Coulomb gap is smeared out and disappears if only short range interactions are considered.

There is no clear evidence from measurements on lightly doped III-V compounds for either $T^{-1/4}$ or $T^{-1/2}$ law. Measurements on wide range of

temperatures at zero magnetic field as well as in presence of the field are important in order to verify which law is most likely to be obeyed.

2.6 Variable Range Hopping in a Magnetic Field:

Variable-range hopping in presence of a magnetic field has been treated by many authors (see, e. g., Shklovskii 1973, 1982; Tokumoto et al. 1980, 1982 and Shklovskii and Efros 1984).

As it has been mentioned elsewhere, the effect of a magnetic field on the wave function becomes stronger with increasing distance from the impurity centre, therefore in the VRH regime and at sufficiently low temperatures one would expect a large positive magnetoresistance. A weak magnetic field makes a relatively small contribution to the resistivity exponent ξ_{ij} , while strong magnetic field has a pronounced effect. Now, for the case of constant density of states at the Fermi level and in the weak-field case, according to (2.45), the contribution due to the magnetic field can be written as

$$\Delta\xi_{ij} = \frac{r_{ij}^3 a \sin^2\theta}{12\lambda^4} \tag{2.62}$$

where θ is the angle between the vector r_{ij} and the magnetic field, and λ is magnetic length given by (2.44). If the effect of the weak magnetic field on the characteristic hopping length is negligible then by substituting (2.57) into (2.62) one finds that the contribution to the threshold percolation parameter ξ_c, in order of magnitude equals to

$$\frac{a^4}{\lambda^4}\left[\frac{T_0}{T}\right]^{3/4}$$

Hence, the magnetoresistance in this case is given by

$$\ln\frac{\rho(H)}{\rho(0)} = t_1\frac{e^2a^4H^2}{c^2\hbar^2}\left[\frac{T_0}{T}\right]^{3/4} \tag{2.63}$$

Shklovskii and Efros (1984) estimate the dimensionless parameter t_1 as 0.0025.

The case of an arbitrary power-law dependence of the density of states on energy has been considered by the above authors. Using the fact that

$< r_{ij}^3 >= \gamma_{(p)}(a\xi_c/2)^3$, where $\gamma_{(p)} < 1$, and that $\xi_c = (T_0/T)^x$, then in this case

$$\ln\left(\frac{\rho(H)}{\rho(0)}\right) = t_p \frac{a^4}{\lambda^4}\left[\frac{T_0}{T}\right]^{3x} \tag{2.64}$$

where $t_p = \gamma_{(p)}/144$. If the density of states is governed by the Coulomb gap ($p = 2$), in this case equation (2.64) takes the form

$$\ln\left(\frac{\rho(H)}{\rho(0)}\right) = t_2 \frac{a^4}{\lambda^4}\left[\frac{T_0}{T}\right]^{3/2} \tag{2.65}$$

The parameter $t_2 \approx 0.0015$, (SE).

Variable range hopping in strong magnetic field has been considered by many authors (e. g., Shklovskii 1977; Tokumoto et al. 1982; Shklovskii 1982), (see also Shklovskii and Efros (1984)). The temperature dependence of the resistivity depends on the shape of the wave function assumed in the treatment of the overlap integral. For a wave function of YKA type;

$$\Psi_{YKA} = \left[\left(2\pi\right)^{3/2} a_\perp^2 a_\parallel\right]^{-1/2} \exp\left(-\frac{x_i^2 + y_i^2}{4a_\perp^2} - \frac{z_i^2}{4a_\parallel^2}\right) \tag{2.66}$$

the resistivity is given by (2.61), with $x = 2(p+1)/(2p+5)$. For a constant density of states at the Fermi level, $p = 0$, thus $x = 2/5$ and $T_0 = S_3(g_0 a_\perp^2 a_\parallel k_B)^{-1}$ with $S_3 = 0.433$. For the case when the density of states is governed by equation (2.58) with $p = 2$, then x becomes $2/3$ and

$$T_0 = S_4(g_0 a_\perp^2 a_\parallel k_B)^{-1/3} \tag{2.67}$$

and $S_4 = 1.62$.

For a wave function of Hasegawa-Howard type (1961) (eq. (2.48)), a similar expression was obtained by Tokumoto et al. (1982) with $x = (p+1)/(p+3)$. Hence, for a constant density of states ($p = 0$), one gets $x = 1/3$. In this case $T_0 = S_5(g_0 \lambda^2 a_\lambda k_B)^{-1}$ with $S_5 = 5.8$. When the Coulomb gap becomes important ($p = 2$), then $x = 3/5$ and $T_0 = S_6(g_0 \lambda^2 a_\lambda k_B^3)^{-1/3}$ where $S_6 = 4.21$.

Shklovskii (1982) has proposed a novel new approach to VRH in a large magnetic field. He pointed out that the magnetic field creates a barrier to transverse hopping which increases in proportion to the square of the hopping

distance perpendicular to the direction of the magnetic field. Shklovskii has used a wave function of the form

$$\Psi(\rho', z) \propto \exp\left(-\frac{z}{a_H} - \frac{\rho'}{b}\right) \tag{2.68}$$

where ρ' is the hopping distance perpendicular to the field and b depends on the strength of the magnetic field. As a result, the resistivity was found to be

$$\rho = \rho_0 \exp\left(T_0/T\right)^x \tag{2.69}$$

The exponent x here is equal to $(p+1)/(p+4)$. This gives $x = 1/2$ for a density of states proportional to ε^2 with $T_0 = S_7 e^2 (a_H b^2)^{-1/3}/k_B\epsilon$ and $S_7 = 7.52$. For a constant density of states, $p = 0$, $x = 1/4$, $T_0 = S_8(a_H b^2)^{-1}/g_0 k_B$ and $S_8 = 63.02$. The theoretical predictions of the exponent x suggested for different models are summarised in table 2.1.

	$g(\varepsilon)$=constant		$g(\varepsilon) = g_0\varepsilon^2$	
donor wave function	x	T_0	x	T_0
zero magnetic field	1/4	$S_1(g_0 a^3 k_B)^{-1}$	1/2	$S_2(g_0^{1/3} a_B)^{-1}$
large field and Ψ_{YKA}	2/5	$S_3(g_0 a_\perp^2 a_\parallel k_B)^{-1}$	2/3	$S_4(g_0 a_\perp^2 a_\parallel k_B)^{-1/3}$
large field and Ψ_{HH}	1/3	$S_5(g_0\lambda^2 a_\lambda k_B)^{-1}$	3/5	$S_6(g_0\lambda^2 a_\lambda k_B^3)^{-/3}$
large field and Ψ_{Sh}	1/4	$S_8(a_H b^2)^{-1}/g_0 k_B$	1/2	$S_7 e^2 (a_H b^2)^{-1/3}/k_B\epsilon$

Table 2.1: Values of the exponent x together with the temperature T_0 in equation (2.69) obtained by different models.

2.7 Alternating Current Hopping Conductivity:

It has been discussed earlier that at low temperatures the transport occurs due to hopping of electrons. The charges are considered to move by discontinuous " hopping " jumps between well defined localized states within the solid, spending most of the time at rest on these sites. The lowest energy state is achieved when the majority impurity nearest to a given minority is ionized. The presence of

an electric field yields a current which can pass only under the condition that the thermal energy is sufficient to overcome the Coulomb potential around the minority impurity. In the case if the thermal energy is insufficient, the presence of the electric field will change the potential and consequently a new equilibrium has to be established. This would lead to a polarization which can be investigated as a current in a.c. experiment.

When a harmonically varying field $E(\omega)$ is applied to a dielectric sample, the produced time-dependent polarization in the frequency domain $P(\omega)$ is given by (Jonscher 1983)

$$P(\omega) = \epsilon_0 \chi(\omega) E(\omega) \tag{2.70}$$

where ϵ_0 is the permittivity of free space, and χ is the dielectric susceptibility represented by a complex form as

$$\chi(\omega) = \chi_1(\omega) - i\chi_2(\omega) \tag{2.71}$$

Here, the imaginary part χ_2 is termed the "dielectric loss", and the current due to it is in phase with the harmonic driving field. The components of the dielectric susceptibility are related to those of the complex relative permittivity $\epsilon(\omega) = \epsilon_1(\omega) - i\epsilon_2(\omega)$

$$\epsilon_1(\omega) = 1 + \chi_1(\omega) \tag{2.72}$$

$$\epsilon_2(\omega) = \chi_2(\omega) \tag{2.73}$$

The real part of the a.c. conductivity is expressed in terms of the dielectric loss as

$$Re\sigma(\omega) = \epsilon_0 \omega \epsilon_2(\omega) \tag{2.74}$$

and the imaginary part is written as

$$Im\sigma(\omega) = \epsilon_0 \omega \epsilon_1(\omega) \tag{2.75}$$

In random systems, it is assumed that a (broad) distribution $n(\tau)$ of relaxation times, τ, should exist if relaxation occurs by processes involving distances or activation energies related to the disordered structure of the material. Thus,

one can assume that each individual microscopic process giving rise to a given relaxation time τ is independent of all others, and therefore the overall conductivity is given by a summation over all contributions. Thus for continuous distribution of $n(\tau)$, the real part of the a.c. conductivity can be written in the form

$$Re\sigma(\omega) = \int_0^\infty \alpha' n(\tau) \frac{\omega^2 \tau}{1+\omega^2\tau^2} d\tau \tag{2.76}$$

Here α' is the polarizability of a pair of sites. The form of $n(\tau)$ required in the calculations implies that the relaxation time τ must be an exponential function of a random variable, η', say

$$\tau = \tau_0 \exp(\eta') \tag{2.77}$$

where τ_0 is a constant characteristic relaxation time. Generally, the physical microscopic relaxation mechanisms that can give rise to functional form for τ in equation (2.77) are (Elliott 1987 for review)

(1) Phonon-assisted quantum-mechanical tunnelling (QMT) of electrons through the barrier separating two equilibrium positions, in which case

$$\eta' = 2\alpha r \tag{2.78}$$

(2) Classical hopping of carriers over the potential barrier separating two energetically favourable sites, in this case

$$\eta' = W/k_B T \tag{2.79}$$

2.7.1 Modelling for a.c. conductivity. Two-site Model:

To calculate the a.c. conductivity, three quantities have to be found. These are; (a) the polarizability α', (b) the distribution function for the relaxation times $n(\tau)$ and (c) the relaxation time expressed in terms of the variable η'.

The first attempts towards a theoretical understanding of $\sigma(\omega)$ were taken by Pollak and Geballe (1961), who introduced a two-site model as a mechanism of relaxation losses in lightly doped semiconductors for investigating the a.c. hopping conductivity. The basic assumption of this pioneering model is that the a.c. conductivity is due to electrons that tunnel back and forth between two donors and not among larger groups of donors. This is valid at frequencies high enough that during half a period of the oscillation of the external electric field electrons can hop solely between nearest-neighbour sites. At low frequencies, however, during half a period of the oscillation of the external field, electrons may perform many hops. The current then was proposed to arise from transitions within highly conducting clusters of sites, (coupled via capacities of nonconducting parts), the size of which increases with decreasing frequency, so that it becomes macroscopically large for $\omega \rightarrow 0$. Such an arrangement of resistors and capacitors demonstrates an impedance with real and imaginary parts. Since an electron can tunnel only from an ionized donor to a neutral one, a pair must be singly ionized to contribute to the a.c. conductivity.

The main distinguishing feature of the a.c. conduction from the d.c. one lies in the fact that in the former it is necessary to transfer an electron between a pair of sites, while in the latter a continuous percolation path between the electrodes has to be formed for the current to perpetuate. This suggests the approach of considering the absorption of an isolated pair of states with one electron and to sum up the losses due to such pairs so as the total response of a bulk sample can be obtained.

At frequencies where conduction is due to relaxation mechanisms, one can assume that the external electric field slightly changes the equilibrium occupation

numbers of sites and causes relaxation to the equilibrium state which is determined by an instantaneous value of the field. The transition between the sites is suggested to be due to phonon-assisted tunnelling and has the characteristic frequency

$$\tau^{-1} = \nu_{ph} exp(-2r/a) \tag{2.80}$$

where $\nu_{ph} \sim 10^{12}$ Hz, r is the distance between sites of pair, and a is the localization length. It should be borne in mind that the main contribution to the conductivity is given by the pairs with the transition frequency τ^{-1} of the order of ω, i.e. pairs at a separation

$$r_\omega = \frac{a}{2} \ln(\nu_{ph}/\omega) \tag{2.81}$$

The current density in the field direction is given by

$$j = \dot{p} \tag{2.82}$$

where

$$p = \frac{1}{\Omega} \sum_i e X_i f_i \tag{2.83}$$

and Ω is the volume over which the summation extends, X_i is the distance between the ith majority impurity and the nearest minority impurity along the field direction. The function f_i is the occupancy probability of the ith majority impurity and is given by the solution of

$$\dot{f}_i = \sum_j \Gamma_{ij} f_j - \sum_j \Gamma_{ji} f_i \tag{2.84}$$

where Γ_{ij} is the transition rates given by MA (2.25). PG simplified the solution of equation (2.84) by considering that the hopping occurs exclusively between pairs of majority impurities and assuming that the jumping in a given pair is independent of the others, i. e. the electric field at one hopping centre is just the applied field. Considering the conductivity of 1 cm^3 with n identical jumping centres each of which is consisting of a pair of majority atoms separated by a distance r, energy ε and having the same orientation θ with respect to the applied field. Labeling the pair with 1 and 2, then from (2.84) one has

$$\begin{aligned} \dot{f}_1 &= \Gamma_{12} f_2 - \Gamma_{21} f_1 \\ &= -(\Gamma_{21} + \Gamma_{12}) f_1 + \Gamma_{12} \end{aligned} \tag{2.85}$$

and (2.83) gives

$$p = ne(X_1 f_1 + X_2 f_2) = ne(X_1 - X_2) f_1 + neX_2 \tag{2.86}$$

thus

$$j = \dot{p} = ne(X_1 - X_2)\dot{f}_1 = ner\dot{f}_1 \cos\theta \tag{2.87}$$

where $f_1 + f_2 = 1$. In the presence of an external electric field $E(\omega)$, PG solved equation (2.87) in the limits of $t = 0$ and $t = \infty$ and they obtained the current density in a frequency-dependent form as

$$\frac{j(\omega)}{E(\omega)} = \frac{1}{4} nr^2 \cos^2\theta e^2 \frac{1}{k_B T \cosh^2(\varepsilon/2k_B T)} \tau^{-1} \left[\frac{\omega^2\tau^2}{1+\omega^2\tau^2} + i\frac{\omega\tau}{1+\omega^2\tau^2} \right] \tag{2.88}$$

As the pairs are considered to be at random, and there is no interaction between hopping centres, the total conductivity is obtained by an additive function of the contributions from all pairs, the integration over θ yields

$$d\sigma(r,\varepsilon,\omega) = \frac{e^2}{12k_B T} dp(r,\varepsilon) N_A r^2 \tau^{-1} \left[\frac{\omega^2\tau^2}{1+\omega^2\tau^2} + i\frac{\omega\tau}{1+\omega^2\tau^2} \right] \frac{1}{\cosh^2(\varepsilon/2k_B T)} \tag{2.89}$$

where $dp(r,\varepsilon)$ is the number of pairs of energy separation ε and spacing separation r and is given by (PG)

$$dp(r,\varepsilon) = 4\pi N_D r^2 dr \tag{2.90}$$

Pollak and Geballe have simplified the problem by considering the high temperature case and reduced the double integration over r and ε to a single integral over r. Hence, the real part of the conductivity, $Re(\sigma)$, is obtained at high enough temperature to be

$$\begin{aligned} Re(\sigma) = {} & (4\pi/12) N_D N_A (e^2/k_B T)(14.8 - \frac{1}{2}\ln\omega)^4 (a^5/2)\omega \\ & \left\{ \frac{\pi}{2} - \arctan[5.5 \times 10^{-13} \times \omega (14.8 - \frac{1}{2}\ln\omega)^{3/2} \tanh(\varepsilon/2k_B T)] \right\} \end{aligned} \tag{2.91}$$

Equation (2.91) predicts that the frequency dependence of the conductivity is of the form $\sigma \propto \omega^s$ with $s \approx 0.8$, a behaviour which has been already observed in many disordered materials. One of several discrepancies between the above formula and experimental findings is the temperature dependence of the conductivity.

While the conductivity was found experimentally to increase with temperature the theory predicts that it should decrease as $1/T$.

The problem of a.c. conductivity in disordered materials has been discussed by many authors (see, e. g., Pollak 1971, Böttger and Bryksin 1976, Butcher and Hayden 1977, Efros 1981). For the case of QMT of electrons, the relaxation time is suggested to be given by $\tau \propto \exp(2\alpha r)$. Efros (1981) has tackled the problem as follows. The conductivity of one pair is calculated then an averaging over all pairs is performed. The main property of the pairs which is considered important here is that the transitions of electrons between the two sites of the pair are much faster than the transitions between any site of the pair and any other site of the system. By considering a pair as a closed system with an induced dipole moment

$$\mathbf{d}(\omega, \varepsilon, \mathbf{r}) = e\mathbf{r}\frac{(e\mathbf{E}.\mathbf{r})}{k_B T}\frac{1}{4\cosh^2 \varepsilon/2k_B T}\frac{1}{1+i\omega\tau} \tag{2.92}$$

the dipole moment of the unit volume is

$$\mathbf{P} = \int\int \mathbf{d}(\omega, \varepsilon, \mathbf{r}) F(\varepsilon, r) d\varepsilon d\mathbf{r} \tag{2.93}$$

$F(\varepsilon, r)$ is the distribution function of pairs such that the probability of finding a pair in a volume containing both empty and occupied sites with a distance between them within the range $(r, r+dr)$ and an activation energy in the range $(\varepsilon, \varepsilon + d\varepsilon)$ is given by $4\pi F(\varepsilon, r) d\varepsilon r^2 dr$. Integrating equation (2.93) over the angles corresponding to the vector $\mathbf{r}$ and using equation (2.80) gives (Efros 1981)

$$\sigma(\omega) = \frac{\pi^2}{6} e^2 \left(\frac{a}{2}\right)^5 \omega \left(\ln \frac{\nu_{ph}}{\omega}\right)^4 \int \frac{d\varepsilon F(\varepsilon, r_\omega)}{k_B T \cosh^2 \varepsilon/2k_B T} \tag{2.94}$$

Efros (1981) has used Austin and Mott (1969) one-electron approximation in which the energy of an electron on site i is independent of the occupation numbers of all other sites. Accordingly, the distribution function $F(\varepsilon, r)$ was found to be given by

$$F(\varepsilon, r) = \frac{\varepsilon g_0^2}{\tanh(\varepsilon/2k_B T)}$$

Thus equation (2.94) becomes

$$\sigma(\omega) = \frac{\pi^4}{12} e^2 k_B T g_0^2 (\frac{a}{2})^5 \omega \ln^4 \left(\nu_{ph}/\omega\right) \tag{2.95}$$

Böttger and Bryksin (1976) have obtained a similar equation. The same functional form (of the frequency and temperature dependences) was also obtained by different authors (see, e.g., Pollak 1971, Mott and Davis 1979). The frequency dependence of the conductivity predicted by the QMT then can be written as

$$s = \frac{d\ln\sigma}{d\ln\omega} \tag{2.96}$$

Hence,

$$s = 1 - \frac{4}{\ln(\nu_{ph}/\omega)} \tag{2.97}$$

Accordingly, the QMT model predicts that s is less than unity (typically $s \approx 0.8$ for $\omega \approx 10^4$ Hz and $\nu_{ph} = 10^{12}$ Hz) and is temperature-independent but frequency-dependent, s decreases with increasing frequency. On the other hand, the QMT predicts that $\sigma(\omega)$ is only weakly temperature dependent.

Pollak (1971) was the first to consider the effect of intersite correlation between electrons on neighbouring sites. Subsequently, Efros (1981), Long (1982) and more recently Efros and Shklovskii (1985) have dealt with this problem. The pair approximation is also invoked in the discussion of correlation, since it is suggested that the intersite Coulomb interaction affects just the close neighbours, (i.e., pairs of sites), the Coulomb interaction is assumed to be screened out for further neighbours and hence the occupation of a given site by an electron is assumed not to affect the occupation of such further neighbouring sites. For this case Efros finds that the distribution function $F(\varepsilon, r)$ is given by

$$F(\varepsilon, r) = g_0^2(\varepsilon + \frac{e^2}{\epsilon r})$$

Accordingly, the conductivity takes the form

$$\sigma(\omega) = \frac{\pi^3}{3}\left(\frac{a}{2}\right)^4 \frac{e^4}{\epsilon}\omega \ln^3\left(\frac{\nu_{ph}}{\omega}\right) g_0^2 \tag{2.98}$$

The frequency dependence is more pronounced in this case as

$$s = 1 - \frac{3}{\ln(\nu_{ph}/\omega)} \tag{2.99}$$

Further developments of the theory of a.c. conductivity in lightly doped semiconductors described by PG have been made by Golin (1963); Pollak (1964);

Baranovskii and Uzakov (1980, 1981). The main idea behind the mechanism used by these authors is the same as that originally proposed by PG, i. e., pairs of impurity centres, one filled and one empty, are considered and the electron states are assumed to be localized at the sites. In presence of the electric field, polarization is created by electron jumps in the pairs from the occupied to empty sites. The contribution made to the conductivity by one pair averaged over all orientations of a pair relative to the field direction is given by (2.89). It has been shown by Pollak and Watt (1965) that in the process of integration with respect to r the term $[\omega\tau + (\omega\tau)^{-1}]^{-1}$ can be replaced by $\pi a\delta(r - r_\omega)/4$, and the term $(1 + \omega^2\tau^2)^{-1}$ with $\theta(r_\omega - r)$, where $\theta(x)$=0 for $x < 0$ and $\theta(x)$=1 for $x > 1$.

Baranovskii and Uzakov (1981) have considered the case of low temperatures when k_BT is much less than $e^2/\epsilon r_D$ which is the energy of the Coulomb interaction when the average distance between donors is r_D. They assumed that only the donor nearest to the acceptor is ionized on condition that its distance from the acceptor does not exceed $r_\mu = e^2/\epsilon\mu$ where μ is the Fermi energy. The case when there are two ionized donors near an acceptor is ignored. Following Baranovskii and Uzakov, the conductivity of the system is found by integrating $d\sigma$ over all values of r and ε, multiplying by the probability that in a unit volume a pair of one filled and one empty site can be found within a distance r to $r + dr$ and specified by energy in the range ε to $\varepsilon + d\varepsilon$. This probability has been denoted by $4\pi^2 F(\varepsilon, r)dr d\varepsilon$. With a simple shape of the distribution function $F(\varepsilon, r)$ these authors have obtained the real part of the conductivity to be given by

$$\sigma(\omega) = \frac{\pi^2}{12}\left(\frac{a}{2}\right)^4 a\frac{\epsilon\omega}{k_BT}\ln^4(\nu_{ph}/\omega)I(K, r, T) \qquad (2.100)$$

where K is the compensation ratio, r and a are measured in unites of $N_D^{-1/3}$, k_BT is measured in units of $e^2N_D^{1/3}/\epsilon$ and $I(K, r, T)$ was calculated by numerical integration (Baranovskii and Uzakov 1980).

2.8 Extended Pair Approximation and Scaling formula:

Butcher (1980) has used the MA equivalent circuit to generate a rate equation. A finite array of N_s sites in a macroscopic volume Ω is considered. Each site may be occupied by one and only one electron. This system is then assumed to be subjected to an electric field $E\exp(-i\omega t)$ in the x-direction. According to Butcher (1980) (see also Summerfield and Butcher 1982), the rate equations linearized in E are given by

$$-i\omega C_i\Big(V_i + Ex_i\Big) = \sum_j g_{ij}\Big(V_i - V_j\Big) \tag{2.101}$$

where sites are labelled by indices i. Here, the voltages V_i are related to the field perturbation of the site-occupation probabilities, the capacitance C_i associated with site i is determined by the equilibrium occupation probability of this site and is a function of the energy ε_i, the conductance g_{ij} (between two sites i and j) is determined by the equilibrium occupation probabilities of sites i and j and the transition rate between them and the voltage generators $-Ex_i$ accounts for the applied field. Equation (2.101) is identical with Kirchhoff's equations for the Miller-Abrahams equivalent circuit. The left-hand side of this equation is the time derivative of the electric charge on site i. Hence, by calculating the time derivative of the macroscopic polarization Summerfield and Butcher (1982) obtained

$$\sigma = -\frac{1}{2\Omega E}\sum_i g_{ij}V_{ij}x_{ij} \tag{2.102}$$

where

$$V_{ij} = V_i - V_j \tag{2.103}$$

$$x_{ij} = x_i - x_j \tag{2.103a}$$

The real part of the conductivity then is written as (Butcher and Summerfield 1981, Summerfield and Butcher 1982)

$$Re\sigma(\omega) = \frac{1}{2\Omega E^2}\sum_{ij} g_{ij} \mid V_{ij} \mid^2 \tag{2.104}$$

The a.c. conductivity in a pair approximation (Summerfield and Butcher 1982) is obtained by considering two arbitrary sites labelled 1 and 2, and neglecting all

conductances except g_{12}, then eqn. (2.101) takes the form

$$-i\omega C_1\Big(V_1 + Ex_1\Big) = -g_{12}V_{12} \tag{2.105}$$

$$-i\omega C_2\Big(V_2 + Ex_2\Big) = -g_{12}V_{12} \tag{2.105a}$$

Hence

$$V_{12} = -Ex_{12}/Z_p g_{12} \tag{2.106}$$

where the impedance Z_p is given by

$$Z_p = \frac{1}{g_{12}} - \frac{1}{i\omega C_1} - \frac{1}{i\omega C_2} \tag{2.107}$$

Equation (2.106) is the elementary pair approximation to V_{12}. When $\omega \rightarrow 0$, $Z_p \rightarrow \infty$ and $V_{12} \rightarrow 0$, thus one obtains no d.c. conductivity. However, when $\omega \neq 0$, and $g_{12} \rightarrow 0, V_{12} \rightarrow -Ex_{12}$. Therefore, the pair approximation is consistent with the macroscopic boundary condition provided that $\omega \neq 0$.

The failure of the pair approximation theory to account for the d.c. limit of the conductivity, (when $\omega = 0$), led Butcher and Summerfield (1981) (BS) (see also Summerfield and Butcher 1982 (SB)) to work out the effect of the external network on the pair labelled 1 and 2.

In the exact equations for V_1 and V_2 there are additional terms on the right hand sides of (2.105) and (2.105a) which allow for both the current flowing into other sites and the voltage generations Ex_k associated with other sites. A series combination of an admittance Y_i and a voltage generator e_i between site i and the ground with $i = 1$ and 2 was proposed to take into account these effects, i.e. $-Y_1(V_1 + e_1)$ and $-Y_2(V_2 + e_2)$ has to be added to the R.H.S. of equations (2.105) and (2.105a). Solving for V_{12} yields (SB 1982)

$$V_{12} = -\frac{Ex_{12}}{Zg_{12}} + \frac{1}{Zg_{12}}\left[\frac{Y_1}{Y_1 - i\omega C_1}\Big(Ex_1 - e_1\Big) - \frac{Y_2}{Y_2 - i\omega C_2}\Big(Ex_2 - e_2\Big)\right] \tag{2.108}$$

where

$$Z = \frac{1}{g_{12}} + \frac{1}{Y_1 - i\omega C_1} + \frac{1}{Y_2 - i\omega C_2} \tag{2.109}$$

If the sites are macroscopically separated then one has $V_{12} \rightarrow -Ex_{12}$ for sites with $g_{12} = 0$. Consequently, the quantity in the square brackets should vanish when sites 1 and 2 are macroscopically separated. In this case one gets

$$V_{12} = -Ex_{12}/Zg_{12} \tag{2.110}$$

which is similar to eqn. (2.106) except that Z_p is replaced by Z.

A complete formalism of the extended pair approximation has been obtained by BS (1981) who have calculated Y_i which represents the average admittance of the rest of the circuit to current flowing out of site i, i.e., its external admittance seen from site i=1 averaged over all stochastic variables except ε_1 and ε_2. Since site 2 is assumed to be remote from site 1, then $Y_1 = Y(\varepsilon_1)$ and $Y_2 = Y(\varepsilon_2)$. SB 1982 have used a first order approximation to $Y(\varepsilon_i)$ given by a mean field approach shown in Figure 2.2.

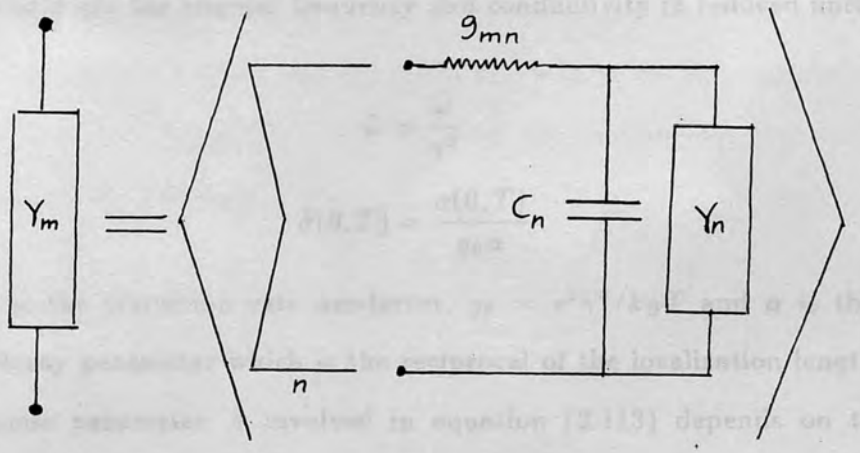

Figure 2.2

Schematic representation of the mean-field approximation to Y_m (SB 1982).

The N-1 conductances g_{ij} connecting site i to all other sites j and the associated capacitances C_j are taken into account. The mean value $Y(\varepsilon_i)$ replaces

the admittance of the rest of the network seen from site j. With the system averages written explicitly, an extended pair approximation equations for $Y(\varepsilon_i)$ and $\sigma(\omega)$ in a 3-dimensional system are obtained (SB 1982)

$$Y(\varepsilon_i) = 4\pi B_c^{-1} \int_{-\infty}^{\infty} g(\varepsilon_j) d\varepsilon_j \int_0^{\infty} r_{ij}^2 \left(\frac{1}{g(\varepsilon_i, \varepsilon_j, r_{ij})} + \frac{1}{Y(\varepsilon_j) - i\omega C(\varepsilon_j)} \right)^{-1} dr_{ij} \tag{2.111}$$

$$\sigma(\omega) = \frac{2\pi}{3} \int_{-\infty}^{\infty} g(\varepsilon_i) d\varepsilon_i \int_{-\infty}^{\infty} g(\varepsilon_j) d\varepsilon_j \int_0^{\infty} r_{ij}^4 \times \left(\frac{1}{g(\varepsilon_i, \varepsilon_j, r_{ij})} + \frac{1}{Y(\varepsilon_i) - i\omega C(\varepsilon_i)} + \frac{1}{Y(\varepsilon_j) - i\omega C(\varepsilon_j)} \right)^{-1} dr_{ij} \tag{2.112}$$

Recently, Summerfield (1985) has used the EPA theory developed by BS and SB to scale the a.c. conductivity into its d.c. limit in a very simple formula of the form

$$\frac{\sigma(\omega, T)}{\sigma(0, T)} = f[\frac{A\tilde{\omega}}{\tilde{\sigma}(0, T)}] = f(x) \tag{2.113}$$

where $\tilde{\omega}$ and $\tilde{\sigma}$ are the angular frequency and conductivity in reduced units given by

$$\tilde{\omega} = \frac{\omega}{\gamma^0}$$

$$\tilde{\sigma}(0, T) = \frac{\sigma(0, T)}{g_0 \alpha} \tag{2.114}$$

where γ^0 is the transition rate pre-factor, $g_0 = e^2\gamma^0 / k_B T$ and α is the wave function decay parameter which is the reciprocal of the localization length. The dimensionless parameter A involved in equation (2.113) depends on the site statistics and the function $f(x')$ is believed to be universal and is approximated by (Summerfield 1985)

$$f(x) = 1 + x'^{0.725} \tag{2.115}$$

Summerfield examined some solutions of the EPA in the region of low-frequency response defined as the region where the exponent s (defined as d ln σ (ω) / d ln ω) is a monotonically increasing function of the frequency ω. In tackling the problem, Summerfield has considered random sites in three dimensions and quantum tunnelling with transition rates whose spatial dependence on intersite separation r is given by $(\alpha r)^{\nu_1} \exp(-2\alpha r)$ where the parameter ν_1 is associated with the

symmetry of the localized wave functions. Using the definitions of $\tilde{\sigma}(\omega)$ and $\tilde{\omega}$ described above, the EPA equations (2.111) and (2.112) takes the form

$$\tilde{\sigma}(\omega) = \frac{\pi}{48\alpha^6} \int g(\varepsilon_1) g(\varepsilon_2) d\varepsilon_1 d\varepsilon_2 W(\varepsilon_1, \varepsilon_2) I_4^{\nu_1} \Big(W(\varepsilon_1, \varepsilon_2); \varepsilon_1, \varepsilon_2 \Big) \tag{2.116}$$

where

$$W(\varepsilon_1, \varepsilon_2) = \left[\frac{1}{Y(\varepsilon_1) - i\tilde{\omega} C(\varepsilon_1} + \frac{1}{Y(\varepsilon_2) - i\tilde{\omega} C(\varepsilon_2)} \right]^{-1} \tag{2.117}$$

and

$$Y(\varepsilon_1) = \frac{\pi}{2\alpha^3 B_c} \int g(\varepsilon_2) d\varepsilon_2 \Big[Y(\varepsilon_2) - i\tilde{\omega}(\varepsilon_2) \Big] I_2^{\nu_1} \Big[Y(\varepsilon_2) - i\tilde{\omega} C(\varepsilon_1); \varepsilon_1, \varepsilon_2 \Big] \tag{2.118}$$

The integration $I_n^{\nu_1}(z; \varepsilon_1, \varepsilon_2)$ is given by

$$I_n^{\nu_1}(z; \varepsilon_1, \varepsilon_2) = \int_0^\infty \frac{x^n dx}{1 + z \exp[Q(\varepsilon_1, \varepsilon_2) + x - \nu_1 \ln x/2]} \tag{2.119}$$

The analytical approximations to $I_n^{\nu_1}$ are developed by Summerfield and Butcher (1983). The functions $C(\varepsilon)$ and $Q(\varepsilon_1, \varepsilon_2)$ are related to the equilibrium site occupancy $f_0(\varepsilon) = 1/\exp\beta(\varepsilon - \mu) + 1$ and the equilibrium transition rate $\gamma_{12}(r, \varepsilon_1, \varepsilon_2)$ via the relations

$$C(\varepsilon) = f_0(\varepsilon) \Big[1 - f_0(\varepsilon) \Big] = \exp \Big[-Q(\varepsilon_1, \varepsilon_2) \Big] \tag{2.120}$$

$$\gamma_{12}(r, \varepsilon_1, \varepsilon_2) f_0(\varepsilon_1) \Big[1 - f_0(\varepsilon_2) \Big] = \gamma^0 (\alpha r)^{\nu_1} \exp \Big[-2\alpha r - Q(\varepsilon_1, \varepsilon_2) \Big] \tag{2.121}$$

In the MA theory

$$\exp \Big[-Q(\varepsilon_1, \varepsilon_2) \Big] = \frac{f_0(\varepsilon_1) \Big[1 - f_0(\varepsilon_2) \Big] \beta(\varepsilon_2 - \varepsilon_1)}{\exp \Big[\beta(\varepsilon_2 - \varepsilon_1) \Big] - 1} \tag{2.122}$$

where $\beta = 1/k_B T$. Summerfield shows that results of the extended pair approximation (EPA) calculations for different models with various density of states distribution appear very similar in such a way that it scales as (2.113). The exponent (0.725) in equation (2.115) is a median fixed by trial and error (Summerfield 1985).

2.9 Some aspects related to Metal-Insulator Transition in Doped Semiconductors:

It has been well established that a metal-insulator (MI) transition in doped semiconductors could be induced by varying the concentration of the impurity centres in the material. This has been extensively studied in materials such as Ge and Si (see, e.g., Mott 1974, Mott and Davis 1979, Resenbaum et al. 1980, 1983, Newman and Holcomb 1983, Hirsch and Holcomb 1987). Mott (1949) was the first to show that this transition occurs at a certain value of the impurity concentration given by

$$(N^c a_B^{*3})^{1/3} = 0.25 \tag{2.123}$$

Experimental evidence that this law is well obeyed has been shown by many authors (see, e.g., Edwards and Sienko 1978) with the right hand side of equation (2.123) being 0.26 ± 0.05.

MI-transition can be observed in doped semiconductors not only by varying the impurity concentration but also it could be induced by applying an external agents such as a magnetic field. The basic effect of it on a hydrogen-like atom is to shrink the Bohr radii of the donor wave functions and to increase the binding energy of the donor centres. This effect has been already described by the dimensionless parameter γ (see section 2.2). In materials such as n-InSb, inducing MI-transition by varying the concentration of donors seems to be quite difficult. This comes from the fact that the dielectric constant of this material is large (~ 17.64) and the effective mass of the electron is so small ($m^* = 0.0145 m_0$). This gives a large effective Bohr radius ($\sim 650 \mathring{A}$). However, the possibility of changing the spatial extent between donors using a reasonable magnetic field makes it possible to induce the MI-transition and consequently putting the material on the insulator side. This excellent tool has been used successfully by many authors (see for example, Ferre et al. 1975; Mansfield et al. 1985; Abdul-Gader et al. 1987). The magnetic field-induced metal-insulator transition in other materials such as InP and Si has also been reported by many authors (see, e. g., Biskupski et al. 1984, Long and Pepper 1984, 1985). According to Ishida and Otsuka (1977),

for moderate compensation ratio, (~ 0.5), the magnetic field induced MI-transition occurs at a critical (threshold) value H_{cr} which can be deduced from the formula

$$\left(N_D a_{\parallel} a_{\perp}^2\right)^{1/3} = 0.26 \tag{2.124}$$

where N_D is the donor concentration, $a_{\parallel}$ and $a_{\perp}$ are the YKA parameters. This equation is simply Mott's criterion (2.123) with allowance to the anisotropy of the donor wavefunction due to the magnetic field. Robert et al. (1980) have shown that the critical field for weak compensated material can be evaluated from the relationship

$$H_{cr} \propto \left(N_D - N_A\right)^{0.84} \tag{2.125}$$

where N_A is the acceptor concentration. In the present work, the magnetic-field-induced MI-transition will be employed to locate the n-InSb samples on the insulator side of the MI-transition so as the a.c. hopping conductivity and related phenomena can be investigated.

The conduction in the insulating state of doped semiconductors is of an activated nature. In the metallic state however the conduction has a finite value σ_0 at $T \rightarrow 0$. According to the scaling formula of localization given by Abrahams et al. (1979) (see also Rosenbaum et al. 1983) σ_0 tends continuously to zero as the electron concentration approaches the critical value;

$$\sigma_0 = c' \frac{e^2}{\hbar l_c} \tag{2.126}$$

where c' is a constant and l_c is a scale length diverging as $n \rightarrow n_c$,

$$l_c = l_0 \left(\frac{n}{n_c} - 1\right)^{-\nu} \tag{2.127}$$

ν here is a critical exponent and l_0 is the value of l_c far from MI-transition.

In studying MI-transition from the insulator side, the variation of the dielectric constant with donor contents has been investigated. Castner et al. (1980) have observed an enhancement in the dielectric constant as the excess donors ($N_D - N_A$) in n-Ge is increased. A gradual linear increase in the dielectric constant above the host crystal dielectric constant is observed which then becomes

very rapid as the concentration is increased towards the critical value. It has been suggested that the scaling theory of localisation predicts that the dielectric constant ϵ should diverge as the critical concentration is approached (see e. g., Ionov et al. 1983 and Thomas 1983). The variation of the dielectric constant with concentration has also been reported by Capizzi et al. (1980). Capizzi et al. have used a scaling formula of the form

$$\epsilon = \epsilon_c \left(\frac{n_c}{n_D} - 1 \right)^{-\nu'} \tag{2.128}$$

to discuss their results, and they found that the parameter ν' is twice the theoretical predictions, ($\nu' = 2\nu$). Similar results were found by Ionov et al. (1983).

CHAPTER 3

Experimental Technique And Details

3.1 Sample Preparation :

The disc-shaped n-InSb samples used in the a.c. measurements were cut from ingot slices (supplied by MCP Electronic Materials Ltd., England) by a spark erosion machine. For concentration and compensation ratio (K) measurements, bar-shaped samples were prepared from the same ingot slices. 2-5 μm fine alumina powder was used to polish the samples and grind them to the appropriate size. They were then cleaned in an ultrasonic cleaner for at least two hours. A standard CP4 solution (made up of a mixture of hydrofluric, nitric and acetic acids in ratios 3 : 5 : 3) was then used as an etchant to remove surface damage and for extra cleaning of the specimens. It has been pointed out by Mansfield and Kusztelan (1978) that as the temperature is lowered or the magnetic field is increased, the resistance increases so that the material becomes a near insulator. These authors have reported that the high bulk resistance of the sample could be masked by a surface conducting layer unless suitable precautions are taken. This work confirms this conclusion and careful etching is important and necessary to avoid the surface conducting layer. Mansfield and Kusztelan, also suggested that resistivity measurements could be extended to higher resistivity by using disc-shaped samples instead of the bar-shaped ones which are used normally in electrical measurements. Good agreement between measurements with bar-shaped and disc-shaped samples were reported by many authors (see, for example, Tokumoto et al. 1982 and Walton and Dutt 1977).

The disc-shaped samples were electroplated with pure indium as follows. Samples were coated with Kodak KPR3 photoresist varnish, dried for at least 4 hours and then they enveloped in masks (Scribecoat Acetate Film) with two identical opaque circles facing the flat surfaces of the samples. For experimental reasons, the diameter of the opaque circle was chosen to be in the range of 5

mm to 6.5 mm depending on the carrier concentration. Specimens then were exposed to an UV light for about 5 minutes. This process is necessary to harden the photoresist apart from the well protected areas facing the opaque circles. With the samples taken out of the the masks, KPR3 developer was applied to dissolve the unhardened parts of the photoresist. This step leaves the specimens coated with Kodak KPR3 photoresist varnish except tow opposite circular areas on each sample. Indium plating solution was used to electroplate the samples with the current being $\approx$ 25 mA during this process. A platinum wire (of 0.13 mm diameter) was soldered to one electroplated circular spot with pure indium using a fine soldering iron and applying "Superior" No. 30 flux, while the other circular spot was soldered onto a head of a copper screw and the screw was then firmly bolted to the specimen holder. Finally, the photoresist which was protecting the sample during plating and soldering processes was removed by using "analar" quality acetone. The residual flux was then removed.

The bar-shaped samples used for concentration measurements, after being etched with the CP4 solution, were provided with current and potential probe leads of platinum or 40 SWG enamelled copper wires. A pure indium solder was used to make the soldering and the superior flux No. 30 was applied. Specimens were then washed thoroughly to remove the residual flux so that the effects of the surface contamination could be avoided.

The bar-shaped n-InP samples used in d.c. measurements were prepared from ingot slices supplied by the same suppliers mentioned above. Surfaces of the specimens were polished with 0.25 μm diamond compound and then ultrasonically cleaned in analar acetone. Current and potential probes were made by the same way as explained above.

For the carrier concentration and compensation ratio measurements, a conventional ^{4}He cryostat has been used. The excess donor concentrations $N_D - N_A$ for the n-InSb samples were determined from the Hall coefficient measured at 77 K and $N_D + N_A$ from measurements of the conductivity in the temperature range 10-30 K where impurity scattering dominates and the Brooks-

Herring theory can be used (Mansfield and Kusztelan 1978).

The values of $N_D - N_A$ of the n-InP samples were originally determined from the Hall coefficient measurements at 77 K. The compensation ratio $K = N_A/N_D$ for each sample was determined from the resistivity in zero magnetic field over the temperature range 10 to 300 K. The details of the procedure has been explained by Mansfield et al. (1988).

3.2 Sample Holder and Superconducting magnet:

The disc-shaped n-InSb samples were mounted on the platform of a multi-pillar sample holder in a parallel configuration with respect to the magnetic field, while the bar-shaped n-InP samples were mounted in parallel then perpendicular arrangements so that both longitudinal and transverse resistivities were measured. The sample holder is made up from one-piece of oxygen-free high conductivity copper rod (OFHC). This sample holder has been designed in such a way to accommodate disc- and bar-shaped samples simultaneously. A schematic diagram of the sample holder is given in Figure 3.1. The holder is firmly fixed to the mixing chamber of the ^{3}He-^{4}He dilution refrigerator (DR) via a screw which is a part from the same sample holder.

The electrical terminals for the a.c. measurements are formed from two coaxial cables in the DR. The wires coming out of the samples were soldered to the coaxial cables via 40 SWG copper wires which were thermally anchored to the body of the sample holder with a very thin layer of GE7031 varnish. All the wires as well as the samples were electrically isolated from the the body of the DR.

For the d.c. measurements a small teflon block was fixed on the sample holder. The wires coming out of the bar-shaped samples were soldered into the ends of the terminals on the teflon piece to which a bunch of 40 SWG copper wires were soldered and then thermally anchored to the body of the sample holder. These wires are soldered to superconducting wires which ran up to the 4.2 K flange in the DR.

To minimize the thermal radiation, a small cylindrical hollow jacket made

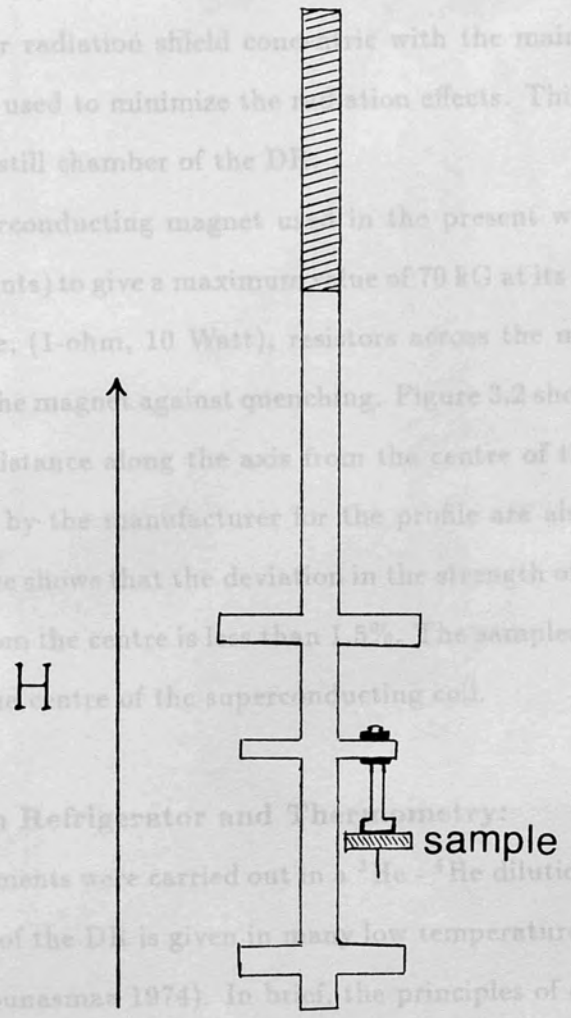

Figure 3.1

A Schematic diagram of the sample holder with a disc-shaped in position.

up from the same material as the sample holder itself was fitted firmly to a shoulder on the sample holder in such a way that the samples can be accommodated securely inside it. The eddy currents due to the usage of high magnetic fields were reduced by providing this cylindrical jacket with a very narrow slit along its axis. An additional copper radiation shield concentric with the main vacuum chamber of the DR was also used to minimize the radiation effects. This radiation shield was anchored to the still chamber of the DR.

The superconducting magnet used in the present work was designed (by Oxford Instruments) to give a maximum value of 70 kG at its centre at a rate of 1.38 kG/Amp. Three, (1-ohm, 10 Watt), resistors across the magnet terminals were used to protect the magnet against quenching. Figure 3.2 shows the calculated field variation with distance along the axis from the centre of the coil. Experimental points provided by the manufacturer for the profile are also shown on the same figure. The figure shows that the deviation in the strength of the field at a distance of about 1cm from the centre is less than 1.5%. The samples were located as much as possible at the centre of the superconducting coil.

3.3 Dilution Refrigerator and Thermometry:

Measurements were carried out in a ^{3}He - ^{4}He dilution refrigerator (DR). A full description of the DR is given in many low temperature technique books (see, for example, Lounasmaa 1974). In brief, the principles of operation of ^{3}He - ^{4}He dilution refrigerator are as follows. Firstly, the system is pre-cooled down to the nitrogen temperature (77 K) and then down to the ^{4}He temperature (4.2 K). The ^{4}He pot is pumped till its temperature reaches 1.2 K. As the ^{3}He - ^{4}He mixture is introduced to the dilution unit it liquifies in the mixing chamber. When the condensation is complete, the mixture is cooled further by continuous pumping on the still chamber and hence ^{3}He-^{4}He mixture until at 0.8 K the mixture separates into a ^{3}He-rich phase floating on the top of a ^{4}He-rich phase. Cooling now occurs because the ^{4}He-rich phase has superfluid properties and the ^{3}He atoms dissolved in it behave as a Fermi gas and can move freely through it. ^{3}He atoms

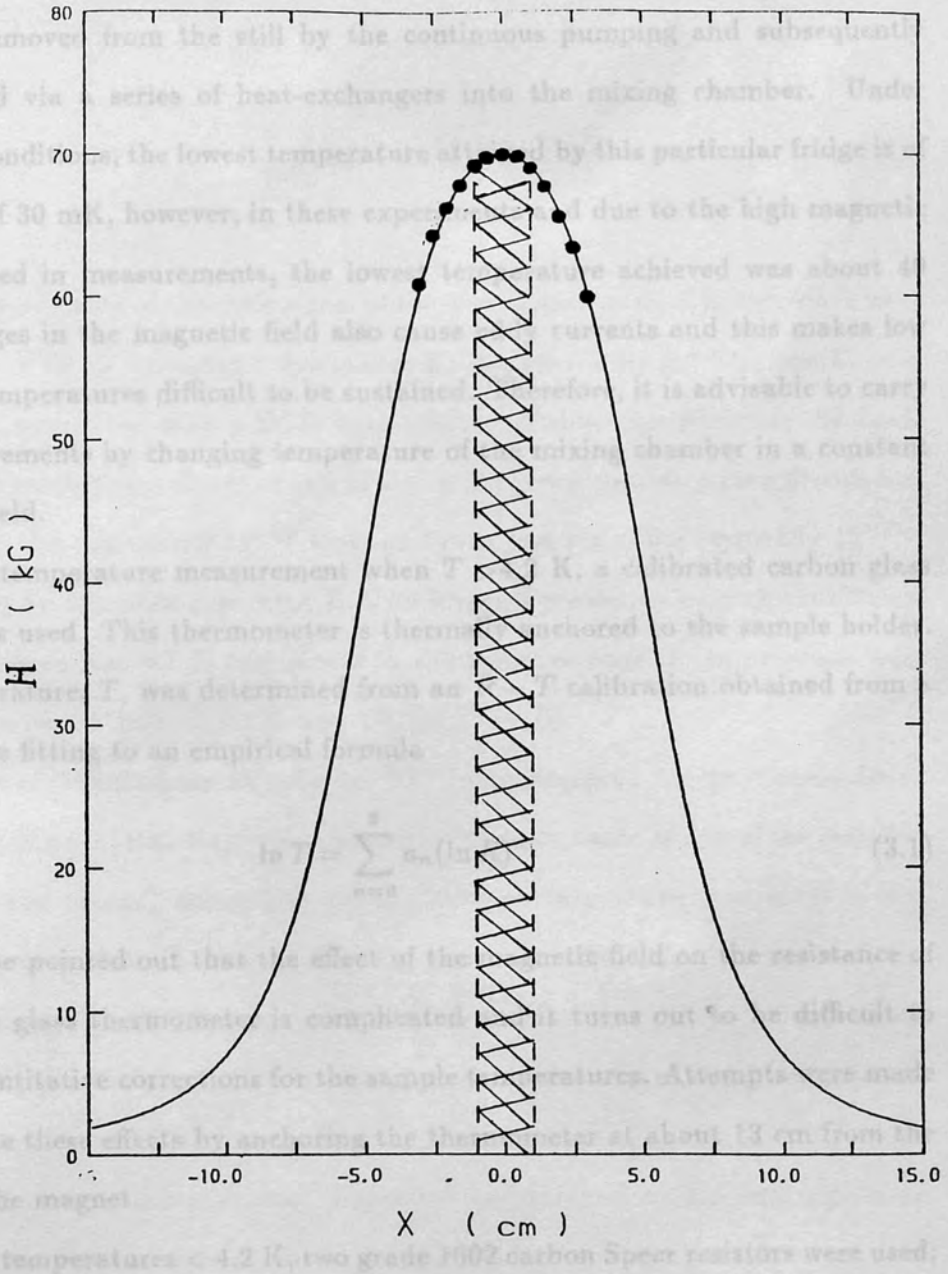

Figure 3.2

The variation of the magnetic field with the distance along the axis of the 70 kG superconducting magnet. The solid line is the calculation from the formula that relates H and I for a solenoid. The circles are the experimental points provided by the manufacturer.

therefore evaporate across the phase boundary thus cooling the mixture. They are then removed from the still by the continuous pumping and subsequently recondensed via a series of heat-exchangers into the mixing chamber. Under optimum conditions, the lowest temperature attained by this particular fridge is of the order of 30 mK, however, in these experiments and due to the high magnetic field involved in measurements, the lowest temperature achieved was about 40 mK. Changes in the magnetic field also cause eddy currents and this makes low constant temperatures difficult to be sustained. Therefore, it is advisable to carry out measurements by changing temperature of the mixing chamber in a constant magnetic field.

For temperature measurement when T >4.2 K, a calibrated carbon glass resistor was used. This thermometer is thermally anchored to the sample holder. The temperature, T, was determined from an $R-T$ calibration obtained from a least-square fitting to an empirical formula

$$\ln T = \sum_{n=0}^{9} a_n (\ln R)^n \tag{3.1}$$

It should be pointed out that the effect of the magnetic field on the resistance of the carbon glass thermometer is complicated and it turns out to be difficult to obtain quantitative corrections for the sample temperatures. Attempts were made to minimize these effects by anchoring the thermometer at about 13 cm from the centre of the magnet.

For temperatures < 4.2 K, two grade 1002 carbon Speer resistors were used; R8 (470Ω,1/2 Watt) and R4 (100Ω,1/2 Watt), above and below 1 K respectively, both thermally anchored to the sample holder at about 13 cm away from the centre of the magnet where the magnetic field strength is very small (less than 2 kG if the maximum field is 70 kG at the centre of the coil). R8 was calibrated against a carbon glass (628) resistor and checked against the saturated vapour pressure of ^{4}He. The resistor R4 had been calibrated against a CMN magnetic susceptibility, ^{60}Co-nuclear-orientation, Superconducting Reference Material (SRM)767 unit and calibrated Ge-thermometer. The calibration curves R(T) for R8 and R4 are shown

in Figures 3.3 and 3.4; the curves are a least-square fit of the calibration points to the formula

$$\frac{1}{T} = aR + b\sqrt{R} + c \tag{3.2}$$

Measurements of the resistances of the thermometers used in this work were made by an AVS-45 Automatic Resistance Bridge (made by R4-Electronikka Oy of Finland), and fitted with a BCD data transfer option. To minimize the Joule heating, the excitation voltage of the bridge was chosen so that power dissipation in the sensor did not exceed 10^{-10} Watt and even less than that (typically 10^{-12} - 10^{-16} Watt) for temperatures <0.1 K. The bridge's resolution over the resistance range of interest was 0.1 Ω and errors in the measurement of temperature were estimated to be 1.5% for T <1 K and 1% for T >1 K.

An a.c. Wheatstone Cryobridge S72 (manufactured by the Czechoslovak Academy of Science) was employed to monitor the resistance of one of the resistors on the sample holder, depending on the temperature range and gives a d.c. output voltage which, in turn, is directly related to the difference between the required temperature of the sample holder determined by the resistance set on the cryobridge, and its actual temperature. The error signal was introduced as an input to an Oxford Instruments Digital Temperature Controller (DTC2) which has the capability of proportional, derivative and integral action and regulating the voltage applied to a heater on the sample holder.

3.4 Electrical Measurements:

3.4.1 Direct Current Measurements:

For the d.c. resistivity and Hall coefficient measurements of the n-InP samples a conventional four-terminal d.c. electrical method was used. A typical circuit diagram is shown in Figure 3.5. High quality Elma rotary switches were used in this circuit. The different components of the circuit were enclosed in a metal box so that the pick-up problems can be reduced. The required resistivity

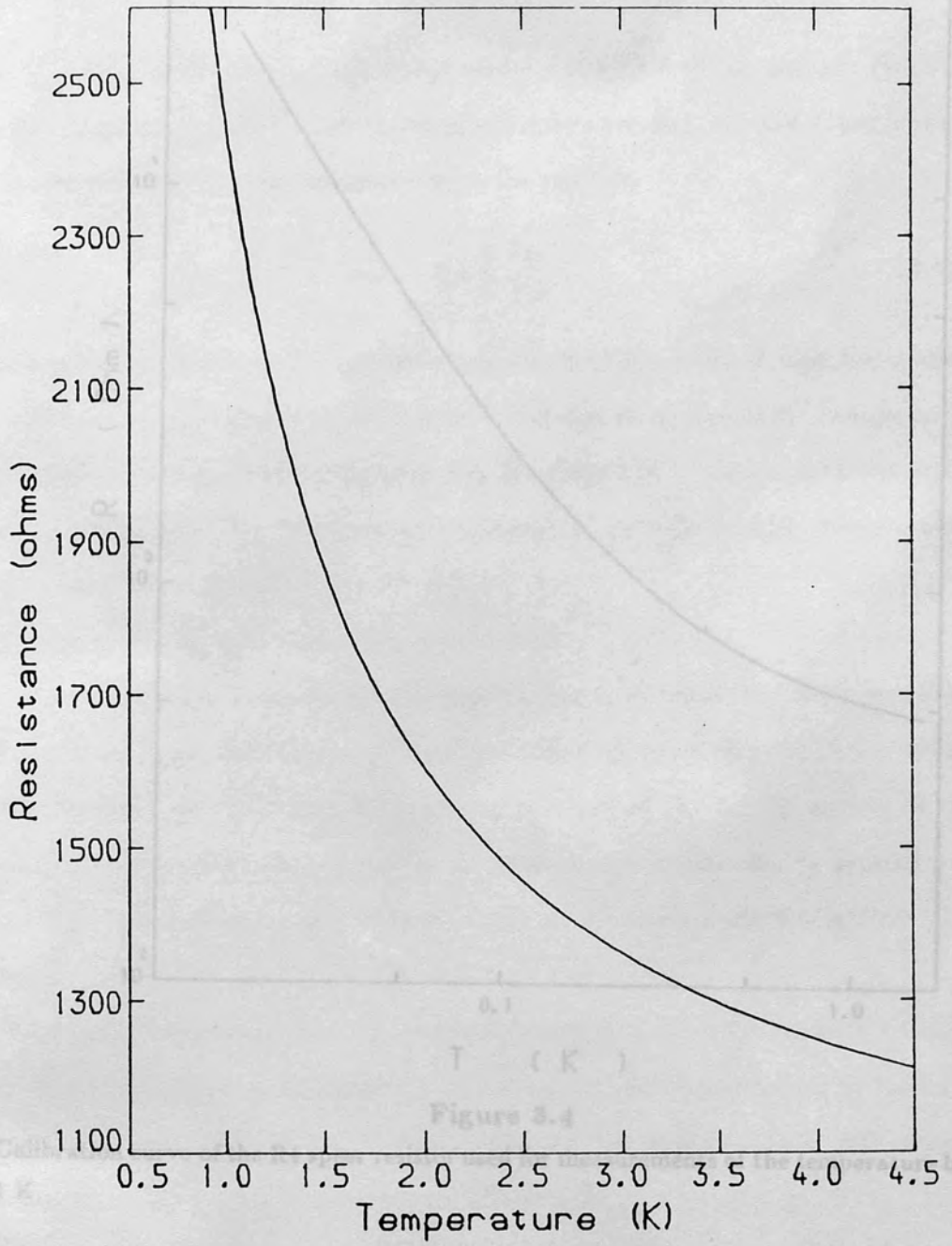

Figure 3.3

Calibration curve of the R8 speer resistor used for measurements of the temperatures 5 K$\gtrsim$ $T$$\gtrsim$1 K.

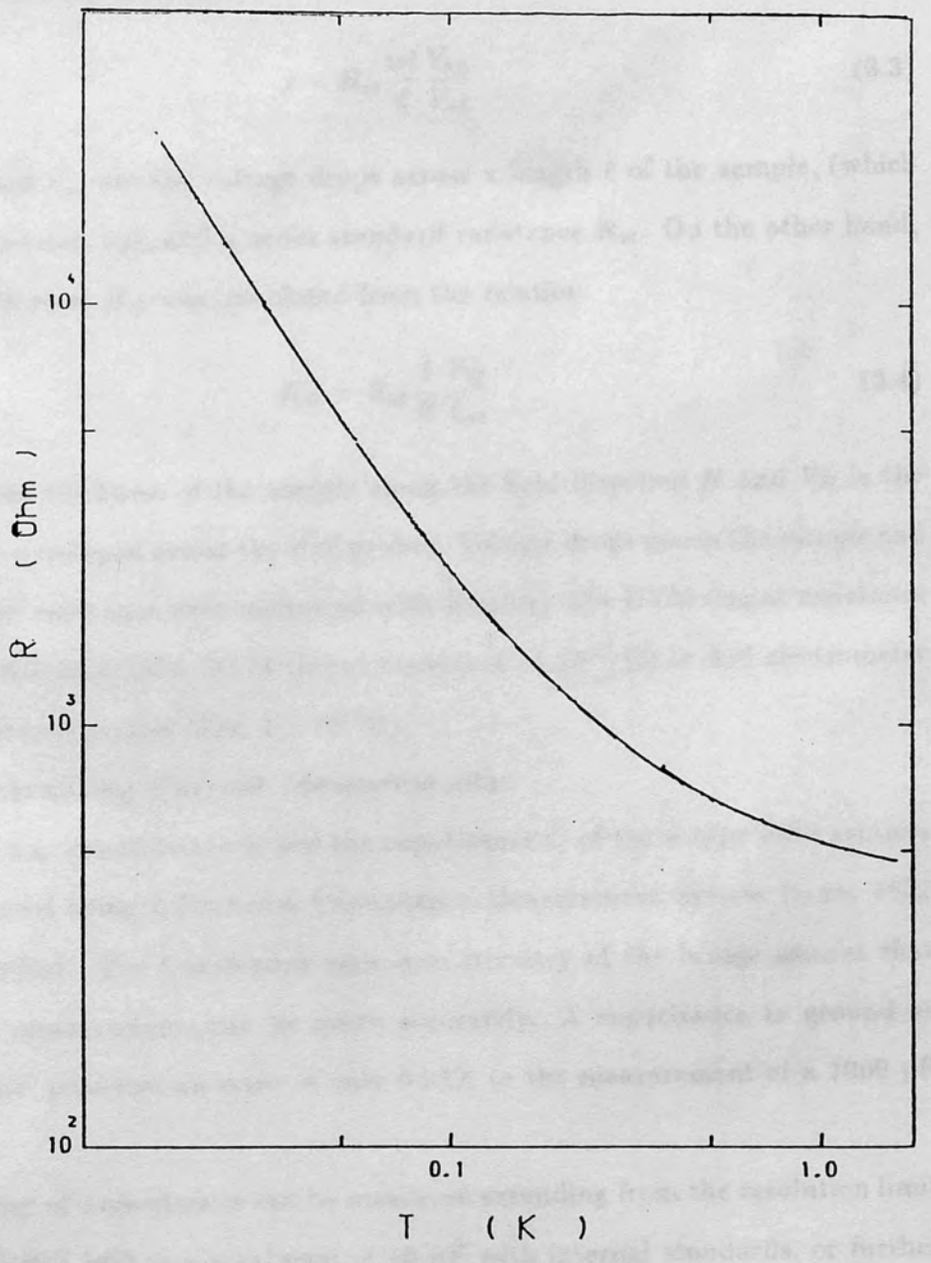

Figure 3.4

Calibration curve of the R4 speer resistor used for measurements of the temperature below 1 K.

was calculated from the formula

$$\rho = R_{st} \frac{wt}{\ell} \frac{V_{sp}}{V_{st}} \tag{3.3}$$

where V_{sp} and V_{st} are the voltage drops across a length ℓ of the sample, (which has a cross section wt), and a series standard resistance R_{st}. On the other hand, the Hall coefficient R_H was calculated from the relation

$$R_H = R_{st} \frac{t}{H} \frac{V_H}{V_{st}} \tag{3.4}$$

where t is the thickness of the sample along the field direction H and V_H is the Hall voltage developed across the Hall probes. Voltage drops across the sample and the standard resistance were measured with Keithley 174 DVM (input resistance of 10^9 Ω), Keithley 195A DVM (input resistance of 10^{11} Ω) or 616 electrometer (input resistance greater than $2 \times 10^{14} \Omega$).

3.4.2 Alternating Current Measurements:

The a.c. conductance G and the capacitance C of the n-type InSb samples were measured using a Precision Capacitance-Measurement System (type; 1621 General Radio). The transformer-ratio-arm circuitry of the bridge assures that 3-terminal measurements can be made accurately. A capacitance to ground as high as 1 μF produces an error of only 0.03% in the measurement of a 1000 pF capacitor.

A wide range of capacitances can be measured extending from the resolution limit of 0.1 aF (10^{-7} pF) to a maximum of 10 μF with internal standards, or further with external standards. The conductance also can be measured in a wide range extending from 0:1 f mho to a maximum of 1 m mho, a range of 1 to 10^{13}.

The 1621 Precision Capacitance-Measurement System consists of 1616 Precision Capacitance Bridge, 1316 Oscillator and 1238 Detector. The BCD outputs of the bridge were employed for automatic data processing via a "Universal G.P.I.B. Interface" unit (made by Mr. A.K. Betts in the department electronic workshop). The output measuring voltage of the bridge was measured by a Precision 9503 Lock-in-Amplifier and the signal was kept as low as possible

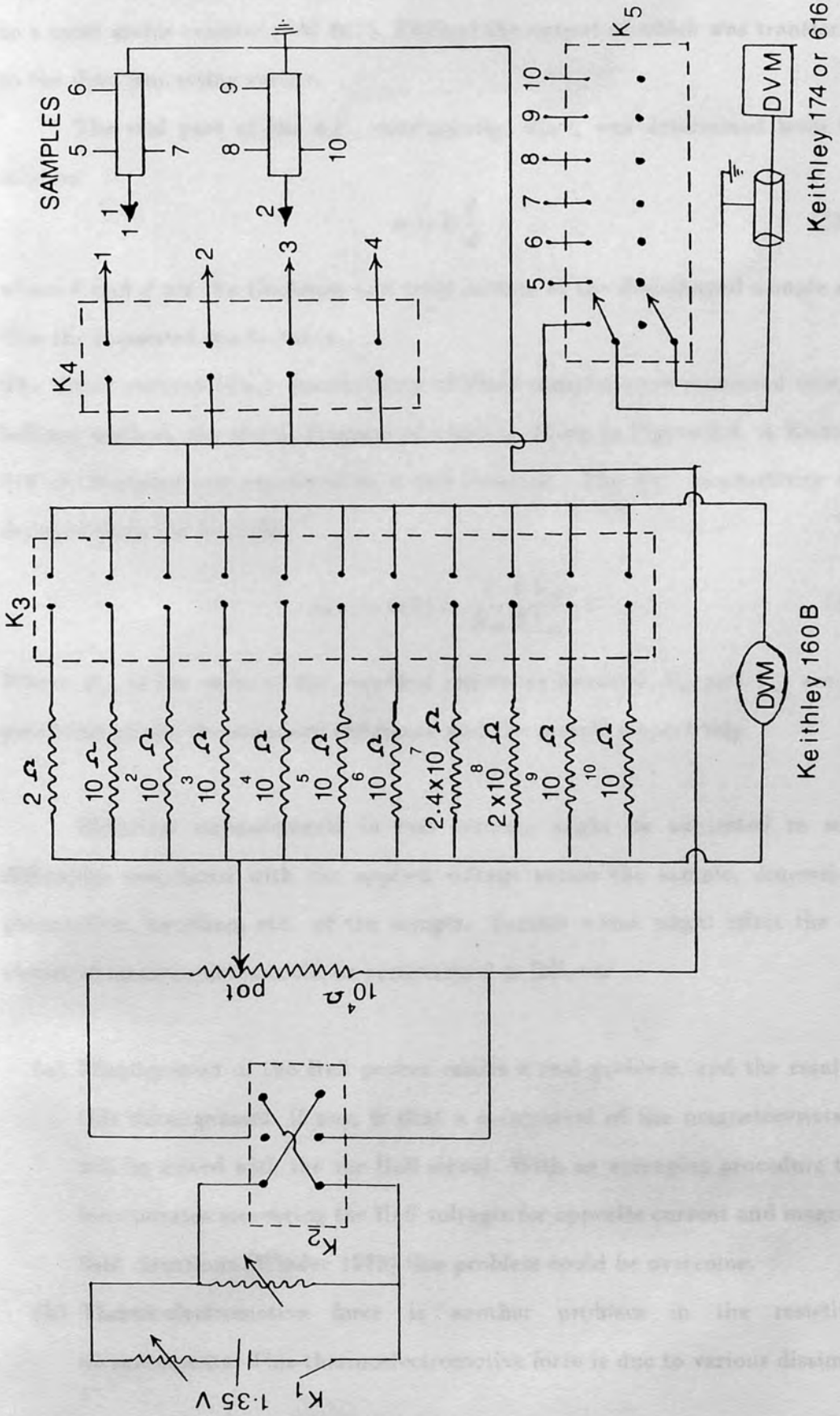

Figure 3.5
The circuit diagram used for the d.c. electrical measurements of the n-type InP samples.

to ensure that the resistance of the samples stays in the ohmic region. With the help of the synchronizing circuit, the 1316 Oscillator was conveniently connected to a more stable counter (PM 6615, Philips) the output of which was transferred to the data processing system.

The real part of the a.c. conductivity, $\sigma(\omega)$, was determined from the relation

$$\sigma = G\frac{\ell}{d} \tag{3.5}$$

where ℓ and d are the thickness and cross section of the disc-shaped sample and G is the measured conductance.

The direct current (d.c.) conductivity of these samples were measured using a balance method, the circuit diagram of which is shown in Figure 3.6. A Keithley 616 electrometer was employed as a null detector. The d.c. conductivity was deduced from the formula

$$\sigma_{d.c.} = \sigma(0) = \frac{1}{R_{st}}\frac{\ell}{d}\frac{V_{st}}{V_{sp}} \tag{3.6}$$

Where R_{st} is the value of the standard resistance involved, V_{st} and V_{sp} are the potentials across the standard resistance and the sample respectively.

Electrical measurements in real systems might be subjected to some difficulties associated with the applied voltage across the sample, dimensions, preparation, handling, etc. of the sample. Factors which might affect the d.c. electrical measurements could be summarised as follows:

(a) Misalignment of the Hall probes causes a real problem, and the result of this misalignment, if any, is that a component of the magnetoresistance will be mixed with the the Hall signal. With an averaging procedure that incorporates measuring the Hall voltages for opposite current and magnetic field directions (Wieder 1979) this problem could be overcome.

(b) Thermoelectromotive force is another problem in the resistivity measurements. This thermoelectromotive force is due to various dissimilar

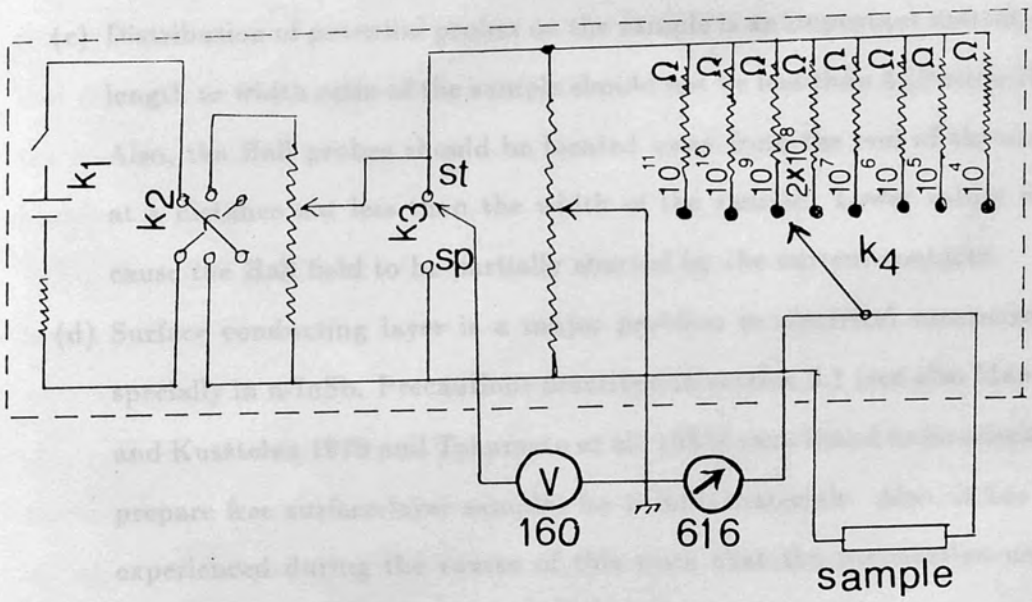

Figure 3.6

The circuit diagram of the balance bridge used for the d.c. resistivity of the n-InSb disc-shaped samples.

metals which connects the sample holder up through the DR. It can be eliminated if one reverses the current through the sample and the standard resistance so that the average values of the potential drops can be obtained.

(c) Distribution of potential probes on the sample is an important matter. The length to width ratio of the sample should not be less than 4 (Putley 1968). Also, the Hall probes should be located away from the end of the sample at a distance not less than the width of the sample. Lower values would cause the Hall field to be partially shorted by the current contacts.

(d) Surface conducting layer is a major problem in electrical measurements specially in n-InSb. Precautions described in section 3.1 (see also Mansfield and Kusztelan 1978 and Tokumoto et al. 1982) were found to be adequate to prepare free surface-layer samples for n-InSb materials. Also, it has been experienced during the course of this work that the preparation method described in section 3.1 is appropriate for n-InP samples.

(e) Non-ohmic and self-heating effects are also problems particularly at low temperatures. However, by applying very low voltages and varying the current passing through the sample one can minimise and check whether they cause a significant effect on the measurements.

(f) In a.c. measurements the stray capacitance is another problem. By making use of the three-terminal measurements, and using coaxial cables, this stray capacitance can be minimised.

3.5 Data Acquisition:

Data were recorded by a Hewlett-Packard HP9816 microcomputer. Figure 3.7 shows the schematic diagram of such data acquisition system. A disc drive as well as dot-matrix printer were interfaced to the microcomputer using the Hewlett-Packard General Purpose Interface Bus (HPIB). The Keithley 174 DVM was connected to the HP9816 through a BCD interface, while the Keithley 195A was interfaced via HPIB (IEEE).

The other devices involved in measurements with interface other than HPIB

compatible, were connected to the HP9816 through two interface boxes, designated AKB1 and AKB2, (designed and built in the department of Physics workshop). The interfacing box coded AKB1 was acting as an interface between the HP9816 microcomputer and both the General Radio 1616 Precision Capacitance Bridge and the AVS-45 Resistance Bridge. This box converts the BCD representation of the data into IEEE format which, consequently, is sent to the microcomputer for processing.

The Philips PM6615 frequency counter was interfaced to the HP9816 via box AKB2 which translates the BCD data into IEEE format to be sent to the microcomputer.

Now, the HP9816 was employed to record the resistance of the thermometers, the real and the imaginary parts of the conductance, the frequency of the AC measurements, and the voltages across the samples and the standard resistances for DC measurements. From these data, the temperature, real and imaginary parts of the a.c. conductivity as well as the DC conductivity were calculated and displayed graphically by the microcomputer. Data, also, were stored on a disc for later transfer to the main VAX computer system for further processings and investigations.

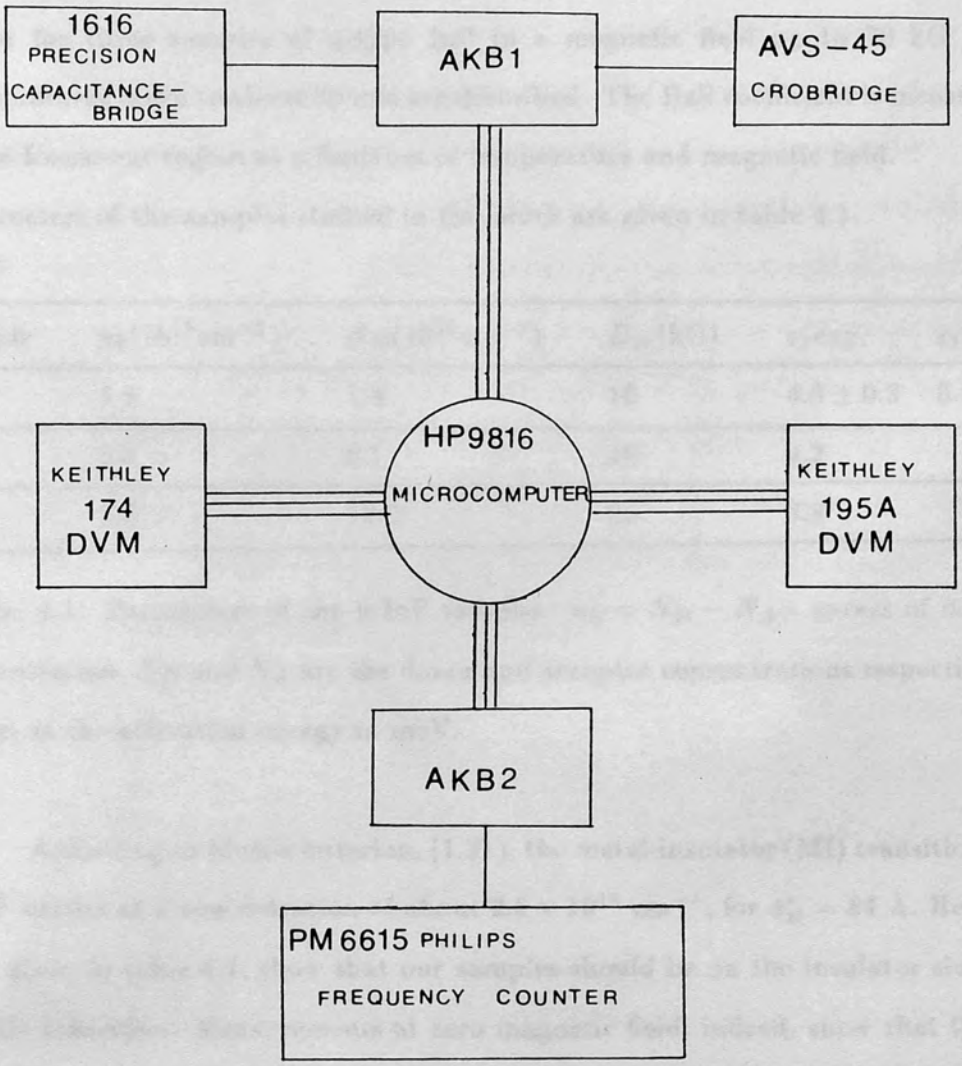

Figure 3.7

A schematic diagram of the system used for data acquisition.

CHAPTER 4

DC Conduction In n-type InP

4.1 Introduction:

In the present chapter, measurements of the components of the resistivity tensor for three samples of n-type InP in a magnetic field up to 70 kG and temperatures down to about 80 mK are described. The Hall coefficient is measured in the freeze-out region as a function of temperature and magnetic field. Parameters of the samples studied in this work are given in table 4.1.

Sample	$n_0(10^{15}\text{cm}^{-3})$	$N_D(10^{15}\text{cm}^{-3})$	H_{cr}(kG)	$\varepsilon_1$exp.	$\varepsilon_1$thr.
I	4.8	7.4	16	4.6 ± 0.3	5.5
II	5.9	9.1	18	4.2	
III	7.8	12.0	22	3.8	

Table 4.1: Parameters of the n-InP samples. $n_0 = N_D - N_A$= excess of donor concentration, N_D and N_A are the donor and acceptor concentrations respectively and ε_1 is the activation energy in meV.

According to Mott's criterion, (1.21), the metal-insulator (MI) transition in n-InP occurs at a concentration of about 2.6×10^{16} cm^{-3}, for $a_B^* = 84$ Å. Hence, data given in table 4.1, show that our samples should be on the insulator side of the MI-transition. Measurements at zero magnetic field, indeed, show that these samples behave like an insulator as $T \rightarrow 0$.

At higher temperatures freeze-out of the electrons from the conduction band onto the donor sites occurs. In a magnetic field, similar behaviour is observed with an activation energy, ε_1, being a function of the field. In this region, the Hall coefficient increases sharply, reaches a maximum and then decreases, due to the advent of hopping conduction. The temperature and magnetic field dependence of the resistivity, activation energy and the Hall coefficient in this regime will be

discussed in section 4.2.

The freeze-out of conduction electrons with decreasing temperature is followed by a situation in which the main contribution to the conductivity is due to hopping of electrons between the impurity centres without being excited to the conduction band. In this process electron hops, or jumps, from an occupied donor to a nearest neighbour empty one due to compensation with an activation energy ε_3 which slightly increases with the field. The temperature and magnetic field dependences of the resistivity in the nearest-neighbour hopping region are discussed in section 4.3. Further reduction in the temperature leads to a situation in which electrons prefer to hop to more remote sites than to the nearest-neighbour ones, in order to reduce the energy required for the hop. In this range and in absence of the field, Mott's $T^{-1/4}$-law predicted for VRH seems to be followed. In presence of the magnetic field $T^{-3/4}$-law is obeyed which is in line with the $T^{-1/4}$-law. Section 4.4 considers the behaviour of the resistivity in this regime. In the whole range of temperature the resistivity in absence of the magnetic field can be described by the equation

$$\rho^{-1}(T) = \rho_1^{-1}\exp\left(-\frac{\varepsilon_1}{k_B T}\right) + \rho_3^{-1}\exp\left(-\frac{\varepsilon_3}{k_B T}\right) + \rho_0^{-1}\exp\left(-\frac{T_0}{T}\right)^{1/4} \qquad (4.1)$$

The first term corresponds to the band conduction, where the conductivity is due to electrons in the conduction band, and is dominant above about 5 K and mainly determined by the freeze-out of electrons (sect.4.2). The second term is attributed to the hopping process in the nearest-neighbour hopping region and becomes dominant for temperatures below 5 K (section 4.3). The third term is due to the variable range hopping (VRH) and is dominant below 1.5 K (section 4.4).

Measurements in this work were made, mainly, by varying the temperature while the magnetic field is kept constant. This method has the advantage of avoiding heating effects caused by changing the magnetic field.

4.2 Temperature and magnetic field dependence of the resistivity and Hall Coefficient in the freeze-out region:

In n-type InP, freeze-out of carriers can be observed in absence of magnetic field provided that the isolation condition (1.1) is satisfied. Figures 4.1-4.3 display the temperature and magnetic field dependences of the transverse resistivity for the samples I, II and III respectively. Data presented here are restricted to temperatures above 1 K. In the temperature range down to about 5 K a sharp increase in the resistivity is observed.

As the electrons freeze out off the conduction band, one would expect the conductivity to decrease sharply with the reduction of the temperature. The temperature dependence of the carrier concentration in this region is given by (Blakemore 1974)

$$\frac{n(N_A+n)}{N_D-N_A-n}=\frac{N_c}{2}\exp\left(-\frac{E_D}{k_BT}\right) \tag{4.2}$$

where n is the concentration of free electrons in the conduction band, N_D and N_A are the donor and acceptor concentrations respectively.

$$N_c=4.83\times10^{15}\left(\frac{m^*}{m_0}T\right)^{3/2}cm^{-3}=1.05\times10^{14}T^{3/2}cm^{-3} \tag{4.3}$$

for n-InP. The temperature dependence of the concentration of the carriers in the conduction band, indeed, depends on the relation between the number of empty donors due to compensation, ($KN_D = N_A$), and the number of empty positions $n(T)$ due to thermal excitation of electrons from donor levels to the conduction band. Thus. equation (4.2) takes two limiting forms:

(a) $N_A \ll n(T)$, i.e., the number of empty donors is much less than $n(T)$. In this case equation (4.2) reduces to the form

$$n(T)=\left(\frac{N_DN_c}{2}\right)^{1/2}\exp\left[-\frac{E_D}{2k_BT}\right] \tag{4.4}$$

This dependence holds in an intermediate temperature range, i.e., $KN_D \ll n(T) \ll N_D$. Apparently, its validity requires low enough compensation ratio which is not the case of our samples.

(b) $N_A \gg n(T)$. In this case the Fermi level is close to the isolated-donor level

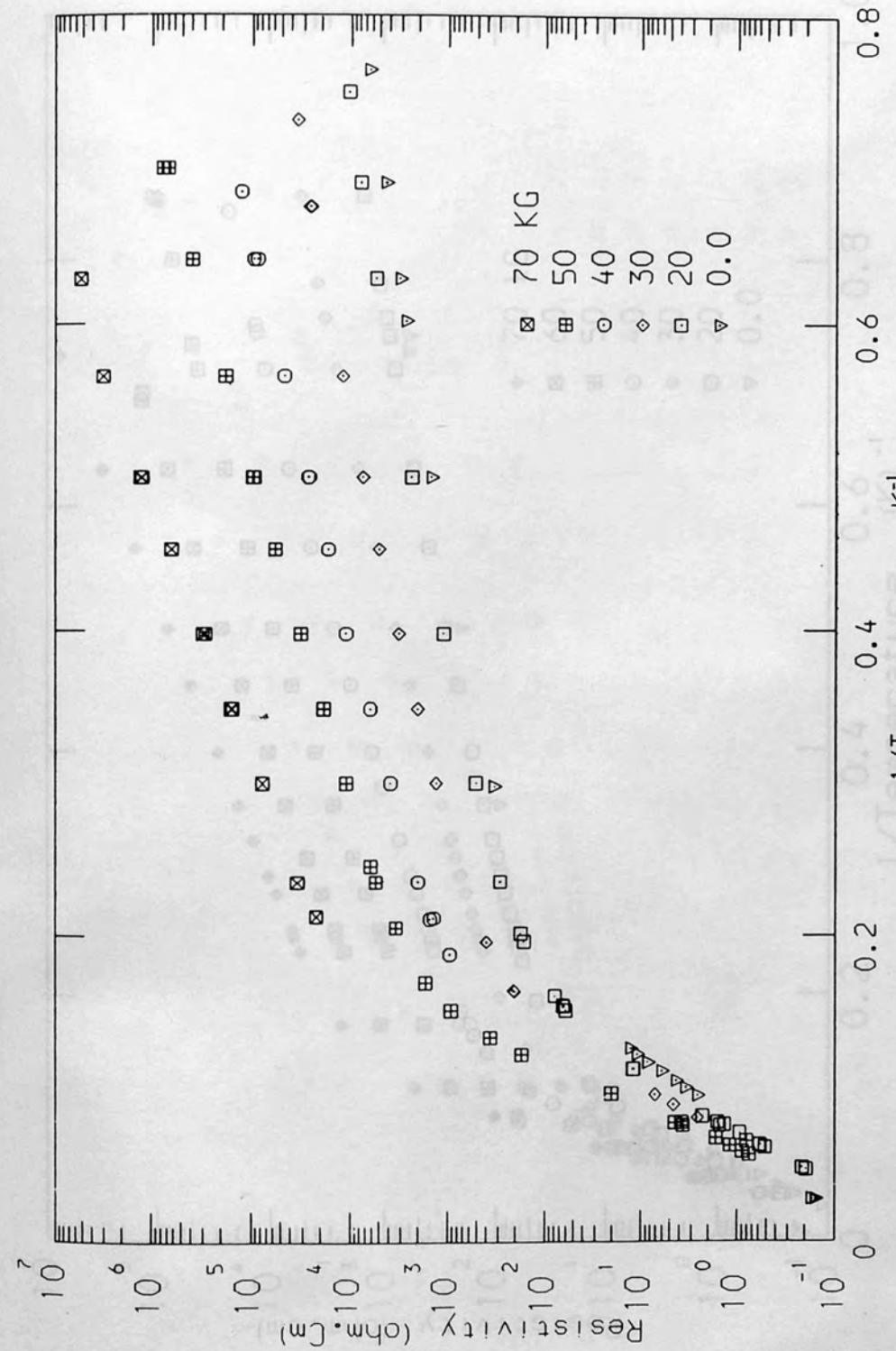

Figure 4.1

Transverse resistivity of sample I as a function of T^{-1} in the freeze-out and nearest-neighbour hopping regions.

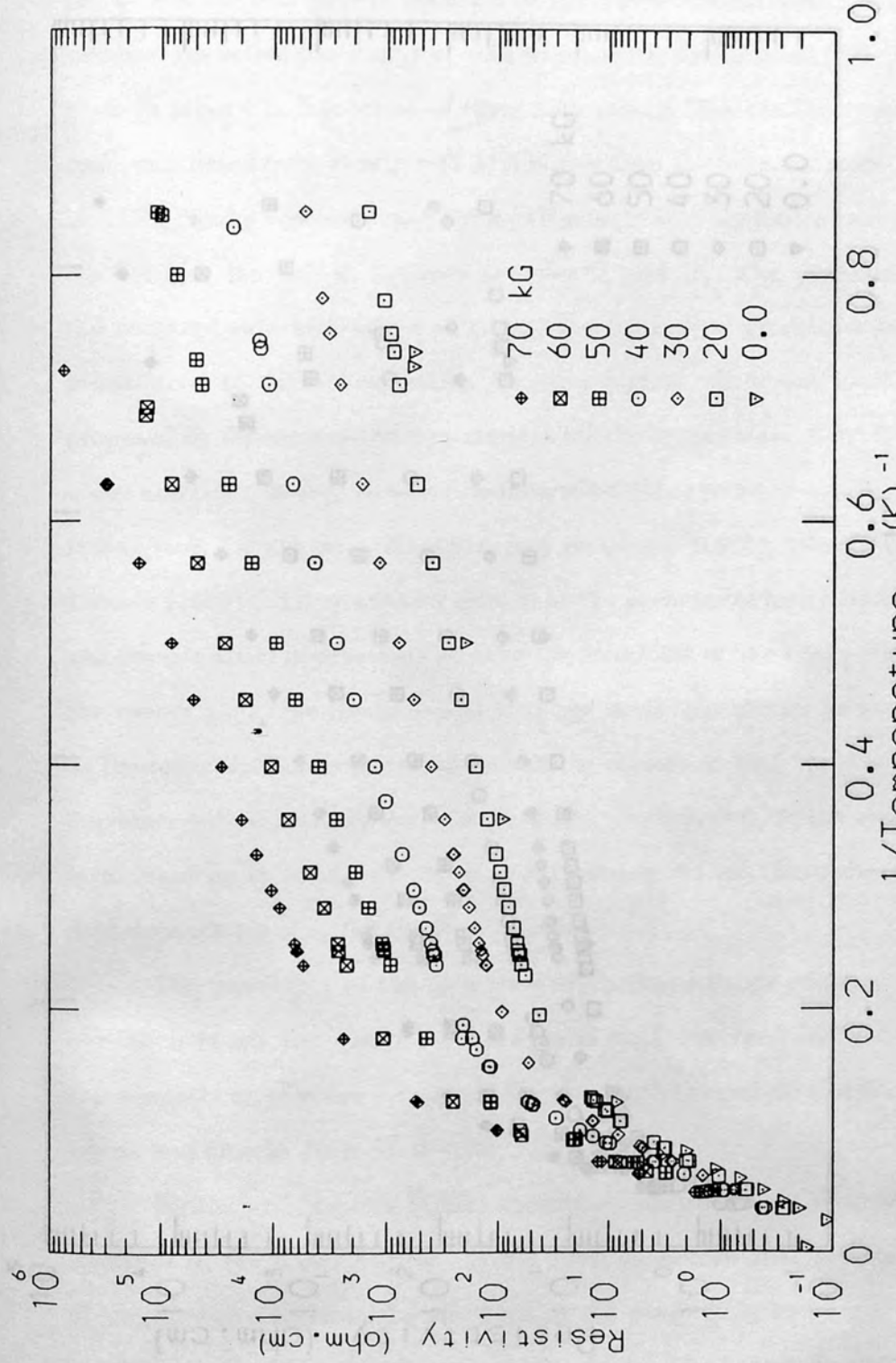

Figure 4.2

Transverse resistivity of sample II as a function of T^{-1} in the freeze-out and nearest-neighbour hopping regions.

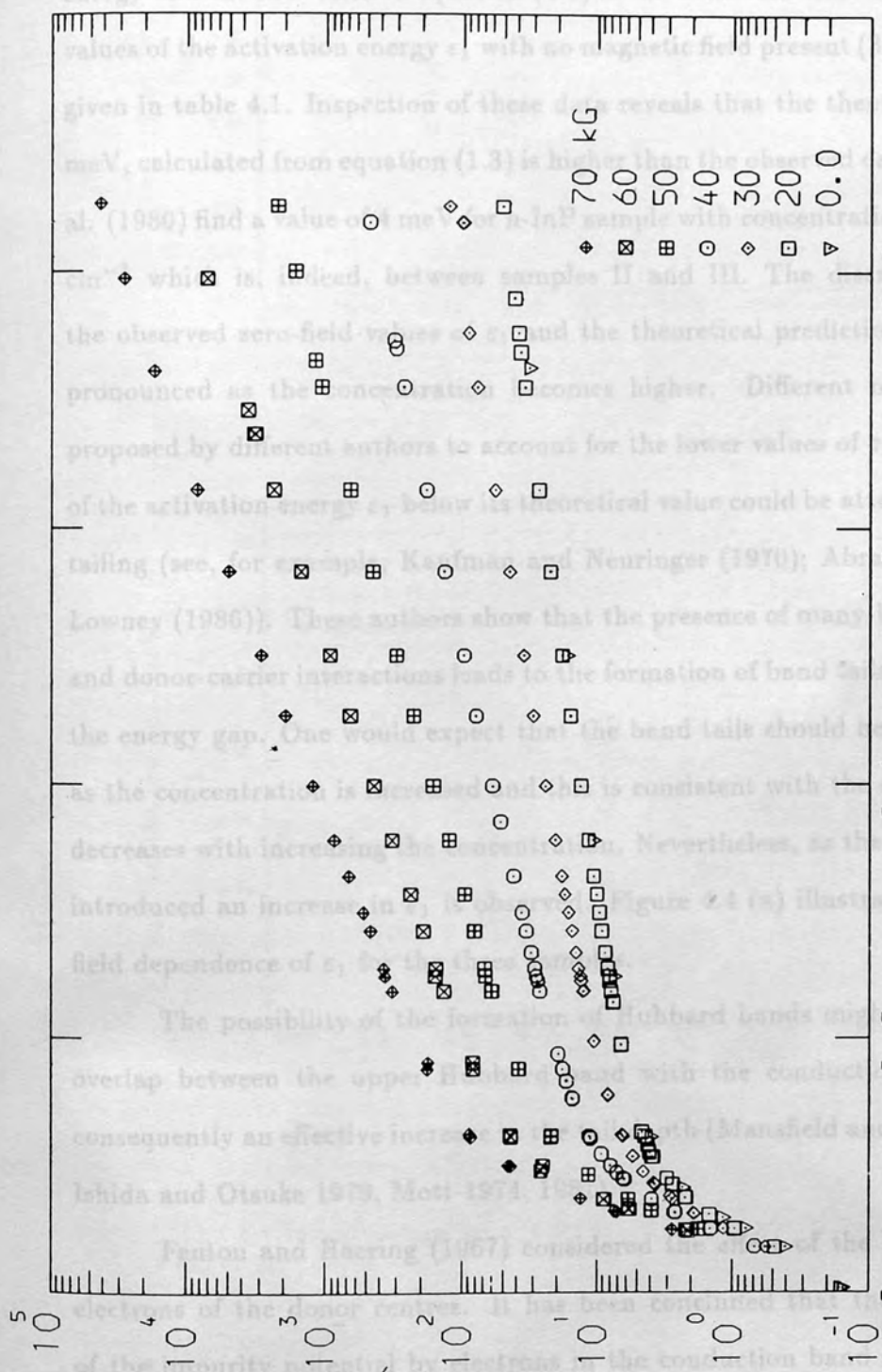

Figure 4.3 Transverse resistivity of sample III as a function of T^{-1} in the freeze-out and nearest-neighbour hopping regions.

and one would have

$$n(T) = \frac{N_c(N_D - N_A)}{2N_A} \exp\left(-\frac{E_D}{k_B T}\right) \tag{4.5}$$

Analyses of the experimental data of the resistivity in the freeze-out region showed that the temperature dependence of the resistivity has only one activation energy and the first term in equation (4.1) is the dominant one. The experimental values of the activation energy ε_1 with no magnetic field present (3.8 - 4.6 meV) are given in table 4.1. Inspection of these data reveals that the theoretical value, 5.5 meV, calculated from equation (1.3) is higher than the observed ones. Biskupski et al. (1980) find a value of 4 meV for n-InP sample with concentration $n = 6.6 \times 10^{15}$ cm^{-3} which is, indeed, between samples II and III. The discrepancy between the observed zero-field values of ε_1 and the theoretical prediction becomes more pronounced as the concentration becomes higher. Different mechanisms were proposed by different authors to account for the lower values of ε_1. The reduction of the activation energy ε_1 below its theoretical value could be attributed to a band tailing (see, for example, Kaufman and Neuringer (1970); Abram et al. (1984); Lowney (1986)). These authors show that the presence of many-body interactions and donor-carrier interactions leads to the formation of band tails which decreases the energy gap. One would expect that the band tails should be more important as the concentration is increased and this is consistent with the observation as ε_1 decreases with increasing the concentration. Nevertheless, as the magnetic field is introduced an increase in ε_1 is observed. Figure 4.4 (a) illustrates the magnetic field dependence of ε_1 for the three samples.

The possibility of the formation of Hubbard bands might also lead to an overlap between the upper Hubbard band with the conduction band tail and consequently an effective increase in the tail depth (Mansfield and Kusztelan 1978, Ishida and Otsuka 1979, Mott 1974, 1981).

Fenton and Haering (1967) considered the effect of the screening by free electrons of the donor centres. It has been concluded that the screening effect of the impurity potential by electrons in the conduction band might reduce the binding energy. This screening effect, thus, is opposite to the effect of the magnetic

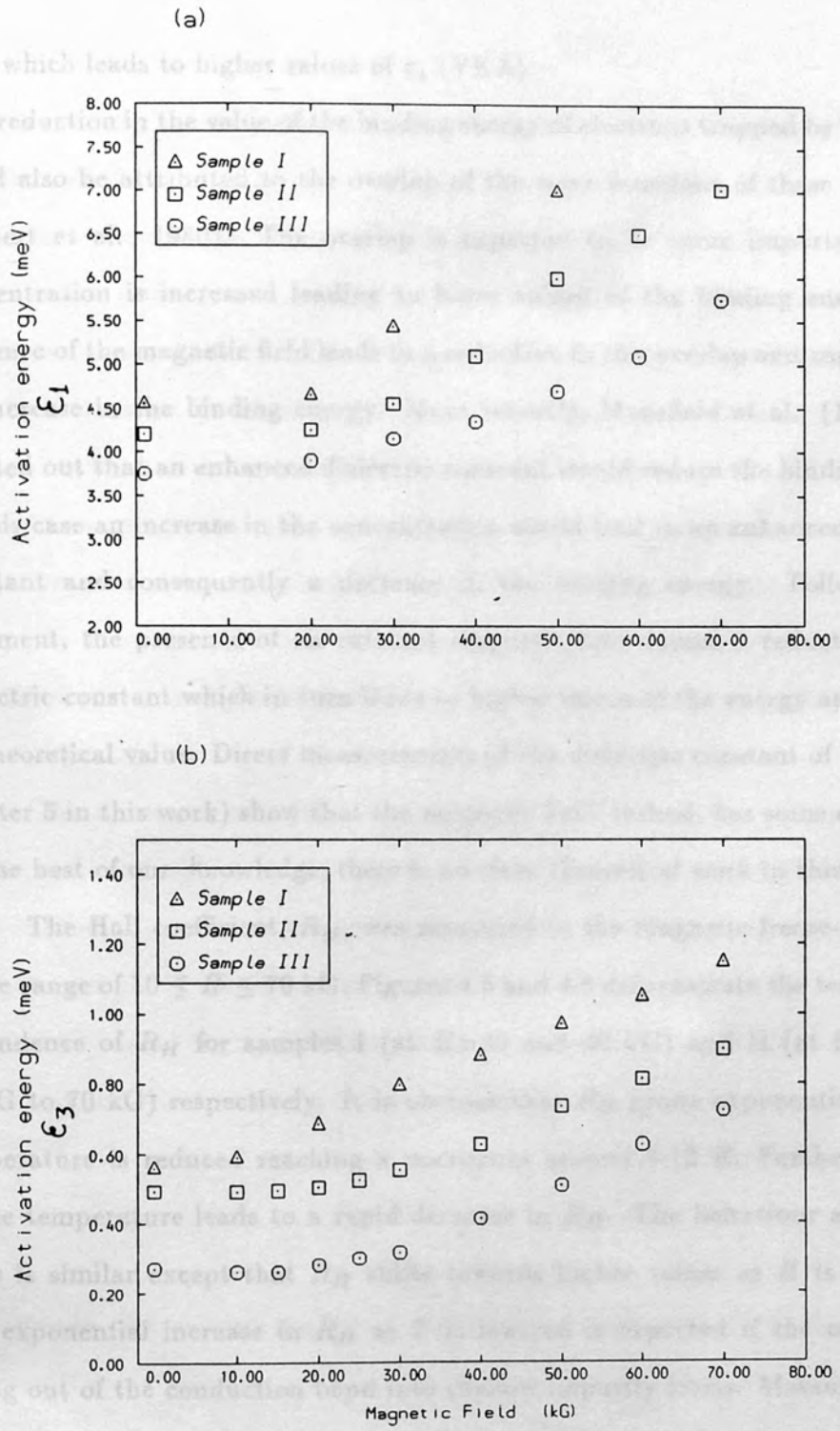

Figure 4.4

The activation energy as a function of the magnetic field;
(a) ε_1 and (b) ε_3.

field which leads to higher values of ε_1 (YKA).

The reduction in the value of the binding energy of electrons trapped by impurities could also be attributed to the overlap of the wave functions of these impurities (Robert et al. 1980). The overlap is expected to be more important as the concentration is increased leading to lower values of the binding energy. The presence of the magnetic field leads to a reduction in this overlap and consequently an increase in the binding energy. More recently, Mansfield et al. (1988) have pointed out that an enhanced dielectric constant would reduce the binding energy. In this case an increase in the concentration would lead to an enhanced dielectric constant and consequently a decrease in the binding energy. Following this argument, the presence of an external magnetic field causes a reduction in the dielectric constant which in turn leads to higher values of the energy approaching its theoretical value. Direct measurements of the dielectric constant of n-InSb (in chapter 5 in this work) show that the magnetic field, indeed, has some effect on ϵ. To the best of our knowledge, there is no clear theoretical work in this respect.

The Hall coefficient, R_H, was measured in the magnetic freeze-out region in the range of $10 \leq H \leq 70$ kG. Figures 4.5 and 4.6 demonstrate the temperature dependence of R_H for samples I (at H=20 and 40 kG) and II (at fields from 10 kG to 70 kG) respectively. It is obvious that R_H grows exponentially as the temperature is reduced reaching a maximum around 8-12 K. Further decrease in the temperature leads to a rapid decrease in R_H. The behaviour at different fields is similar except that R_H shifts towards higher values as H is increased. The exponential increase in R_H as T is lowered is expected if the carriers are falling out of the conduction band into shallow impurity levels. Measurements of the resistivity in this temperature range, indeed, confirm this argument where a freeze-out of electrons is observed. However, the Hall coefficient, R_H, does not continue to increase as the temperature is further reduced, but passes through a maximum followed by a decrease as the temperature is reduced. This behaviour could be due to :

(a) A surface conducting layer which short out the bulk conduction as can occur

in n-InSb at low temperatures,

(b) Conduction in an impurity band produced by strong overlap of the wave functions of the donors, or

(c) Onset of hopping conduction.

In the present work, careful precautions were taken during the preparation of the samples to avoid surface contamination. Re-treatment of sample I with new Hall leads yields similar behaviour. Therefore the formation of a surface conducting layer is unlikely. On the other hand, the variation of $\rho(T)$ in the same temperature range shows the advent of the activated hopping with a constant activation energy, ε_3, (see Section 4.3). Thus, the formation of an impurity band leading to a metallic-like behaviour can be excluded. One, then, might conclude that the decrease in R_H as temperature is lowered is related to the onset of hopping conduction.

The appearance of the bump in $R_H(T)$ can be explained with the help of the two-band model (Shklovskii and Efros 1984 (SE)) in which all electrons participating in electrical conduction are divided into two groups : conduction-band electrons with conductivity $\sigma_c = n(T)e\mu_c$ and Hall coefficient $R_c = 1/n(T)e$; and impurity band electrons with hopping conductivity σ_h and Hall coefficient R_h. Shklovskii and Efros (1984) give a phenomenological expression at zero magnetic field limit;

$$R_H = \frac{R_c\sigma_c^2 + R_h\sigma_h^2}{(\sigma_c + \sigma_h)^2} \tag{4.6}$$

This simple picture may explain the temperature dependence of R_H, with the hopping Hall mobility $\mu_h = R_h\sigma_h$ being much smaller than the band mobility $\mu_c = R_c\sigma_c$. Now, when the temperature is not very low, the second term in the numerator can be neglected with respect to the first one. Thus the formula predicts a sharp maximum at $\sigma_c \approx \sigma_h$, at which the conduction changes from band to hopping mechanism. At high temperatures, to the left of the maximum, $\sigma_c \gg \sigma_h$, thus

$$R_H = R_c = \frac{1}{n(t)e} \propto \exp\left[E_D/k_BT\right] \tag{4.7}$$

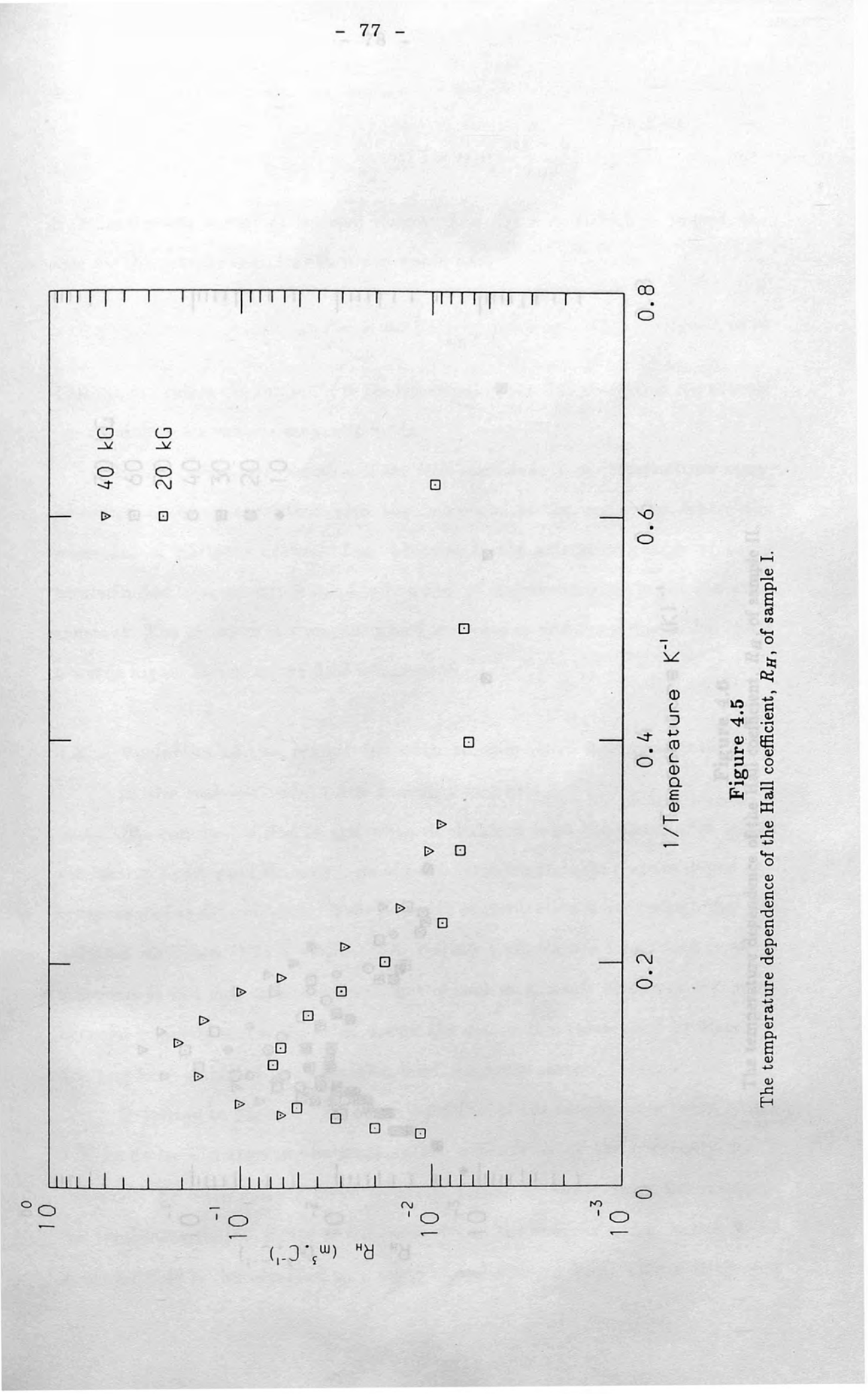

Figure 4.5

The temperature dependence of the Hall coefficient, R_H, of sample I.

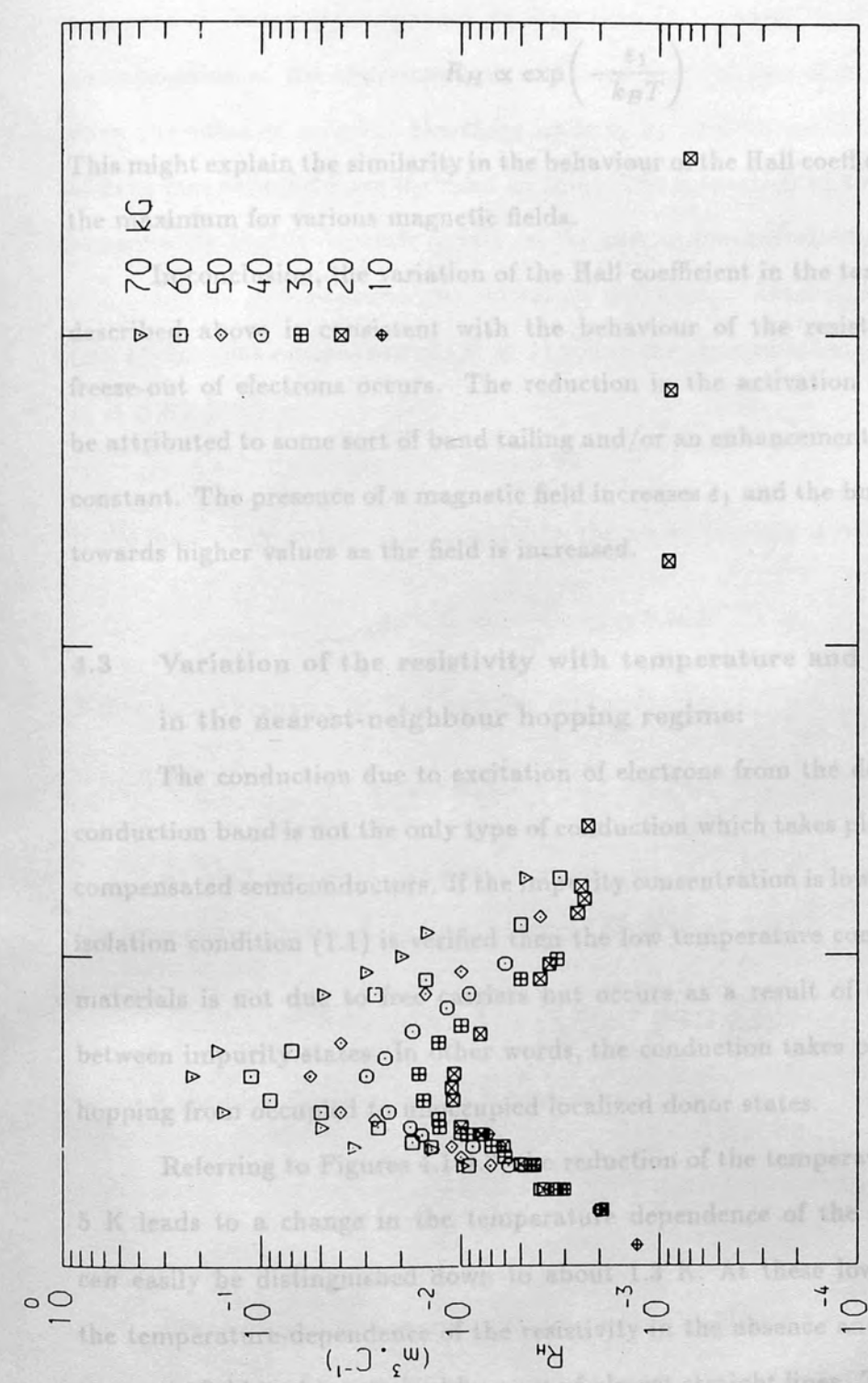

Figure 4.6
The temperature dependence of the Hall coefficient, R_H, of sample II.

At lower temperatures, $\sigma_c \ll \sigma_h$, hence

$$R_H = \frac{R_c \sigma_c^2}{\sigma_h^2} = \frac{\mu_c^2 e}{\sigma_h^2} n(T) \propto \exp\left(\frac{2\varepsilon_3 - E_D}{k_B T}\right) \tag{4.8}$$

If the activation energy ε_3 is small compared to $E_D \equiv \varepsilon_1$ (which is, indeed, the case for the present samples) then one would have

$$R_H \propto \exp\left(-\frac{\varepsilon_1}{k_B T}\right) \tag{4.9}$$

This might explain the similarity in the behaviour of the Hall coefficient R_H around the maximum for various magnetic fields.

In conclusion, the variation of the Hall coefficient in the temperature range described above is consistent with the behaviour of the resistivity where the freeze-out of electrons occurs. The reduction in the activation energy ε_1 could be attributed to some sort of band tailing and/or an enhancement in the dielectric constant. The presence of a magnetic field increases ε_1 and the bump in R_H shifts towards higher values as the field is increased.

4.3 Variation of the resistivity with temperature and magnetic field in the nearest-neighbour hopping regime:

The conduction due to excitation of electrons from the donor sites to the conduction band is not the only type of conduction which takes place in doped and compensated semiconductors. If the impurity concentration is low enough that the isolation condition (1.1) is verified then the low temperature conduction in these materials is not due to free carriers but occurs as a result of charge transport between impurity states. In other words, the conduction takes place by electrons hopping from occupied to unoccupied localized donor states.

Referring to Figures 4.1-4.3, the reduction of the temperature below about 5 K leads to a change in the temperature dependence of the resistivity which can easily be distinguished down to about 1.3 K. At these lower temperatures the temperature-dependence of the resistivity in the absence and presence of the magnetic field is characterised by a set of almost straight lines. This is attributed

to the fact that the conduction due to nearest-neighbour hopping dominates over the free electron conduction. The resistivity in this range obeys the activated-conduction law (1.7), (second term in equation (4.1)), which is typical of hopping conduction between impurities with a non-vanishing activation energy ε_3.

The experimental values of the activation energy ε_3 as well as the pre-exponential factor ρ_3 appeared in equation (4.1) were obtained as follows. Extrapolation of the experimentally obtained straight line of ln $\rho(T)$ to $1/T=0$ gives the value of ρ_3 while the slope leads to ε_3. Values calculated by this way at zero magnetic field are included in table 4.2. Inspection of these data reveals immediately that it depends clearly on the carrier concentration.

Let us now examine the activation energy ε_3. According to Efros et al. (1972), for weak compensation ($K \ll 1$) and in the absence of long-range potential, ε_3 is given by

$$\varepsilon_3 = 0.99\frac{e^2 N_D^{1/3}}{\epsilon} \tag{4.10}$$

If the long-range potential is considered, the above formula is replaced by

$$\varepsilon_3 = 0.99\frac{e^2 N_D^{1/3}}{\epsilon}(1 - 0.29K^{1/4}) \tag{4.11}$$

Miller and Abrahams derived another expression for ε_3,

$$\varepsilon_3 = 1.61\frac{e^2 N_D^{1/3}}{\epsilon}\left(1 - 1.35K^{1/3}\right) \tag{4.12}$$

At high degree of compensation, i.e., for $(1 - K) \ll 1$, and in absence of the long-range potential, ε_3 has the form (Efros et al. 1972);

$$\varepsilon_3 = \left(\frac{2\pi}{3}\right)\left(\frac{e^2 N_D^{1/3}}{\epsilon(1-K)^{1/3}}\right) \tag{4.13}$$

while if the long-range potential is considered;

$$\varepsilon_3 = C_1\frac{e^2 N_d^{1/3}}{\epsilon(1-K)^{1/3}} \tag{4.14}$$

where C_1 is a numerical constant of the order of unity.

The experimental values of ε_3 are plotted in Figure 4.7 (a) as a function of $N_D^{1/3}$. The dependence of ε_3 on the donor concentration deduced from equations

(4.11) and (4.14) at K = 0.2 and 0.6 respectively is also given in the same graph. (we have used C_1=0.6, Gadzhiev and Shlimak 1973). It is obvious that data do not fit any of these theoretical predictions. An exact comparison of the results with the theory is quite difficult. The reason is that the existing theories are applicable either for weak or strong compensation which is not the case of our samples. Another discrepancy is that, despite the theoretical predictions, ε_3 is actually found to decrease as the impurity concentration is increased.

Low values of ε_3 have been observed in many semiconductor materials. ε_3 does not vary with concentration as predicted from simple theory. Instead of increasing monotonically with increasing concentration, it has been found that ε_3 deviates from the theoretical prediction, exhibiting a peak at a concentration N_p (see for example Emelyanenko et al. 1974). At concentrations higher than N_p, ε_3 starts to decrease gradually with increasing concentration and falls below the value predicted from simple theory.

According to Shklovskii and Shlimak (1972) and Shklovskii and Efros (1984) as N_D increases, ε_3 deviates from the classical theoretical predictions showing a peak and then gradually decreases to zero as the nonmetal-metal transition is approached. These authors attributed this behaviour to the effect of enhanced overlap between the donor wave functions. The quantum interpretation of deviation from the classical prediction may be confirmed more spectacularly by applying an external agent such as uniaxial compression, magnetic field, etc. If the doping level is very low so that the overlap between the adjacent donors is extremely small then one would expect that ε_3 does not vary under the external agent. In this case the overlap plays no role even at zero external agent. This has been shown by Shklovskii and Shlimak (1972) by applying pressure. On the other hand, if the overlap is not negligible then it might be possible to reduce its effect by applying a uniaxial compression. The study of Shklovskii and Shlimak on Ge samples, also, shows that the application of a uniaxial compression leads to a strong enhancement in ε_3 and its value closely approaches the straight line predicted by the theoretical approach.

In a similar experiment by Averous et al. (1976) on p-GaSb they have shown that ε_3 increases with the pressure. It has been concluded that the volume of acceptor states is decreased under pressure, which leads to a rather considerable enhancement of ε_3. The effect of the magnetic field on the donor wavefunctions is also important. A strong magnetic field reduces the wave function overlap. Its effect on ε_3 is believed to be similar to that of the uniaxial compression. Thus, at extremely low concentrations, the magnetic field should have no effect on ε_3, whereas as the concentration is increased the field must enhance ε_3, eliminating the deviation from the classical predictions.

In Figure 4.4 (b) we plot ε_3 as a function of the magnetic field H. Although a high magnetic field has some effect on ε_3, however, the highest value of ε_3 obtained at $H = 70$ kG is still not in a satisfactory agreement with the theory. With the available magnetic field it is difficult to conclude whether or not ε_3 should approach its theoretical value.

The quantum interpretation described above is not the only explanation to account for the lower values of the activation energy ε_3 below theoretical predictions, an alternative explanation is discussed by Knotek and Pollak (1972, 1974). In their approach, Knotek and Pollak have considered the effect of the correlation effects. According to these authors, the correlation effect consists of the movement of two (or more) electrons simultaneously whenever it lowers the energy difference between initial and final states of the system. This correlation lowers the activation energy below the one electron process. As the resistance in the hopping region is given by expression (2.36) (together with (2.36a) and (2.37)), the single hops are dominant if the first term in equation (2.37) is much larger than the second term. An increase of the carrier concentration leads to a decrease in the average distance between donors which in turn leads to a decrease of the first term. Thus the second term becomes important (provided that the temperature is low) and this results in correlated hopping. The transition from single to multi-correlated hops occurs when $r = r_o$ (Knotek 1977), hence

$$N_0 = \frac{3}{4\pi}\left(\frac{2\epsilon k_B T}{e^2 a}\right)^{3/2}$$

For temperature T= 5 K, say, the above equation gives $N_0 = 7 \times 10^{15}$ cm^{-3}. This value is clearly less than the lowest concentration in our samples (see table 4.1). So one cannot ignore the effect of the correlated hopping, and this again could explain the lower values of the activation energy ε_3.

More recently, Mansfield et al. (1988) have pointed out that to derive the activation energy ε_3 one has to use the explicit expression, appropriate for nearest neighbour hopping which is based on the Miller-Abrahams model;

$$\rho = C\frac{k_B T(N_D^{1/3}a)^{1-\gamma'}}{\varepsilon_3}\exp(\alpha_1/N_D^{1/3}a)\exp(\varepsilon_3/k_B T) \qquad (4.15)$$

where $C = \frac{27\pi v_s^5 d_5 \hbar^4 \epsilon^2}{2E_1^2 e^6}$,

v_s=velocity of sound = 5.15 $\times 10^5$ cm s^{-1}, d_s=density= 4.787 gm cm^{-3} for InP

γ'=scaling parameter = 0.85, ϵ=dielectric constant = 14 and

E_1 = deformation potential = 14 eV.

The pre-exponential factor thus is temperature dependent, (it indeed, depends linearly on T), so one has to plot ln (ρ/T) versus $1/T$ to determine ε_3. We have found that values of ε_3 obtained by this method differ appreciably from those obtained from simple plots of ln (ρ) versus $1/T$ (see table 4.2). It has also been suggested by the above authors that as ε_3 depends on both N_D and ϵ, thus the effect of the enhanced dielectric constant by the donor centres should not be ignored.

	ε_3 (meV) from		
Sample	lnρ vs. $1/T$	ln(ρ/T) vs. $1/T$	ρ_3 (Ω.cm)
I	0.56	1.07	66.1
II	0.48	0.76	15.7
III	0.27	0.56	3.51

Table 4.2: Values of the activation energy ε_3 at zero magnetic field derived from plots of ln ρ versus $1/T$ and ln (ρ/T) versus $1/T$ as well as ρ_3 from ln ρ vs. $1/T$ plot.

Although the experimental values of ε_3 are small compared to the theoretical predictions, the conductivity is believed to be of hopping nature. Our investigation of the resistivity support this hypothesis. According to the percolation theory (reviewed by Shklovskii and Efros 1984; Böttger and Bryksin 1985), the value of ρ_3 is an exponential function of the donor concentration since it is governed by the probability of a jump which proportional to the overlap integral of the wave functions of impurities;

$$\rho_3 = \rho_{03} \exp\Big(f(N_D) \Big),\ f(N_D) = \alpha_1 / N_D^{1/3} a_B^*$$

Extensive studies of the hopping conduction were carried out on Si and Ge. Although these crystals can be obtained in a highly homogeneous form and with known impurity concentrations which is a considerable advantage over other semiconductors, the complex band structure of these materials makes it difficult to compare quantitatively the experimental and theoretical results. The case of n-InP is considered as a simple case, because it has a very simple parabolic and spherically isotropic conduction band. So one can compare the experimental and theoretical results in a more comprehensive way.

Values of ρ_3 deduced from the ln ρ versus $1/T$ plots are plotted in Figure 4.7 (b) as a function of the parameter $(N_D^{1/3} a_B^*)^{-1}$. The value of a_B^* is assumed to be 84 $\mathring{A}$. A best fit of these data gives a slope ($\alpha_1 = 3.2$) which differs substantially from the theoretical prediction of the percolation theory ($\sim$ 1.73). Following the argument of Mansfield et al. (1988) and as it has been already mentioned before one would expect better agreement if we plot ln (ρ/T) versus $1/T$ and deduce the corresponding values. This procedure (see Figure 4.7 (b)) yields a value of 2.4 for the parameter α_1 which still considerably higher than the theoretical value. It is emphasized by the above authors that since the pre-exponential factor varies with the dielectric constant ϵ, N_D and ε_3, and ε_3 is affected by both N_D and ϵ (as it will be shown later that ϵ is enhanced by the donor centres) then it might be possible to compare the slope with 1.73 if the dielectric enhancement is considered.

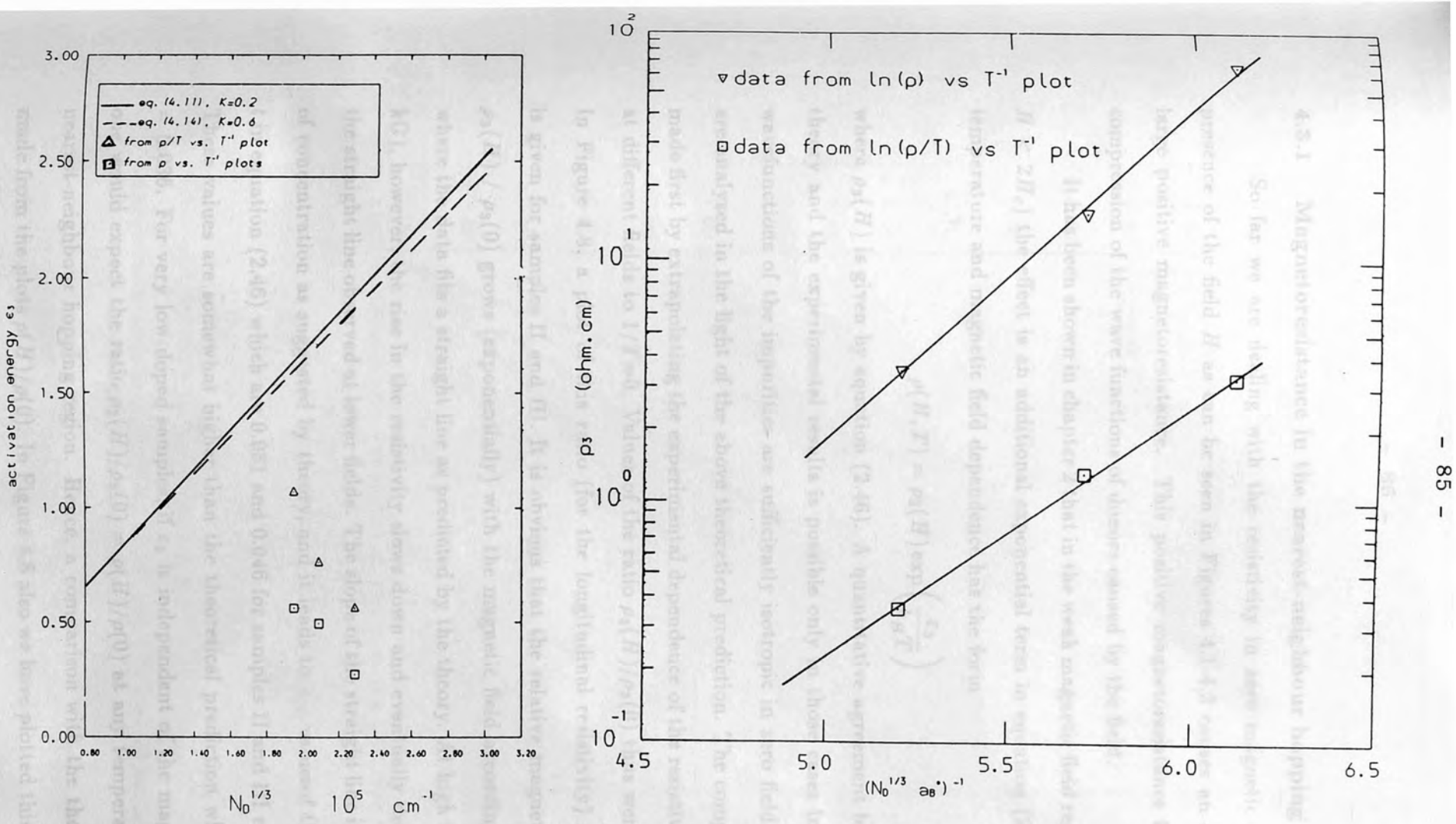

Figure 4.7

(a) The activation energy ε_3 (meV) as a function of majority concentration. The solid line is the theoretical calculations from eq.(4.11) at $K = N_A/N_D$=0.2. Dashed line represents eq.(4.14) with K=0.6. (b) The resistivity ρ_3 as a function of $(N_D^{1/3}a_B^*)^{-1}$.

4.3.1 Magnetoresistance in the nearest-neighbour hopping regime:

So far we are dealing with the resistivity in zero magnetic field. The presence of the field H as can be seen in Figures 4.1-4.3 causes an exponential large positive magnetoresistance. This positive magnetoresistance is due to a compression of the wave functions of donors caused by the field.

It has been shown in chapter 2 that in the weak magnetic field region (where $H < 2H_c$) the effect is an additional exponential term in equation (2.45a). The temperature and magnetic field dependence has the form

$$\rho(H,T) = \rho_3(H)\exp\left(\frac{\varepsilon_3}{k_B T}\right) \tag{4.16}$$

where $\rho_3(H)$ is given by equation (2.46). A quantitative agreement between this theory and the experimental results is possible only in those cases in which the wavefunctions of the impurities are sufficiently isotropic in zero field. The data are analysed in the light of the above theoretical prediction. The comparison was made first by extrapolating the experimental dependence of the resistivity $\rho(H,T)$ at different fields to $1/T$=0. Values of the ratio $\rho_3(H)/\rho_3(0)$ thus were obtained. In Figure 4.8, a plot of this ratio (for the longitudinal resistivity) against H^2 is given for samples II and III. It is obvious that the relative magnetoresistance $\rho_3(H)$ / $\rho_3(0)$ grows (exponentially) with the magnetic field according to (2.46), where the data fits a straight line as predicted by the theory. At high fields ($\geq$ 35 kG), however, the rise in the resistivity slows down and eventually deviates from the straight line observed at lower fields. The slope of the straight line is a function of concentration as suggested by theory, and it leads to values of the constant t in equation (2.46) which are 0.051 and 0.046 for samples II and III respectively. These values are somewhat higher than the theoretical prediction which gives t = 0.036. For very low-doped samples, if ε_3 is independent of the magnetic field, one would expect the ratio $\rho_3(H)/\rho_3(0) = \rho(H)/\rho(0)$ at any temperature in the nearest-neighbour hopping region. Hence, a comparison with the theory can be made from the plots $\rho(H)/\rho(0)$. In Figure 4.8 also we have plotted this parameter against H^2 for the lowest doped sample (sample I) at T = 2 K. This graph shows

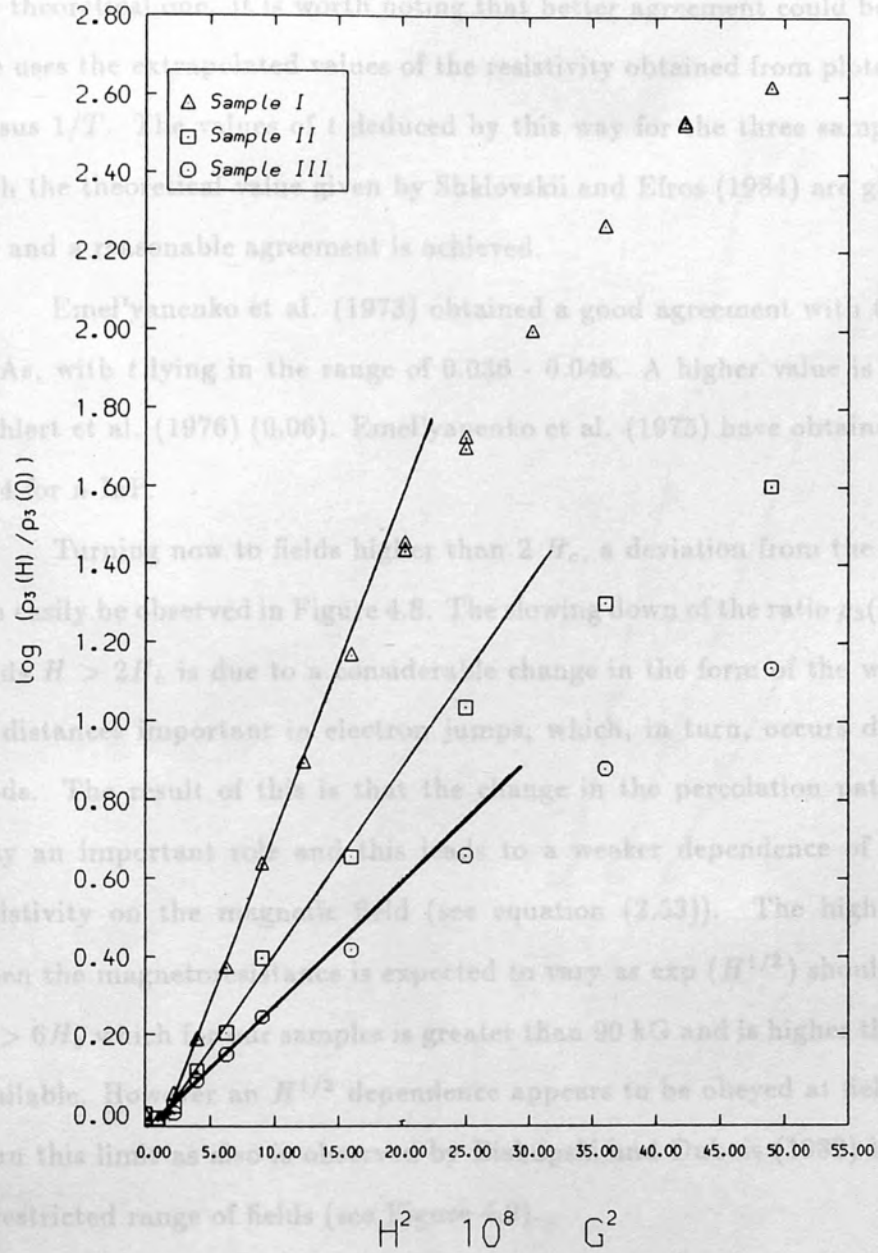

Figure 4.8

Magnetoresistance ln $(\rho_3(H)/\rho_3(0))$ of samples I, II and III against the H^2 in the nearest-neighbour hopping region.

that a good agreement is observed in the low-field limit, however, the deduced value of t by this method ($\sim$ 0.076) is considerably (almost twice) higher than the theoretical one. It is worth noting that better agreement could be obtained if one uses the extrapolated values of the resistivity obtained from plots of ln (ρ/T) versus $1/T$. The values of t deduced by this way for the three samples together with the theoretical value given by Shklovskii and Efros (1984) are given in table 4.3 and a reasonable agreement is achieved.

Emel'yanenko et al. (1973) obtained a good agreement with theory for n-GaAs, with t lying in the range of 0.036 - 0.046. A higher value is obtained by Kahlert et al. (1976) (0.06). Emel'yanenko et al. (1975) have obtained a value of 0.04 for n-InP.

Turning now to fields higher than 2 H_c, a deviation from the straight line can easily be observed in Figure 4.8. The slowing down of the ratio $\rho_3(H)/\rho_3(0)$ for fields $H > 2H_c$ is due to a considerable change in the form of the wavefunctions at distances important in electron jumps, which, in turn, occurs due to strong fields. The result of this is that the change in the percolation paths begins to play an important role and this leads to a weaker dependence of the hopping resistivity on the magnetic field (see equation (2.53)). The high field region when the magnetoresistance is expected to vary as exp $(H^{1/2})$ should start when $H > 6H_c$ which for our samples is greater than 90 kG and is higher than the fields available. However an $H^{1/2}$ dependence appears to be obeyed at fields much less than this limit as also is observed by Biskupski and Dubois (1982) but only over a restricted range of fields (see Figure 4.9).

Let us now discuss the anisotropy in the magnetoresistance of the studied samples in the nearest-neighbour hopping region. When a magnetic field H is applied, the wave functions of the impurity centres are no longer isotropic, instead, anisotropy builds up. Shklovskii (1977) has calculated the anisotropy in presence of magnetic fields. It has been found that the parallel and the perpendicular components of the resistivity, ($\rho_{\|}$ and $\rho_{\perp}$) are related to the magnetic field H via

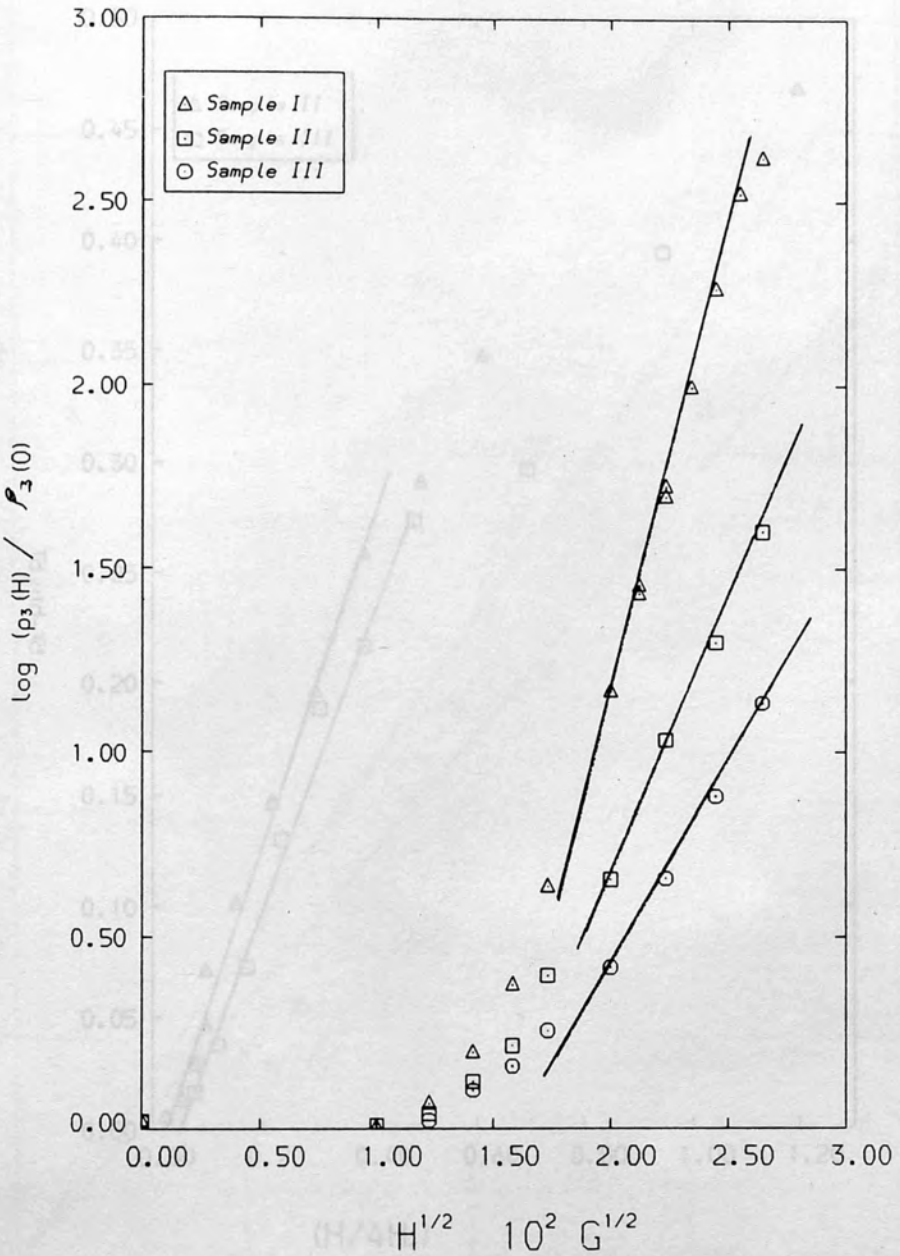

Figure 4.9

Magnetoresistance ln $(\rho_3(H)/\rho_3(0))$ of samples I, II and III against the $H^{1/2}$ in the nearest-neighbour hopping region.

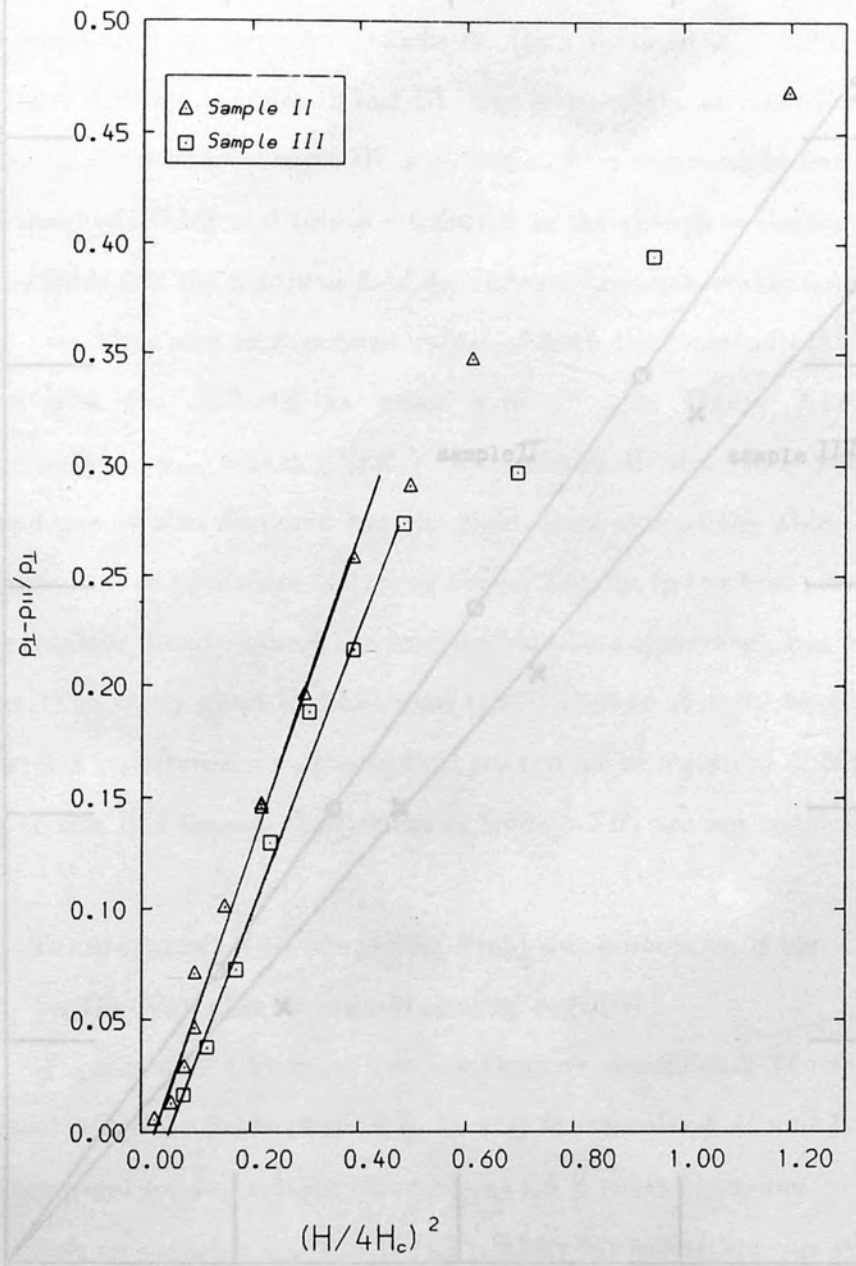

Figure 4.10

Magnetic field dependence of the anisotropy in the nearest-neighbour hopping region of samples II and III.

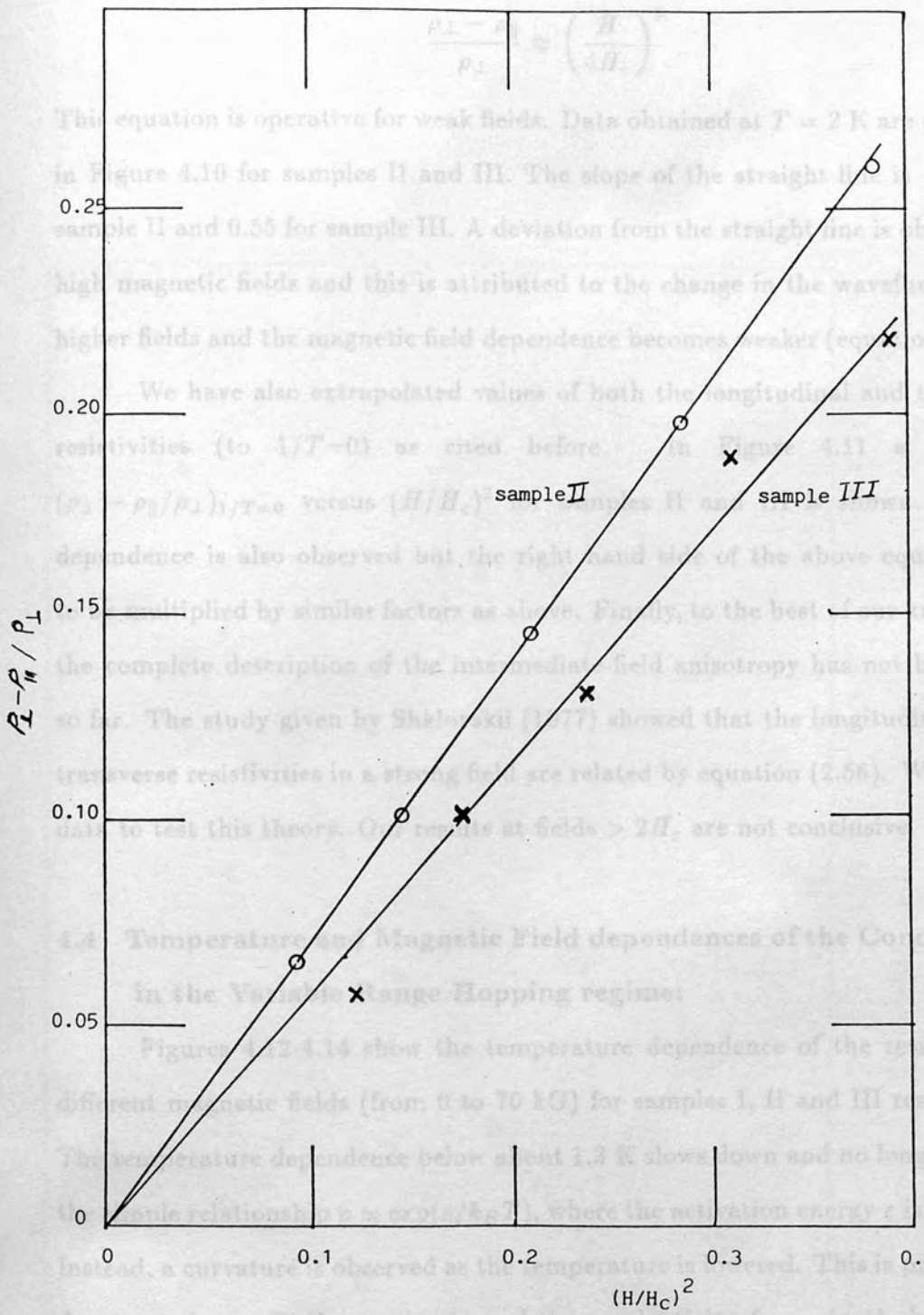

Figure 4.11

Magnetic field dependence of the anisotropy of samples II and III. (the extraploted values of the resistivity to $1/T=0$ are used).

equation (2.55);

$$\frac{\rho_\perp - \rho_\parallel}{\rho_\perp} \approx \left(\frac{H}{4H_c}\right)^2 \tag{4.17}$$

This equation is operative for weak fields. Data obtained at $T = 2$ K are presented in Figure 4.10 for samples II and III. The slope of the straight line is ~0.70 for sample II and 0.55 for sample III. A deviation from the straight line is observed at high magnetic fields and this is attributed to the change in the wavefunctions at higher fields and the magnetic field dependence becomes weaker (equation (2.56)).

We have also extrapolated values of both the longitudinal and transverse resistivities (to $1/T$=0) as cited before. In Figure 4.11 a plot for $(\rho_\perp - \rho_\parallel/\rho_\perp)_{1/T=0}$ versus $(H/H_c)^2$ for samples II and III is shown. An H^2 dependence is also observed but the right hand side of the above equation has to be multiplied by similar factors as above. Finally, to the best of our knowledge, the complete description of the intermediate-field anisotropy has not been done so far. The study given by Shklovskii (1977) showed that the longitudinal to the transverse resistivities in a strong field are related by equation (2.56). We have no data to test this theory. Our results at fields $> 2H_c$ are not conclusive.

4.4 Temperature and Magnetic Field dependences of the Conductivity in the Variable Range Hopping regime:

Figures 4.12-4.14 show the temperature dependence of the resistivity at different magnetic fields (from 0 to 70 kG) for samples I, II and III respectively. The temperature dependence below about 1.3 K slows down and no longer follows the simple relationship $\rho \propto \exp(\varepsilon/k_B T)$, where the activation energy ε is constant. Instead, a curvature is observed as the temperature is lowered. This is presumably due to a change in the mechanism of the conductivity from simple hopping of electrons between nearest neighbouring sites (with constant activation energy as described in the preceeding section) to a variable-range hopping with decreasing activation energy. It has been mentioned earlier that at very low temperatures, typical resistances between neighbouring impurities might become higher than those connecting some remote impurities whose energies happen to be very close

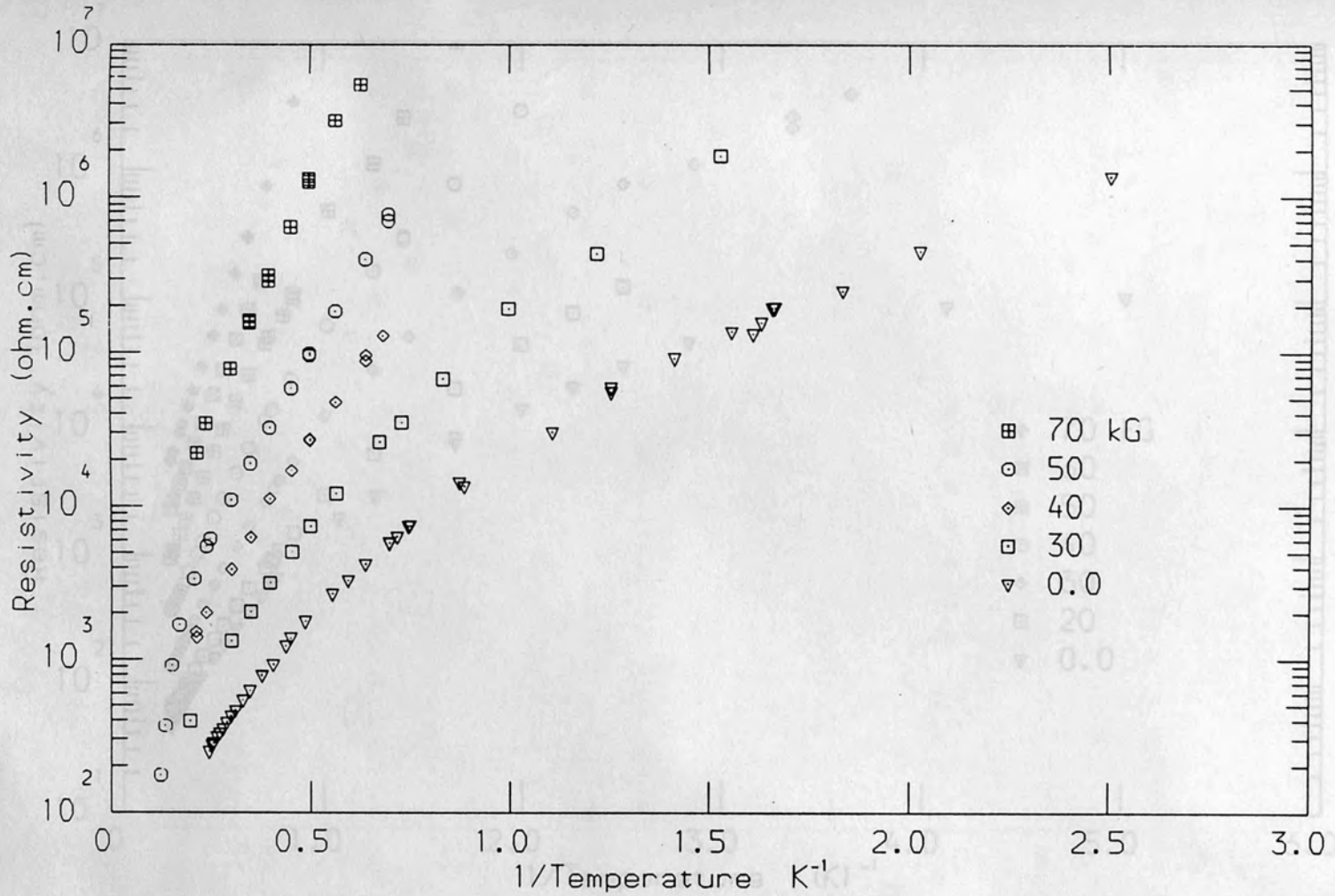

Figure 4.12
Resistivity of sample I in both nearest-neighbour and variable-range hopping regions.

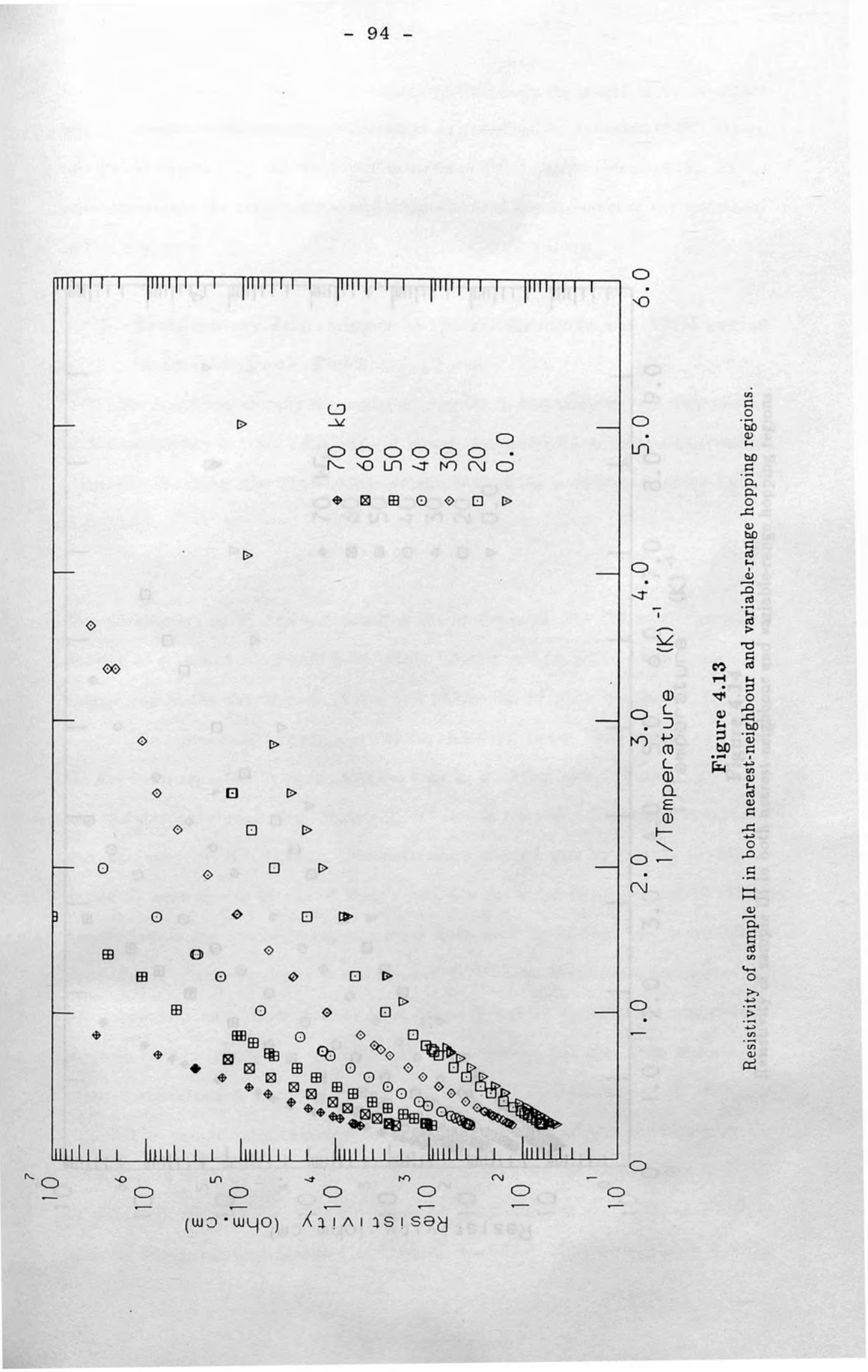

Figure 4.13

Resistivity of sample II in both nearest-neighbour and variable-range hopping regions.

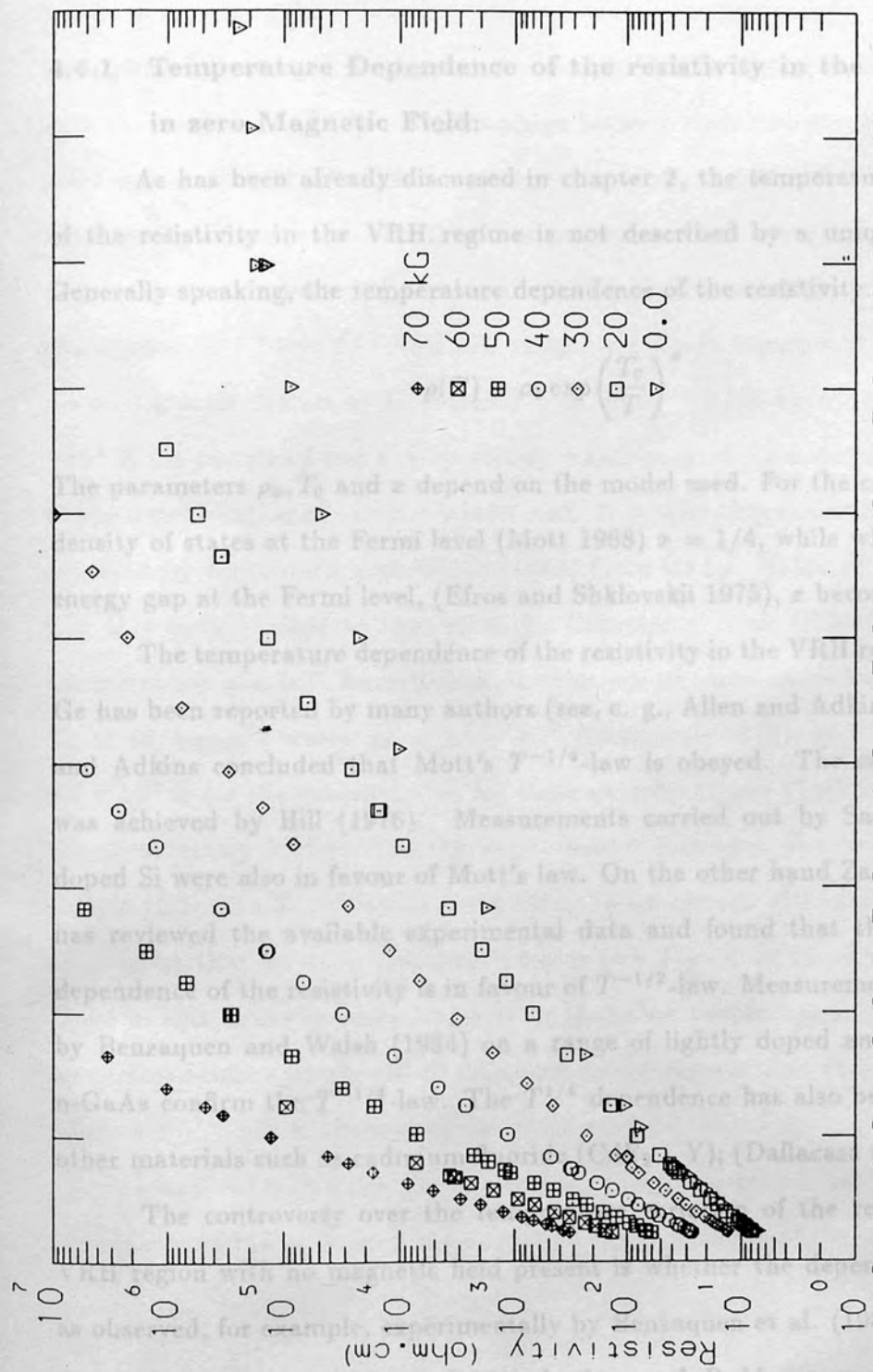

Figure 4.14

Resistivity of sample III in both nearest-neighbour and variable-range hopping regions.

to the Fermi level. In this case the characteristic hopping length is not constant but it increases with lowering temperature as described by equation (2.57). Thus, one would expect that the conductivity to be of VRH nature (Mott 1968). Let us now investigate the temperature and magnetic field dependences of the resistivity in this regime.

4.4.1 Temperature Dependence of the resistivity in the VRH region in zero Magnetic Field:

As has been already discussed in chapter 2, the temperature dependence of the resistivity in the VRH regime is not described by a unique expression. Generally speaking, the temperature dependence of the resistivity is given by

$$\rho(T) = \rho_0 \exp\left(\frac{T_0}{T}\right)^x \tag{4.18}$$

The parameters ρ_0, T_0 and x depend on the model used. For the case of constant density of states at the Fermi level (Mott 1968) $x = 1/4$, while when there is an energy gap at the Fermi level, (Efros and Shklovskii 1975), x becomes $1/2$.

The temperature dependence of the resistivity in the VRH regime of n-type Ge has been reported by many authors (see, e. g., Allen and Adkins 1972). Allen and Adkins concluded that Mott's $T^{-1/4}$-law is obeyed. The same conclusion was achieved by Hill (1976). Measurements carried out by Sasaki (1985) on doped Si were also in favour of Mott's law. On the other hand Zabrodskii (1977) has reviewed the available experimental data and found that the temperature dependence of the resistivity is in favour of $T^{-1/2}$-law. Measurements carried out by Benzaquen and Walsh (1984) on a range of lightly doped and compensated n-GaAs confirm the $T^{-1/4}$-law. The $T^{1/4}$ dependence has also been observed in other materials such as cadmium fluoride (CdF_2 : Y); (Dallacasa et al. 1988).

The controversy over the temperature variation of the resistivity in the VRH region with no magnetic field present is whether the dependence is $T^{-1/4}$ as observed, for example, experimentally by Benzaquen et al. (1985) or $T^{-1/2}$ as seen by Finlayson and Mason (1986), both on n-InP. Measurements on a wider

temperature range at lower limit are necessary to verify whether $T^{-1/4}$ or $T^{-1/2}$-law is obeyed.

Now, let us discuss the temperature dependence of the resistivity of our samples in absence of the magnetic field. It has been seen in Figures 4.12-4.14 that the variation of ρ with T (at lower temperatures) is no longer be described by the nearest-neighbour hopping with constant activation energy. In Figure 4.15 (a) a plot of ρ versus $T^{-1/4}$ is given for sample I, while Figure 4.15 (b) is plotted with the x-axis being $T^{-1/2}$. A comparison between these two graphs shows that a good agreement with $T^{-1/4}$-law is observed in support of Mott's law. This indeed confirms Benzaquen et al. (1985) results, but over a much wider temperature range and consequent variation of ρ. A similar result is obtained with sample II. A plot of ρ against $T^{-1/4}$ and $T^{-1/2}$ for this sample is given in Figure 4.16 (a) and (b) on a semi-log scale. Values of T_0 deduced from the $T^{-1/4}$ plots are 7.3 $\times 10^4$ and 2.2 $\times 10^4$ K for samples I and II respectively which seem to be a decreasing function as the concentration of carriers is increased. A similar behaviour has already been reported by Benzaquen and Walsh (1984) for n-GaAs. Value of T_0 for sample I in this work is close to that given by Benzaquen et al. (1985) for a similar concentration of n-InP. Nevertheless, the theoretical calculations from the relation $T_0 = 49/k_B g_0 a^3$, where $g_0 = \epsilon N_D^{2/3} e^{-2}$ (Shklovskii 1973), give 2.6 $\times$ 10^5 and 2.3 $\times$ 10^5 K for the parameter T_0 for these samples (I and II respectively) which are considerably higher than the experimental findings. For the most impure sample (III), the $T^{-1/4}$-law is more likely to be obeyed although the fit is not as good as that for the other two samples (see Figure 4.17). The temperature range in this figure is much larger than the other two samples. Results on the magnetoresistance which will be discussed below suggest that this sample should follow a $T^{-1/4}$-law in absence of the magnetic field.

Mansfield et al. (1988) have used the explicit expression for the temperature dependence of the resistivity in this regime. An expression of the form (Allen and

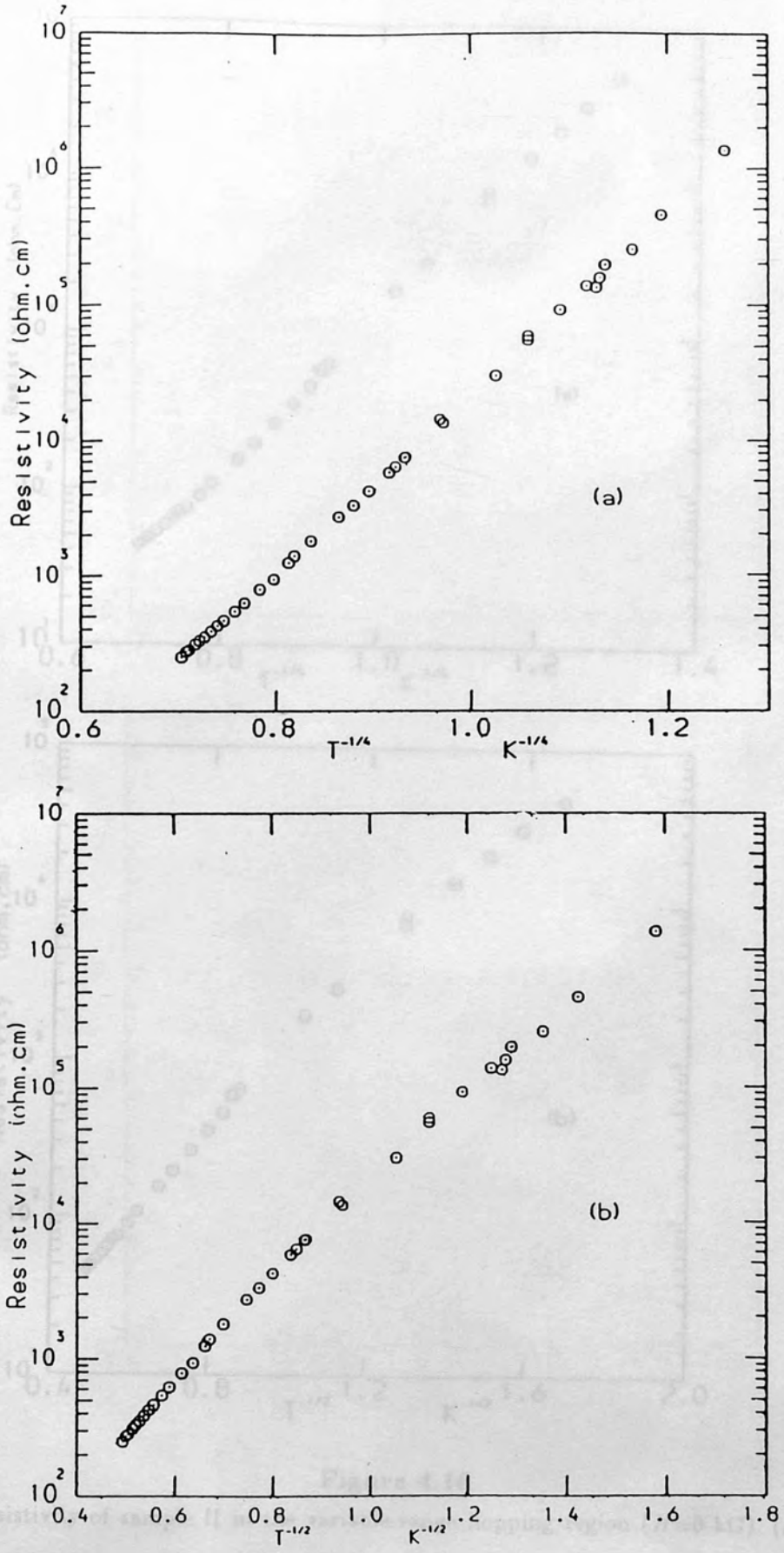

Figure 4.15

The resistivity of sample I in the variable-range hopping region (H=0 kG). (a) log ρ against $T^{-1/4}$. (b) log ρ against $T^{-1/2}$.

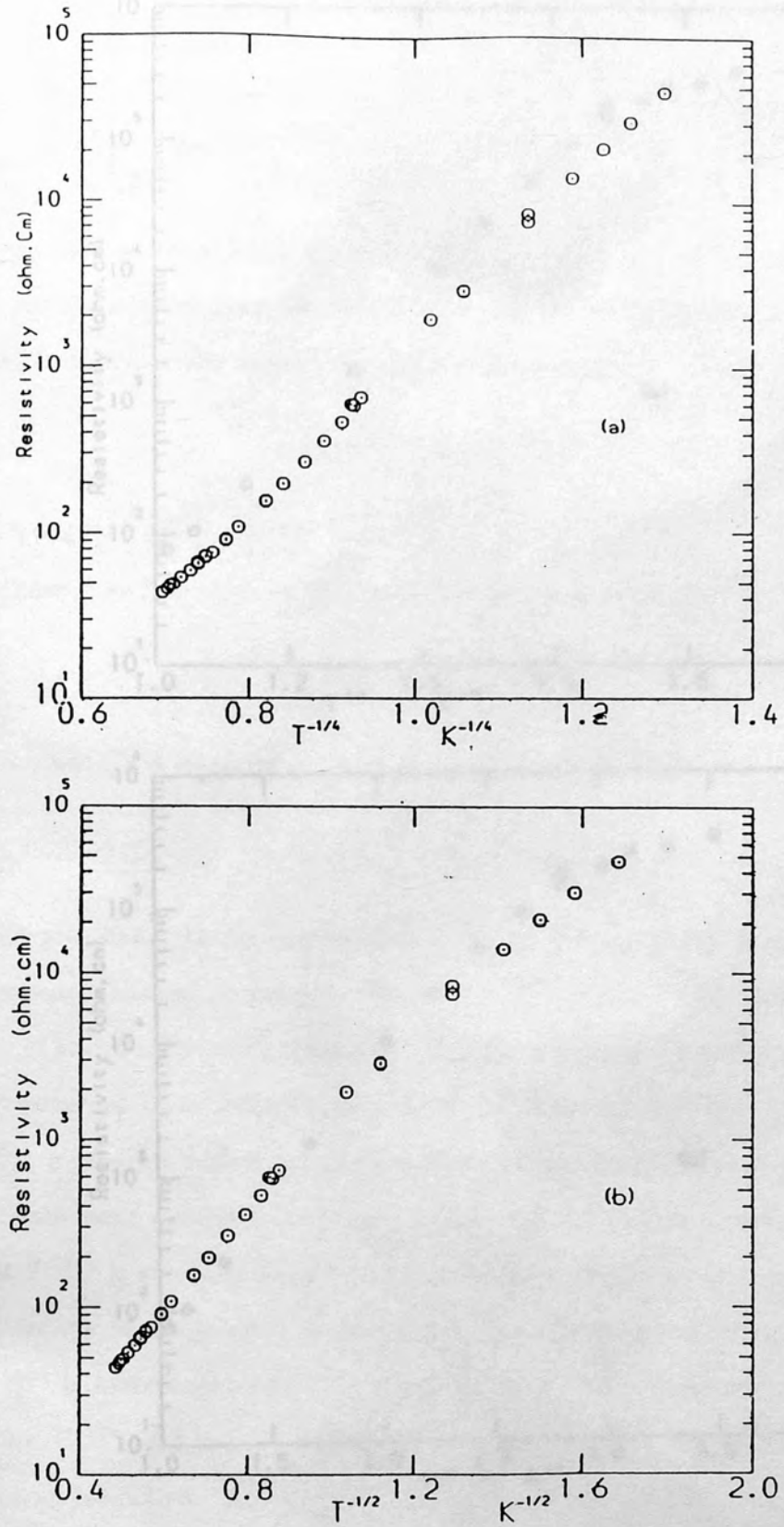

Figure 4.16

The resistivity of sample II in the variable-range hopping region (H=0 kG). (a) log ρ against $T^{-1/4}$. (b) log ρ against $T^{-1/2}$.

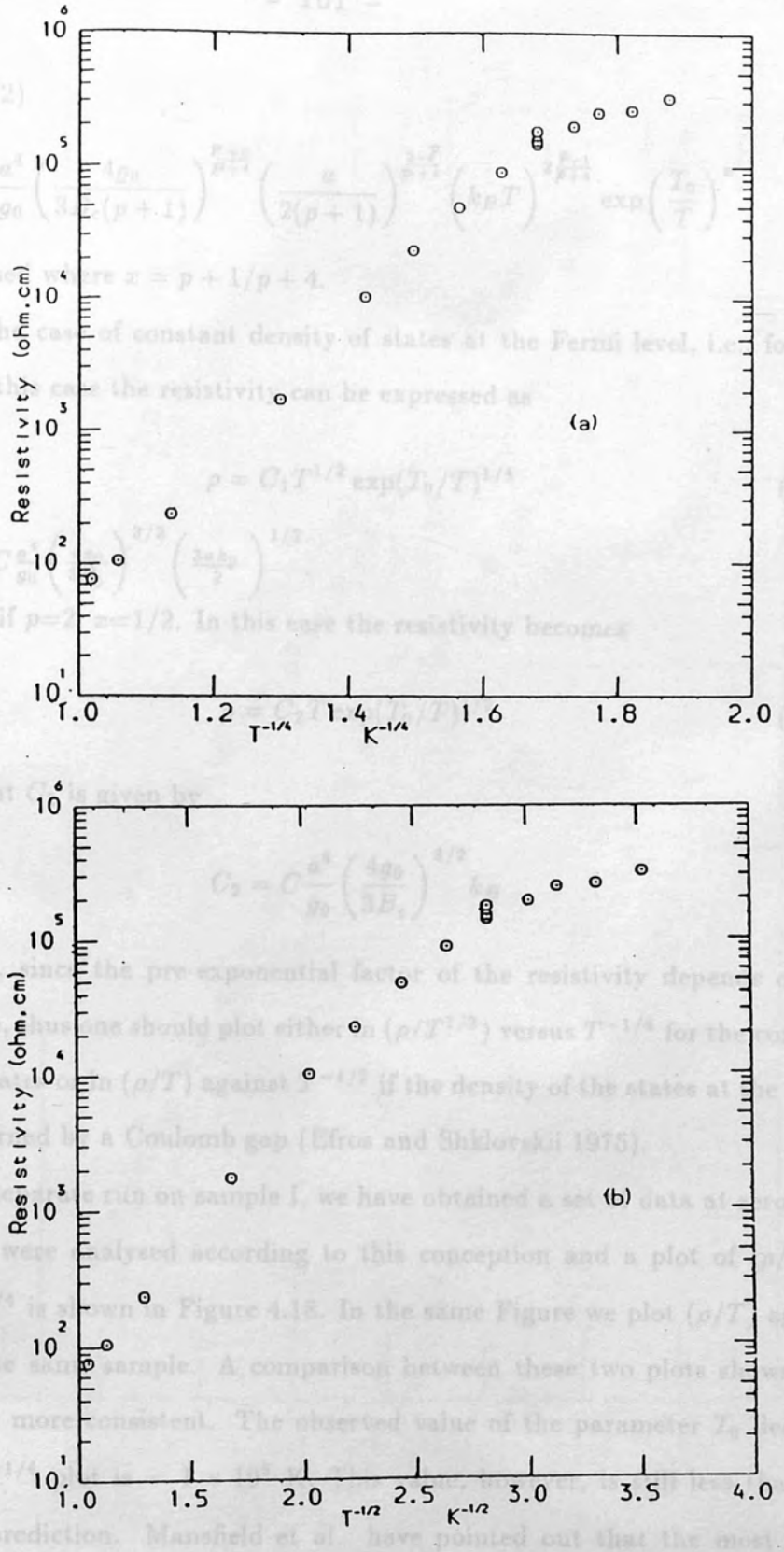

Figure 4.17

The resistivity of sample III in the variable-range hopping region (H=0 kG). (a) log ρ against $T^{-1/4}$. (b) log ρ against $T^{-1/2}$.

Adkins 1972)

$$\rho = C\frac{a^4}{g_0}\left(\frac{4g_0}{3B_c(p+1)}\right)^{\frac{p+6}{p+4}}\left(\frac{a}{2(p+1)}\right)^{\frac{2-p}{p+4}}\left(k_BT\right)^{2\frac{p+1}{p+4}}\exp\left(\frac{T_0}{T}\right)^{x} \qquad (4.19)$$

has been used where $x = p + 1/p + 4$.

Thus, for the case of constant density of states at the Fermi level, i.e., for p=0, x=1/4. In this case the resistivity can be expressed as

$$\rho = C_1T^{1/2}\exp(T_0/T)^{1/4} \qquad (4.19a)$$

with $C_1 = C\frac{a^4}{g_0}\left(\frac{4g_0}{3B_c}\right)^{3/2}\left(\frac{3ak_B}{2}\right)^{1/2}$.

In the case if p=2, x=1/2. In this case the resistivity becomes

$$\rho = C_2T\exp(T_0/T)^{1/2} \qquad (4.19b)$$

The constant C_2 is given by

$$C_2 = C\frac{a^4}{g_0}\left(\frac{4g_0}{3B_c}\right)^{3/2}k_B$$

Accordingly, since the pre-exponential factor of the resistivity depends on the temperature, thus one should plot either ln $(\rho/T^{1/2})$ versus $T^{-1/4}$ for the constant density of states or ln (ρ/T) against $T^{-1/2}$ if the density of the states at the Fermi level is governed by a Coulomb gap (Efros and Shklovskii 1975).

In a separate run on sample I, we have obtained a set of data at zero field. These data were analysed according to this conception and a plot of $(\rho/T^{1/2})$ against $T^{-1/4}$ is shown in Figure 4.18. In the same Figure we plot (ρ/T) against $T^{-1/2}$ for the same sample. A comparison between these two plots shows that the $T^{-1/4}$ is more consistent. The observed value of the parameter T_0 deduced from the $T^{-1/4}$ plot is $\sim 1 \times 10^5$ K. This value, however, is still less than the theoretical prediction. Mansfield et al. have pointed out that the most likely candidate for such a discrepancy is the dielectric constant which has been used in the theoretical calculation ($\epsilon = 14$ for n-InP). These authors have suggested that in order to obtain agreement between the theoretical and observed values of ε_3 in the nearest-neighbour hopping region it is necessary to enhance the dielectric

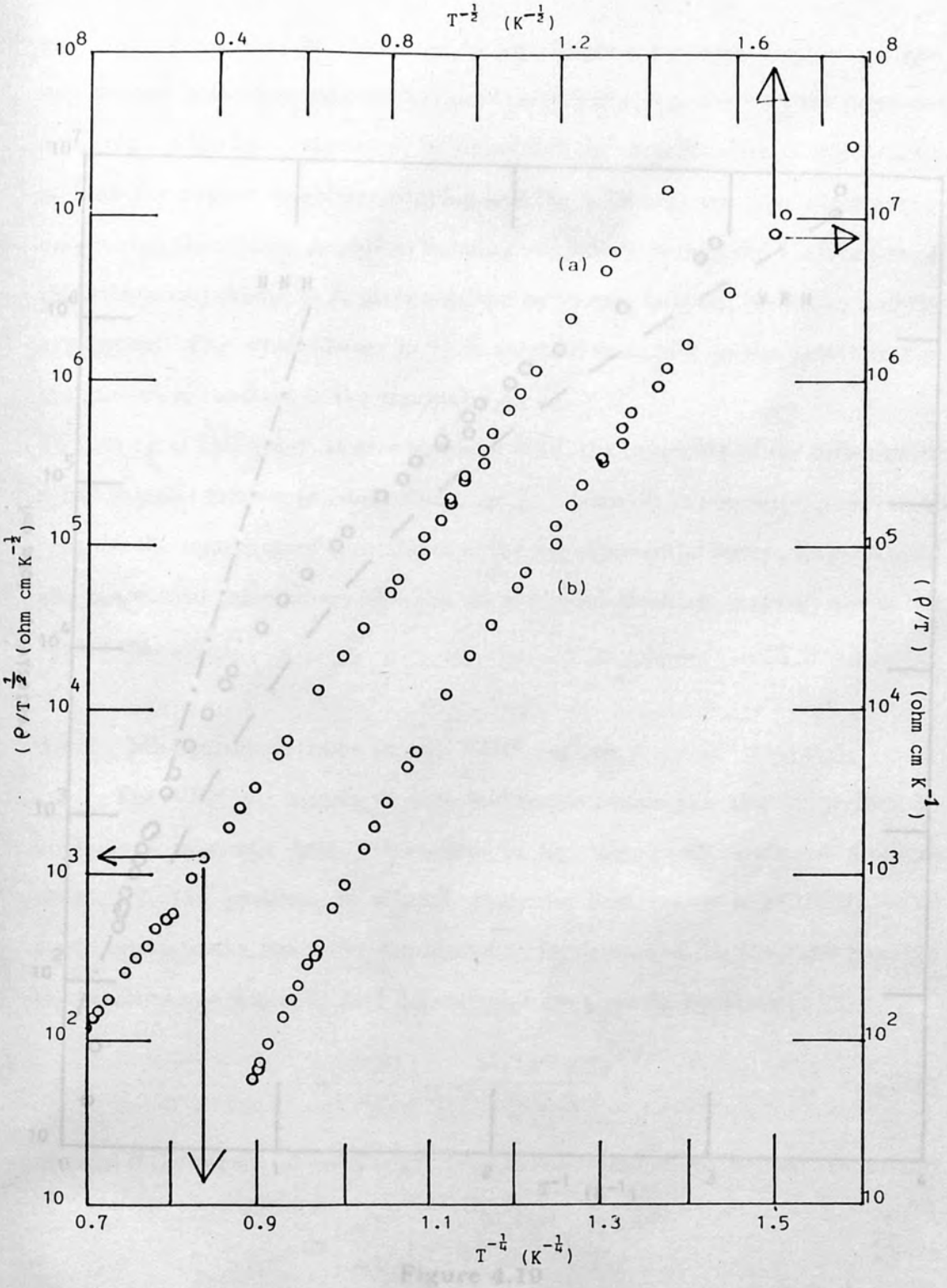

Figure 4.18

The resistivity of sample I in the variable-range hopping region (H=0 kG). A comparison is made between (a) a log ($\rho/T^{1/2}$) against $T^{-1/4}$ plot and (b) a log (ρ/T) against $T^{-1/2}$ plot.

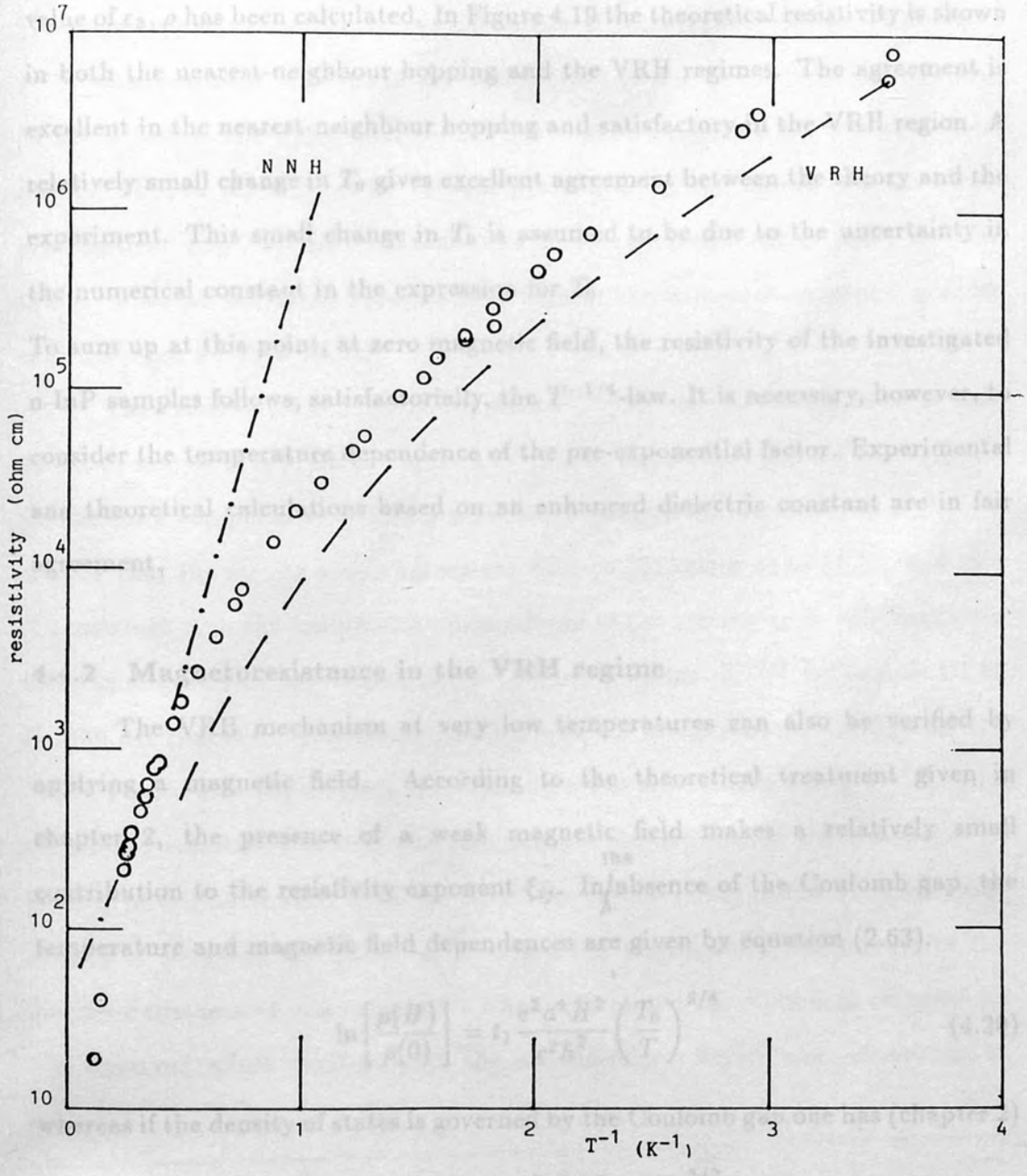

Figure 4.19

Comparison of the theoretical and experimental resistivity of sample I in zero magnetic field. The dash-dotted curve is the resistivity deduced for the NNH using eq. (4.15). The dashed curve is the resistivity for the the VRH using eq. (4.19).

constant. A value of 26 instead of 14 for sample I has been used in the pre-exponential factor in equations (2.47) and (4.19a) and, together with the measured value of ε_3, ρ has been calculated. In Figure 4.19 the theoretical resistivity is shown in both the nearest-neighbour hopping and the VRH regimes. The agreement is excellent in the nearest-neighbour hopping and satisfactory in the VRH region. A relatively small change in T_0 gives excellent agreement between the theory and the experiment. This small change in T_0 is assumed to be due to the uncertainty in the numerical constant in the expression for T_0.

To sum up at this point, at zero magnetic field, the resistivity of the investigated n-InP samples follows, satisfactorially, the $T^{-1/4}$-law. It is necessary, however, to consider the temperature dependence of the pre-exponential factor. Experimental and theoretical calculations based on an enhanced dielectric constant are in fair agreement.

4.4.2 Magnetoresistance in the VRH regime

The VRH mechanism at very low temperatures can also be verified by applying a magnetic field. According to the theoretical treatment given in chapter 2, the presence of a weak magnetic field makes a relatively small contribution to the resistivity exponent ξ_{ij}. In the absence of the Coulomb gap, the temperature and magnetic field dependences are given by equation (2.63),

$$\ln\left[\frac{\rho(H)}{\rho(0)}\right] = t_1 \frac{e^2 a^4 H^2}{c^2 \hbar^2} \left(\frac{T_0}{T}\right)^{3/4} \tag{4.20}$$

whereas if the density of states is governed by the Coulomb gap one has (chapter 2)

$$\ln\left[\frac{\rho(H)}{\rho(0)}\right] = t_2 \frac{e^2 a^4 H^2}{c^2 \hbar^2} \left(\frac{T_0}{T}\right)^{3/2} \tag{4.21}$$

Let us now discuss the temperature dependence of the magnetoresistance of the three n-InP samples in the light of the above formulae.

The variation of $\ln \rho_{\parallel}(H)/\rho(0)$ against $T^{-3/4}$ for sample I at H=30 kG is shown in Figure 4.20 (a). A fit to a straight line in the whole temperature range is not satisfactory. In Figure 5.20 (b) we replot $\ln \rho_{\parallel}(H)/\rho(0)$ against $T^{-3/2}$ for this

sample at the same field. It seems that neither law can describe the behaviour of the resistivity in the whole temperature range. In Figure 4.20 (a) data are also presented for this sample at a field of 20 kG. A reasonable straight line is achieved. The departure in the temperature dependence of the magnetoresistance from the $T^{-3/4}$ observed at $H = 30$ kG in this figure could be due to the fact that the field 30 kG is just at the upper limit of H^2-dependence suggested for the weak field case ($< 2H_c$) as H_c =16 kG for this sample. However, one cannot rule out other possibilities. (e.g., an experimental error in the measurement of $\rho(H)$ for this sample since its resistance becomes very high in this temperature range; greater than 10^9 ohm for $T = 0.5$ K).

The variation of $\ln \rho_\perp(H)/\rho(0)$ with $T^{-3/4}$ at constant fields, $H = 20$ and 30 kG of sample II is given in Figure 4.21 (a). In Figure 4.21 (b) the plot is given for the same sample at $H = 30$ kG with the horizontal axis replaced by $T^{-3/2}$. It is clear that the results are in agreement with (4.20) rather than (4.21) and this is consistent with the temperature dependence of the resistivity in zero magnetic field. In Figure 4.22 (a) we plot $\ln(\rho\ (H)/\rho(0))$ against $T^{-3/4}$ for sample III at H =30 kG (parallel configuration) and H=20 kG (perpendicular configuration). While Figure 4.22 (b) displays the same data but with x-axis being $T^{-3/2}$. The immediate conclusion is that the temperature dependence of the resistivity is, indeed, in fair agreement with the $T^{-3/4}$-law which is suggested for a constant density of states at the Fermi level. From the temperature dependence of the magnetoresistance of these samples we have calculated the numerical constant t_1. The observed values together with the theoretical prediction are summarised in table 4.3.

Sample code	t from $\ln(\rho/T)$ vs. $1/T$ plot	t_1 from $T^{-3/4}$-law	H^2-law
I	0.042	0.0044	0.0044
II	0.047	0.0072	0.0083
III	0.044	0.0049	0.0066
Theoretical values		t=0.036	t_1=0.0025

Table 4.3: The experimental and theoretical values of the numerical parameters t and t_1.

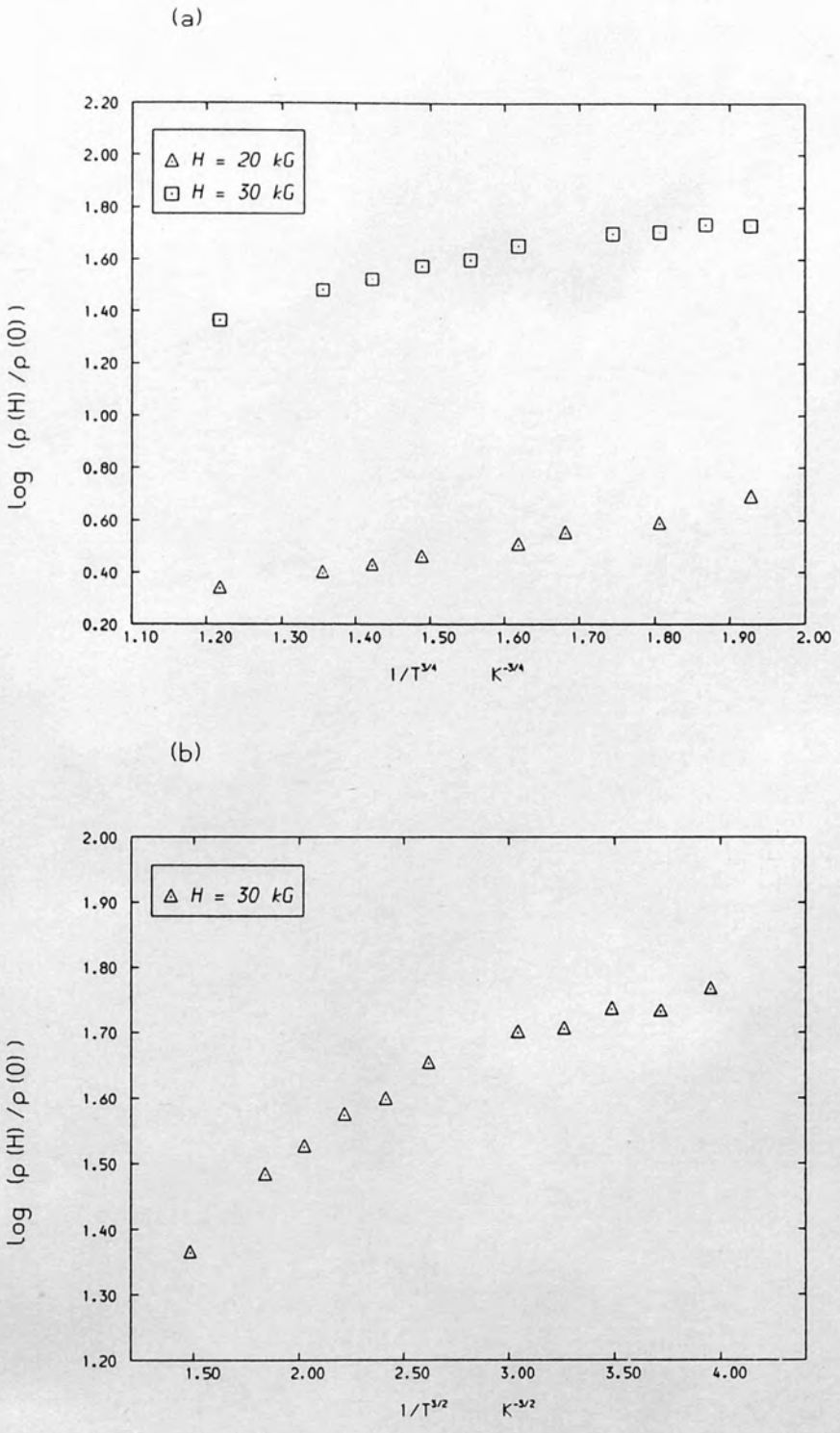

Figure 4.20

The magnetoresistance of sample I in the VRH region. The logarithm of the ratio $(\rho_{\parallel}(H)/\rho(0))$ of the resistivity in a field H divided by the resistivity in zero field is plotted as a function of (a) $T^{-3/4}$, and (b)$T^{-3/2}$.

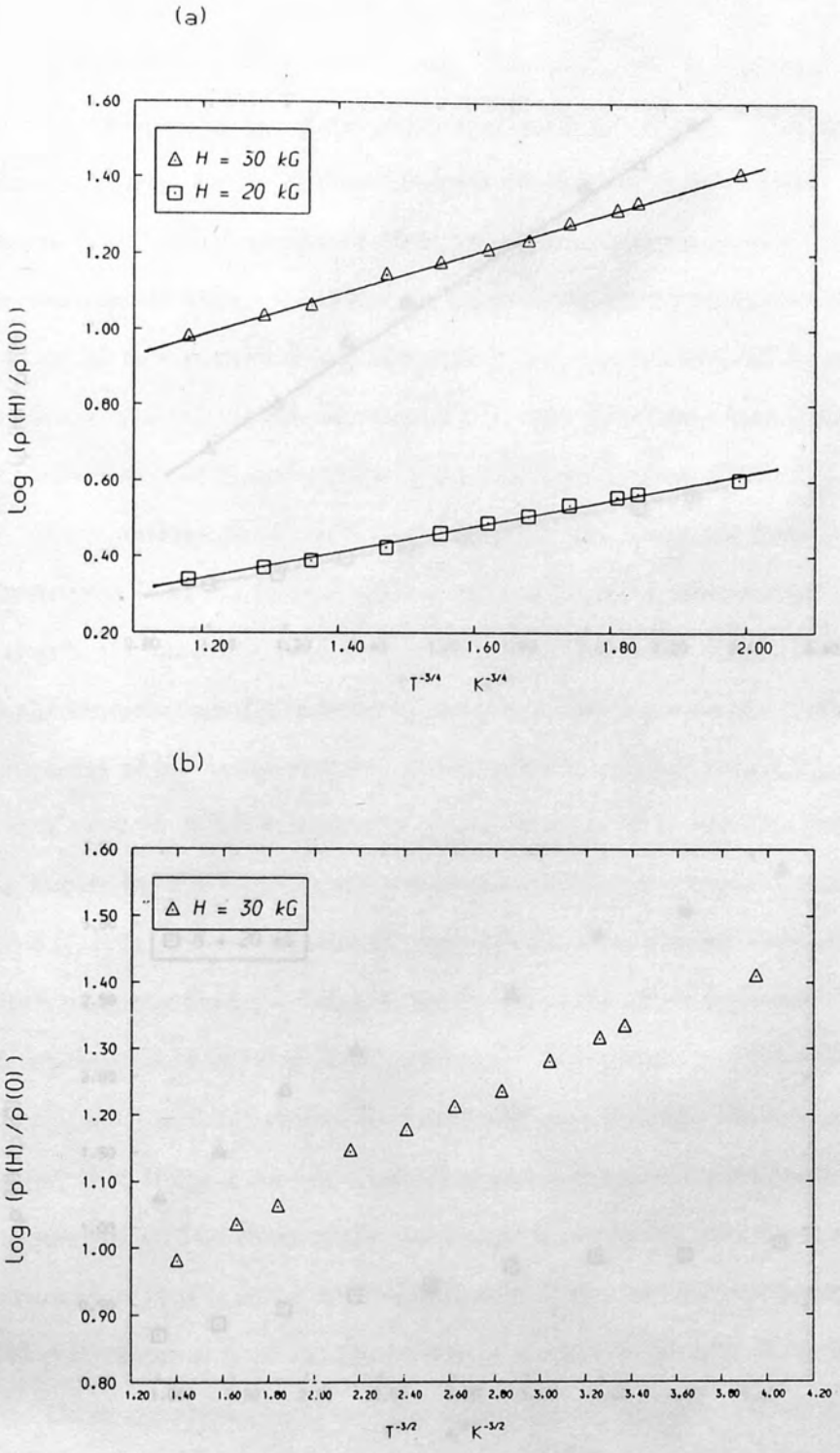

Figure 4.21

The magnetoresistance of sample II in the VRH region. The logarithm of the ratio $(\rho_\perp(H)/\rho(0))$ of the resistivity in a field H divided by the resistivity in zero field is plotted as a function of (a) $T^{-3/4}$, and (b) $T^{-3/2}$.

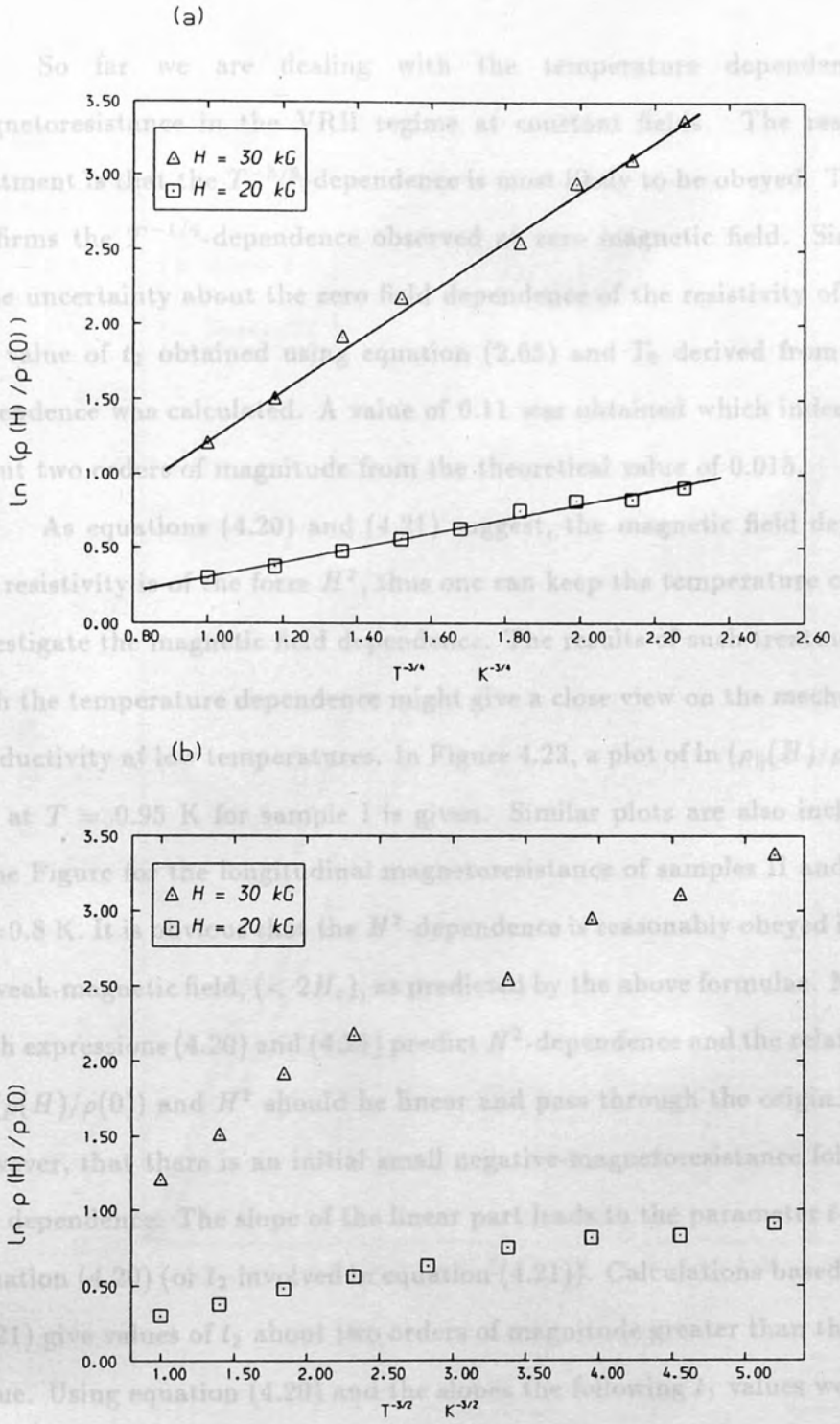

Figure 4.22

The magnetoresistance of sample III in the VRH region. The logarithm of the ratio $(\rho(H)/\rho(0))$ of the resistivity in a field H divided by the resistivity in zero field is plotted as a function of (a) $T^{-3/4}$, H =30 kG, $\rho_{\parallel}$, H=20 kG, $\rho_{\perp}$] and (b)$T^{-3/2}$ (the same configuration).

So far we are dealing with the temperature dependence of the magnetoresistance in the VRH regime at constant fields. The result of such treatment is that the $T^{-3/4}$-dependence is most likely to be obeyed. This, indeed, confirms the $T^{-1/4}$-dependence observed at zero magnetic field. Since there is some uncertainty about the zero field dependence of the resistivity of sample III, the value of t_2 obtained using equation (2.65) and T_0 derived from the $T^{-1/2}$-dependence was calculated. A value of 0.11 was obtained which indeed differs by about two orders of magnitude from the theoretical value of 0.015.

As equations (4.20) and (4.21) suggest, the magnetic field dependence of the resistivity is of the form H^2, thus one can keep the temperature constant and investigate the magnetic field dependence. The results of such treatment together with the temperature dependence might give a close view on the mechanism of the conductivity at low temperatures. In Figure 4.23, a plot of $\ln(\rho_{\parallel}(H)/\rho(0))$ against H^2 at $T = 0.95$ K for sample I is given. Similar plots are also included in the same Figure for the longitudinal magnetoresistance of samples II and III both at $T = 0.8$ K. It is obvious that the H^2-dependence is reasonably obeyed in the region of weak-magnetic field, ($< 2H_c$), as predicted by the above formulae. Nevertheless, both expressions (4.20) and (4.21) predict H^2-dependence and the relation between $\ln(\rho(H)/\rho(0))$ and H^2 should be linear and pass through the origin. It is found, however, that there is an initial small negative-magnetoresistance followed by an H^2 dependence. The slope of the linear part leads to the parameter t_1 involved in equation (4.20) (or t_2 involved in equation (4.21)). Calculations based on equation (4.21) give values of t_2 about two orders of magnitude greater than the theoretical value. Using equation (4.20) and the slopes the following t_1 values were obtained: 0.0044, 0.0083 and 0.0066 for samples I, II and III respectively. The determination of t_1 is dependent on the measurement of T_0 which is found from the slope of the $\ln(\rho/T^{-1/2})$ versus $T^{-1/4}$ plot in zero magnetic field. It is assumed in deriving (4.20) that T_0 is independent of the magnetic field. This might not be satisfied as the doping level increases causing an increase in the enhancement of the dielectric constant which might be decreased by the magnetic field (Mansfield and Kusztelan

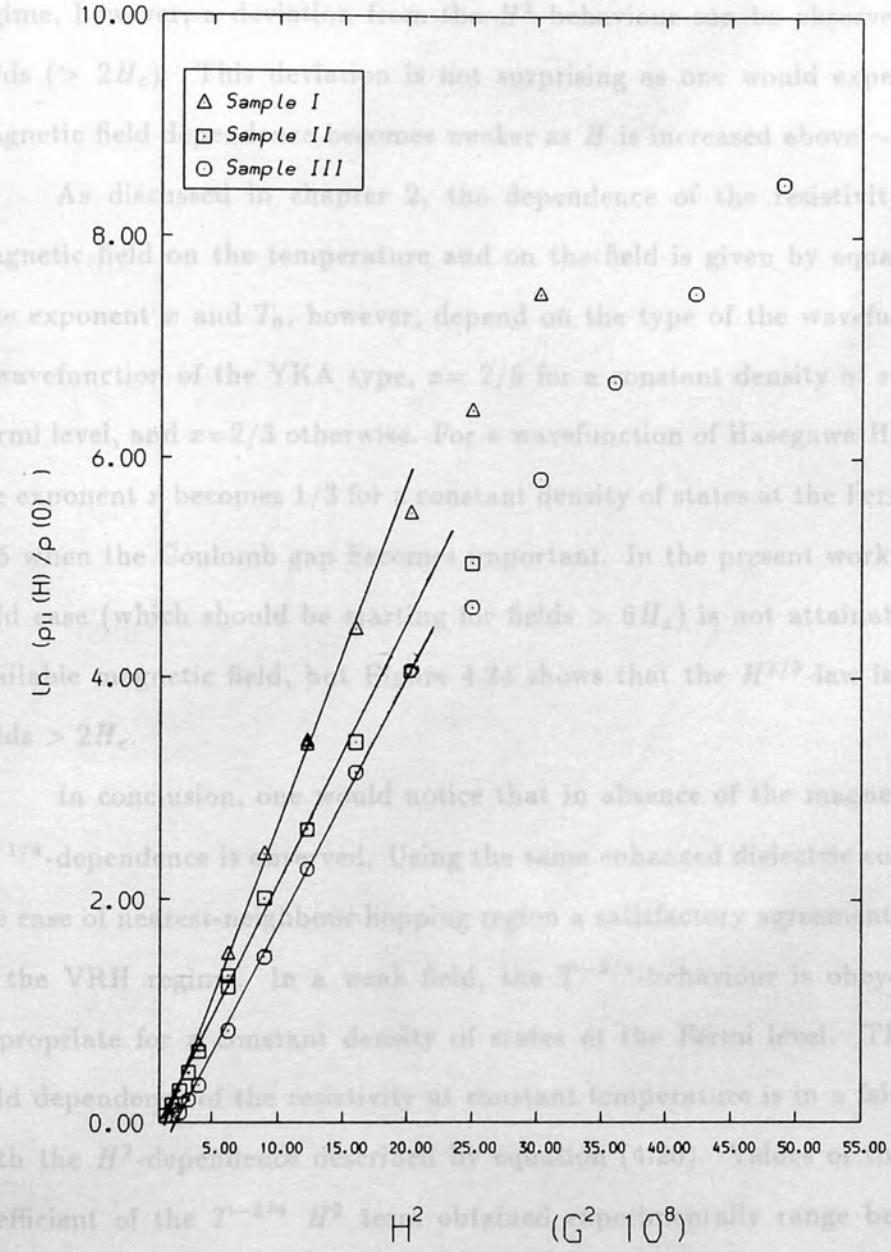

Figure 4.23

The magnetoresistance in the VRH region. The logarithm of the ratio $(\rho_{\parallel}(H)/\rho(0))$ of the resistivity in a field H divided by the resistivity in zero field is plotted as a function of H^2 of Sample I (T=0.95 K), Sample II (T=0.8 K) and Sample III (T=0.8 K)

1978).

It is worth noting that although the H^2 dependence is observed in this regime, however, a deviation from the H^2 behaviour can be observed at higher fields ($> 2H_c$). This deviation is not surprising as one would expect that the magnetic field dependence becomes weaker as H is increased above $\sim 2H_c$.

As discussed in chapter 2, the dependence of the resistivity in strong magnetic field on the temperature and on the field is given by equation (2.69). The exponent x and T_0, however, depend on the type of the wavefunction. For a wavefunction of the YKA type, x= 2/5 for a constant density of states at the Fermi level, and x=2/3 otherwise. For a wavefunction of Hasegawa-Howard type, the exponent x becomes 1/3 for a constant density of states at the Fermi level and 3/5 when the Coulomb gap becomes important. In the present work, the strong field case (which should be starting for fields $> 6H_c$) is not attainable with the available magnetic field, but Figure 4.24 shows that the $H^{1/3}$-law is obeyed for fields $> 2H_c$.

In conclusion, one would notice that in absence of the magnetic field the $T^{-1/4}$-dependence is observed. Using the same enhanced dielectric constant as in the case of nearest-neighbour hopping region a satisfactory agreement is observed in the VRH regime. In a weak field, the $T^{-3/4}$-behaviour is obeyed. This is appropriate for a constant density of states at the Fermi level. The magnetic field dependence of the resistivity at constant temperature is in a fair agreement with the H^2-dependence described by equation (4.20). Values of the numerical coefficient of the $T^{-3/4}$ H^2 term obtained experimentally range between t_1 = 0.0044 to 0.0078, whereas theory predicts a value of 0.0025. This discrepancy could be due to uncertainty in the value of T_0 which has been determined from the zero field behaviour. It has been pointed out that T_0 might vary with magnetic field. This might improve the results for the coefficient t_1.

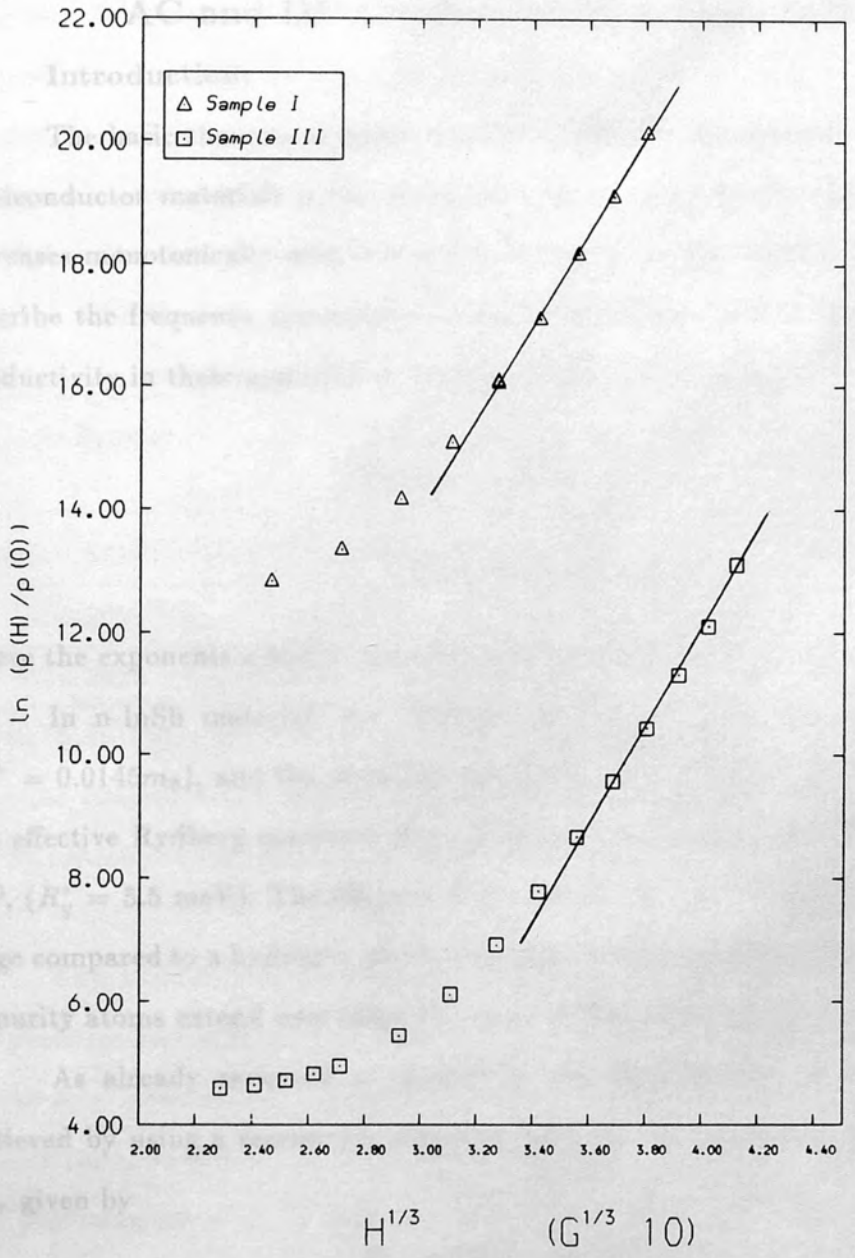

Figure 4.24

The magnetoresistance in the VRH region. The logarithm of the ratio $(\rho_{\parallel}(H)/\rho(0))$ of the resistivity in a field H divided by the resistivity in zero field is plotted as a function of $H^{1/3}2$ of Sample I (T=0.95 K) and Sample III (T=0.8 K)

CHAPTER 5

AC and DC Conduction In n-Type InSb

5.1 Introduction:

The basic theoretical result concerning the a.c. conductivity in disordered semiconductor materials is the assertion that in such systems the conductivity increases monotonically with increasing frequency. It has become a tradition to describe the frequency dependence of the experimental data of the a.c. hopping conductivity in these materials by a relationship of the form

$$Re(\sigma(\omega) - \sigma(0)) \sim \omega^s \tag{5.1}$$

$$Im\sigma(\omega) \sim \omega^{s'} \tag{5.2}$$

where the exponents s and s' are generally less than unity.

In n-InSb material, the effective mass of electron, m^*, is very small, ($m^* = 0.0145m_0$), and the dielectric constant ϵ is very large, ($\epsilon = 17.64$). Thus the effective Rydberg constant, $R_y^* = 0.65$ meV, is much smaller than that of n-InP, ($R_y^* = 5.5$ meV). The effective Bohr radius a_B^* is about 645 $\mathring{A}$, this is very large compared to a hydrogen atom. The wavefunctions associated with the donor impurity atoms extend over large distances in the host crystal.

As already reviewed in chapter 2, the MI-transition in n-InSb can be achieved by using a reasonable magnetic field and this occurs at a critical value H_{cr} given by

$$H_{cr} \propto (N_D - N_A)^{0.85} \tag{5.3}$$

for very small K or

$$(N_D a_{\parallel} a_{\perp}^2)^{1/3} = 0.26 \tag{5.4}$$

for K=0.5, with the different parameters defined in chapter 2.

Parameters of n-InSb samples used in the present work are given in table 5.1. Values of H_{cr} deduced from equation (5.4) are also included in the same table and are an increasing function of concentration. By applying high magnetic

fields ($> H_{cr}$), samples are located on the insulator side of MI-transition where measurements are carried out by changing the temperature and keeping the magnetic field constant. The a.c. conductance and the capacitance of these samples are measured in the frequency range of 110-10^5 Hz as a function of temperature, T, and magnetic field, H (in steps of 5 kG). The d.c. resistance is also measured in the same range of magnetic fields. The magnetic field is kept parallel to the current flow, and the temperature is reduced to a lowest possible value ($\sim$ 40 mK).

Sample	$(N_D - N_A)$ (cm^{-3})	N_D (cm^{-3})	H_{cr} (kG)
5714	5.7×10^{14}	9.63×10^{14}	8
9914	9.9×10^{14}	1.68×10^{15}	18
2015	2.0×10^{15}	3.23×10^{15}	32

Table 5.1: Parameters of the n-InSb samples. N_D and N_A are the donor and acceptor concentrations respectively. H_{cr} is the critical magnetic field (at which MI transition occurs), calculated from equation (5.4).

The variation of real part of the conductivity, $\sigma(\omega)$, with frequency, temperature and magnetic field is presented in section 5.2. It is found that the excess a.c. conductivity, calculated from the relation $\sigma_{a.c.}(\omega) = \sigma(\omega) - \sigma(0)$ follows the power-law ω^s, with the exponent s being temperature-dependent, but becoming constant at very low temperature and high magnetic fields. The temperature dependence of the conductivity is stronger than the linear relationship predicted by the pair approximation theory. In section 5.3 the dependence of the real part of the conductivity on temperature, magnetic field and frequency will be analysed in the light of the scaling formula suggested by Summerfield (1985). In section 5.4 the temperature and magnetic field dependence of the zero frequency limit of the conductivity, $\sigma(0)$, will be discussed. Section 5.5 is devoted to discuss the data obtained from the capacitive part. Analysis of this part shows that the

relative dielectric constant derived from the capacitive part tends to diverge as the magnetic field approaches H_{cr}.

5.2 Temperature, Frequency and Magnetic Field Dependence of the Real Part of the Conductivity:

Measurements on sample 5714 were carried out in magnetic fields $H \geq 15$ kG in steps of 5 kG. The temperature dependence of the real part of the conductivity, $\sigma(\omega)$, and the d.c. component, $\sigma(0)$, at different magnetic fields are shown in Figures 5.1-5.4 as σ versus the reciprocal of temperature, $1/T$. On sample 9914, measurements have been made in magnetic fields ≥ 30 kG. Figures 5.5, 5.6 (a) and (b) show the temperature dependence of this sample at three different magnetic fields (60, 50 and 45 kG respectively). For the more doped sample 2015, the threshold field at which MI-transition occurs is expected to be higher than the other two samples, (refer to table 5.1). For this sample measurements were made for fields ≥ 40 kG. Figures 5.7, 5.8 (a) and (b) show the behaviour of the conductivity of this sample as a function of temperature at different magnetic fields and frequencies. From these graphs one would observe the following:

(a) In the higher temperature range, a sharp exponential drop in the conductivity occurs. In this range, the d.c. conductivity coincides with the low frequency component of the a.c. conductivity. The sharp decrease in σ is due to the freeze-out of electrons from the conduction band onto the donor sites. This is well known as " magnetic-freeze-out", a mechanism which has already been observed, frequently, in these materials (see, e.g., Ferre et al. 1975, Mansfield and Kusztelan 1978, Robert et al. 1980).

(b) As the temperature is reduced, the decrease in $\sigma(\omega)$ is less pronounced. In this region the conductivity is realised to be in the hopping region and it is characterised by an abrupt departure, the a.c. component becomes much less temperature dependent than the d.c. component. In this range $\sigma(\omega)$ is orders of magnitude higher than $\sigma(0)$. The ω^s-dependence is obeyed with the exponent "s" being temperature-dependent and less than unity.

(c) At much lower temperatures, depending on the magnetic field, $\sigma(\omega)$ becomes independent of temperature and weakly dependent on magnetic field for higher values of the field. In this region, the d.c. component becomes too small to measure, and the exponent s is almost unity.

In the case when the a.c. and d.c. conductions are due to totally separate and different processes, or when the same basic process is responsible for both types of conduction, but the states giving rise to the a.c. conductivity are clustered and do not form a percolation path throughout the sample, i. e., do not contribute to the d.c. conduction, then it seems natural to write the total measured conductivity at frequency ω in the form

$$\sigma(\omega) = \sigma(0) + \sigma_{a.c.}(\omega) \tag{5.5}$$

Long and Balkan (1980) (see also Long 1982) have used this formula to analyse their data on amorphous Ge. This is motivated by the fact that the a.c. and d.c. conductivities at high temperatures coincide. The implication of this equation is that there are two independent mechanisms by which charge transfers under the action of an a.c. electric field; the first corresponding to frequency-independent percolating of charges from electrode to electrode and the second to the frequency-dependent mechanism. However, $\sigma(\omega)$ for n-InSb increases monotonically with frequency and it increases only weakly with the temperature. Therefore, the pure a.c. component of the conductivity will dominate at high frequencies and/or low temperatures. This is simply due to the fact that the temperature dependence of the d.c. conductivity is always much greater than that of a.c. part. In such cases, separation of the conductivity into a.c. and d.c. components as in eq. (5.5) will have negligible effect on the analyses.

The temperature dependence of $\sigma(\omega)$ becomes progressively weaker as the temperature is reduced. Detailed analyses on d.c. measurements in a similar temperature range by many authors (see, e.g., Walton and Dutt 1977, Tokumoto et al. (1980), Mansfield and Tokumoto (1983), Abdul-Gader (1984)) show the absence of a wide range constant activation energy at such lower temperatures for these materials and the conductivity is believed to be of the VRH type. The

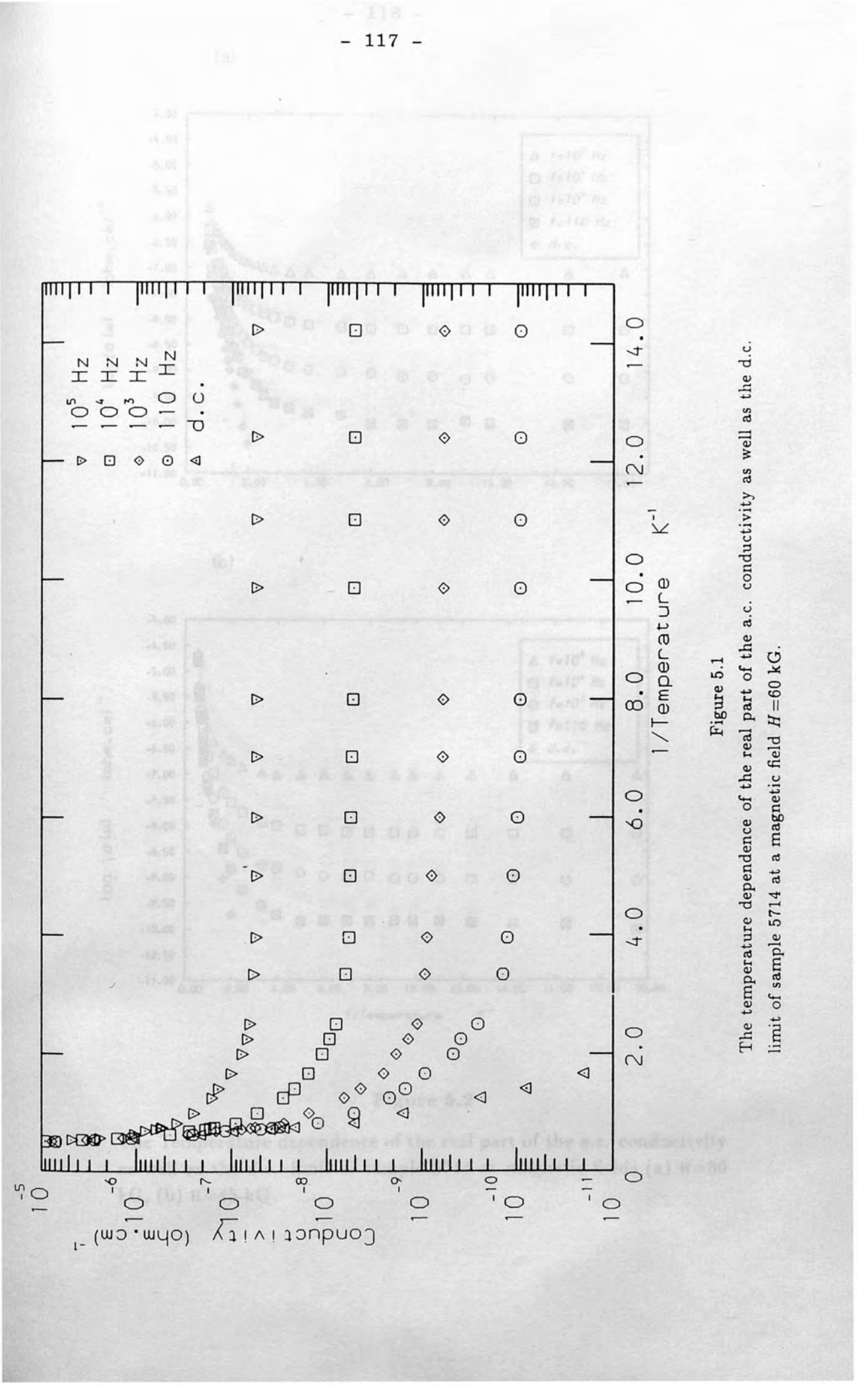

Figure 5.1

The temperature dependence of the real part of the a.c. conductivity as well as the d.c. limit of sample 5714 at a magnetic field H=60 kG.

(a)

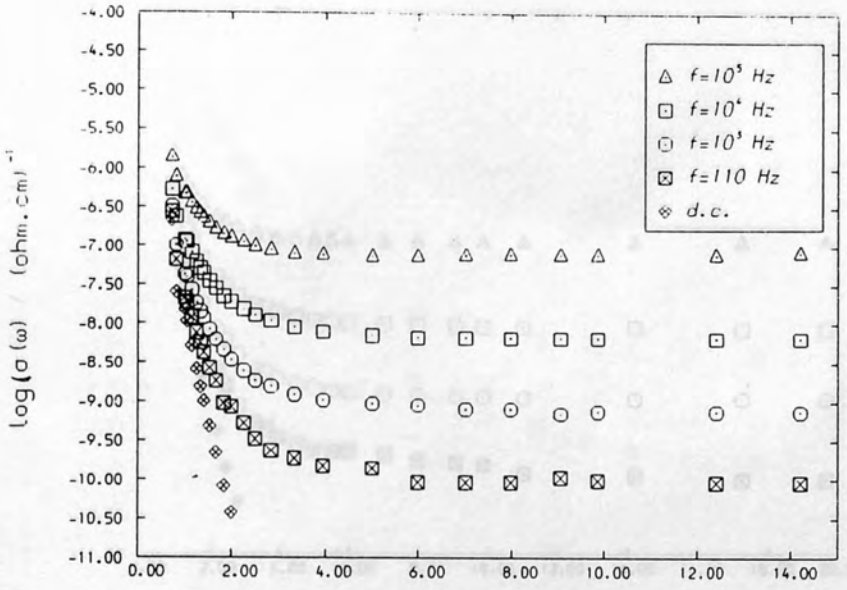

(b)

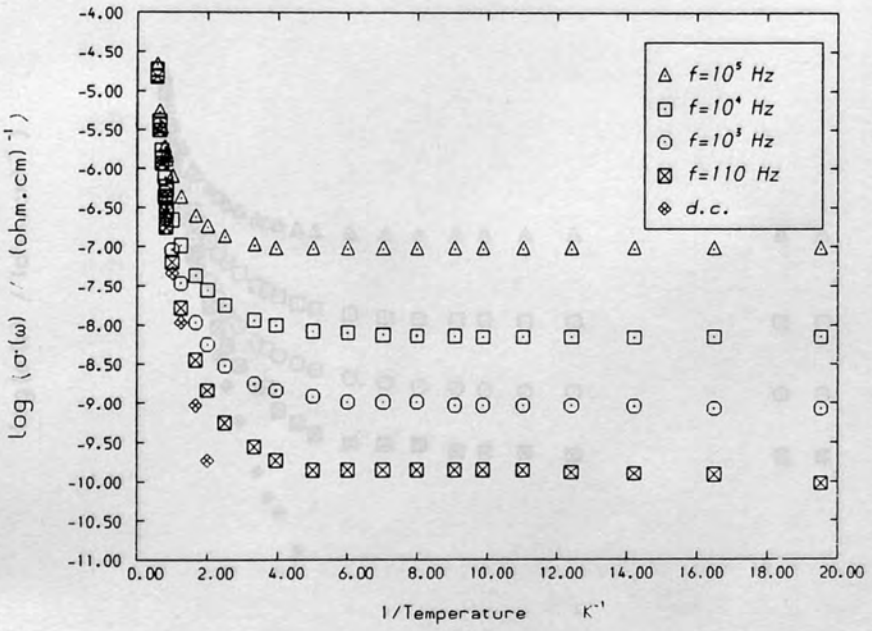

Figure 5.2

The Temperature dependence of the real part of the a.c. conductivity as well as the d.c. limit of sample 5714 at magnetic fields (a) H=50 kG, (b) H=45 kG.

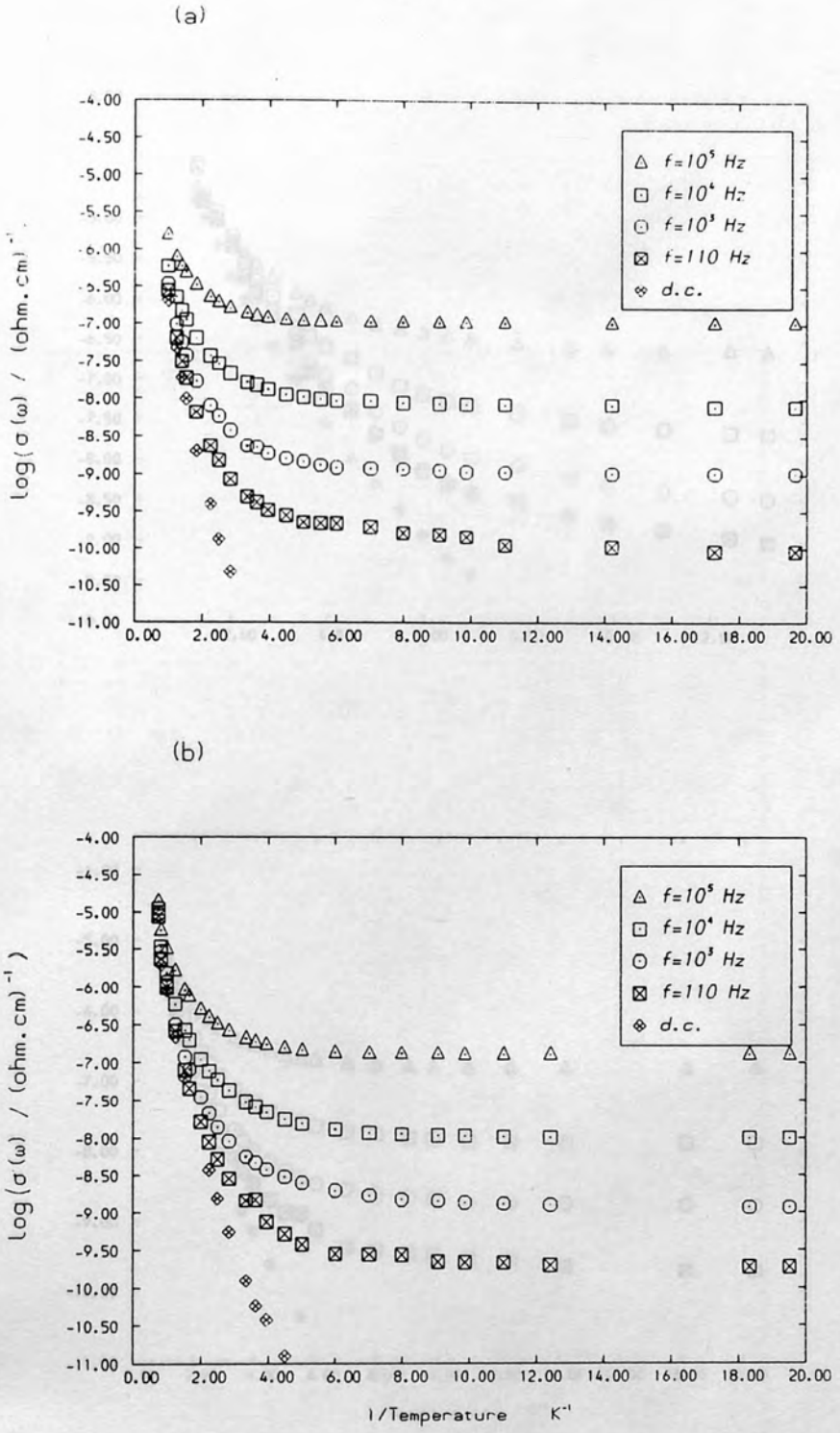

Figure 5.3

The temperature dependence of the real part of the a.c. conductivity as well as the d.c. limit of sample 5714 at magnetic fields (a) H=40 kG, (b) H=35 kG.

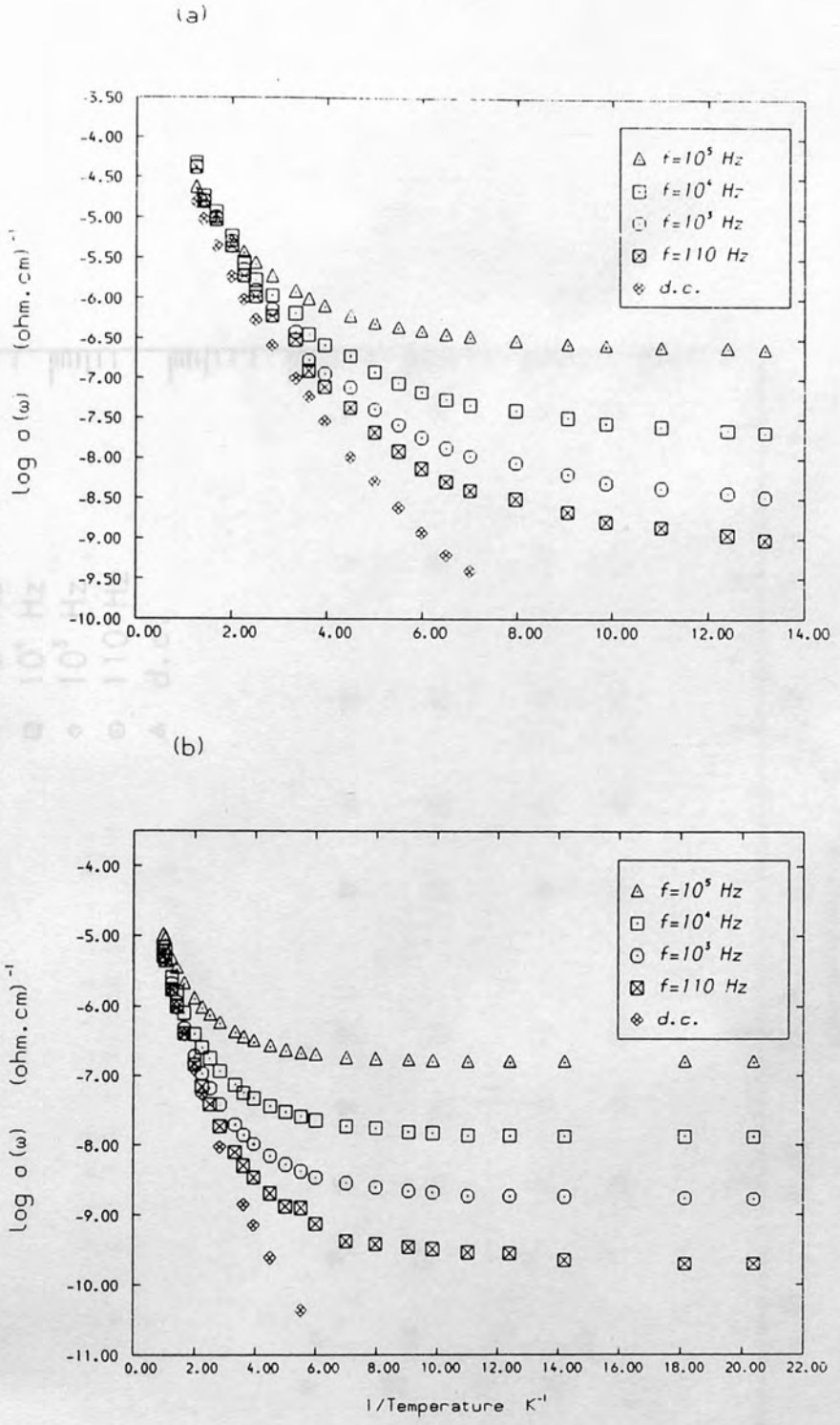

Figure 5.4

The temperature dependence of the real part of the a.c. conductivity as well as the d.c. limit of sample 5714 at magnetic fields (a) H=25 kG, (b) H=30 kG.

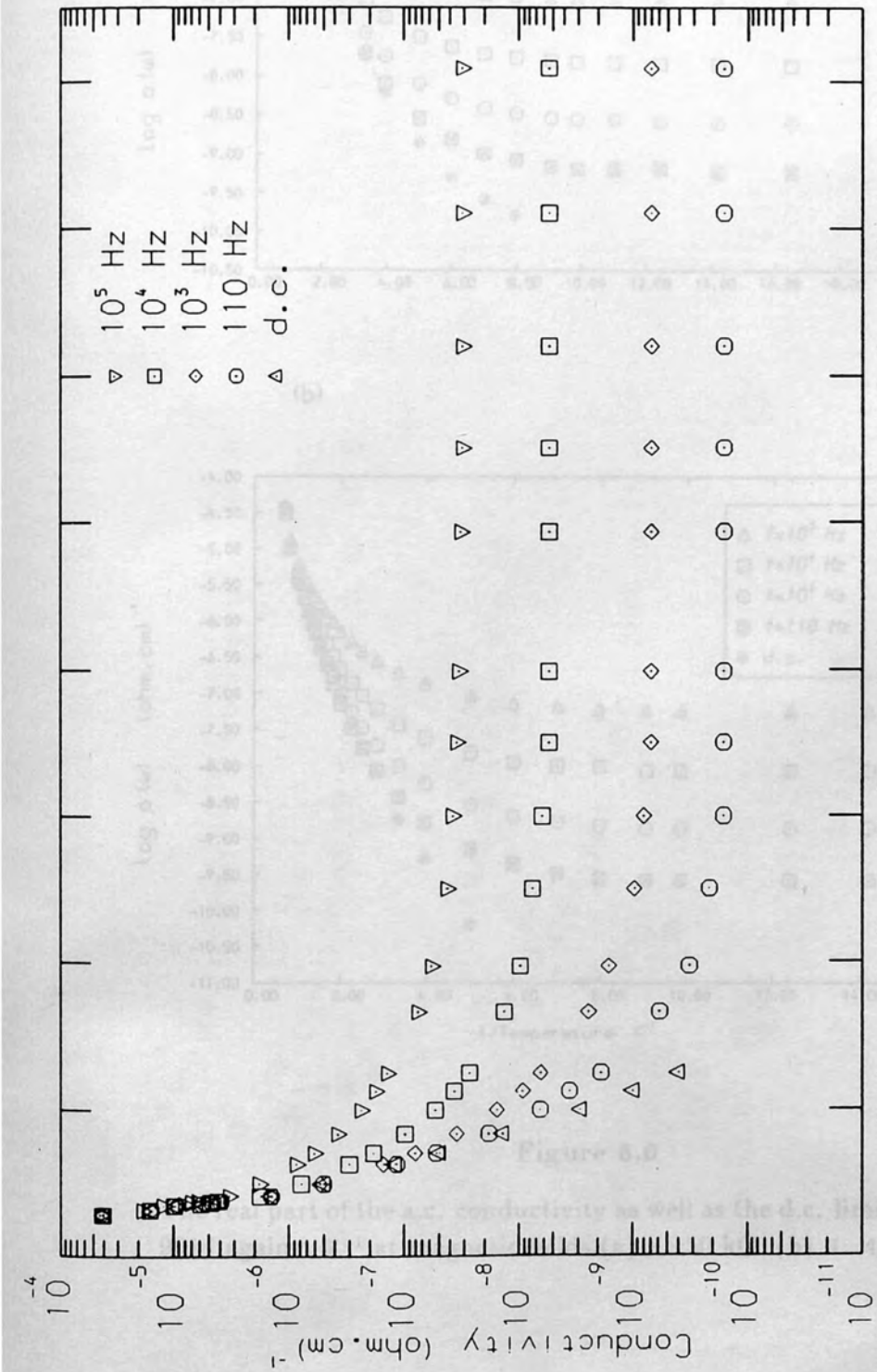

Figure 5.5

The temperature dependence of the real part of the a.c. conductivity as well as the d.c. limit of sample 9914 at a magnetic field H=60 kG.

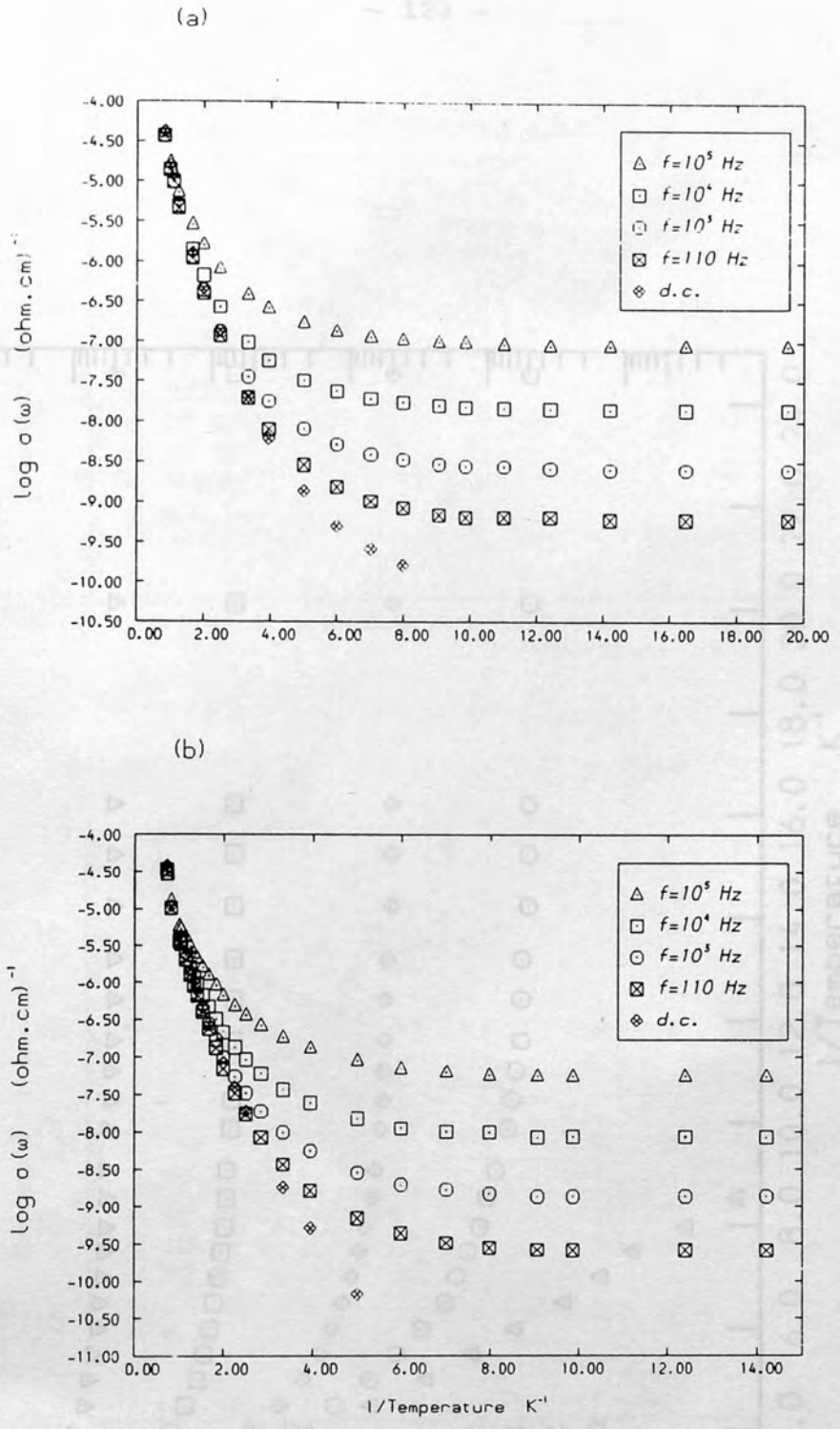

Figure 5.6

The real part of the a.c. conductivity as well as the d.c. limit of sample 9914 against T^{-1} at magnetic fields (a) H=50 kG, (b) H=45 kG.

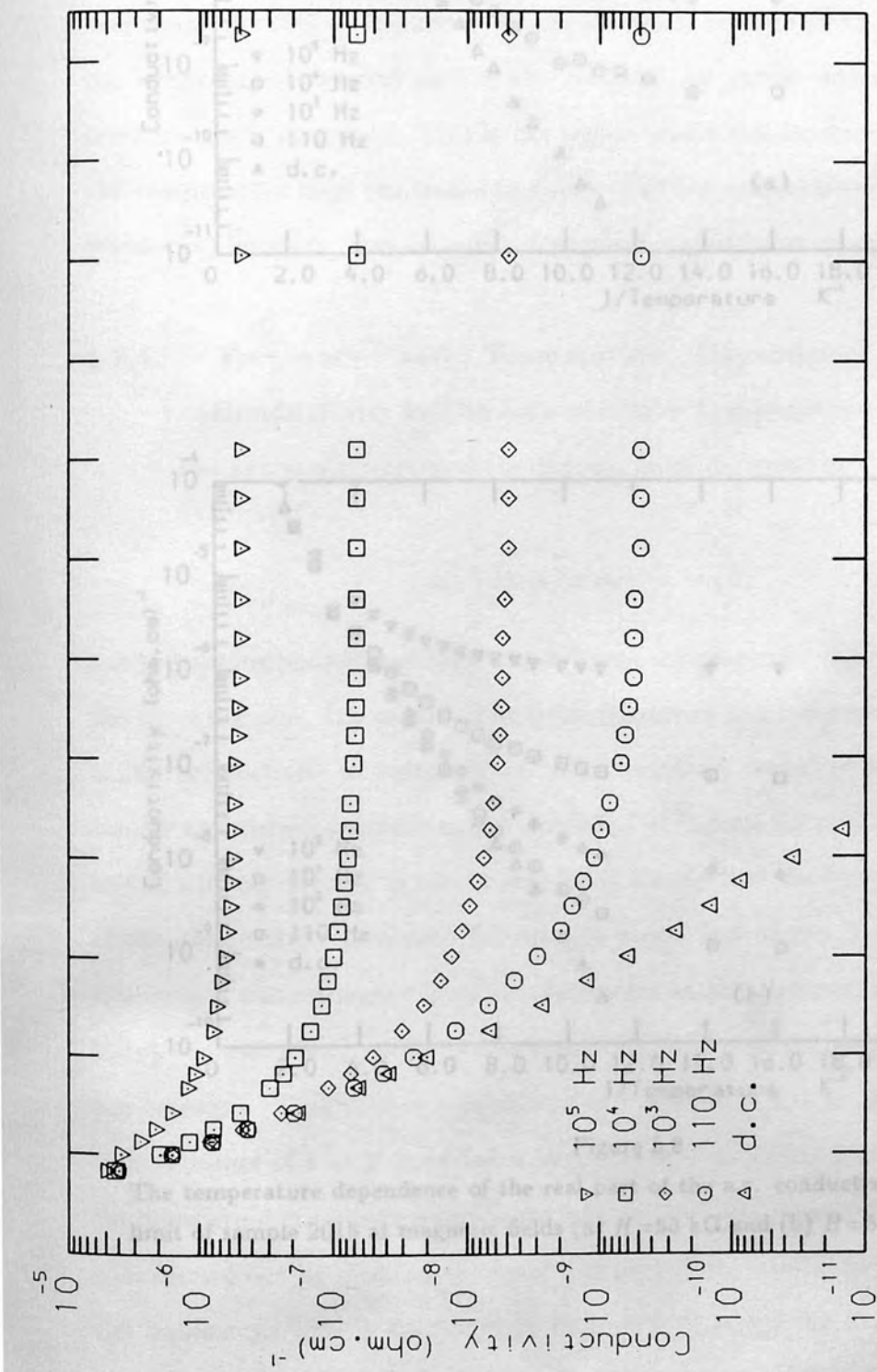

Figure 5.7

The temperature dependence of the real part of the a.c. conductivity as well as the d.c. limit of sample 2015 at a magnetic field H=60 kG.

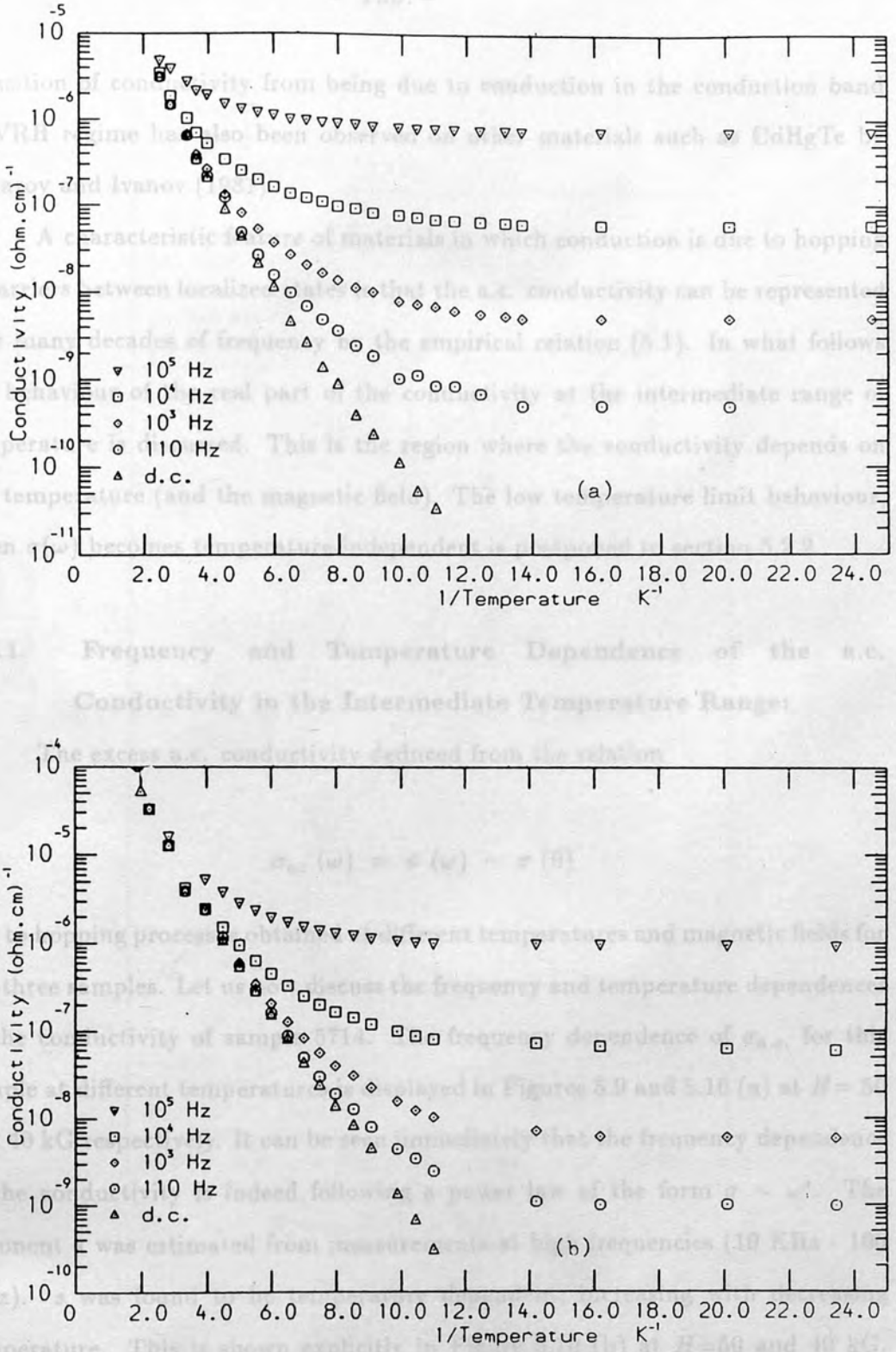

Figure 5.8

The temperature dependence of the real part of the a.c. conductivity as well as the d.c. limit of sample 2015 at magnetic fields (a) H=55 kG and (b) H=50 kG.

transition of conductivity from being due to conduction in the conduction band to VRH regime has also been observed on other materials such as CdHgTe by Elizarov and Ivanov (1981).

A characteristic feature of materials in which conduction is due to hopping of carriers between localized states is that the a.c. conductivity can be represented over many decades of frequency by the empirical relation (5.1). In what follows the behaviour of the real part of the conductivity at the intermediate range of temperature is discussed. This is the region where the conductivity depends on the temperature (and the magnetic field). The low temperature limit behaviour, when $\sigma(\omega)$ becomes temperature-independent is postponed to section 5.2.2.

5.2.1 Frequency and Temperature Dependence of the a.c. Conductivity in the Intermediate Temperature Range:

The excess a.c. conductivity deduced from the relation

$$\sigma_{ac}(\omega) = \sigma(\omega) - \sigma(0)$$

due to hopping process is obtained at different temperatures and magnetic fields for the three samples. Let us now discuss the frequency and temperature dependences of the conductivity of sample 5714. The frequency dependence of $\sigma_{a.c.}$ for this sample at different temperatures is displayed in Figures 5.9 and 5.10 (a) at H= 50 and 40 kG respectively. It can be seen immediately that the frequency dependence of the conductivity is indeed following a power law of the form $\sigma \sim \omega^s$. The exponent s was estimated from measurements at high frequencies (10 KHz - 100 KHz). s was found to be temperature dependent, increasing with decreasing temperature. This is shown explicitly in Figure 5.10 (b) at H=50 and 40 kG. The variation of s as T is varied is also observed for samples 9914 and 2015 and the data are demonstrated in Figure 5.11 (a) and (b) respectively. Analyses are also carried out by plotting the total real part of the conductivity ($\sigma(\omega)$) against the frequency. This is presented in Figures 5.12-14 for the three samples. It is obvious that the slope, dlog$\sigma(\omega)$/dlogω is indeed temperature dependent.

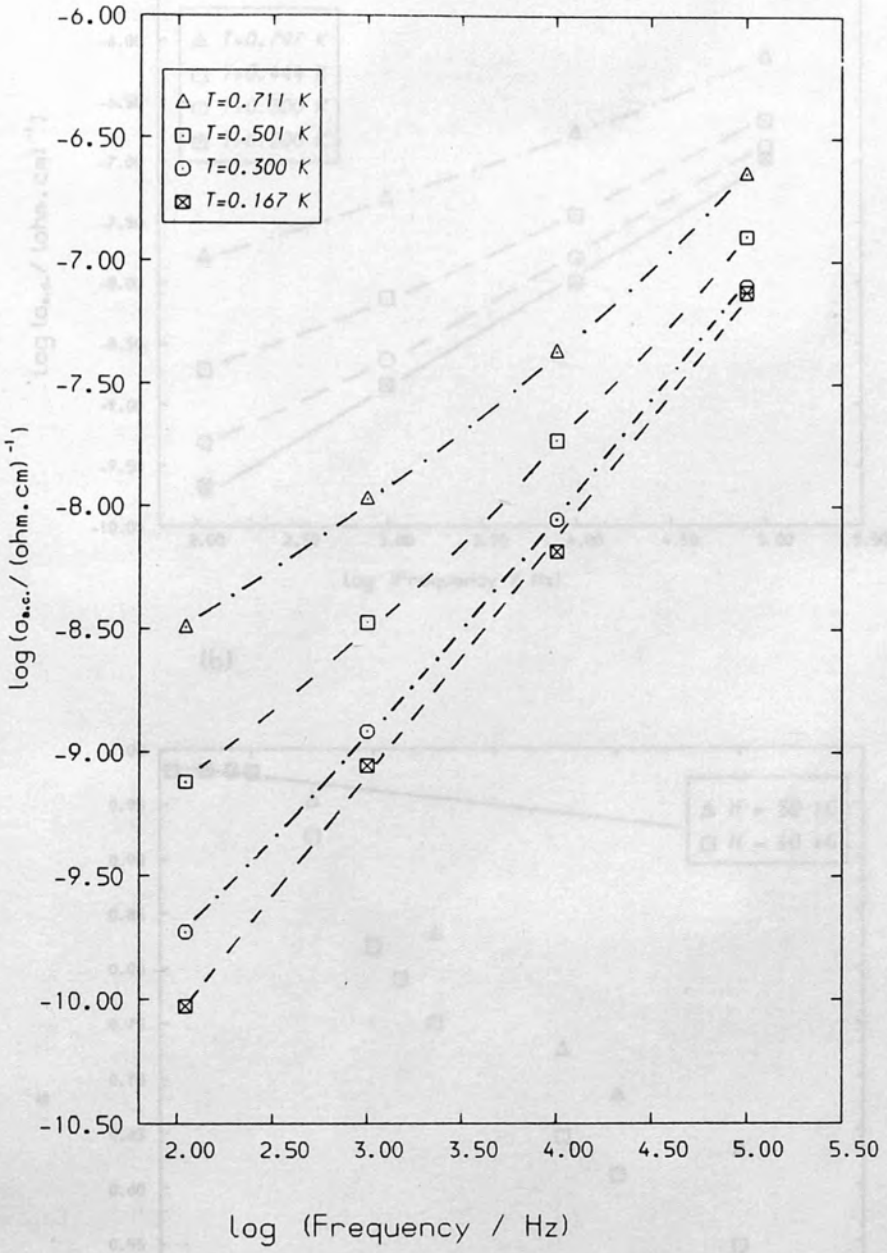

Figure 5.9

The frequency dependence of $\sigma_{a.c.}(\omega)$ of sample 5714 at H=50 kG and different temperatures.

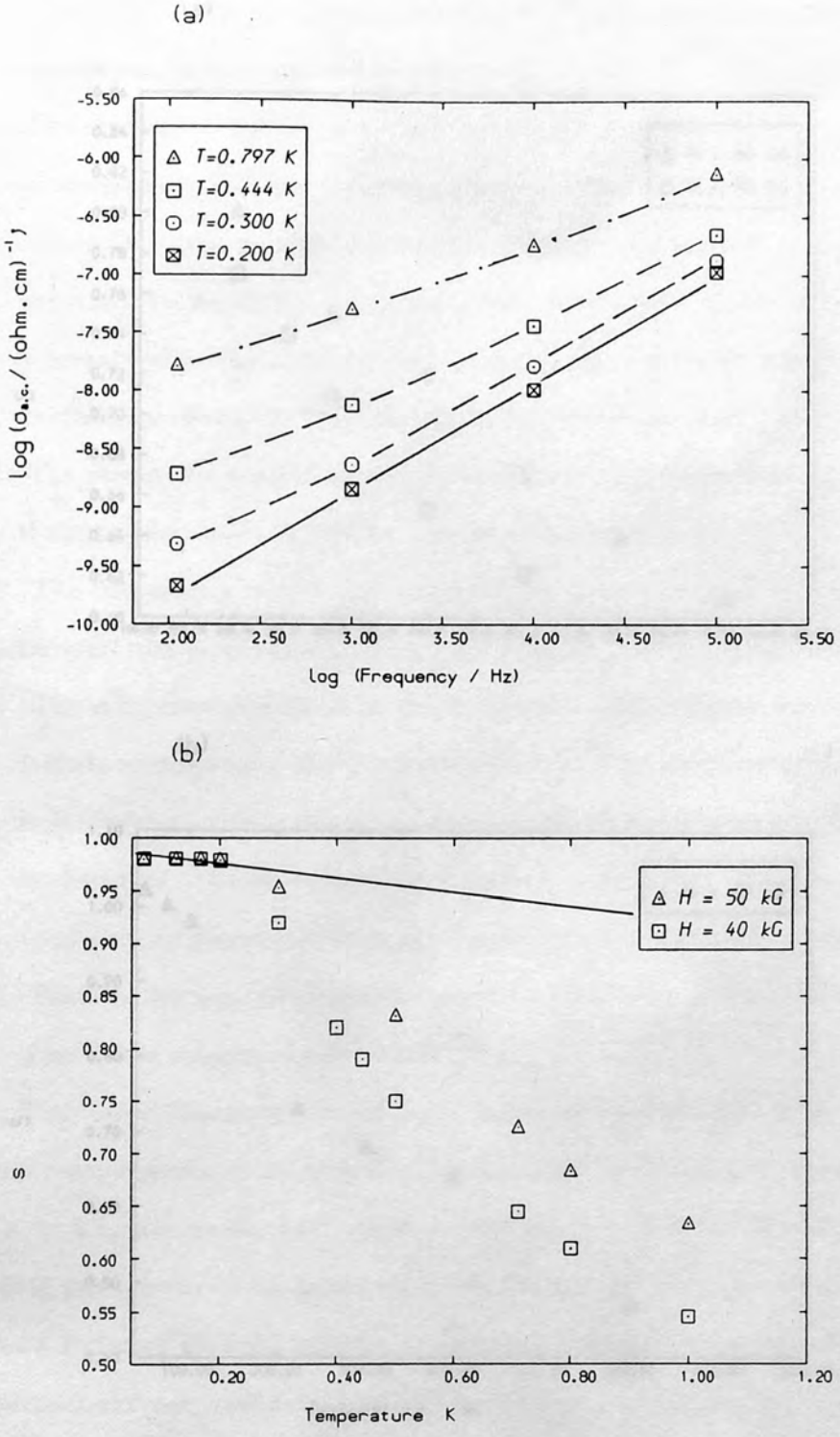

Figure 5.10

(a) The frequency dependence of $\sigma_{a.c.}(\omega)$ of sample 5714 at H=40 kG and different temperatures. (b) The temperature dependence of the exponent s of sample 5714 at fields H=50 kG and 40 kG. The solid line is the calculation from eq.(5.9).

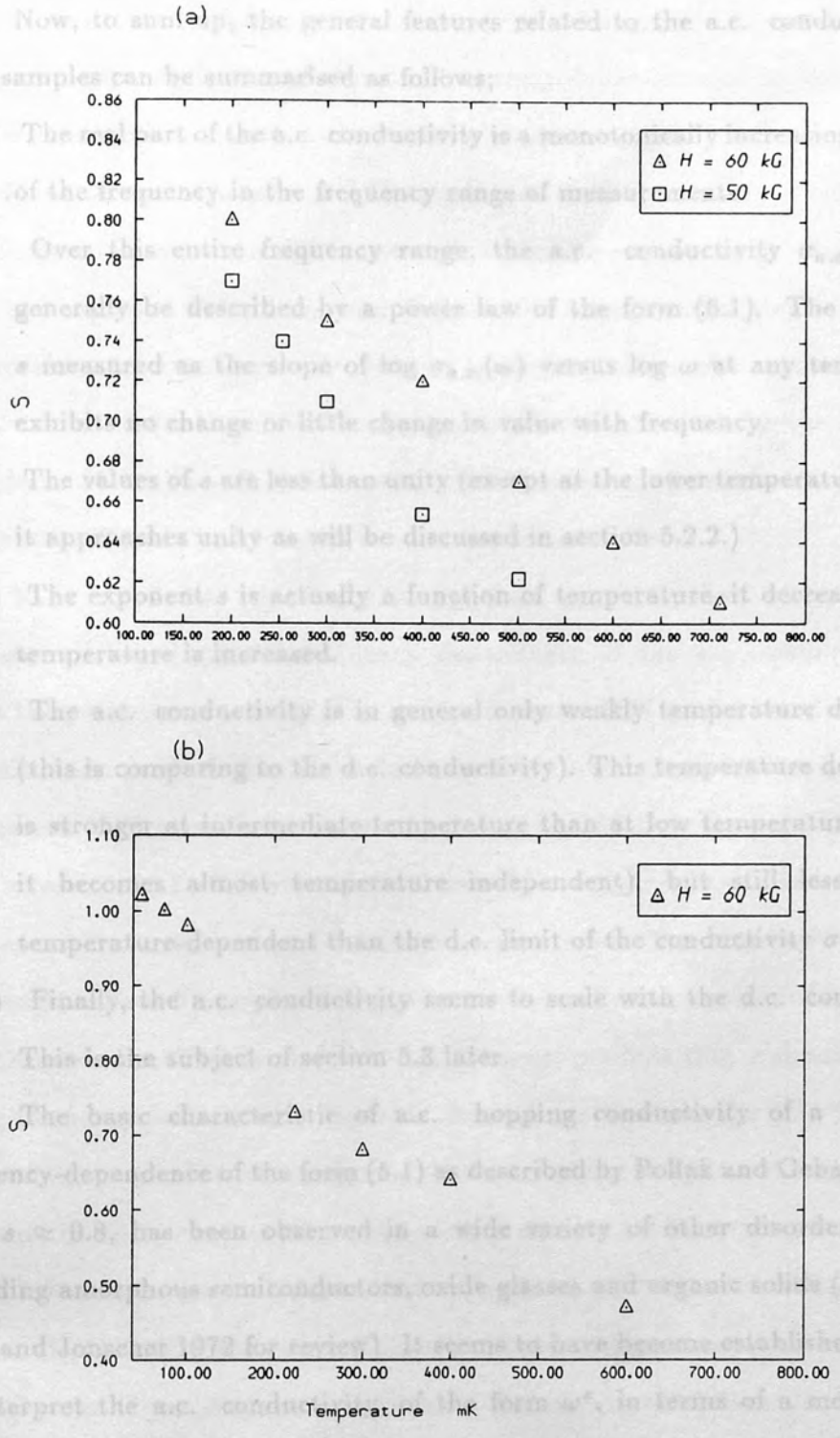

Figure 5.11

The temperature dependence of the exponent s of (a) Sample 9914 and (b) Sample 2015.

Now, to sum up, the general features related to the a.c. conductivity of these samples can be summarised as follows;

(a) The real part of the a.c. conductivity is a monotonically increasing function of the frequency in the frequency range of measurements.

(b) Over this entire frequency range, the a.c. conductivity $\sigma_{a.c.}(\omega)$, can generally be described by a power law of the form (5.1). The exponent s measured as the slope of log $\sigma_{a.c.}(\omega)$ versus log ω at any temperature exhibits no change or little change in value with frequency.

(c) The values of s are less than unity (except at the lower temperatures where it approaches unity as will be discussed in section 5.2.2.)

(d) The exponent s is actually a function of temperature, it decreases as the temperature is increased.

(e) The a.c. conductivity is in general only weakly temperature dependent, (this is comparing to the d.c. conductivity). This temperature dependence is stronger at intermediate temperature than at low temperatures (where it becomes almost temperature independent), but still less strongly temperature-dependent than the d.c. limit of the conductivity $\sigma(0)$.

(f) Finally, the a.c. conductivity seems to scale with the d.c. conductivity. This is the subject of section 5.3 later.

The basic characteristic of a.c. hopping conductivity of a power-law frequency-dependence of the form (5.1) as described by Pollak and Geballe (1961), with $s \approx 0.8$, has been observed in a wide variety of other disordered solids, including amorphous semiconductors, oxide glasses and organic solids (see Elliott 1987 and Jonscher 1972 for review). It seems to have become established practice to interpret the a.c. conductivity, of the form ω^s, in terms of a model which considers conduction to occur by means of tunnelling between neighbouring donor impurity states, randomly distributed in energy and space. This tunnelling model (two-site model) predicts that the frequency dependence of the conductivity is of the type $\sigma \sim \omega^s$, with s given by

$$s = \frac{d \ln \sigma(\omega)}{d \ln \omega} = 1 - 4/\ln(\nu_{ph}/\omega) \qquad (5.6)$$

which implies that the exponent s is temperature independent. Equation (5.6) has been used intensively in interpreting the frequency dependence of the conductivity in some semiconductor materials. However it does not predict the temperature dependence of the exponent s. The variation of the exponent s with T has been observed in some amorphous semiconductor films (see, e. g., Narasimhan, Guha and Agarwal 1976, Long and Balkan 1980). It is interesting to see from the experimental data that some features in the studied n-InSb samples serve to exclude some of the theoretical models used normally to describe the frequency dependence of $\sigma_{a.c.}(\omega)$. In this respect, the behaviour of the exponent s with the temperature T and the frequency ω is an important feature.

It is noted that the experimental data presented here show that the exponent s, describing the frequency dependence of the a.c. conductivity is indeed temperature-dependent, The straightforward QMT model based on the pair approximation predicts that s should be temperature-independent and according to equation (5.6) at an intermediate frequency ($\sim 10^4$ Hz), for $\nu_{ph} = 10^{12}$ Hz, s has a value of ~ 0.8. Our experimental data however show that s is a decreasing function as T is increased and takes values even lower than this prediction. For lower values of $s < 0.8$ one has to consider unphysically small values of ν_{ph} varying with temperature. Furthermore, the QMT model predicts that s should increase as the frequency is decreased. However, no such increase in s (as ω is lowered) is observed in the present measurements. Indeed, the above figures show that if any curvature in $\log \sigma(\omega)$ versus $\log \omega/2\pi$ plots is observed it is in the opposite sense, i. e., s is in fact frequency independent or slowly an increasing function of ω. This fact manifests itself at any magnetic field and temperature as can be seen clearly in these Figures. These discrepancies between the experimental data and the theory might be considered as an evidence against the QMT model. Additional evidence against QMT model as being the dominant mechanism of a.c. conduction can be extracted from the temperature dependence of the conductivity.

In contrast to the d.c. conductivity in the case of VRH regime described by the Mott $T^{-1/4}$-law, the QMT model predicts that $\sigma\ (\omega)$ is varying only linearly

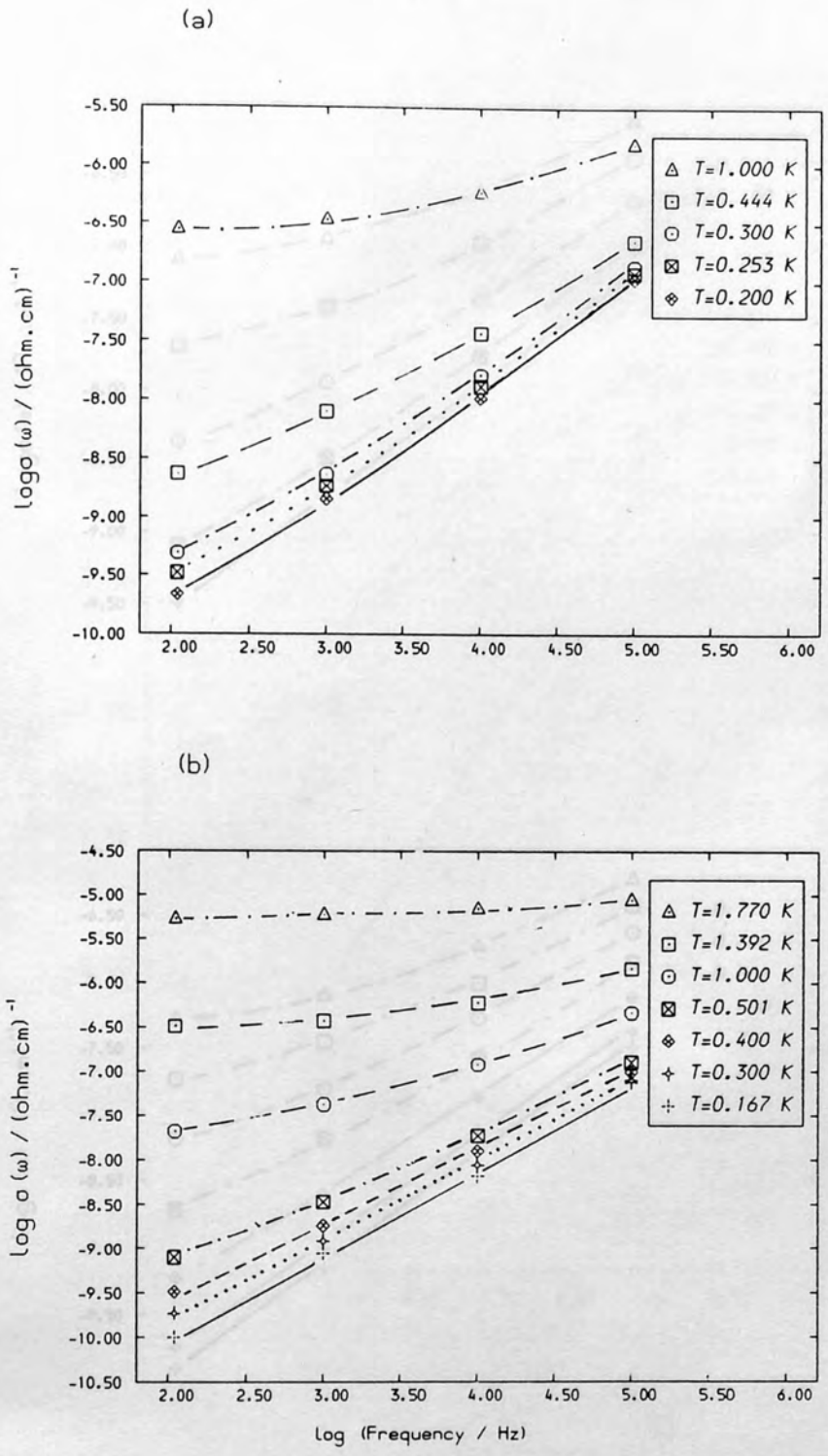

Figure 5.12

The frequency dependence of the conductivity $\sigma(\omega)$ of sample 5714 at different temperatures and at fields (a) H=40 kG, (b) H=50 kG.

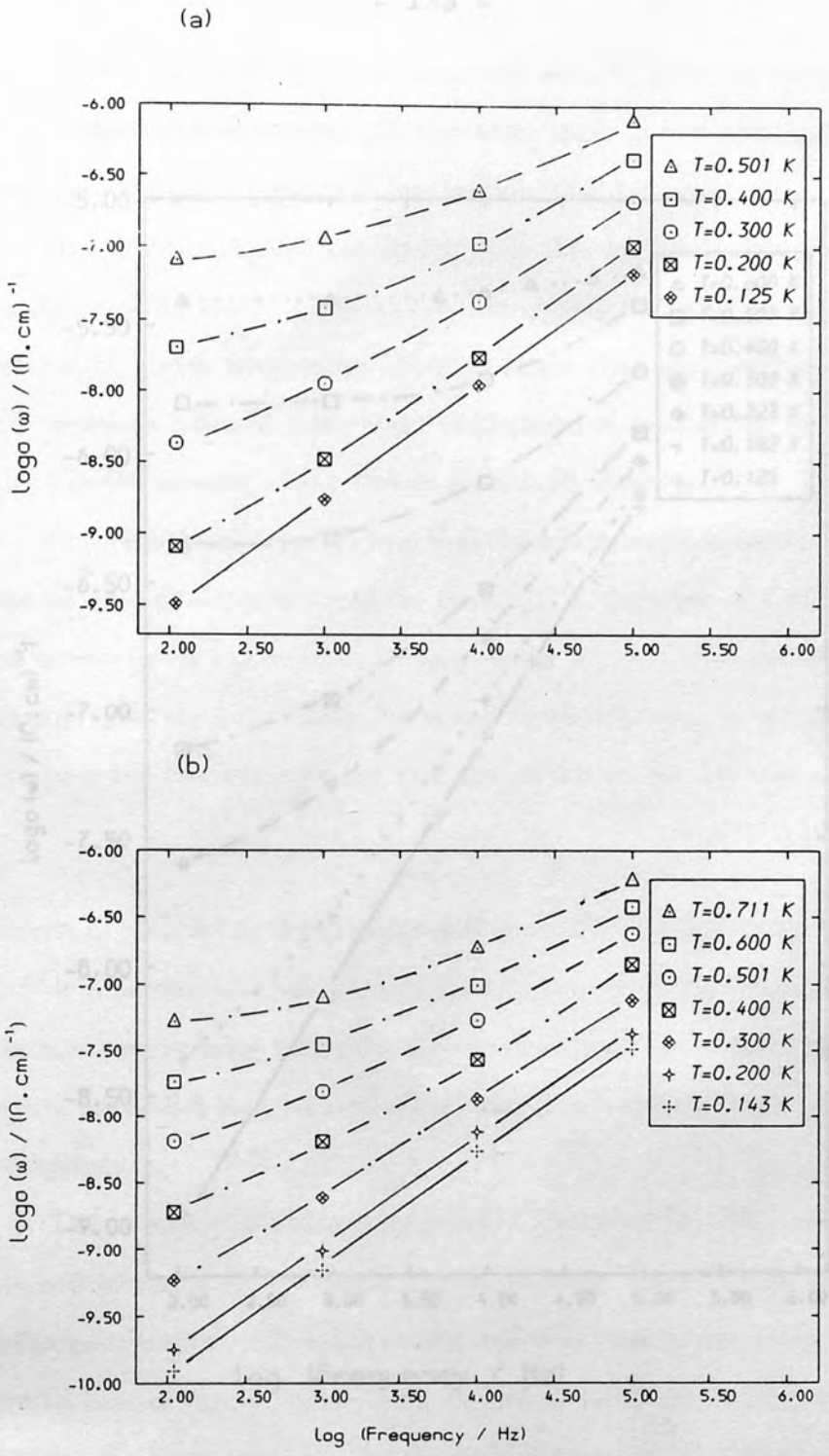

Figure 5.13

The frequency dependence of the conductivity $\sigma(\omega)$ of sample 9914 at different temperatures and at fields (a) H=50 kG, (b) H=60 kG.

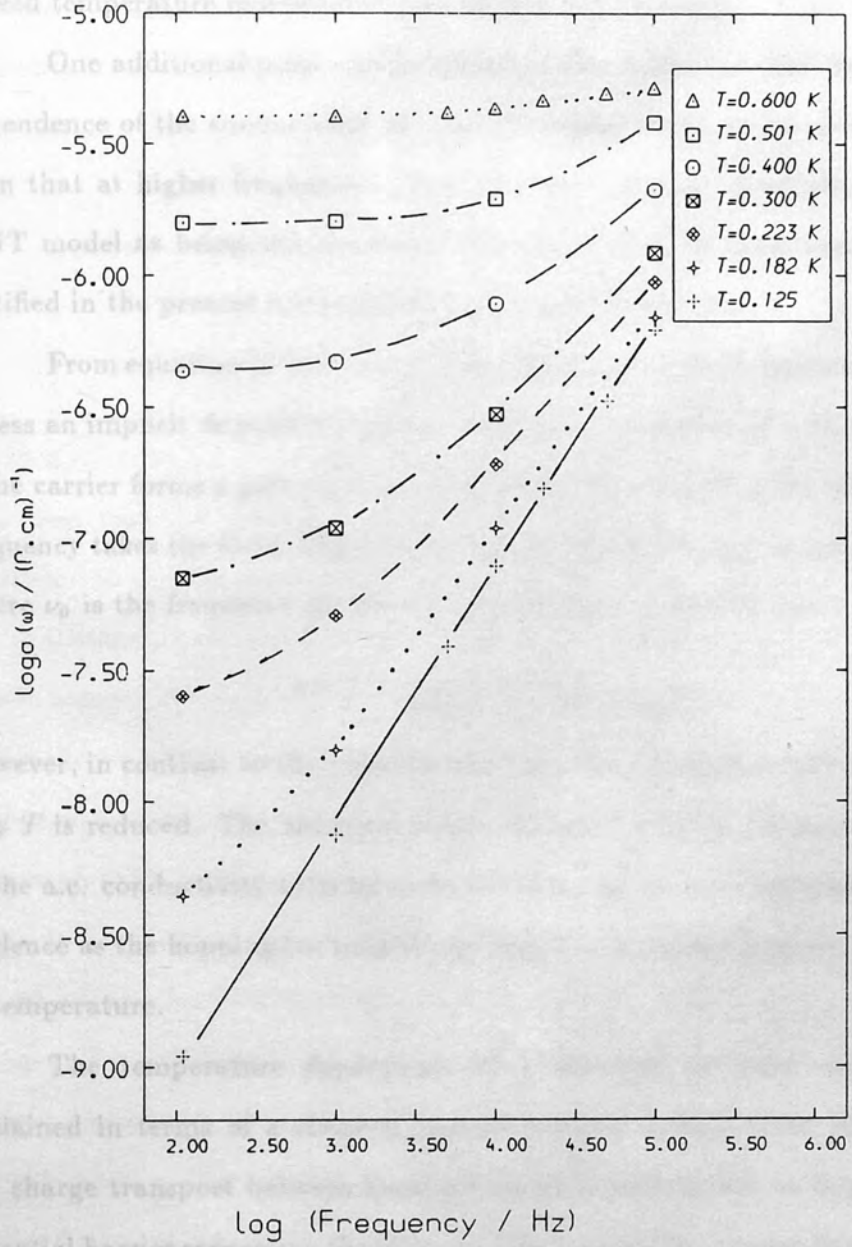

Figure 5.14

The frequency dependence of the conductivity $\sigma(\omega)$ of sample 2015 at different temperatures and at a magnetic field H= 60 kG.

with the temperature T. Such temperature dependence seems to be weaker than the experimental observations. On the other hand, at low temperatures, $\sigma(\omega)$ is indeed temperature independent (see section 5.2.2 below).

One additional point can be added in this respect is that the temperature dependence of the conductivity at lower frequency seems to be more pronounced than that at higher frequencies. Now, it seems that the possibility of using the QMT model as being the dominant mechanism of conduction cannot be totally justified in the present measurements on n-InSb materials.

From equation (5.6) it is seen that there is no explicit dependence of s on T, unless an implicit dependence of the term ν_{ph}. A variation of s with T is possible if the carrier forms a polaron of binding energy W_p; therefore the effective phonon frequency takes the form (Mott, Davis and Street 1975) $\nu_{ph} = \nu_0 \exp(-W_p/2k_BT)$, where ν_0 is the frequency for the undistorted lattice. In this case s is given by

$$s = 1 - \frac{4}{[\ln(\nu_0/\omega) - W_p/2k_BT]} \tag{5.7}$$

However, in contrast to the experimental data this equation predicts a decrease of s as T is reduced. The variation of the exponent s of the frequency dependence of the a.c. conductivity with temperature thus can be considered as an important evidence as the hopping (or tunnelling) length at a certain frequency is a function of temperature.

The temperature dependence of s observed in some oxides has been explained in terms of a classical barrier hopping model, (Pike 1972), in which the charge transport between localised states is mainly due to hopping over the potential barrier separating the sites. In Pike's model the energy barrier is reduced below its maximum value W_m by Coulomb interaction and takes the form

$$W = W_m - \frac{e^2}{\epsilon r} \tag{5.8}$$

where r is the separation of the sites, and ϵ is the dielectric constant. Following the treatment of Pike, Long and Balkan (1980) have shown that for a single electron transfer s is given by

$$s = 1 - \frac{6k_BT}{W_m} \tag{5.9}$$

In Figure 5.10 (b) we plot values of s calculated from equation (5.9) against the temperature T. It is obvious that the agreement becomes very poor as the temperature is increased. Since the derivation of equation (5.9) is based on the assumption of single electron transfer, one would question its validity at higher temperature where multiple hops might take place.

Generally, we can assume that for hopping conduction the conductivity is given by

$$\sigma(\omega, T) \sim \omega^s T^d \tag{5.10}$$

where $d = 1$ and $s \approx 0.8$ for the pair approximation. Firstly, it has already been seen that the frequency dependence of σ might even be weaker than this prediction as the temperature is increased. Secondly, the temperature dependence of σ is stronger than the theoretical prediction. These observations have been also seen in some other materials (see, e. g., Yushida and Arizumi 1976 and Manukyan and Andreev 1976). It has been observed that even the weakest temperature dependence as given in Manukyan and Andreev (1976) and earlier by Owen and Robertson (1970) can be approximated by the above equation with d = 3-5.

In Figures 5.15 we plot for sample 5714 $\sigma_{a.c.}(\omega)$ versus T on log-log scale at H= 50 kG and four different frequencies (namely; 110, 10^3, 10^4 and 10^5 Hz). The exponent d is calculated as the slope of the straight portion of the obtained lines at these frequencies. These are, 3.88, 3.35, 2.69, 2.03 respectively. Figure 5.16 (a) and (b) shows a similar behaviour for the same sample at H= 60 and 40 kG. The obtained data of d at these fields are as follows. At H= 60 kG, d takes the values 3.01, 2.85, 2.21 and 1.66. When H becomes 40 kG the calculated values of the exponent d are 3.76, 3.28, 2.68 and 2. The similarity in the behaviour is obvious that is d is an increasing function as the frequency is decreased and always greater than 1. In Figures 5.17 and 5.18 (a) and (b) we replot for the same sample $\sigma(\omega)$, without subtracting the d.c. limit, against T on log-log scale. Data given here are at three fields 60, 50, 40 kG respectively. The deduced values of d are summarised in table 5.2. These data indeed confirm the previous observations that d is greater

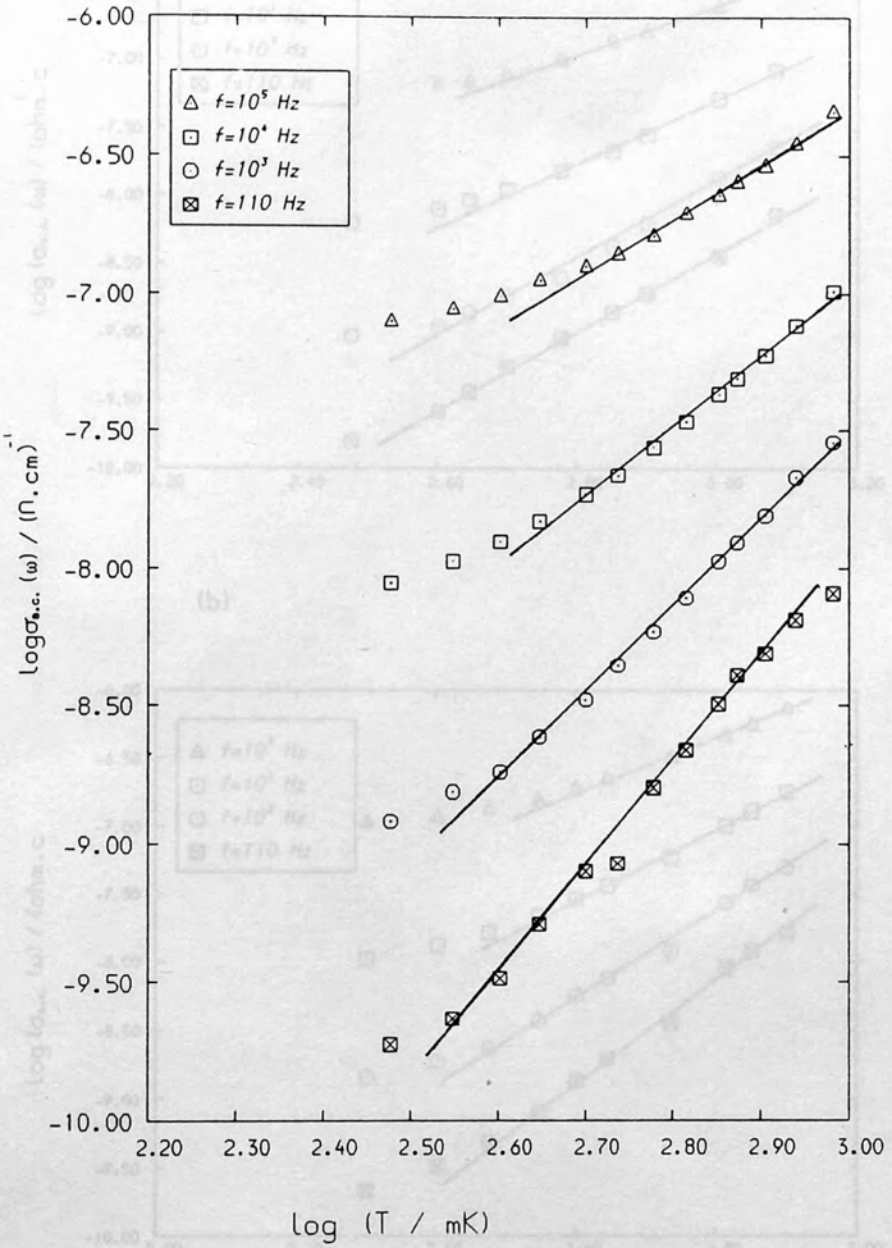

Figure 5.15

The conductivity $\sigma_{a.c.}(\omega)$ of sample 5714 as a function of the temperature T at a magnetic field H=50 kG.

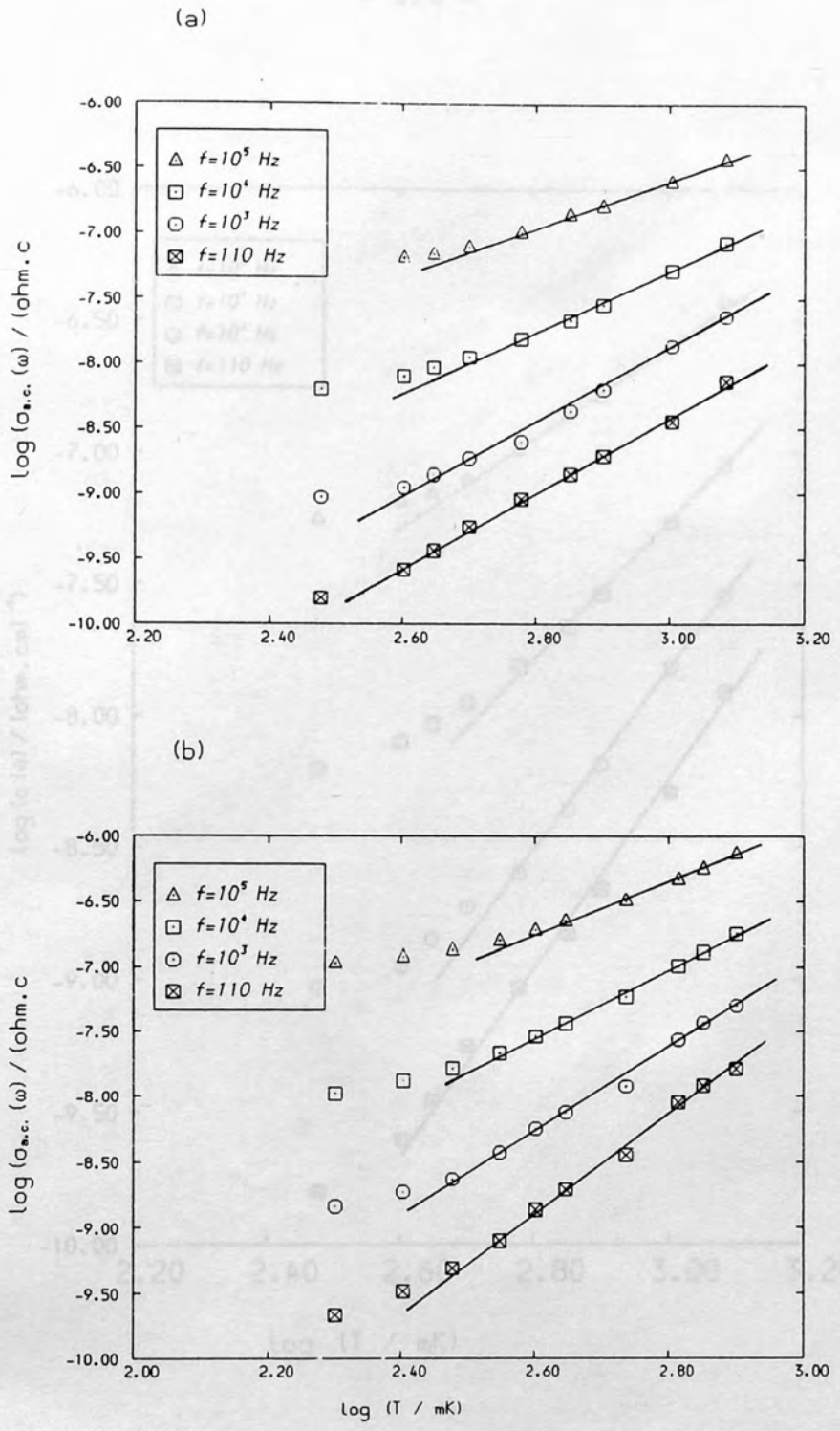

Figure 5.16

The conductivity $\sigma_{a.c.}(\omega)$ as a function of the temperature T, on a log-log scale of sample 5714 at magnetic fields (a) H=60 kG and (b) H=40 kG.

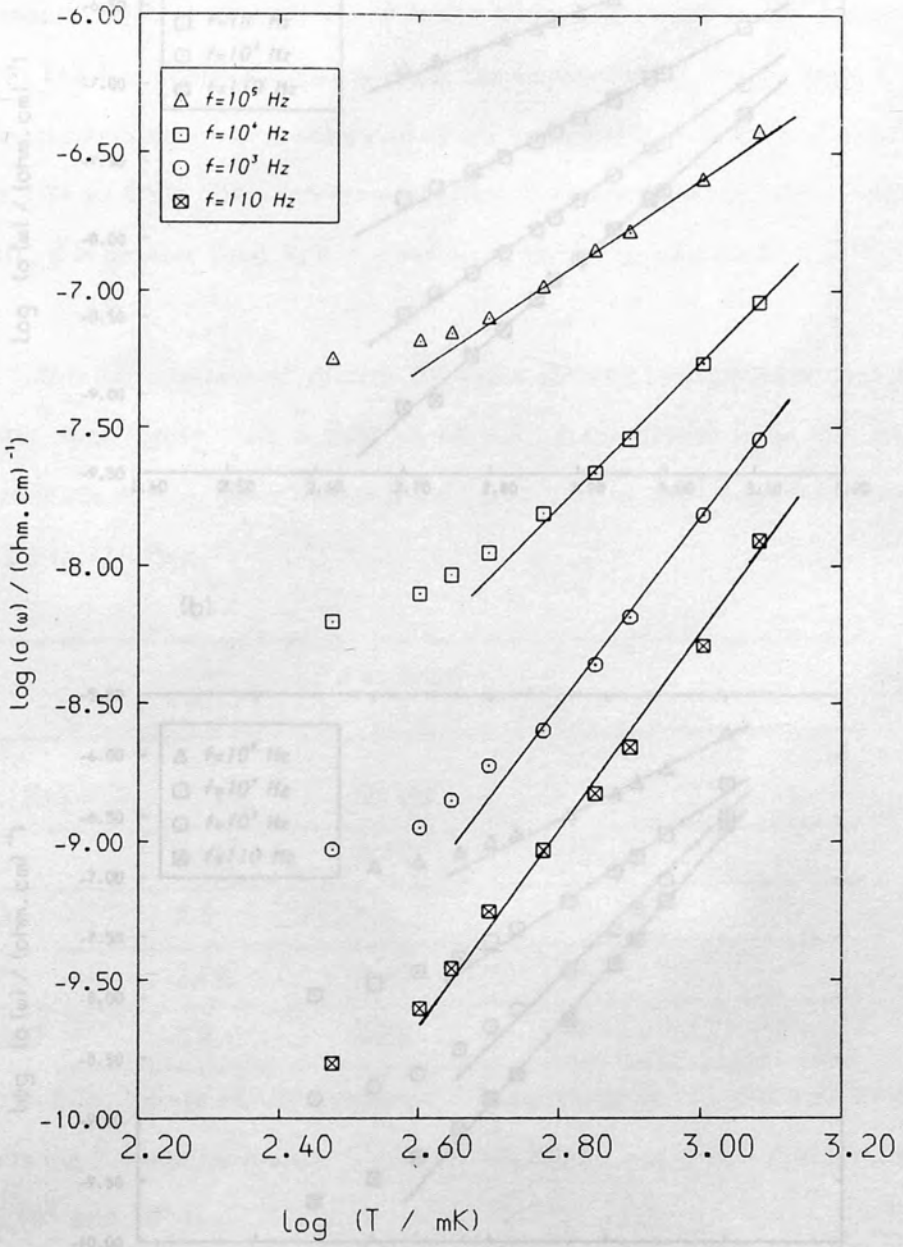

Figure 5.17

The conductivity $\sigma(\omega)$ of sample 5714 as a function of temperature T on a log-log scale at a magnetic field H=60 kG.

(a)

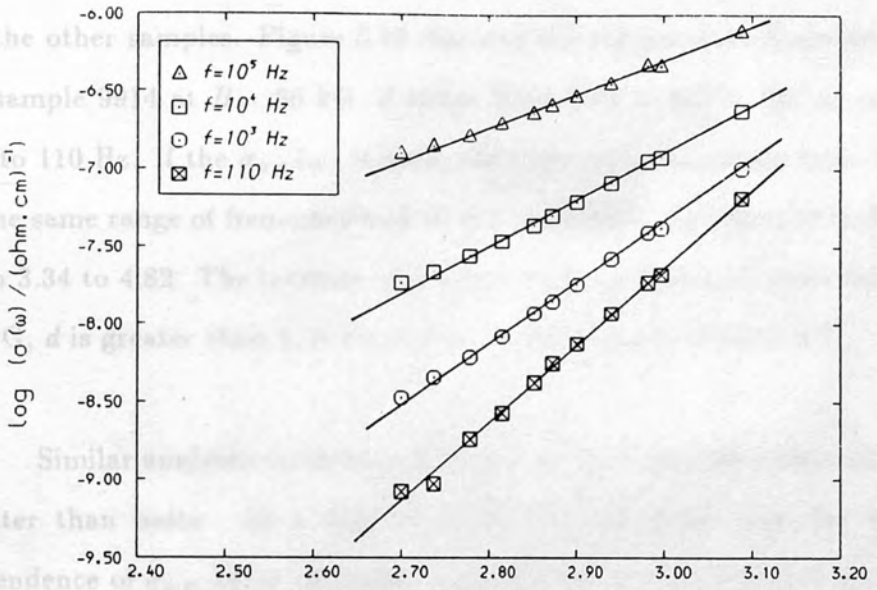

(b)

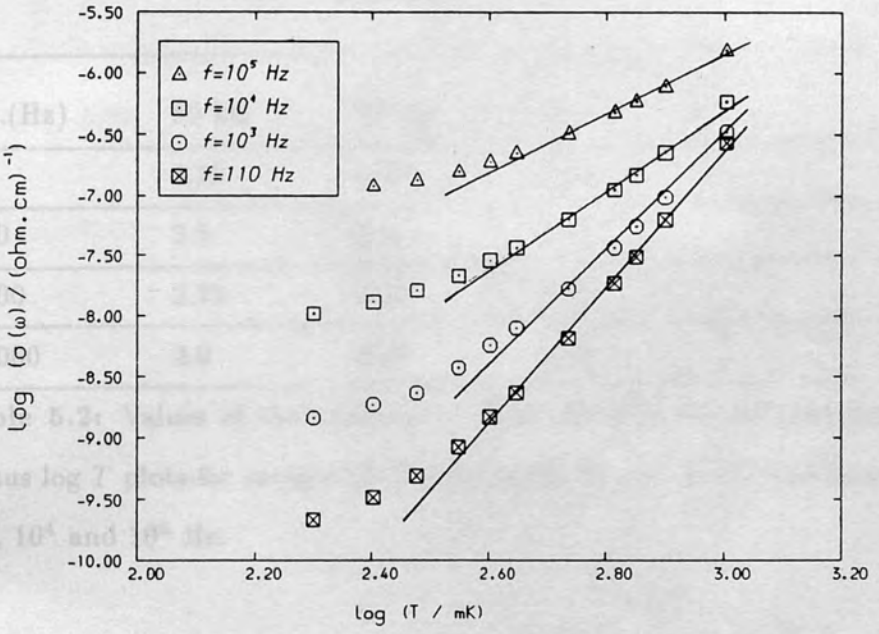

Figure 5.18

The conductivity $\sigma(\omega)$ against the temperature, on log-log scale, of sample 5714 at fields (a) H=50 kG and (b) H=40 kG.

than 1 and increases as the frequency is decreased. Similar behaviour is observed for the other samples. Figure 5.19 displays the temperature dependence of $\sigma(\omega)$ for sample 9914 at $H=$ 60 kG. d varies from 3.23 to 6.2 in the frequency range 10^5 to 110 Hz. If the $\sigma_{a.c.}(\omega)$ is used, the exponent d increases from 2.46 to 4.07 in the same range of frequency and at the same field. At a field of 50 kG, d varies from 3.34 to 4.82. The increase of d above 1 also is found at lower fields. At $H=$ 40 kG, d is greater than 1, it has values in the range of 3.53 to 4.6.

Similar analyses on sample 2015 also showed that the exponent d is indeed greater than unity. At a field of 55 kG, d calculated from the temperature dependence of $\sigma_{a.c.}$ takes values from 1.3 to 2.34 as the frequency decreases from 10^5 Hz to 110 Hz.

	d at fields		
freq.(Hz)	60 kG	50 kG	40 kG
110	4.12	5.44	6.25
1000	3.5	4.2	5.26
10000	2.72	3.28	4.01
100000	2.0	2.48	2.88

Table 5.2: Values of the exponent d in equation (5.10) deduced from log $\sigma(\omega)$ versus log T plots for sample 5714 at fields 60, 50 and 40 kG and frequencies 110, 10^3, 10^4 and 10^5 Hz.

From all these calculations one would observe that the determined values of the exponent d are indeed greater than 1. Its value depends on the frequency, d is smaller for higher frequency. These observations together with the lower values of $s(< 0.8)$ suggest that the pair approximation model is incapable of explaining the observed data. The pair approximation model is based on the assumption that the distance to a third impurity atom is much greater than the distance r_ω

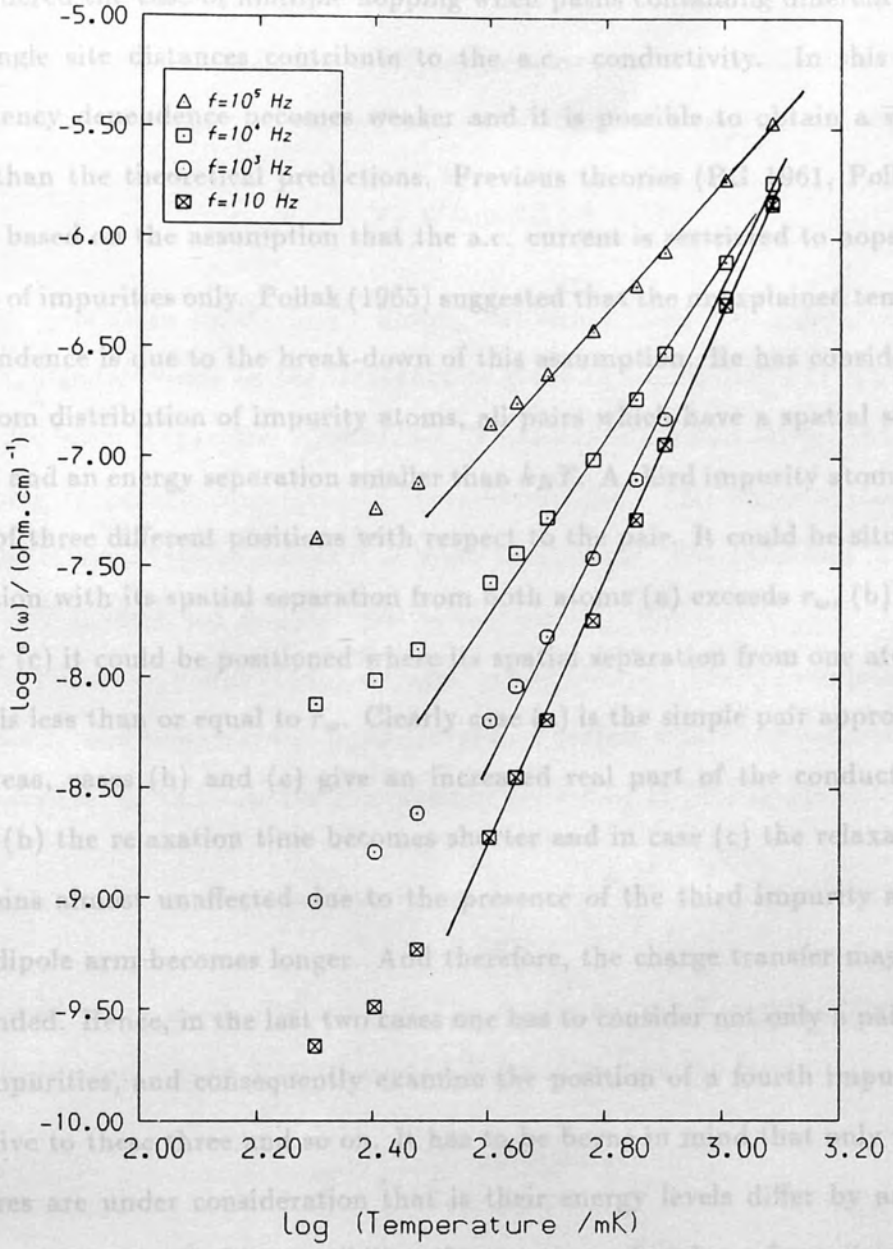

Figure 5.19

The conductivity σ (ω) of sample 9914 against the temperature T on a log-log scale at a magnetic field H=60 kG.

inside the pair. As r_ω is given by equation (2.81), thus, it is governed by the frequency ω, it decreases only slowly with increasing frequency. Pollak (1965) has considered the case of multiple hopping when paths containing different numbers of single site distances contribute to the a.c. conductivity. In this case the frequency dependence becomes weaker and it is possible to obtain a value of s less than the theoretical predictions. Previous theories (PG 1961, Pollak 1964) were based on the assumption that the a.c. current is restricted to hops between pairs of impurities only. Pollak (1965) suggested that the unexplained temperature dependence is due to the break-down of this assumption. He has considered, in a random distribution of impurity atoms, all pairs which have a spatial separation of r_ω and an energy separation smaller than k_BT. A third impurity atom can have one of three different positions with respect to the pair. It could be situated in a position with its spatial separation from both atoms (a) exceeds r_ω, (b) less than r_ω or (c) it could be positioned where its spatial separation from one atom of the pair is less than or equal to r_ω. Clearly case (a) is the simple pair approximation, whereas, cases (b) and (c) give an increased real part of the conductivity. In case (b) the relaxation time becomes shorter and in case (c) the relaxation time remains almost unaffected due to the presence of the third impurity atom, but the dipole arm becomes longer. And therefore, the charge transfer may be more extended. Hence, in the last two cases one has to consider not only a pair but trio of impurities, and consequently examine the position of a fourth impurity atom relative to these three and so on. It has to be borne in mind that only resonance centres are under consideration that is their energy levels differ by an amount not exceeding k_BT. The possibility of occurrence of such configuration increases with increasing k_BT or simply the temperature T. Thus, one might conclude that clusters of three, four etc. centres can be formed and the electron can hop twice, thrice or even more in one half-period of the external electrical field depending on the size of the cluster leading to an increase in the conductivity. It is apparent that the likelihood of such multiplets increases with increasing r_ω. Obviously, such multiplet hopping conduction weakens the frequency dependence but in the

meanwhile strengthens the temperature dependence. An increase dependence of the conductivity on r_ω means a decrease dependence on ω, the multiple hops then will result in a decreased frequency dependence in addition to the increased temperature dependence. The temperature/concentration at which multiple hops will become important is estimated by Pollak (1965) to be given roughly by

$$N_D \sim 0.007 r_T^3 / r_\omega^6 \tag{5.11}$$

where r_T is given by $e^2/\epsilon k_B T$. Hence, this temperature depends inversely upon r_ω^6. r_ω itself depends on the frequency as given by equation (2.81) in such a way that for lower frequencies r_ω is higher. Therefore one would expect that multiple hopping to become important at lower frequencies. This might account for the higher values of the exponent d at lower frequencies. The reduction in the value of s as T is increased also can now be understood.

Following Pollak (1965), Klyatskina and Shlimak (1978) considered only the frequency and temperature dependences of a system where the multiple hopping is operative. In this case the conductivity is written as (Pollak 1965)

$$\sigma(\omega, T) \sim r_\omega r_T \sum_{n_1^2=1}^{n_1} n_1^2 \left(\frac{n_1 r_\omega^2}{r_T} \right)^{n_1} \tag{5.12}$$

where n_1^2 is the number of bonds in the cluster for which $r \leq r_\omega$. This equation has been simplified by Klyatskina and Shlimak to take the form

$$\sigma(\omega, T) \sim \omega^{1 - A_1(2n_1+1)} T^{n_1 - 1} \tag{5.13}$$

where A_1 depends on r_ω/a. Let us now discuss the temperature dependence of the conductivity in the light of this formula. Comparing equations (5.10) and (5.13), then one has

$$n_1 = d + 1$$

Hence, the mean number of hops, n_1^2 can be evaluated. The results of these calculations are included in table 5.3 for samples 5714 and 9914.

sample		5714	9914
H (kG)	freq. (Hz)	n_1^2	n_1^2
60	100000	2.76	6.05
"	10000	4.88	-
"	1000	8.12	-
"	110	10.24	16.56
50	100000	4.12	5.29
"	10000	7.24	-
"	1000	11.22	-
"	110	15.05	17.2

Table 5.3: Number of hops n_1^2 calculated from the temperature dependence of the conductivity $\sigma_{a.c.}(\omega)$ at different frequencies and two magnetic fields, 50 and 60 kG for samples 5714 and 9914.

These data show that n_1^2 is an increasing function of frequency, increases as ω decreases. Thus, the observations can be considered as a satisfactory evidence of the importance of the multiple hopping at higher temperatures in the present measurements. It is interesting to note that higher values for n_1^2 are observed at lower frequencies. This is consistent with the spirit of the multiple hopping ideas. As the multiple hopping becomes important at lower frequencies so one would expect n_1^2 to increase as ω decreases. It is worth noting that the d values obtained above are indeed calculated from the best fit of straight lines at high temperatures. It is obvious that d should decrease as the temperature is reduced as the multiple hopping becomes less favoured.

5.2.2 Frequency and Magnetic Field Dependence of the real part of the conductivity at very low temperatures:

The behaviour of the a.c. conductivity of the studied n-InSb samples at very low temperatures, (when $\sigma(\omega)$ becomes temperature-independent), has been mentioned briefly so far. It is the aim of this section to investigate the frequency and the magnetic field dependences of the conductivity at these temperatures. Referring back to Figures 5.1-5.4 for sample 5714 at very low temperatures depending on the magnetic field $\sigma(\omega)$ becomes temperature-independent and the d.c. component is, practically, not measurable. This temperature-independent a.c. conductivity occurs at lower temperatures for the other two samples, see Figures 5.5-5.8. At these temperatures the frequency dependence becomes stronger. The temperature-independent conductivity has also been observed in other materials such as amorphous Si (see, e.g., Hauser et al. 1981; Deri and Castner 1986).

Since the d.c. component of the conductivity is too small to be measured, (it is indeed too small compared to the a.c. part), so the analyses are carried out based on the actual measured values of $\sigma(\omega)$. The temperature-independent values of $\sigma(\omega)$ were obtained at different fields and frequencies. Figures 5.20 and 5.21 show the variation of these values with the field H for samples 5714 and 9914 respectively. It is obvious that the dependence at high fields is weak , however, as the field is reduced a pronounced change in the conductivity is observed, and the a.c. conductivity strongly depends on H. At high magnetic fields, the wave functions are expected to be strongly (highly) localized, and as the field is reduced towards lower values the wave functions become less localized where a metallic-like behaviour is expected at fields $< H_{cr}$. The estimated values of H_{cr} at which MI-transition occurs (estimated from equation 5.4) are given in table 5.1. However, it seems that the transition occurs at higher values as observed by Abdul-Gader (1984), (see also; Mansfield et al. (1985)).

Let us now discuss the frequency dependence of the conductivity of sample 5714. A typical set of a.c. conductivity data are presented in Figure 5.22 for this

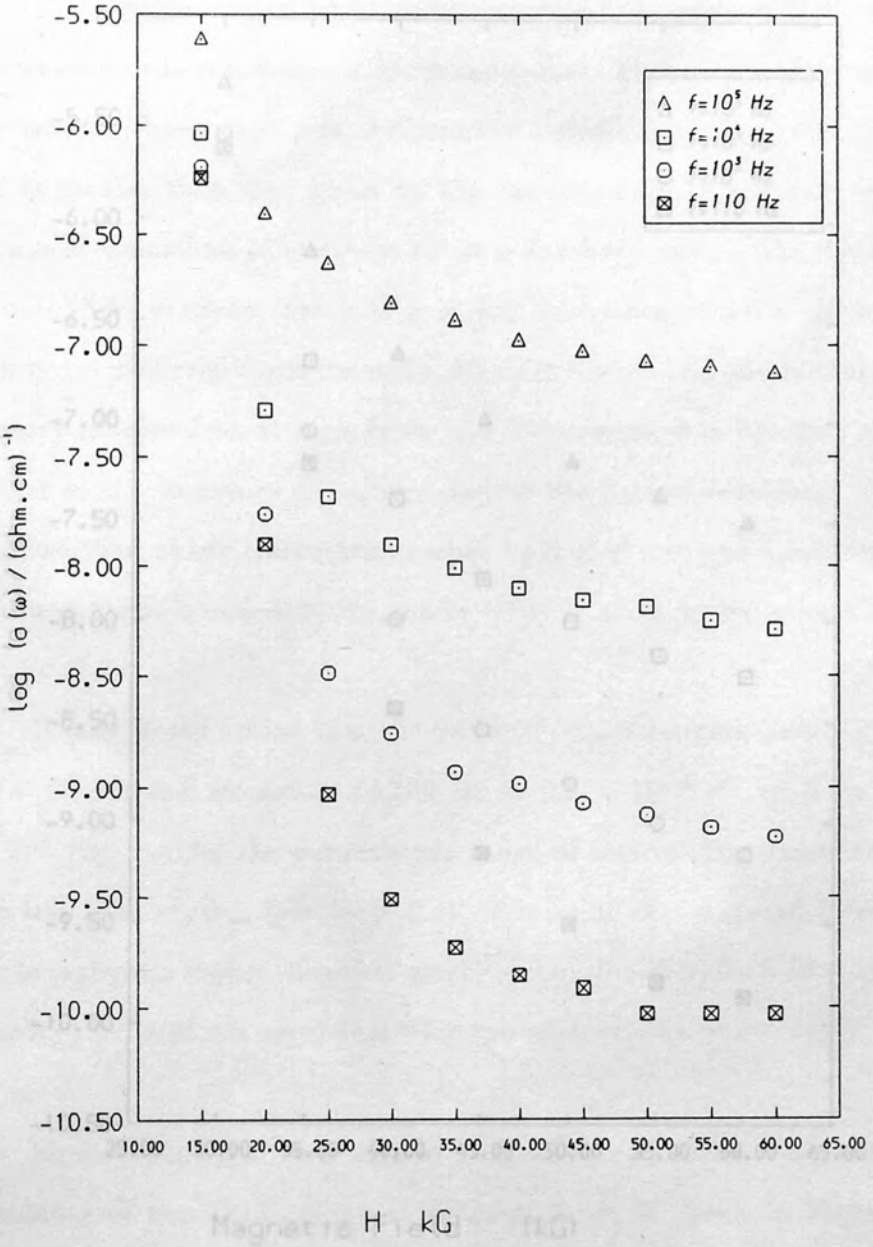

Figure 5.20

The low-temperature limit of the a.c. conductivity $\sigma(\omega)$ of sample 5714 against the magnetic field H. Data are plotted on a semi-log scale.

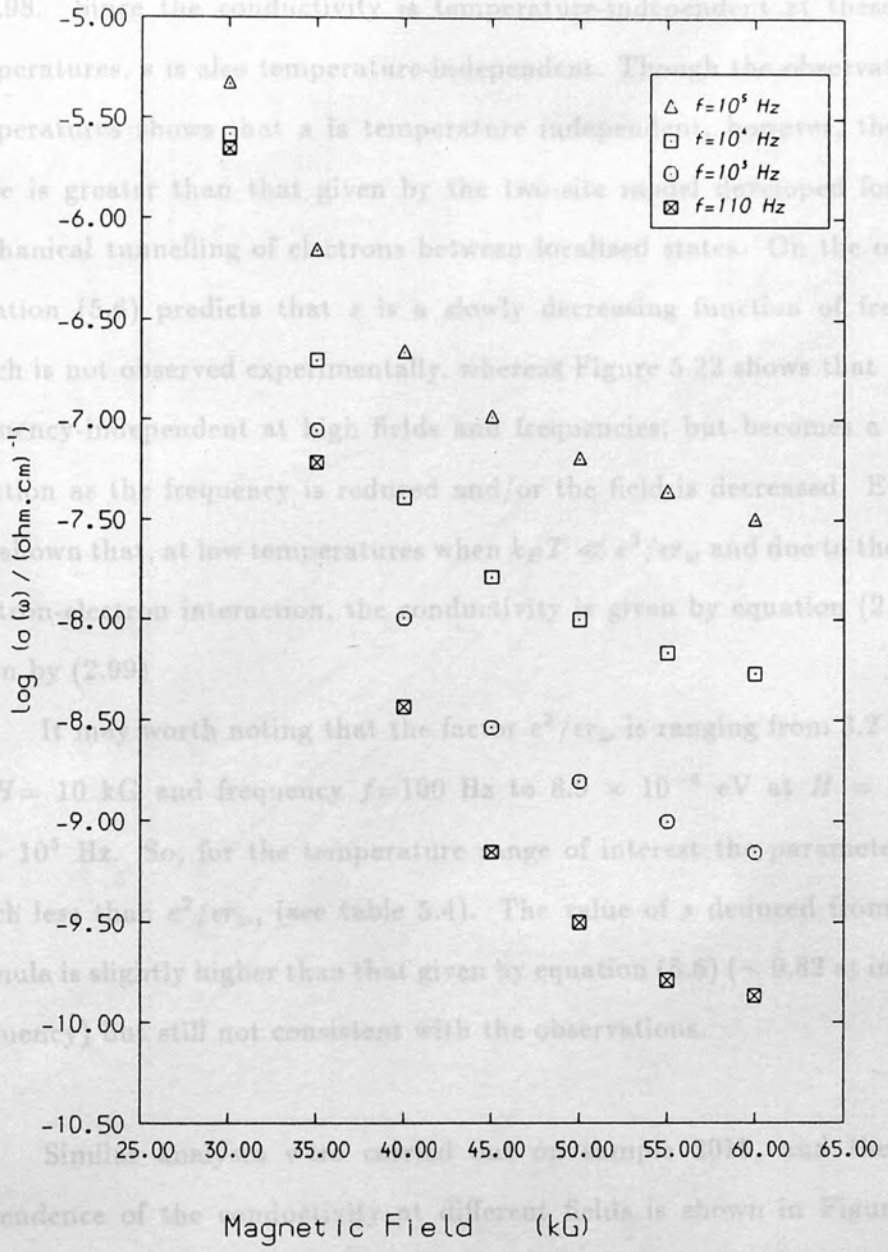

Figure 5.21

The low-temperatyre limit of the a.c. conductivity $\sigma(\omega)$ of sample 9914 against the magnetic field H on a semi-log scale.

sample at several magnetic fields. In this graph the plot is made for log σ (ω) versus log $\omega/2\pi$. The average value of the slope of the straight lines at high frequencies is 0.98. Since the conductivity is temperature-independent at these very low temperatures, s is also temperature-independent. Though the observation at low temperatures shows that s is temperature independent, however, the observed value is greater than that given by the two-site model developed for quantum mechanical tunnelling of electrons between localized states. On the other hand. equation (5.6) predicts that s is a slowly decreasing function of frequency ω, which is not observed experimentally, whereas Figure 5.22 shows that s is almost frequency-independent at high fields and frequencies, but becomes a decreasing function as the frequency is reduced and/or the field is decreased. Efros (1981) has shown that, at low temperatures when $k_BT \ll e^2/\epsilon r_\omega$ and due to the intra-pair electron-electron interaction, the conductivity is given by equation (2.98) with s given by (2.99)

It may worth noting that the factor $e^2/\epsilon r_\omega$ is ranging from 3.2×10^{-4} eV at $H=$ 10 kG and frequency f=100 Hz to 8.9×10^{-4} eV at H = 70 kG and $f = 10^5$ Hz. So, for the temperature range of interest the parameter (k_BT) is much less than $e^2/\epsilon r_\omega$, (see table 5.4). The value of s deduced from the above formula is slightly higher than that given by equation (5.6) ($\sim$ 0.82 at intermediate frequency) but still not consistent with the observations.

Similar analyses were carried out on sample 2015, and the frequency dependence of the conductivity at different fields is shown in Figure 5.23 (a). Plot again was made for $\sigma(\omega)$ versus $\omega/2\pi$ on log-log scale. The average observed value of the exponent s of this sample is 1.02 $\pm$ 0.04. which is again higher than the theoretical findings. As for sample 9914, the frequency dependence of the conductivity is shown in Figure 5.23 (b), a value of 0.83 $\pm$ 0.06 is found for s, which is comparable with that calculated from equation (2.99).

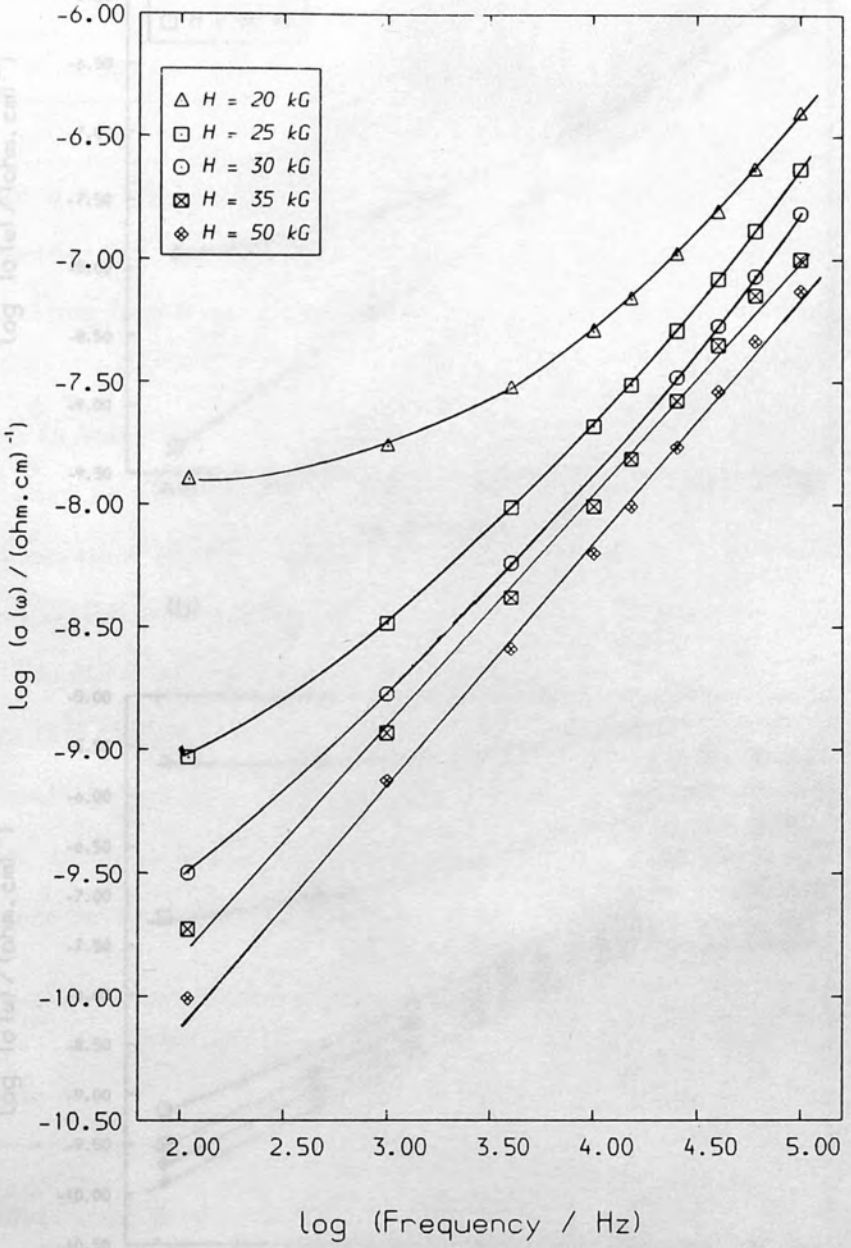

Figure 5.22

The low-temperature limit of the a.c. conductivity $\sigma(\omega)$ of sample 5714 against the frequency $\omega/2\pi$ on a log-log scale.

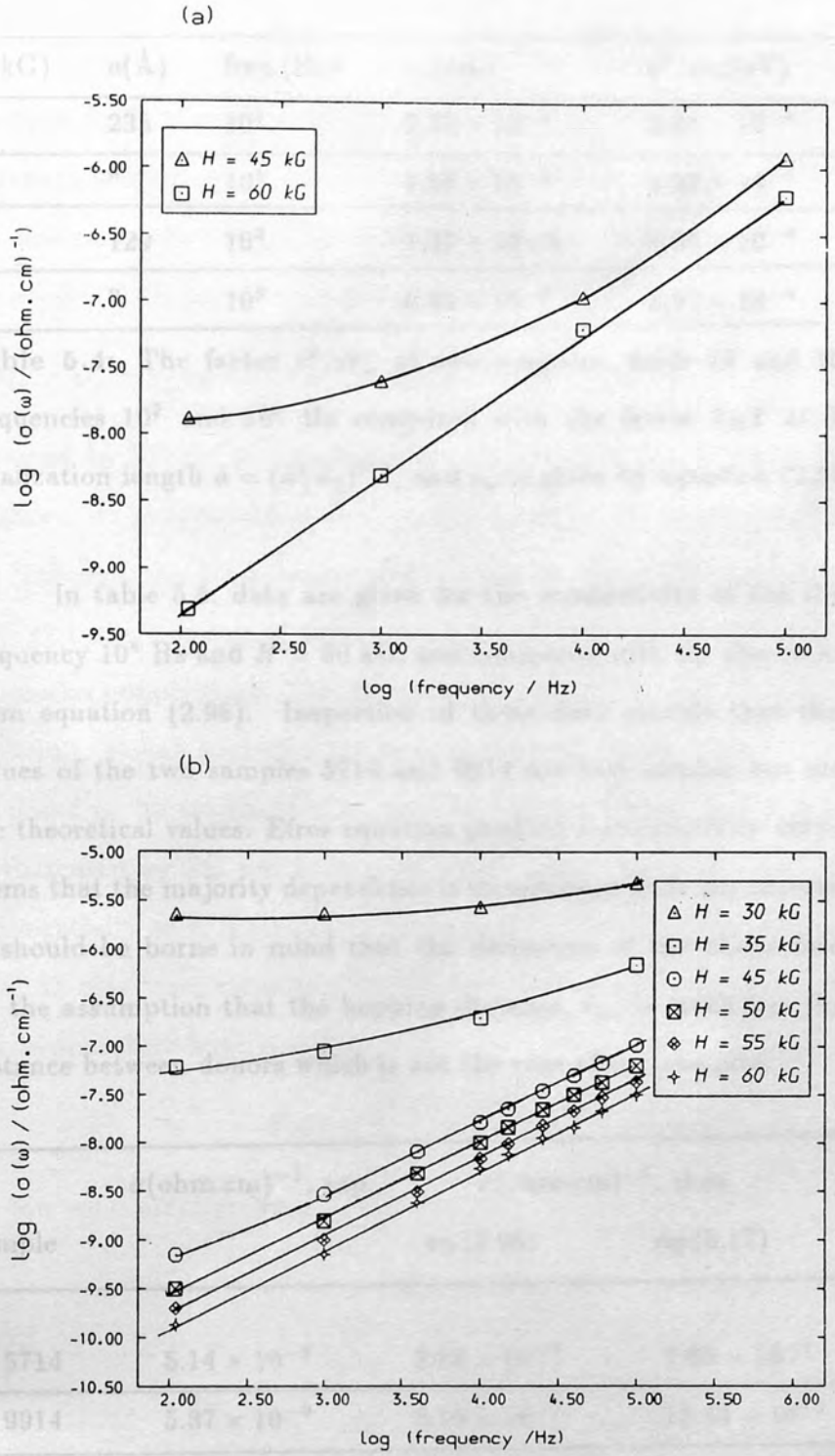

Figure 5.23

The frequency dependence of the low-temperature limit of the a.c. conductivity $\sigma(\omega)$ at different fields for (a) Sample 2015 (b) Sample 9914. Data are presented on a log-log scale.

H(kG)	a(Å)	freq.(Hz)	r_ω(cm)	$e^2/\epsilon r_\omega$(eV)	k_BT at T=0.2 K
10	235	10^2	2.50×10^{-5}	3.31×10^{-4}	1.73×10^{-5}
"	"	10^5	1.68×10^{-5}	4.93×10^{-4}	"
70	129	10^2	$1.37 \times 10{-}5$	6.04×10^{-4}	"
"	"	10^5	0.92×10^{-5}	8.97×10^{-4}	"

Table 5.4: The factor $e^2/\epsilon r_\omega$ at two magnetic fields 10 and 70 kG and two frequencies 10^2 and 10^5 Hz compared with the factor k_BT at T=0.2 K. The localization length $a = (a_\perp^2 a_\parallel)^{1/3}$, and r_ω is given by equation (2.81).

In table 5.5, data are given for the conductivity of the three samples at frequency 10^4 Hz and H = 60 kG, and compared with the theoretical calculations from equation (2.98). Inspection of these data reveals that the experimental values of the two samples 5714 and 9914 are very similar but are smaller than the theoretical values. Efros equation predicts a conductivity varying as $N_D^{4/3}$. It seems that the majority dependence is inconsistent with the observation (see PG). It should be borne in mind that the derivation of the above formulae is based on the assumption that the hopping distance, r_ω, is much less than the average distance between donors which is not the case of our samples.

sample	σ(ohm.cm)$^{-1}$, exp.	σ(ohm.cm)$^{-1}$, theo. eq.(2.98)	eq.(5.17)
5714	5.14×10^{-9}	3.86×10^{-7}	7.65×10^{-7}
9914	5.37×10^{-9}	8.10×10^{-7}	15.43×10^{-7}
2015	6.76×10^{-8}	19.37×10^{-7}	38.40×10^{-7}

Table 5.5: a.c. conductivity of n-InSb samples extrapolated to zero temperature at 10 kHz and 60 kG compared with the theoretical predictions from Efros formula (2.98) and (5.17).

The original analysis of PG, while taking account of the spatial distribution, assumed $k_BT > \varepsilon$ for most pairs. The energy distribution thus was ignored. Following Mott-Conwell model for impurity conduction, Pollak (1964) considered the case when the energy distribution is incorporated in the analysis. Apart from the explicit $1/T$-dependence in the equation

$$d\sigma(r,\varepsilon,\omega) = \frac{1}{12} dp(r,\varepsilon) N_A r^2 \cosh^{-2}(\varepsilon/2k_BT) \times \omega(\omega^{-1}\tau^{-1} + \omega\tau)^{-1} e^2/k_BT \quad (5.14)$$

obtained by PG for the conductivity, the temperature dependence enters to the conductivity in three different ways: (a) Through the hyperbolic function, $\cosh^{-2}$, (b) Through the temperature dependence of τ and (c) by the possibility that $dp(r,\varepsilon)$ (the number of pairs of spacing r and energy separation ε) may also depend on temperature. This is important only for the case of lightly compensated materials. Pollak neglected the explicit dependence of dp on temperature (which is supposed to be satisfactory at very low temperatures) and a procedure similar to that used by PG has been used which makes use of the fact that τ depends exponentially on r. This causes $[\omega\tau + (\omega\tau)^{-1}]^{-1}$ to be a strongly peaked function of r. In this case, according to the treatment of Pollak, the conductivity at the low temperature limit is given by

$$\sigma(\omega) = \frac{\pi^2}{2}\left(\frac{4\pi}{3}\right)^{1/3} K N_D^{4/3} a r_{\omega,T}^3 \epsilon\omega \quad (5.15)$$

for low concentration, $r_{\omega,T} \ll r_D$ with

$$s = 1 - 3/\ln(T/\omega) \quad (5.16)$$

and

$$\sigma(\omega) = \frac{\pi^2}{2} r_{\omega,T}^2 N_A a \epsilon\omega \quad (5.17)$$

for moderate concentration, $r_{\omega,T} \sim r_D$ with

$$s = 1 - 1/\ln(T/\omega) \quad (5.18)$$

where $r_{\omega,T}$ is the r where $[\omega\tau + (\omega\tau)^{-1}]^{-1}$ has a maximum and is given by (Pollak 1964)

$$r_{\omega,T} = \Big[16.3 + 0.53\ln(T/\omega)\Big] a \quad (5.19)$$

At high temperatures the quantum mechanical tunnelling model based on the pair approximation, shows that the conductivity is proportional to ωr_ω^4, while both equations (5.15) and (5.17) show that the frequency dependence of the conductivity should be somewhat more pronounced at very low temperatures than it is at high temperatures. The parameter $r_{\omega,T}$ ranges from $\sim 1.5 \times 10^{-5}$ cm to $\sim 1.8 \times 10^{-5}$ cm for temperatures between 1 down to 0.03 K at magnetic field 70 kG and frequency 10^2 Hz. For the same field and in the same temperature range it becomes slightly less for a frequency of 10^5 Hz (typically 1.2×10^{-5} to 0.95×10^{-5} cm). At lower fields (30 kG, say), these values become slightly higher but still in the order of magnitude of 10^{-5} cm. The average distance between donors for our samples, r_D, ranges from 0.9×10^{-5} to 1.3×10^{-5} cm. These values are comparable with $r_{\omega,T}$ given above. Hence the concentration of our samples can be considered of a moderate type. Equation (5.17) shows that for moderate concentrations, the conductivity is independent of the majority concentration. This has already been observed by PG. At a magnetic field of 50 kG, the lower temperature limit of the conductivity of samples 5714 and 9914 are given in table 5.6.

freq.(Hz)	5714	σ/N_A	9914	σ/N_A
10^5	7.46×10^{-8}	1.9×10^{-22}	8.06×10^{-8}	1.2×10^{-22}
10^4	6.58×10^{-9}	—	1.29×10^{-8}	—
10^3	8.85×10^{-10}	—	2.26×10^{-9}	—
110	9.35×10^{-11}	2.4×10^{-25}	5.08×10^{-10}	7.4×10^{-25}

Table 5.6: Low temperature limit of the conductivity of samples 5714 and 9914 at a magnetic field of 50 kG and different frequencies.

These data reveal that the lack of dependence of σ on N_D is more pronounced at lower frequencies than it is at higher frequencies. As $r_{\omega,T}$ increases with decreasing frequency hence one would expect that the agreement improves when the frequency increases giving rise to values of $r_{\omega,T}$ comparable with r_D.

In Figure 5.24 a comparison between the magnetic field dependence of the low temperature limit conductivity of samples 5714 and 9914 is given at frequency of 10^4 Hz. Following the same argument one would expect that the dependence of conductivity on N_D at high magnetic fields should be less pronounced. This is due to the fact that the parameter $r_{\omega,T}$ has even lower values at high fields and closely approaches r_D. This also agrees with our observations at high fields. Contrary to the case of high fields, the dependence of the conductivity on N_D is much more pronounced at lower values of the magnetic field as $r_{\omega,T}$ becomes relatively higher than r_D and the validity of equation (5.17) is interrupted, (see table 5.7).

freq.(Hz)	$\sigma_{a.c.}(5714)$	$\sigma_{a.c.}/N_A$	$\sigma_{a.c.}(9914)$	$\sigma_{a.c.}/N_A$
10^5	1.5×10^{-7}	3.9×10^{-22}	2.6×10^{-6}	3.7×10^{-21}
110	2.24×10^{-10}	5.7×10^{-25}	8.6×10^{-8}	1.3×10^{-22}

Table 5.7: The low temperature limit of the conductivity of samples 5714 and 9914 at H=30 kG and two frequencies.

The frequency dependence of the conductivity, apart from the explicit dependence on ω is also contained in $r^2_{\omega,T}$ term of equation (5.17). In the frequency range $10^2 - 10^5$ Hz, the frequency dependence of the conductivity should be $\sim \omega^{0.9}$.

It is obvious that the temperature dependence of the conductivity at low temperatures is due to the variation of $r_{\omega,T}$ with T. It is expected then that the hopping conductivity approaches a finite value at very low temperatures when the slight temperature dependence of $r_{\omega,T}$ on T is neglected. The experimental data show that $\sigma(\omega)$ is indeed temperature independent at lower temperatures as already seen in Figures 5.1-5.8.

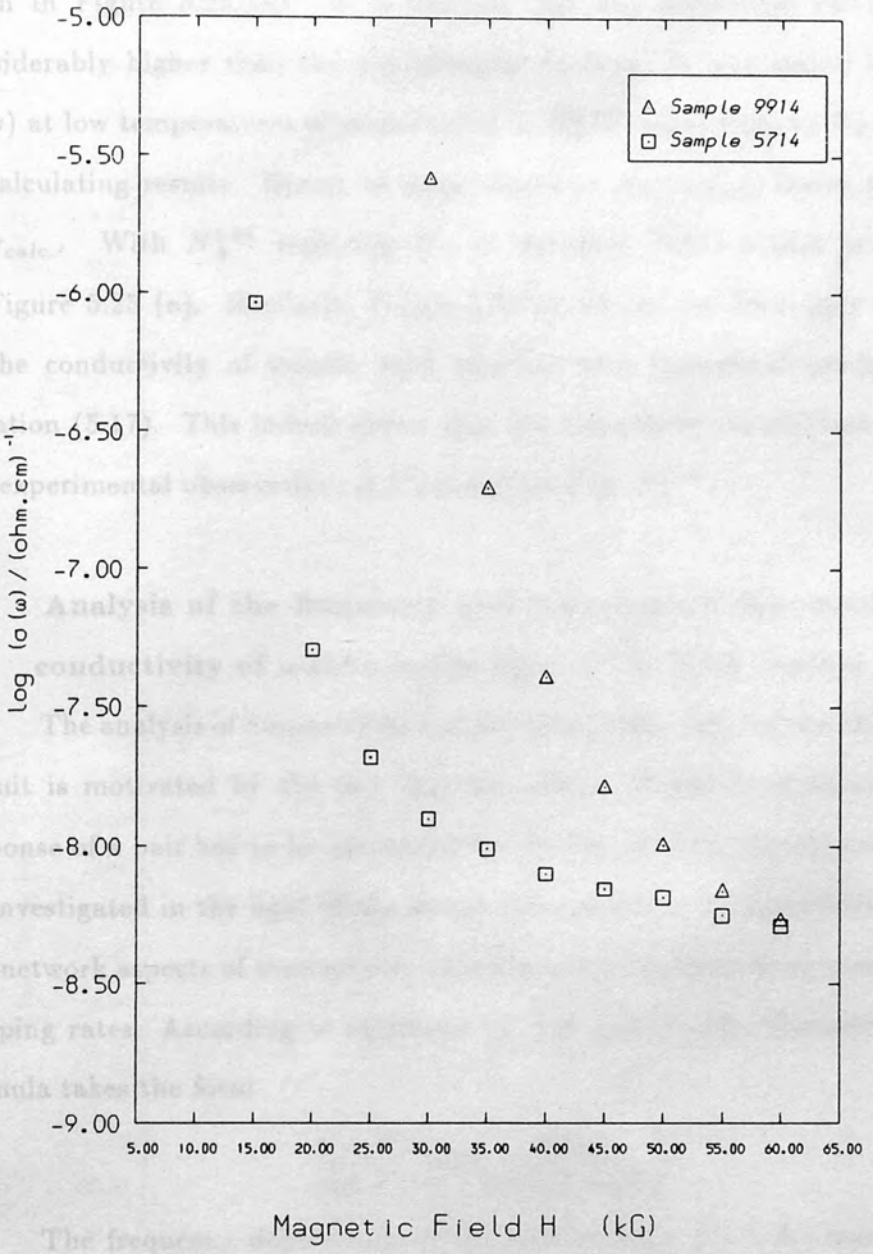

Figure 5.24

A comparison between the magnetic field dependence of the low-temperature limit a.c. conductivity $\sigma(\omega)$ of samples 5714 and 9914 at a frequency of 10^4 Hz.

A comparison between the experimental data of the conductivity at $H=$ 50 kG and the theoretical calculations (from eq. (5.17)) for sample 5714 is given in Figure 5.25 (a). It is obvious that the theoretical calculations are considerably higher than the experimental finding. It was stated by PG that $\sigma(\omega)$ at low temperatures is proportional to $N_A^{0.85}$ rather than to N_A as assumed in calculating results. Hence, at large values of N_A, $\sigma_{meas.}$ seems to fall short of $\sigma_{calc.}$. With $N_A^{0.85}$ replacing N_A in equation (5.17) a plot is also shown in Figure 5.25 (a). Similarly, Figure 5.25 (b) shows the frequency dependence of the conductivity of sample 9914 together with theoretical predictions from equation (5.17). This indeed shows that the theoretical calculations approaches the experimental observations if N_A is replaced by $N_A^{0.85}$.

5.3 Analysis of the frequency and temperature dependences of the conductivity of n-InSb in the light of the EPA theory:

The analysis of Summerfield and Butcher (1982, 1983) of the MA equivalent circuit is motivated by the fact that the effects of neighbouring states on the response of a pair has to be accounted for. In this section, the obtained data will be investigated in the light of the recent observation by Summerfield (1985) that the network aspects of conductivity problem can be isolated from questions of the hopping rates. According to equations (2.113) and (2.114), Summerfield scaling formula takes the form

$$\frac{\sigma(\omega,T)}{\sigma(0,T)} = f\left(\frac{Ae^2\omega\alpha}{\sigma(0,T)k_BT}\right) \tag{5.20}$$

The frequency dependence of the conductivity, $\sigma(\omega)$, for sample 5714 at $T = 0.6$ K is displayed in Figure 5.26 at magnetic fields from 25 kG up to 60 kG. Similar data are demonstrated in Figures 5.27 (a) and (b) for samples 9914 at $T = 0.4$ K and 2015 at $T =$0.154 K. The gradient $d\ ln(\sigma)/d\ ln(\omega)$ is a monotonically increasing function of both frequency and magnetic field H.

In Figure 5.28, we plot for sample 5714, the ratio $\sigma(\omega,H)/\sigma(0,H)$ against $(\omega/2\pi)/\sigma(0,H)$ at T=0.6 K. Interestingly, all the data points follow the same pattern in the whole entire range of frequencies and magnetic fields. In order to

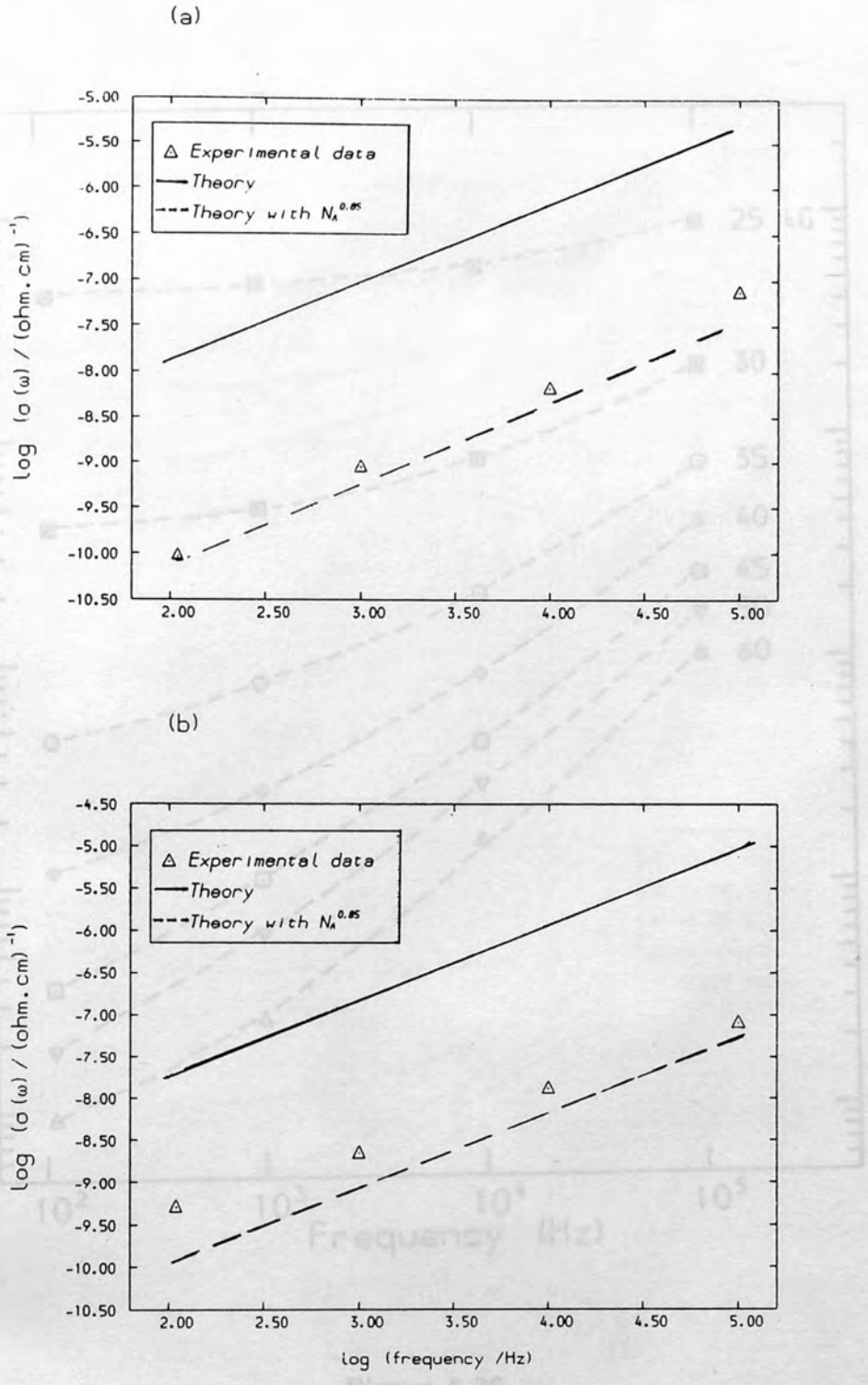

Figure 5.25

The frequency dependence of the low-temperature limit of the a.c. conductivity, $\sigma(\omega)$, at H= 50 kG. The solid line is the theoretical calculation from eq.(5.17). The dashed line is eq.(5.17) but N_A is replaced by $N_A^{0.85}$. (a) Sample 5714, (b) Sample 9914.

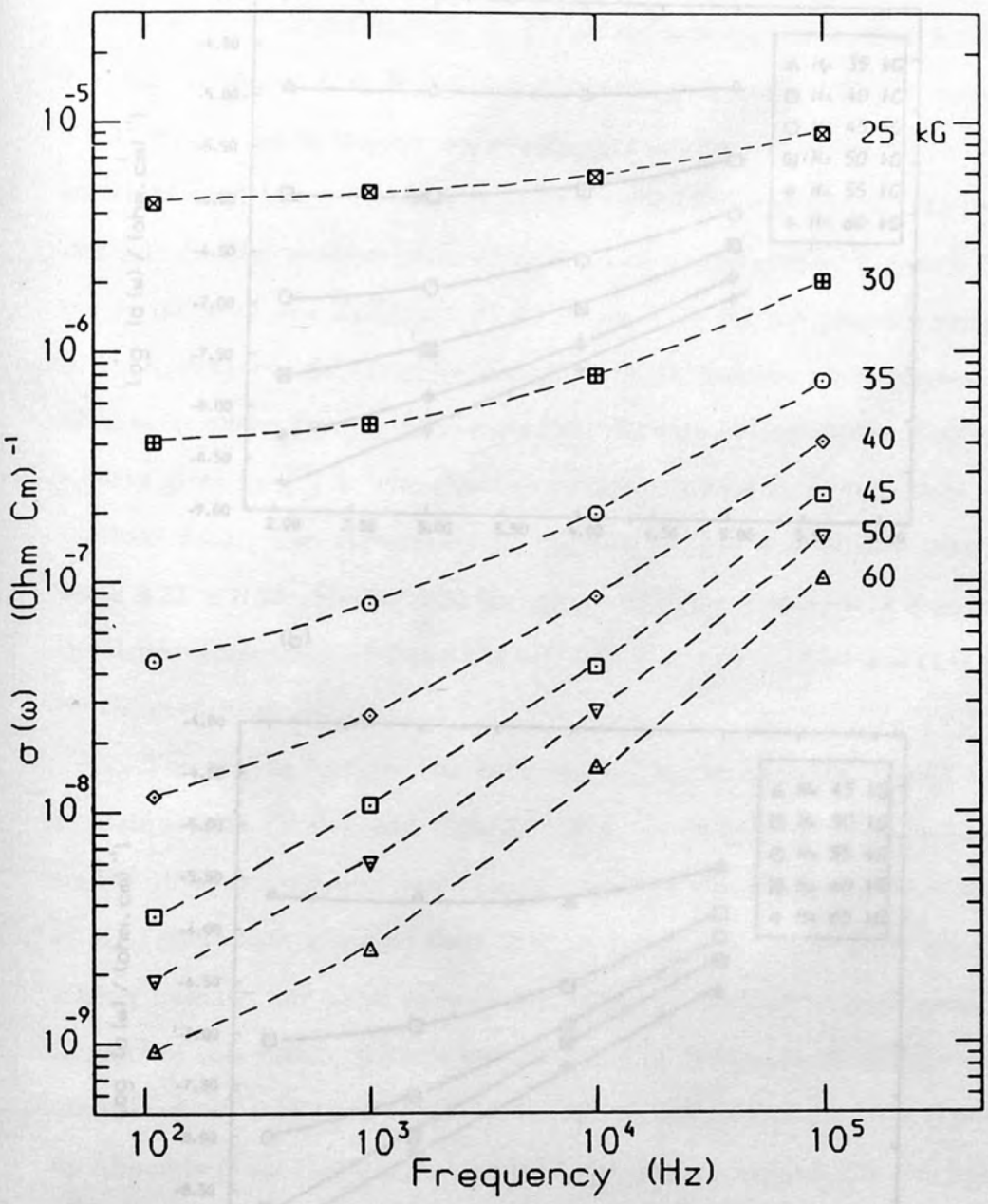

Figure 5.26

The frequency dependence of the a.c. conductivity, $\sigma(\omega)$, of sample 5714 on log-log scale at temperature T=0.6 K and different magnetic fields.

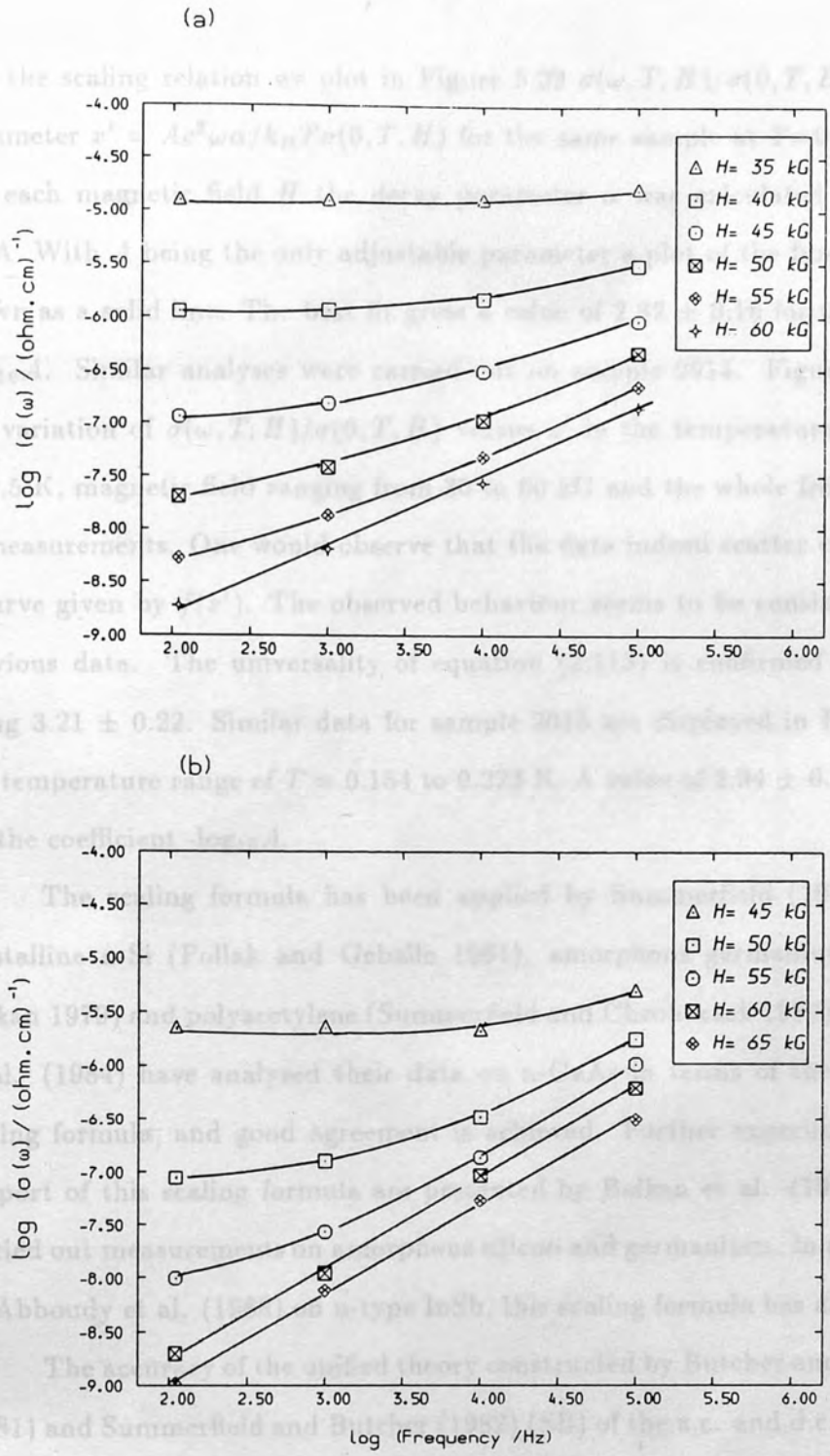

Figure 5.27

The frequency dependence of the a.c. conductivity, $\sigma(\omega)$, of (a) Sample 9914 at T=0.4 K, (b) Sample 2015 at T=0.154 K.

test the scaling relation we plot in Figure 5.29 $\sigma(\omega,T,H)/\sigma(0,T,H)$ versus the parameter $x' = Ae^2\omega\alpha/k_BT\sigma(0,T,H)$ for the same sample at T=0.5 and 0.6 K. For each magnetic field H the decay parameter α was calculated according to YKA. With A being the only adjustable parameter a plot of the function $f(x')$ is shown as a solid line. The best fit gives a value of 2.82 $\pm$ 0.16 for the parameter -$\log_{10}A$. Similar analyses were carried out on sample 9914. Figure 5.30 shows the variation of $\sigma(\omega,T,H)/\sigma(0,T,H)$ versus x' in the temperature range of 0.2 to 0.5 K, magnetic field ranging from 30 to 60 kG and the whole frequency range of measurements. One would observe that the data indeed scatter closely around a curve given by $f(x')$. The observed behaviour seems to be consistent with the previous data. The universality of equation (2.113) is confirmed with -$\log_{10}A$ being 3.21 $\pm$ 0.22. Similar data for sample 2015 are displayed in Figure 5.31 in the temperature range of T = 0.154 to 0.223 K. A value of 2.94 $\pm$ 0.17 is deduced for the coefficient -$\log_{10}A$.

The scaling formula has been applied by Summerfield (1985) to doped crystalline n-Si (Pollak and Geballe 1961), amorphous germanium (Long and Balkan 1979) and polyacetylene (Summerfield and Chroboczek 1984). Chroboczek et al. (1984) have analysed their data on n-GaAs in terms of the Summerfield scaling formula, and good agreement is achieved. Further experimental data in support of this scaling formula are presented by Balkan et al. (1985) who have carried out measurements on amorphous silicon and germanium. In a recent paper by Abboudy et al. (1988) on n-type InSb, this scaling formula has also been used.

The accuracy of the unified theory constructed by Butcher and Summerfield (1981) and Summerfield and Butcher (1982) (SB) of the a.c. and d.c. conductivity of a hopping system was established in SB (1982) by a comparison with exact asymptotic conductivity formulae and results of computer simulations. The EPA theory was used by SB (1983) to analyse data on a range of physical systems in which hopping is believed to be the dominant transport mechanism. Summerfield (1985) has used different types of energy dependence of the transition rate as expressed by the expression Q including those proposed by MA and AHL. The

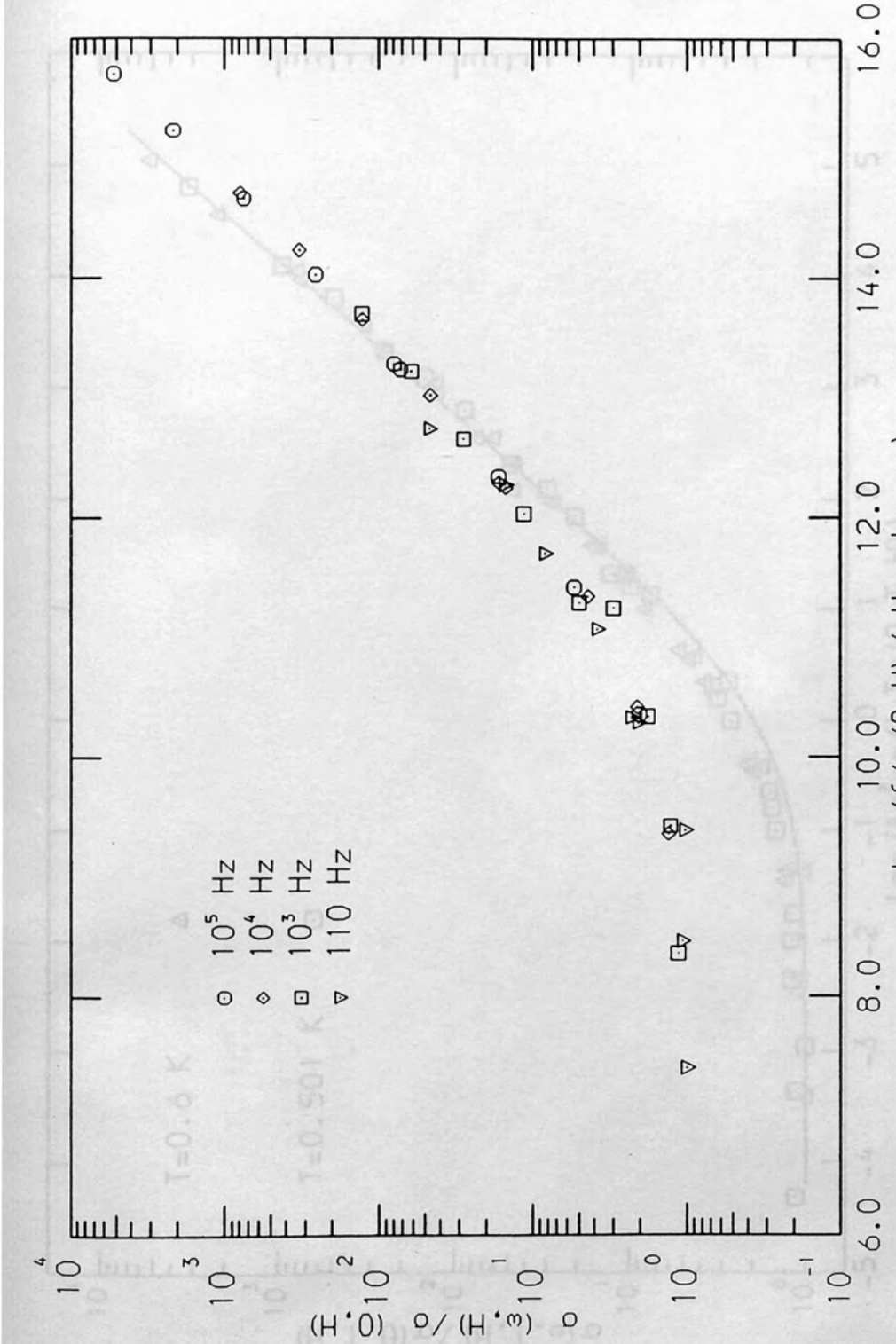

Figure 5.28

The normalized magnetoresistance of sample 5714 against the parameter $((\omega/2\pi)/\sigma(0,H)$ at temperature T=0.6 K. The data include measurements at frequencies from 110 to 10^5 Hz and fields from 20 to 60 kG.

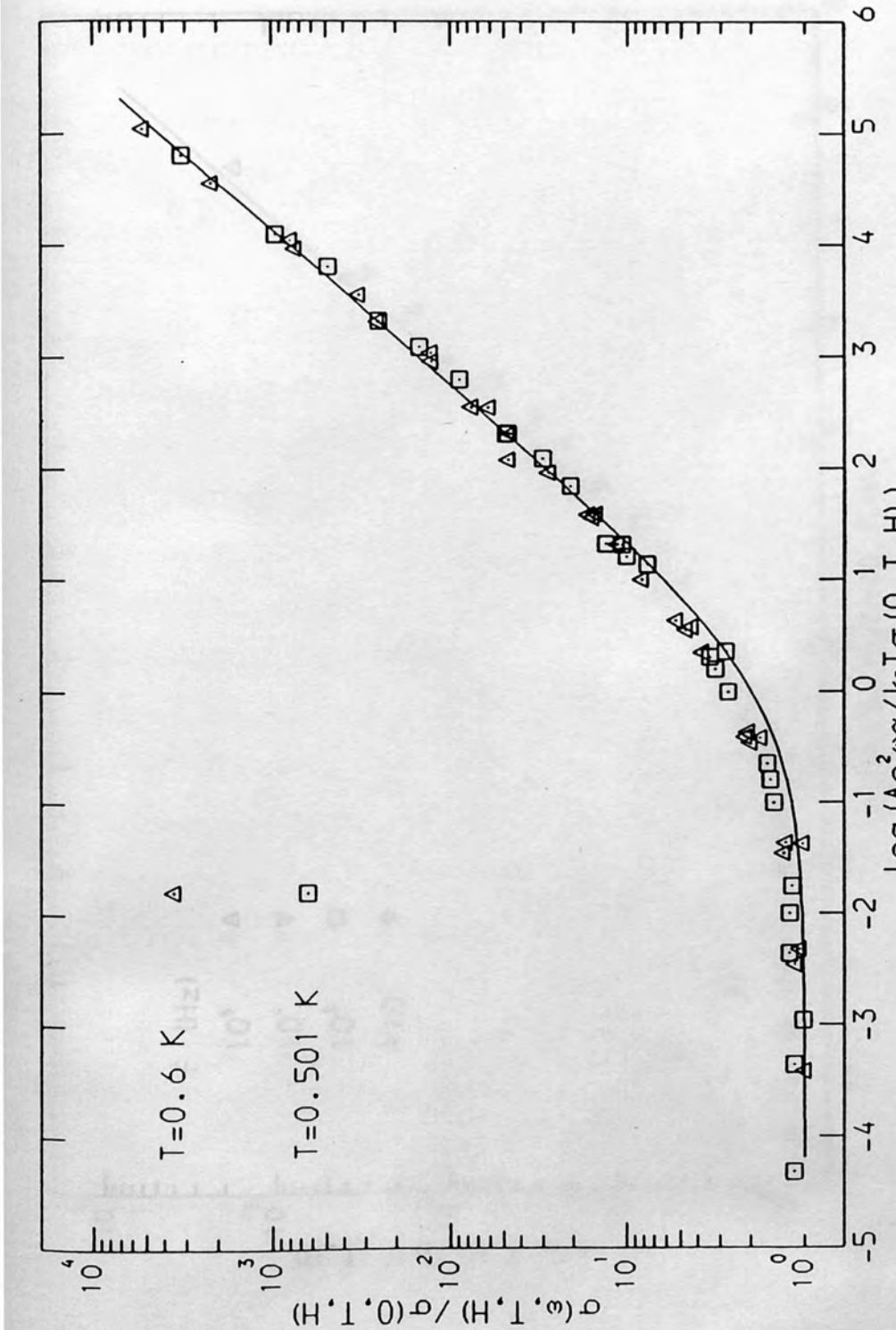

Figure 5.29

The normalized magnetoresistance of sample 5714 against log x' where $x' = A\alpha e^2\omega/k_BT\sigma(0,T,H)$. The data for each temperature include measurements at frequencies 110 to 10^5 Hz and fields from 20 to 60 kG. The parameter - $\log_{10}A = 2.82 \pm 0.16$ was chosen to give the best fit to eq.(2.113), shown as a solid line.

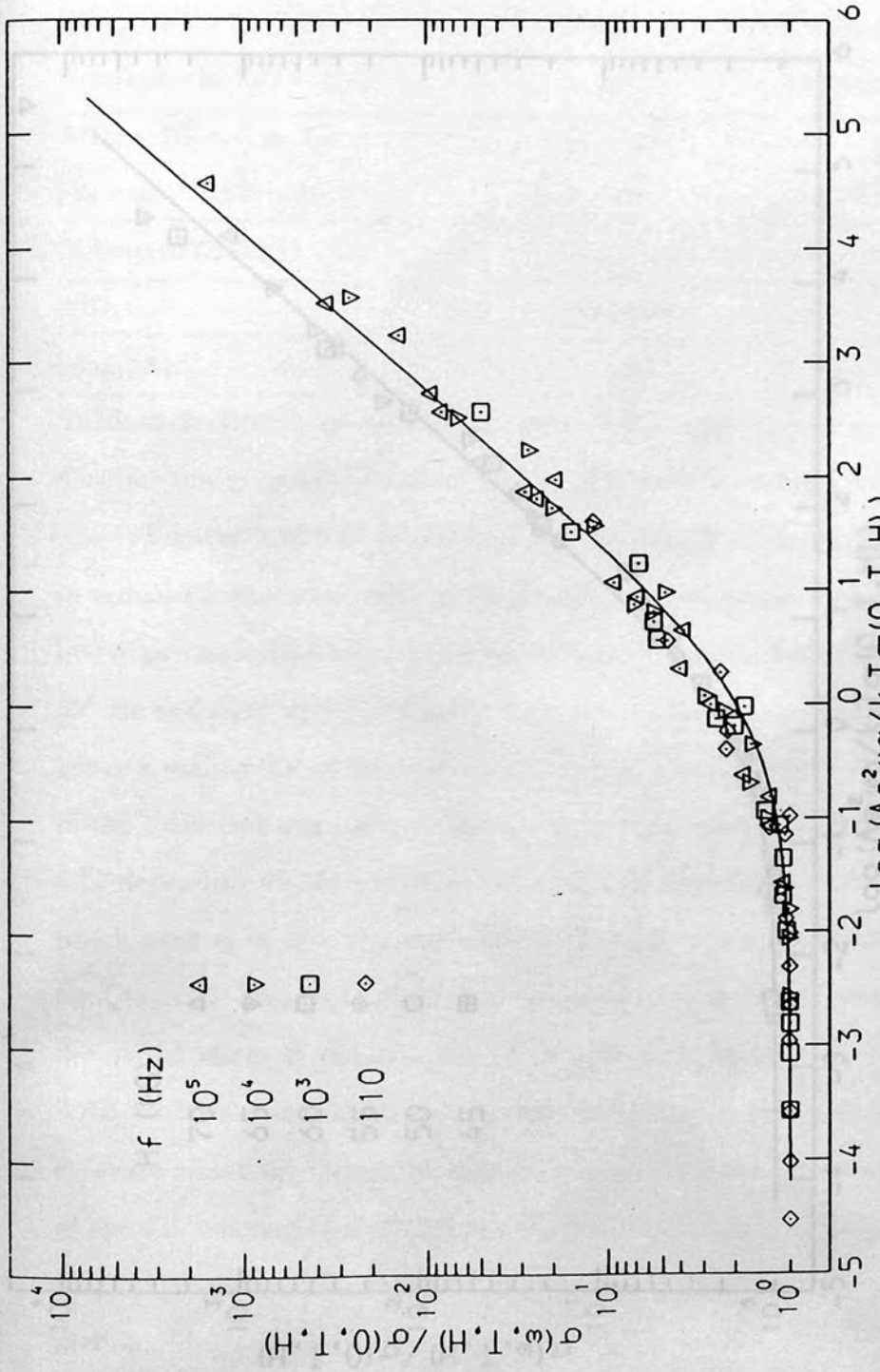

Figure 5.30

The normalized magnetoresistance of sample 9914 against log x' where $x' = A\alpha e^2\omega/k_BT\sigma(0,T,H)$. The data for each frequency include measurements at temperatures from 0.2 to 0.5 K and fields from 30 to 60 kG. The parameter - $\log_{10}A = 3.21 \pm 0.22$ was chosen to give the best fit to eq.(2.113), shown as a solid line.

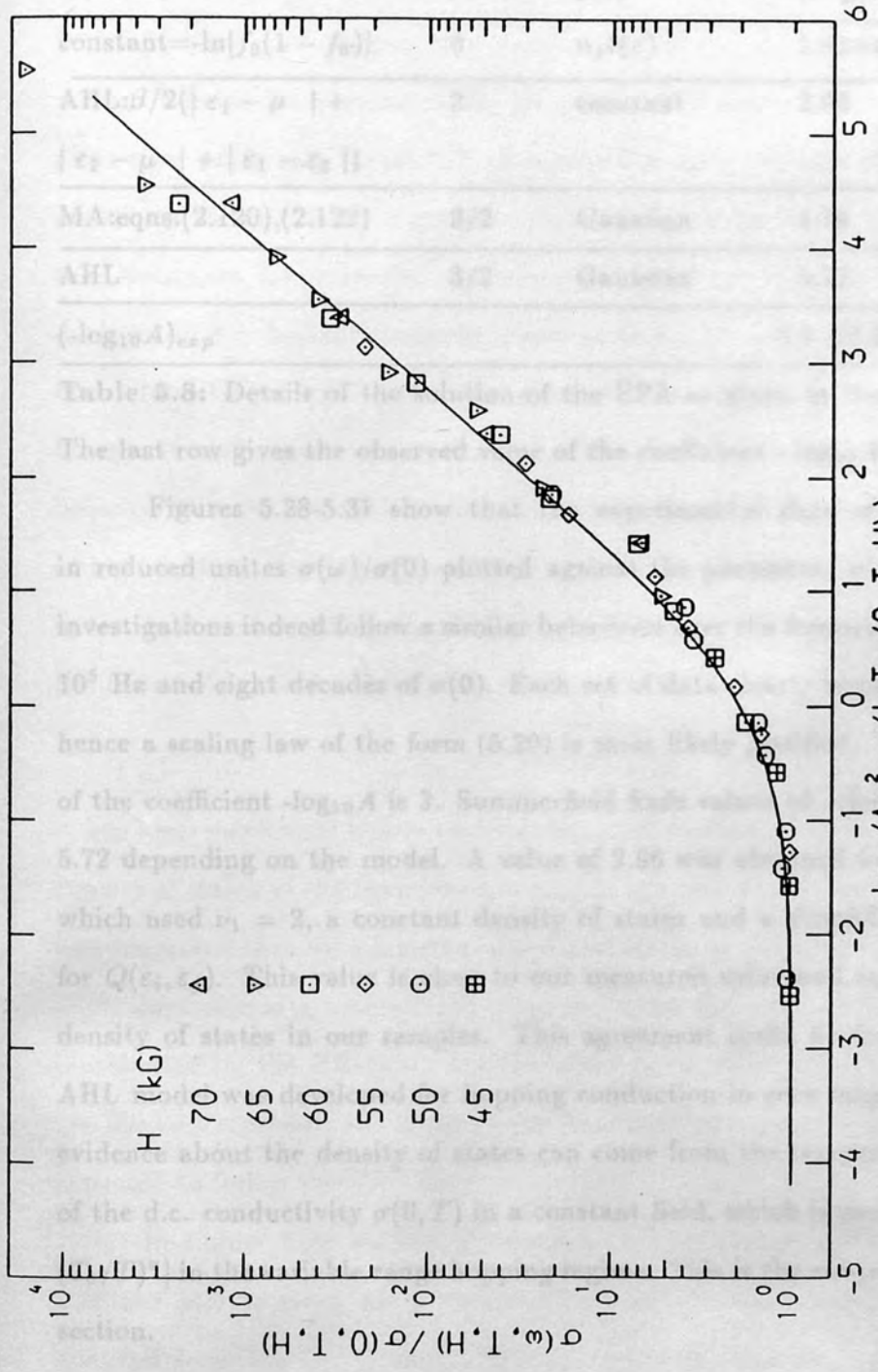

Figure 5.31

The normalized magnetoresistance of sample 2015 against log x' where $x' = A\alpha\epsilon^2\omega/k_BT\sigma(0,T,H)$. The data for each magnetic field include measurements at frequencies 110 to 10^5 Hz and temperatures from 0.154 to 0.223 K. The parameter - $\log_{10}A = 2.94 \pm 0.17$ was chosen to give the best fit to eq.(2.113), shown as a solid line.

parameter ν_1, the shape of the function Q and the density of states $g(\varepsilon)$ define a model. The characteristic parameters of these models are summarised in table (5.8). An empirical scaling formula of the form (2.113) has been implied for a.c. conductivities calculated by the EPA for these models (Summerfield 1985).

$Q(\varepsilon_1, \varepsilon_2)$	ν_1	$g(\varepsilon)$	$(-\log_{10} A)_{thr}$
constant=$-\ln[f_0(1-f_0)]$	0	$n_s\delta(\varepsilon)$	$1.91+Q/\ln 10$
AHL:$\beta/2(\mid \varepsilon_1-\mu \mid + \mid \varepsilon_2-\mu \mid + \mid \varepsilon_1-\varepsilon_2 \mid)$	2	constant	2.96
MA:eqns.(2.120),(2.122)	3/2	Gaussian	4.79
AHL	3/2	Gaussian	5.72
$(-\log_{10} A)_{exp}$			3.0 $\pm$0.2

Table 5.8: Details of the solution of the EPA as given by Summerfield (1985). The last row gives the observed value of the coefficient - $\log_{10} A$.

Figures 5.28-5.31 show that the experimental data of the conductivity in reduced unites $\sigma(\omega)/\sigma(0)$ plotted against the parameter x' of samples under investigations indeed follow a similar behaviour over the frequency range of 110 to 10^5 Hz and eight decades of $\sigma(0)$. Each set of data clearly implies a single curve, hence a scaling law of the form (5.20) is most likely justified. The average value of the coefficient -$\log_{10} A$ is 3. Summerfield finds values of $-\log_{10} A$ from 1.91 to 5.72 depending on the model. A value of 2.96 was obtained for the AHL model which used $\nu_1 = 2$, a constant density of states and a simplified approximation for $Q(\varepsilon_i, \varepsilon_j)$. This value is close to our measured value and suggests a constant density of states in our samples. This agreement could be fortuitous since the AHL model was developed for hopping conduction in zero magnetic field. Other evidence about the density of states can come from the temperature dependence of the d.c. conductivity $\sigma(0,T)$ in a constant field, which is proportional to $\exp[-(T_0/T)^x]$ in the variable range hopping regime. This is the subject of the following section.

5.4 Temperature and Magnetic Field dependence of the DC resistivity of the n-InSb samples:

5.4.1 Temperature Dependence of the resistivity:

d.c. resistivity measurements of the studied n-InSb samples have been carried out in the same range of magnetic field as the a.c. measurements. Figures 5.32-5.34 show the temperature dependence of the d.c. resistivity at various magnetic fields for samples 5714, 9914 and 2015 respectively. In these graphs plots were made as ρ versus $1/T$ on a semi-log scale. At high magnetic fields the resistivity shows a fairly marked increase as the temperature is lowered. As the field decreases, however, the temperature dependence becomes weaker. Detailed analysis on d.c. measurements by many authors (see, e. g., Tokumoto et al. 1980 and Abdul-Gader 1984) show the absence of a wide range constant activation energy at such lower temperatures for these materials and the conductivity is believed to be of the VRH type. Since our measurements are carried out mainly at high fields and low temperatures we will discuss the behaviour of the resistivity in the light of the existing theoretical models suggested for the VRH regime where the resistivity is controlled by the relation (2.69)

$$\rho = \rho_0 \exp\left(\frac{T_0}{T}\right)^x \tag{5.33}$$

It has been mentioned before that the exponent x depends on the behaviour of the density of states at the Fermi level as well as the type of the wave function used. It was suggested that for a constant density of states at the Fermi level ($g = g_0$), the $T^{1/3}$- dependence is theoretically expected when the wavefunctions of donors are represented by the HH-type. On the other hand, when the YKA wavefunctions are used to represent the donor wave functions, the temperature dependence is expected to follow the $T^{2/5}$ law.

In Figure 5.35 we plot ρ versus $T^{-1/3}$ for sample 5714, while in Figure 5.36 the plot is given for ρ versus $T^{-2/5}$ for the same sample. Values of T_0 deduced from the $T^{-1/3}$ and $T^{-2/5}$-dependences together with the theoretical calculations appropriate for each case at $H=$ 60 kG are given in table 5.9. These

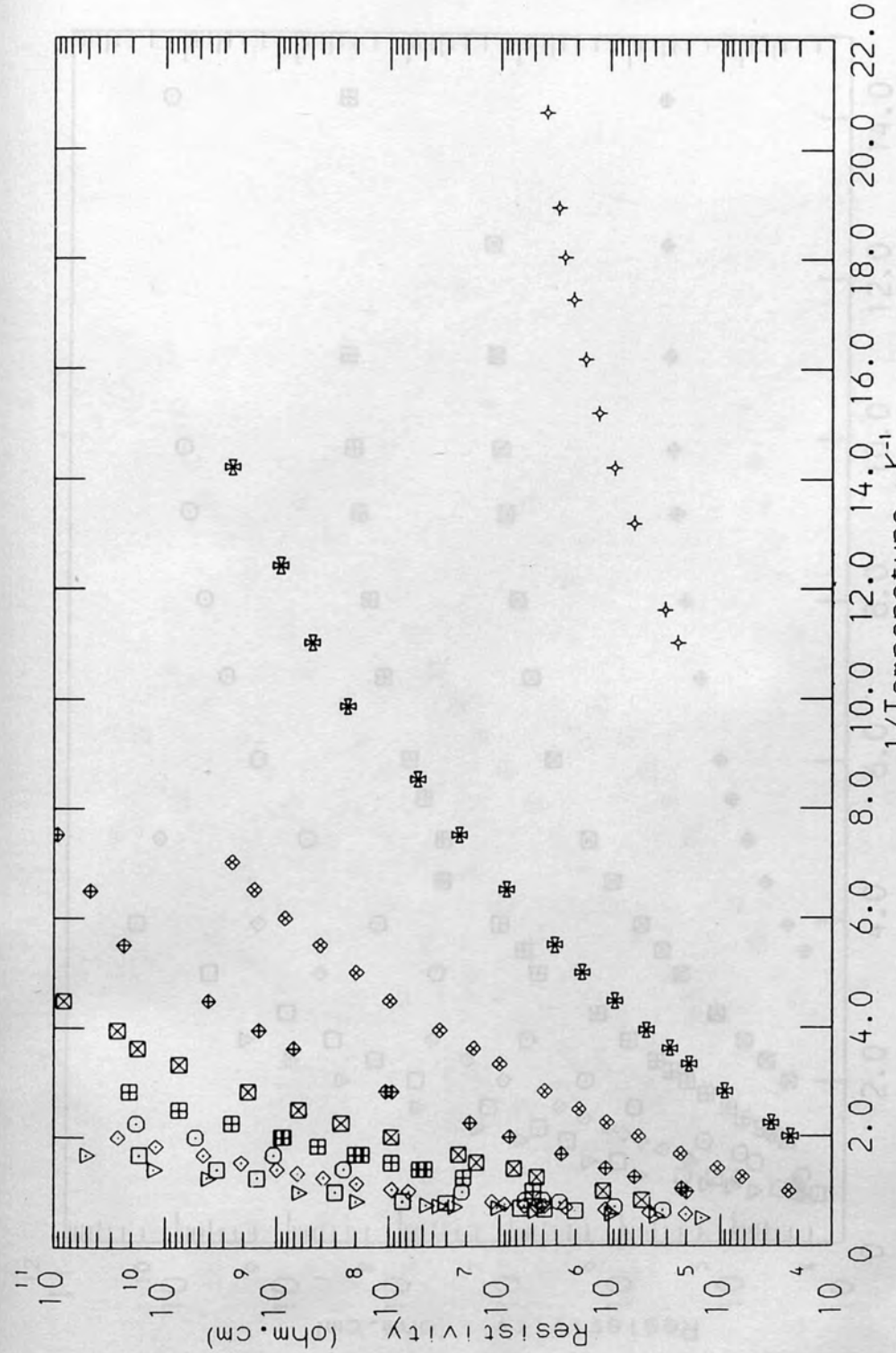

Figure 5.32

The temperature dependence of the d.c. resistivity of sample 5714 at different magnetic fields (from 15 to 60 kG in steps of 5 kG).

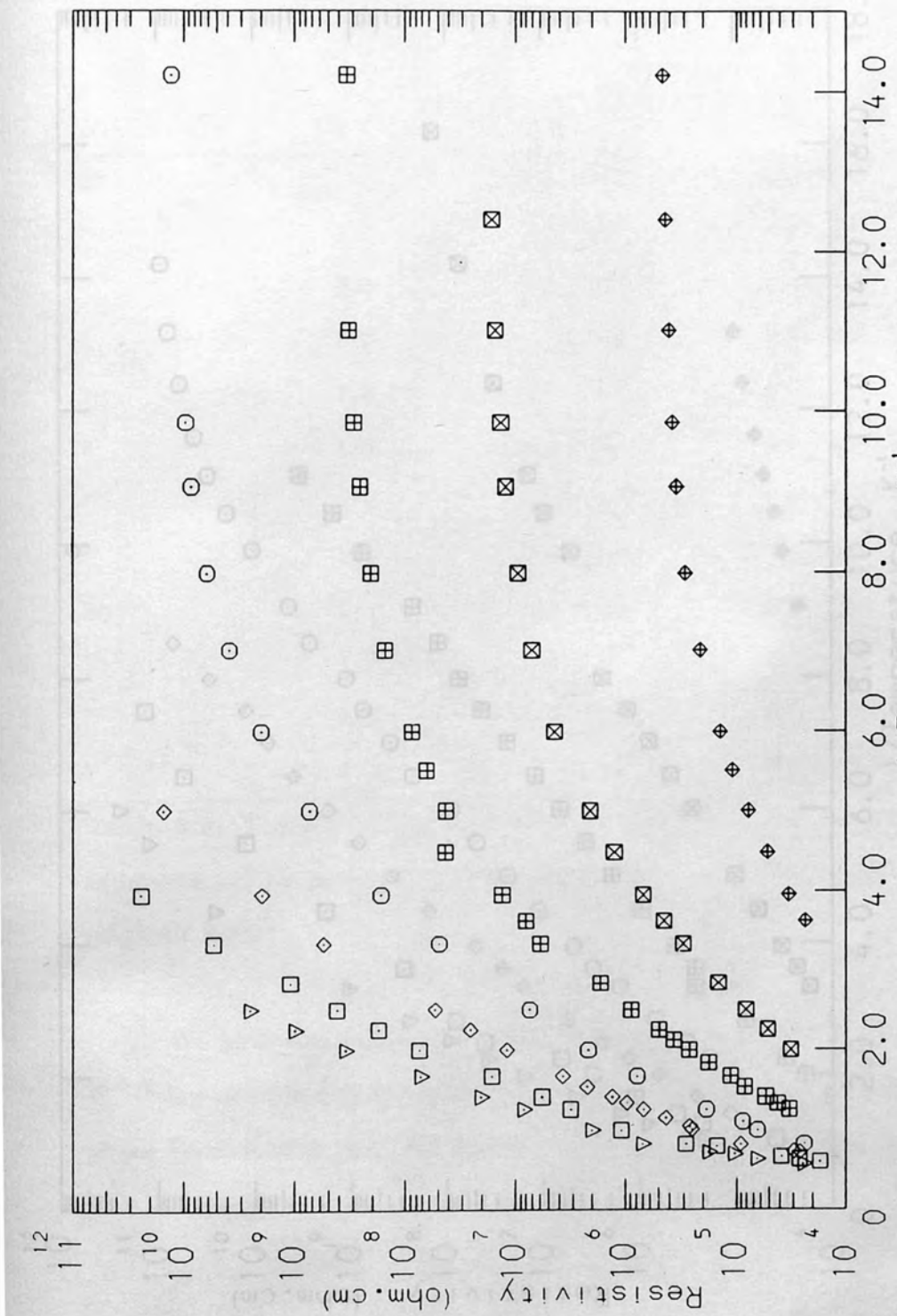

Figure 5.33

The temperature dependence of the d.c. resistivity of sample 9914 at different magnetic fields (from 30 kG to 60 kG, in steps of 5 kG).

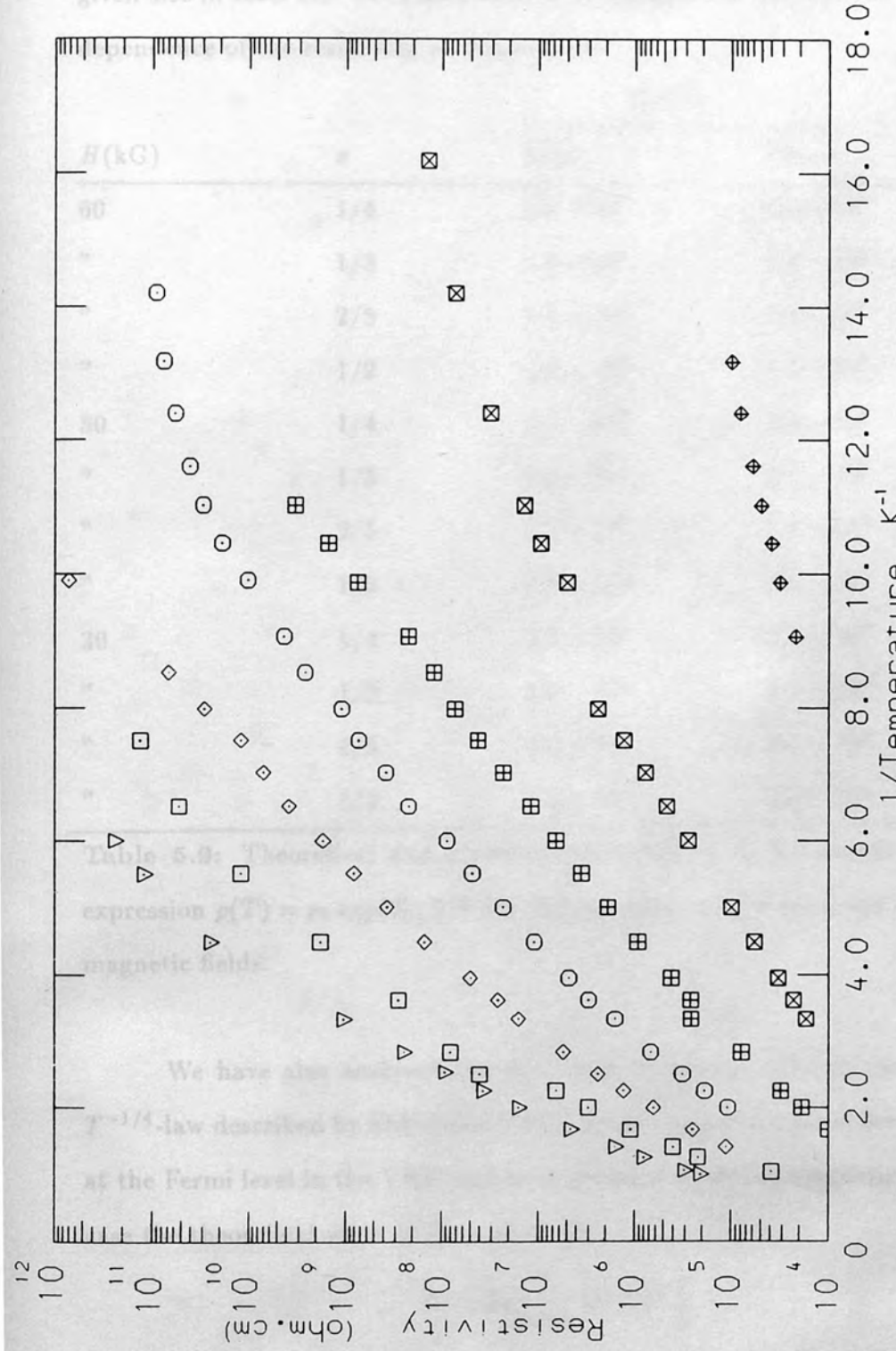

Figure 5.34

The temperature dependence of the d.c. resistivity of sample 2015 at different magnetic fields (from 40 kG to 70 kG, in steps of 5 kG).

data reveal that the observed and the calculated values of T_0 are in the same order of magnitude, (they are, indeed, very similar). At H=50 kG, however, the theoretical values become almost twice as high as the experimental findings. Calculations are also carried out for lower magnetic fields. Data at H= 30 kG are given also in table 5.9. Both laws seem to be adequate to describe the temperature dependence of the resistivity of this sample.

		T_0 (K)	
H(kG)	x	Expt.	Theory
60	1/4	1.0×10^6	3.1×10^5
"	1/3	1.3×10^4	1.2×10^4
"	2/5	1.6×10^3	1.4×10^3
"	1/2	2.2×10^2	5.7×10^2
50	1/4	2.8×10^5	2.4×10^5
"	1/3	4.4×10^3	9.7×10^3
"	2/5	6.2×10^2	1.1×10^3
"	1/2	2.0×10^2	5.3×10^2
30	1/4	2.0×10^5	1.3×10^5
"	1/3	3.0×10^3	5.0×10^3
"	2/5	4.2×10^2	6.0×10^2
"	1/2	6.4×10	4.2×10^2

Table 5.9: Theoretical and experimental values of T_0 for sample 5714 in the expression $\rho(T) = \rho_0 \exp(T_0/T)^x$ for various values of the exponent x at different magnetic fields.

We have also analysed the d.c. data of sample 5714 in the light of the $T^{-1/4}$-law described by Shklovskii (1982) for the case of constant density of states at the Fermi level in the VRH regime in presence of strong magnetic field. In this case the theoretical value of T_0 is given by

$$T_0 = S_8 \frac{1}{g_0 k_B} \left[a(H) b^2 \right]^{-1} \tag{5.34}$$

with S_8=63.02, and b is equal to λ at high fields. In Figure 5.37 we plot $\rho(H)$ versus

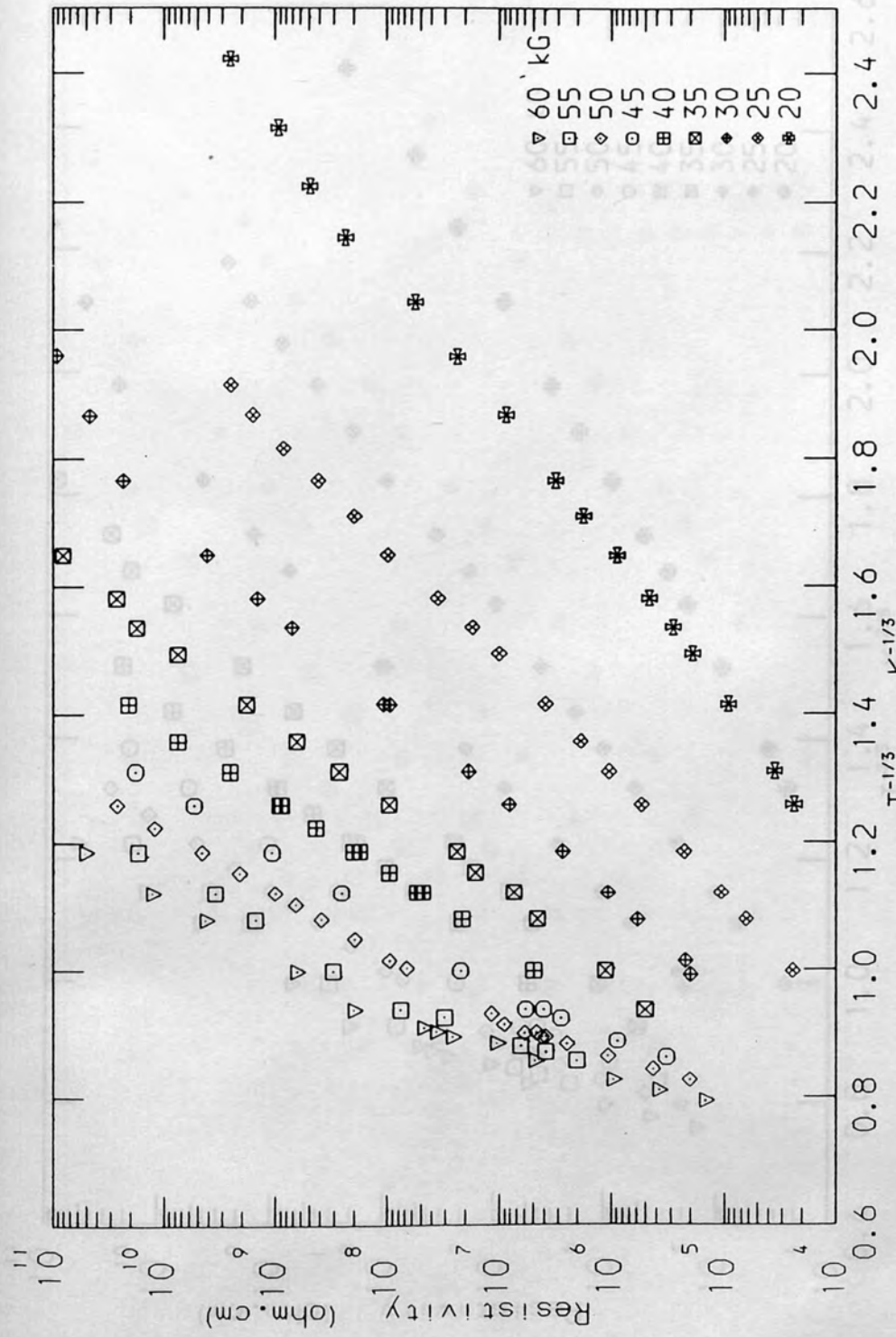

Figure 5.35

The d.c. resistivity of sample 5714 as a function of $T^{-1/3}$ at different fields.

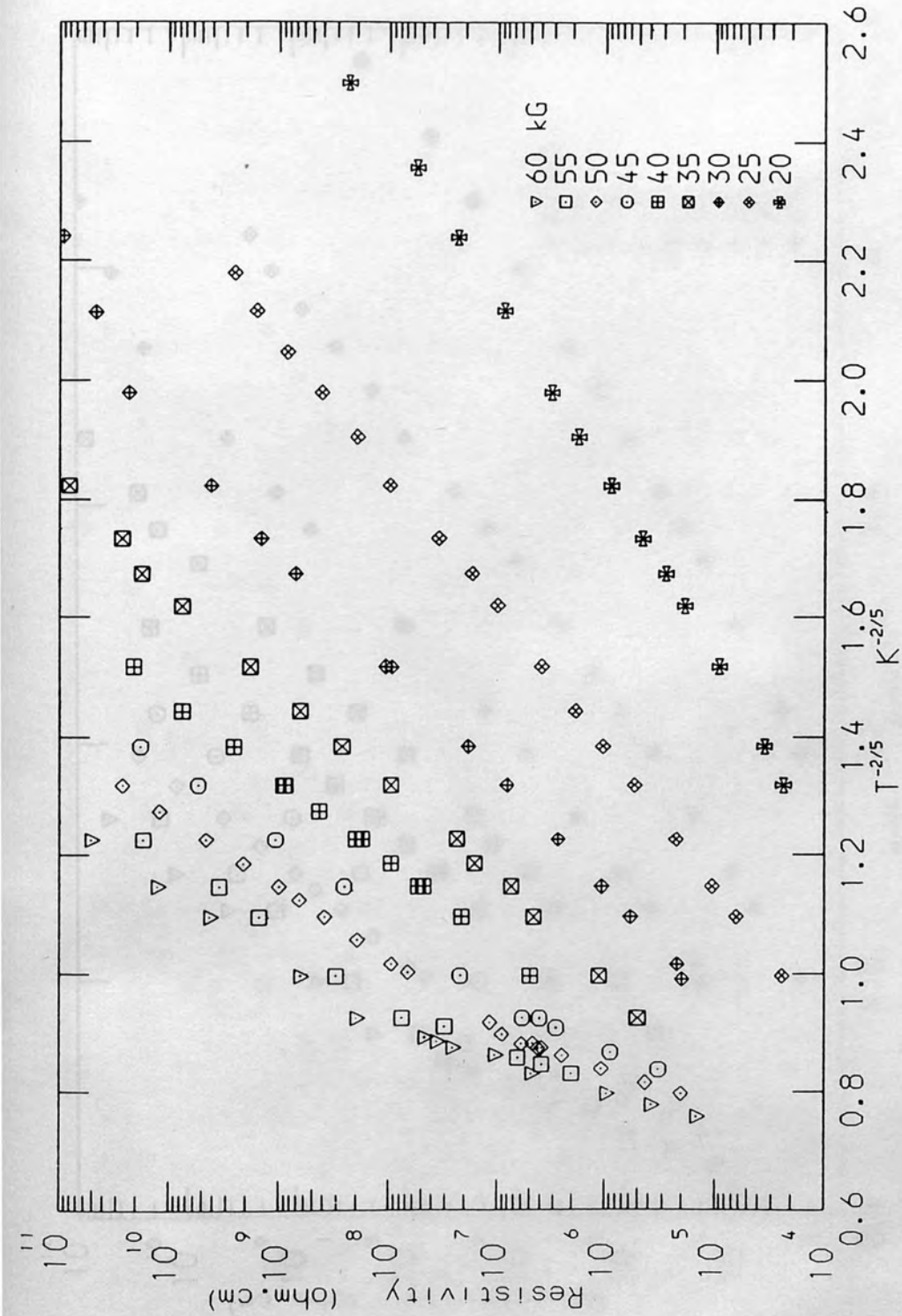

Figure 5.36

The d.c. resistivity of sample 5714 as a function of $T^{-2/5}$ at different fields.

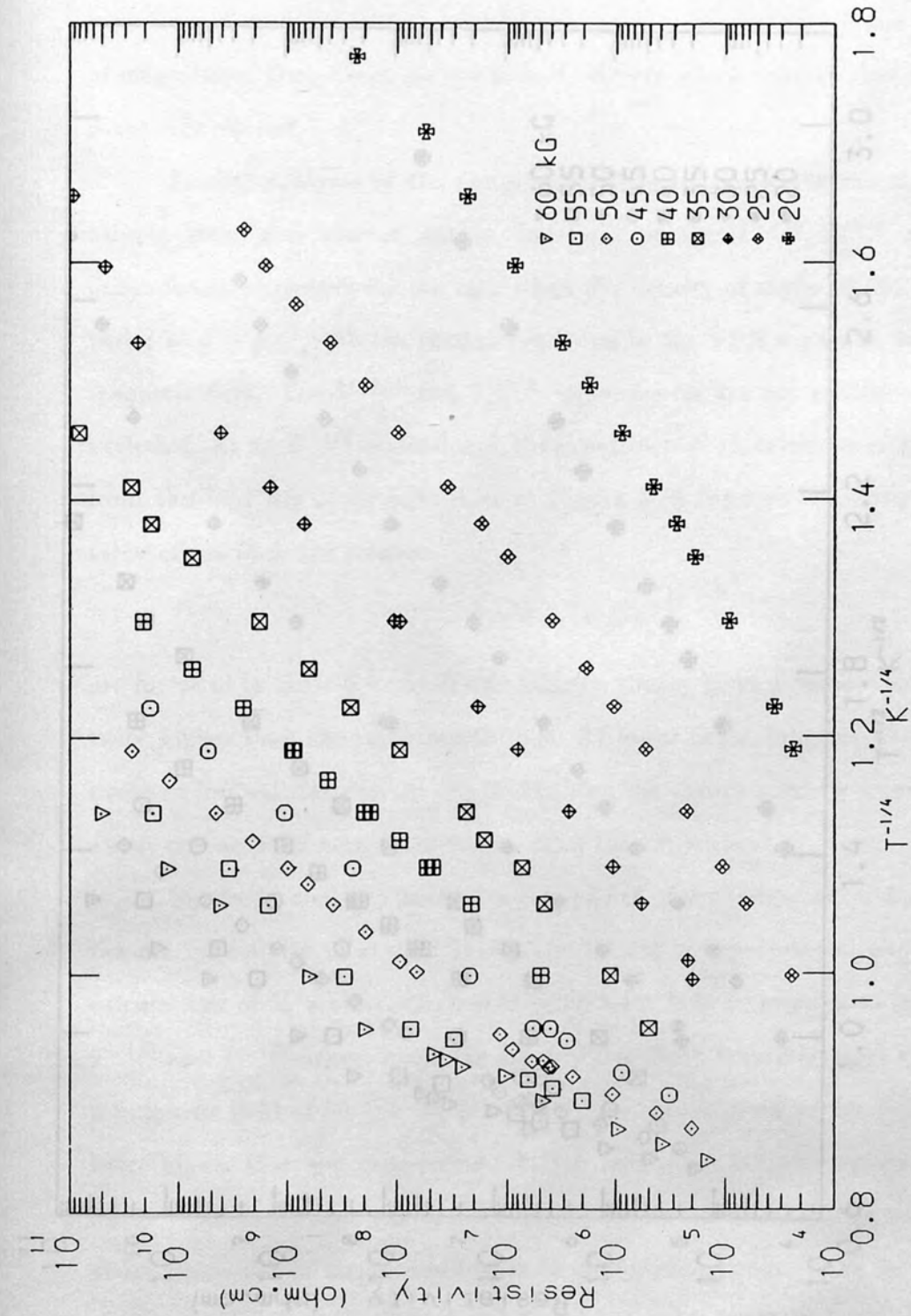

Figure 5.37

The d.c. resistivity of sample 5714 as a function of $T^{-1/4}$ at different fields.

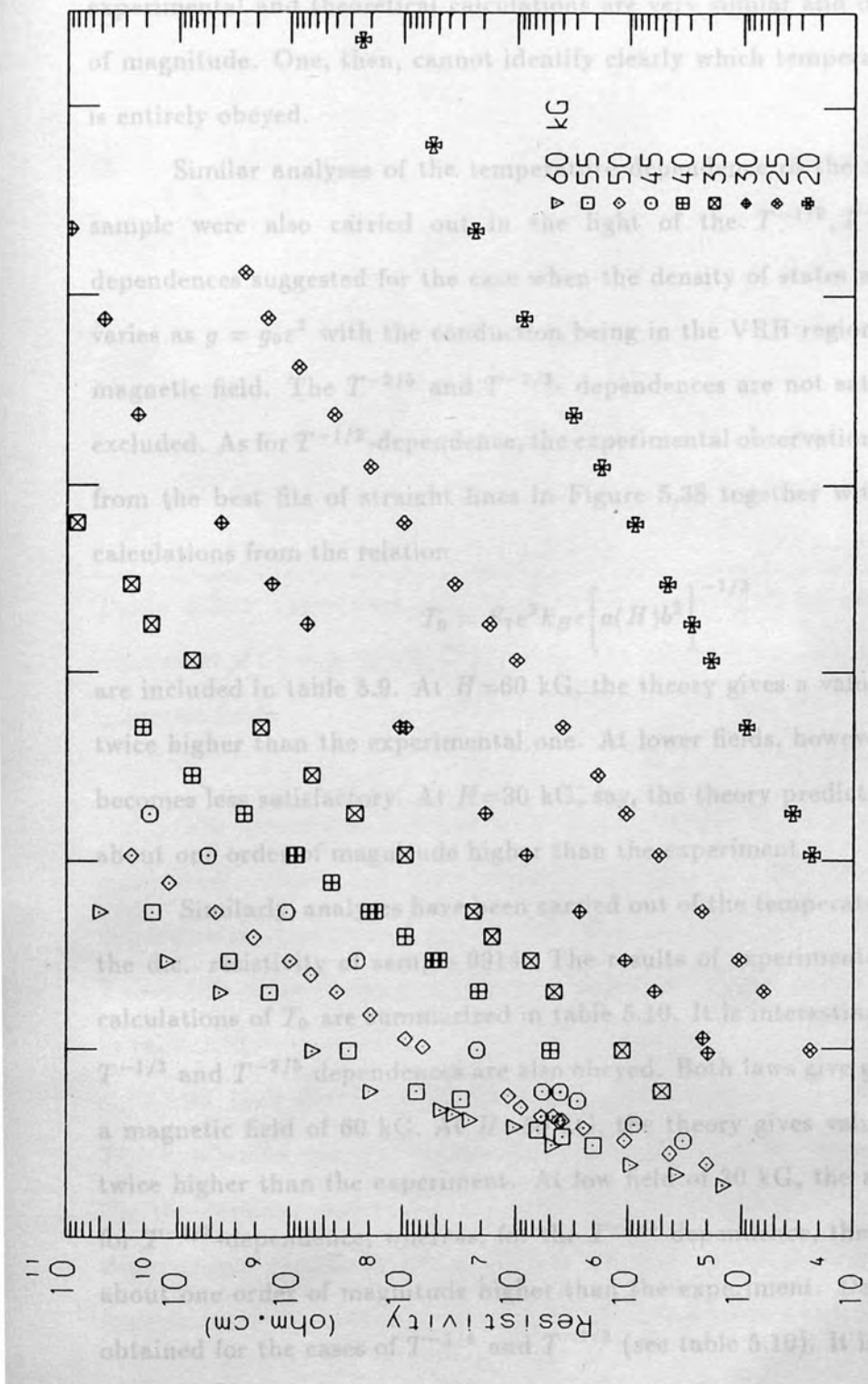

Figure 5.38
The d.c. resistivity of sample 5714 as a function of $T^{-1/2}$ at different fields.

$T^{-1/4}$ for sample 5714. The plots show that the data are reasonably obeyed by this law. The best fits give values of T_0 which varies with the magnetic field. The results of such fitting procedure as well as the calculated parameters at different fields are included in table 5.9. At H=60 kG, the experimental value is only about three times higher than theoretical one. As the field is lowered, however, the experimental and theoretical calculations are very similar and of the same order of magnitude. One, then, cannot identify clearly which temperature dependence is entirely obeyed.

Similar analyses of the temperature dependence of the resistivity of this sample were also carried out in the light of the $T^{-1/2}, T^{-3/5}$ and $T^{-2/3}$-dependences suggested for the case when the density of states at the Fermi level varies as $g = g_0\epsilon^2$ with the conduction being in the VRH region in presence of a magnetic field. The $T^{-3/5}$ and $T^{-2/3}$- dependences are not satisfactory and are excluded. As for $T^{-1/2}$-dependence, the experimental observations of T_0 calculated from the best fits of straight lines in Figure 5.38 together with the theoretical calculations from the relation

$$T_0 = S_7 e^2 k_B \epsilon \left[a(H) b^2 \right]^{-1/3} \tag{5.35}$$

are included in table 5.9. At H=60 kG, the theory gives a value which is almost twice higher than the experimental one. At lower fields, however, the agreement becomes less satisfactory. At H=30 kG, say, the theory predicts a value which is about one order of magnitude higher than the experiment.

Similarly, analyses have been carried out of the temperature dependence of the d.c. resistivity of sample 9914. The results of experimental and theoretical calculations of T_0 are summarized in table 5.10. It is interesting to note that the $T^{-1/3}$ and $T^{-2/5}$-dependences are also obeyed. Both laws give good agreement at a magnetic field of 60 kG. At H=50 kG, the theory gives values (of T_0) almost twice higher than the experiment. At low field of 30 kG, the agreement is good for $T^{-1/3}$-dependence, whereas, for the $T^{-2/5}$-dependence, theory predicts T_0 of about one order of magnitude higher than the experiment. Data for T_0 are also obtained for the cases of $T^{-1/4}$ and $T^{-1/2}$ (see table 5.10). It is obvious that the

agreement is poor for the case of $T^{-1/2}$.

		T_0 (K)	
H(kG)	x	Expt.	Theory
60	1/4	6.0×10^5	2.1×10^5
"	1/3	8.0×10^3	8.4×10^3
"	2/5	1.1×10^3	9.7×10^2
"	1/2	1.5×10^2	5.7×10^2
50	1/4	2.5×10^5	2.4×10^5
"	1/3	3.9×10^3	9.4×10^3
"	2/5	5.4×10^2	9.1×10^2
"	1/2	8.3×10	5.9×10^2
30	1/4	6.7×10^3	8.7×10^4
"	1/3	2.1×10^2	3.4×10^3
"	2/5	4.1×10	4.3×10^2
"	1/2	9.0	4.2×10^2

Table 5.10: Theoretical and experimental values of T_0 for sample 9914 in the expression $\rho(T) = \rho_0 \exp(T_0/T)^x$ for various values of the exponent x at different magnetic fields.

The temperature dependence of the resistivity of sample 2015 is also considered. Data are demonstrated in Figures 5.39-5.42 for the different dependences. One indeed cannot infer clear conclusion from these simple plots. The results of the obtained fitting parameters at different magnetic fields are given in table 5.11.

At high fields, good agreement is obtained for the $T^{-1/3}$, $T^{-2/5}$ and $T^{-1/4}$, whereas, the $T^{-1/2}$-dependence gives T_0 an order of magnitude less than the theoretical calculations. At lower field of 40 kG, $T^{-1/4}$, $T^{-1/3}$ and $T^{-2/5}$ dependences predict values of T_0 only an order of magnitude greater than the experimental observations, while $T^{-1/2}$ predicts a value which is about two orders

of magnitude off the experimental finding.

		T_0 (K)	
H(kG)	x	Expt.	Theory
60	1/4	2.0×10^5	1.4×10^5
"	1/3	2.9×10^3	4.9×10^3
"	2/5	3.8×10^2	8.2×10^2
"	1/2	5.7×10	5.7×10^2
50	1/4	9.7×10^4	1.1×10^5
"	1/3	1.6×10^3	4.3×10^3
"	2/5	2.3×10^2	6.4×10^2
"	1/2	3.6×10	5.3×10^2
40	1/4	1.4×10^4	8.2×10^4
"	1/3	2.7×10^2	2.8×10^3
"	2/5	4.2×10	4.8×10^2
"	1/2	7.3	4.8×10^2

Table 5.11: Theoretical and experimental values of T_0 for sample 2015 in the expression $\rho(T) = \rho_0 \exp(T_0/T)^x$ for various values of the exponent x at different magnetic fields.

It may worth noting that the agreement between the experimental findings and the theoretical calculations deteriorates at lower fields. This might be attributed to the correlation effects (Tokumoto et al. 1982, Mansfield and Tokumoto 1983). It has been suggested that the correlation effects are important for concentrations above

$$N_c = \frac{3\epsilon k_B T}{16\pi\theta e^2 (a_{\|} a_{\perp^2})^{2/3}} \tag{5.36}$$

For fields $\sim$ 70 kG, this gives $N_c \approx 4 \times 10^{14} cm^{-3}$, this reduces to $\sim 2 \times 10^{14} cm^{-3}$ for lower field of about 30 kG. It might be interesting to investigate the behaviour of the resistivity with the magnetic field. This will be examined in the following

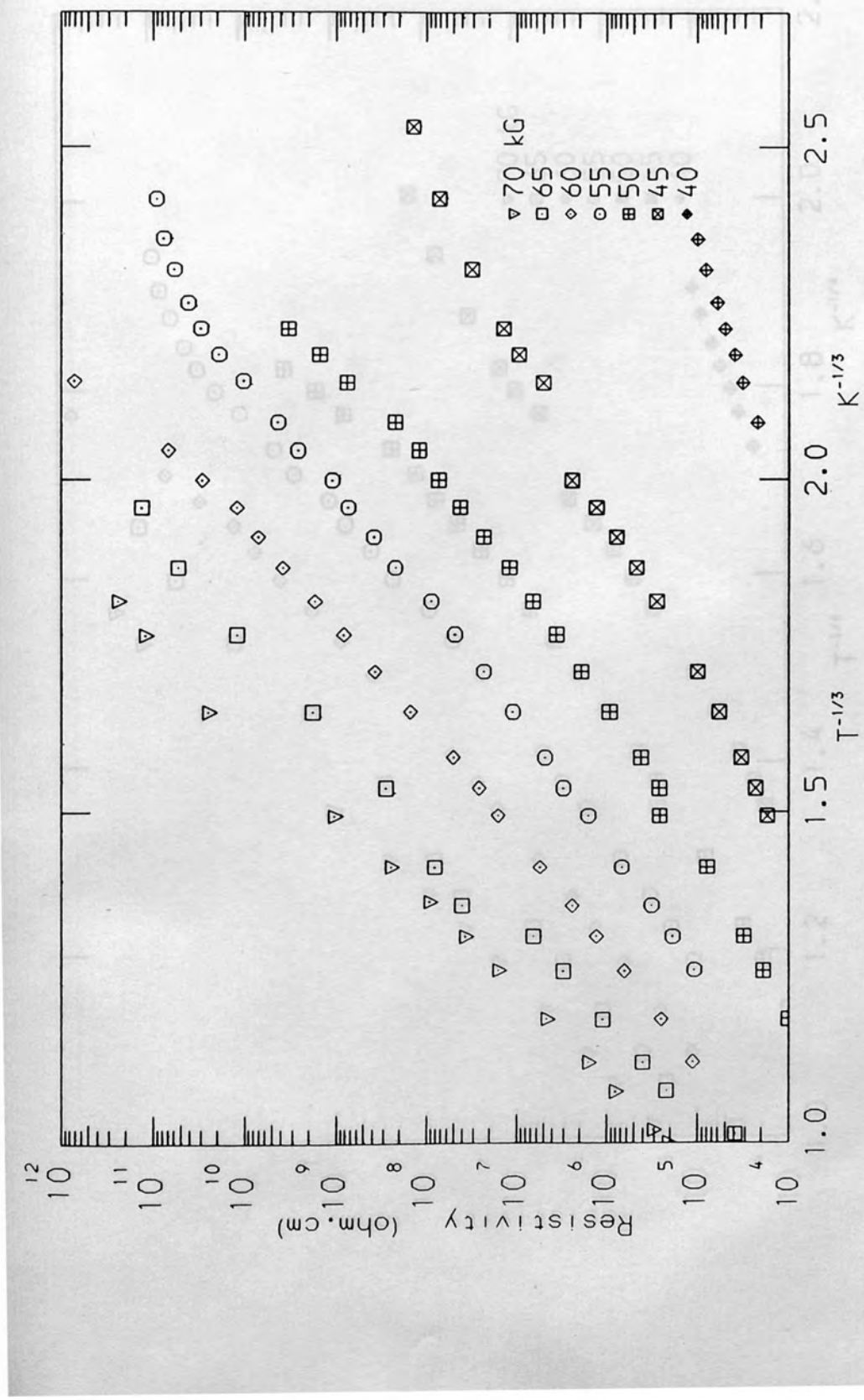

Figure 5.39

The d.c. resistivity of sample 2015 as a function of $T^{-1/3}$ at different fields.

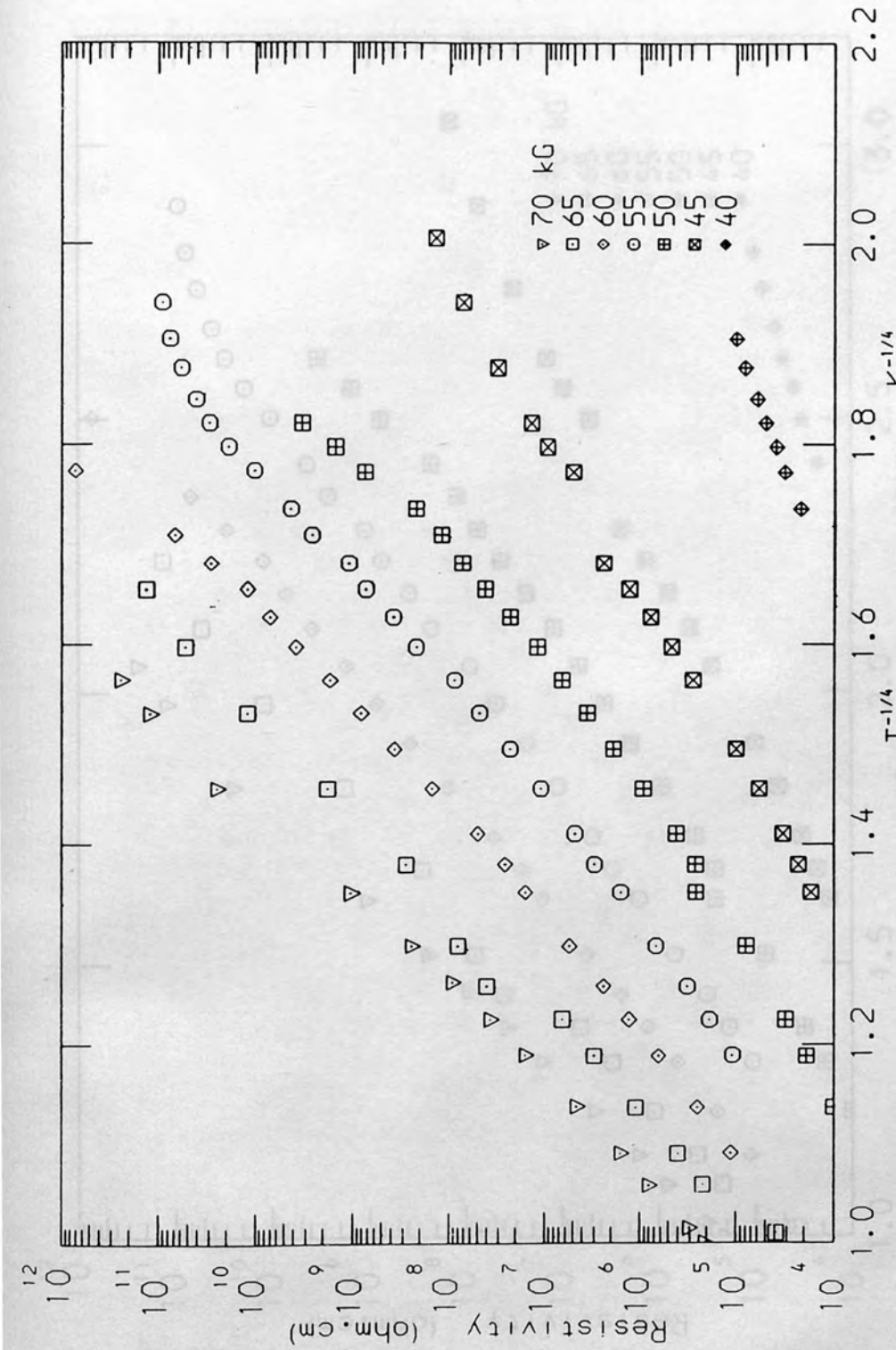

Figure 5.40

The d.c. resistivity of sample 2015 as a function of $T^{-1/4}$ at different fields.

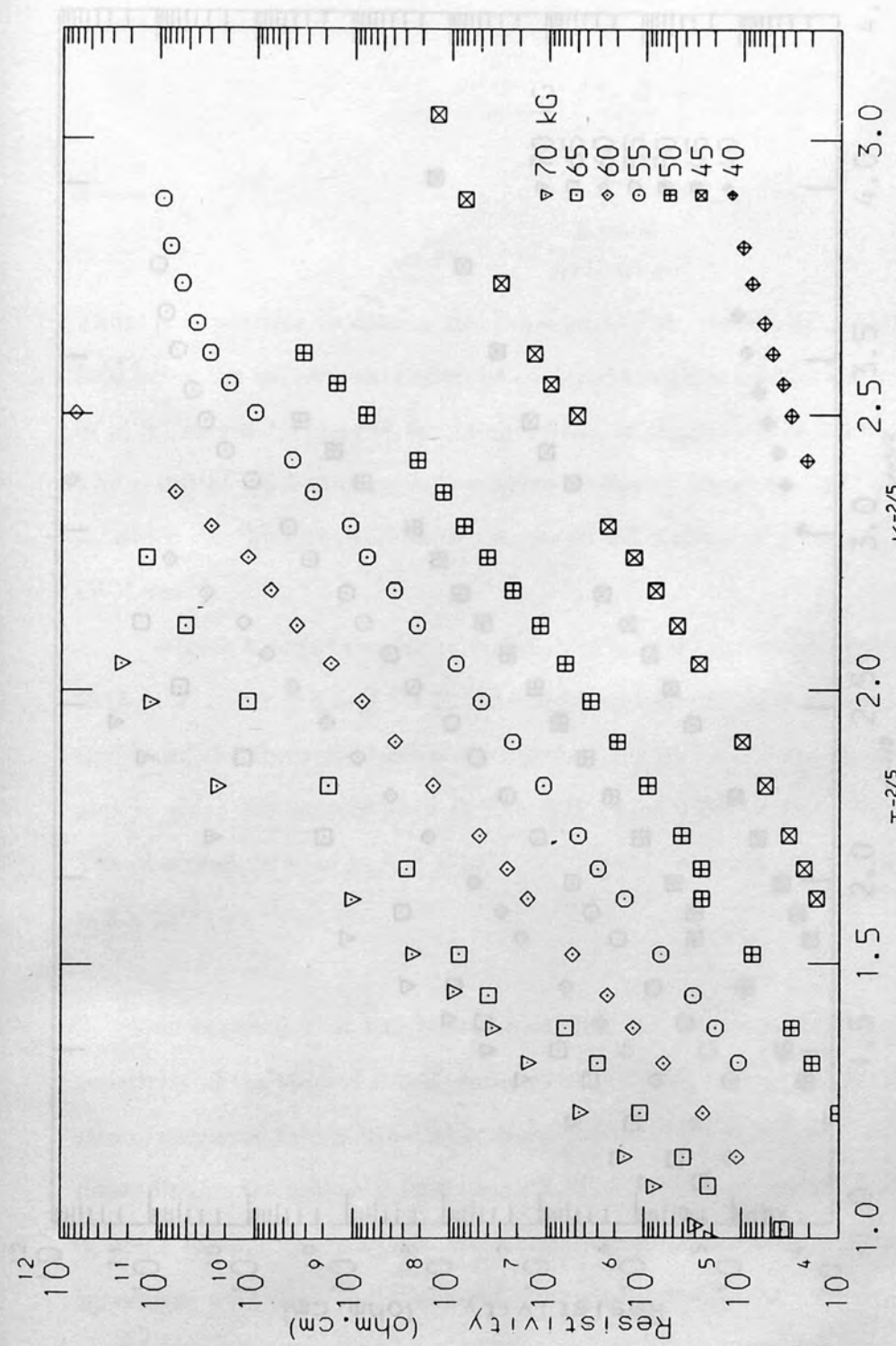

Figure 5.41

The d.c. resistivity of sample 2015 as a function of $T^{-2/5}$ at different fields.

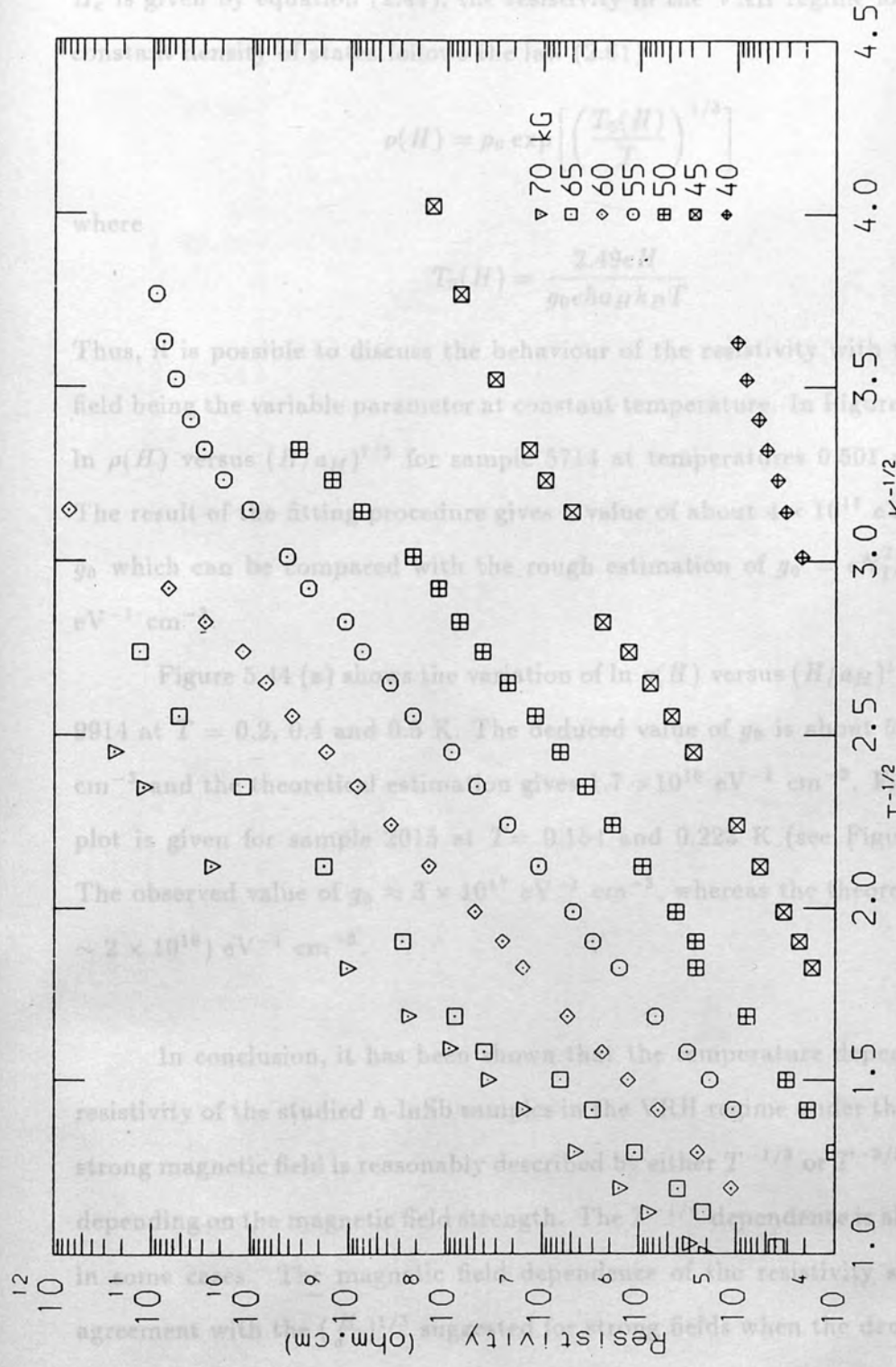

Figure 5.42
The d.c. resistivity of sample 2015 as a function of $T^{-1/2}$ at different fields.

section.

5.4.2 Magnetic Field Dependence of the DC Resistivity:

It has been discussed in chapter 2 that for magnetic fields $H > 6H_c$ where H_c is given by equation (2.47), the resistivity in the VRH regime for the case of constant density of states follows the law (2.61)

$$\rho(H) = \rho_0 \exp\left[\left(\frac{T_0(H)}{T}\right)^{1/3}\right] \tag{5.37}$$

where

$$T_0(H) = \frac{2.49eH}{g_0 c\hbar a_H k_B T} \tag{5.38}$$

Thus, it is possible to discuss the behaviour of the resistivity with the magnetic field being the variable parameter at constant temperature. In Figure 5.43 we plot ln $\rho(H)$ versus $(H/a_H)^{1/3}$ for sample 5714 at temperatures 0.501 and 0.620 K. The result of the fitting procedure gives a value of about 4×10^{17} eV^{-1} cm^{-3} for g_0 which can be compared with the rough estimation of $g_0 = \epsilon N_D^{2/3}/e^2 \approx 10^{18}$ eV^{-1} cm^{-3}.

Figure 5.44 (a) shows the variation of ln $\rho(H)$ versus $(H/a_H)^{1/3}$ for sample 9914 at T = 0.2, 0.4 and 0.5 K. The deduced value of g_0 is about 5×10^{17} eV^{-1} cm^{-3} and the theoretical estimation gives 1.7×10^{18} eV^{-1} cm^{-3}. Finally, similar plot is given for sample 2015 at T= 0.154 and 0.223 K (see Figure 5.44 (b)). The observed value of $g_0 \approx 3 \times 10^{17}$ eV^{-1} cm^{-3}, whereas the theoretical value is $\sim 2 \times 10^{18}$) eV^{-1} cm^{-3}.

In conclusion, it has been shown that the temperature dependence of the resistivity of the studied n-InSb samples in the VRH regime under the influence of strong magnetic field is reasonably described by either $T^{-1/3}$ or $T^{-2/5}$-dependence depending on the magnetic field strength. The $T^{-1/4}$-dependence is also applicable in some cases. The magnetic field dependence of the resistivity shows a good agreement with the $(\frac{H}{a})^{1/3}$ suggested for strong fields when the density of states at the Fermi level is constant. This information together with the a.c. analyses

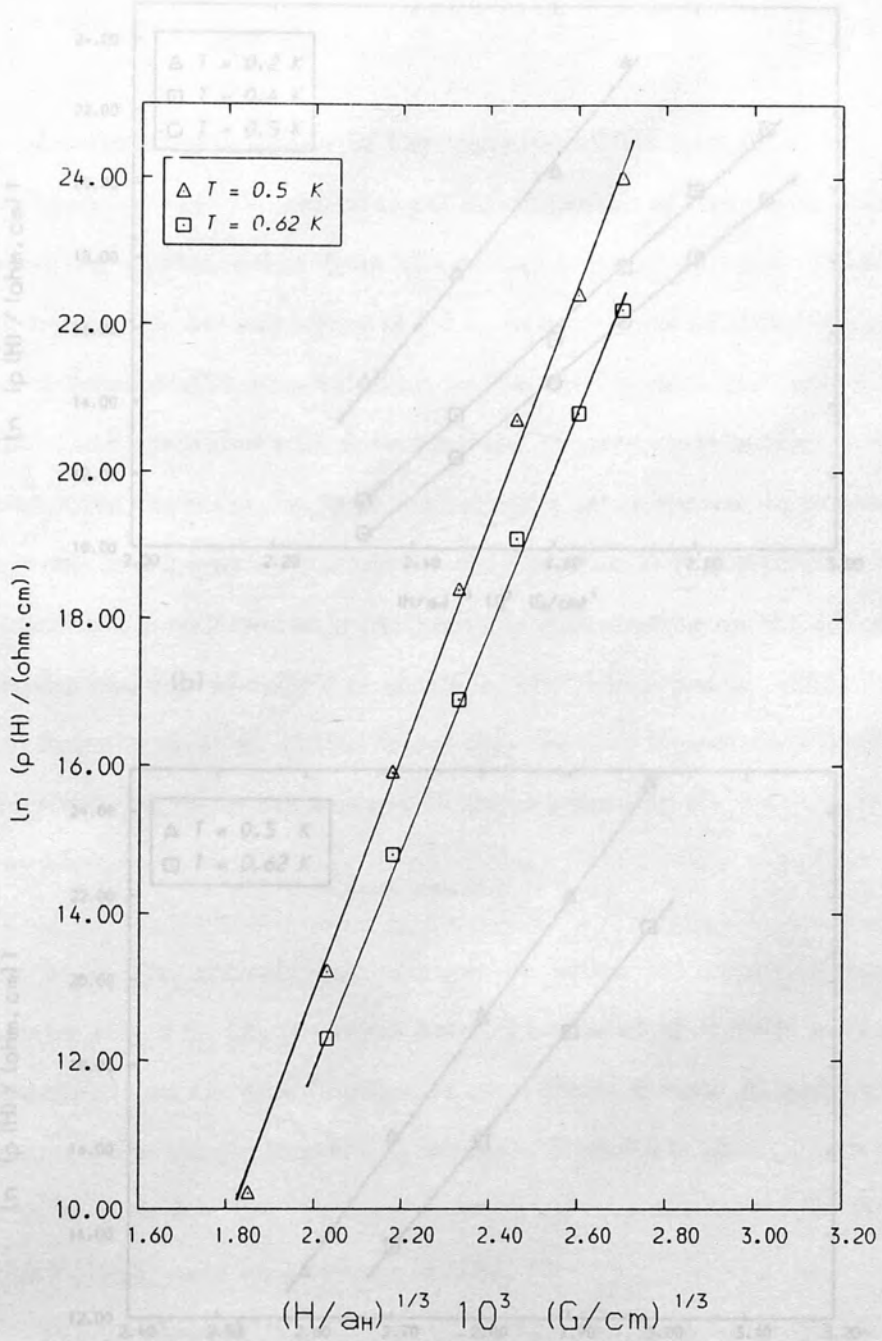

Figure 5.43

The d.c. resistivity of sample 5714 as a function of $(H/a_H)^{1/3}$ at two different temperatures.

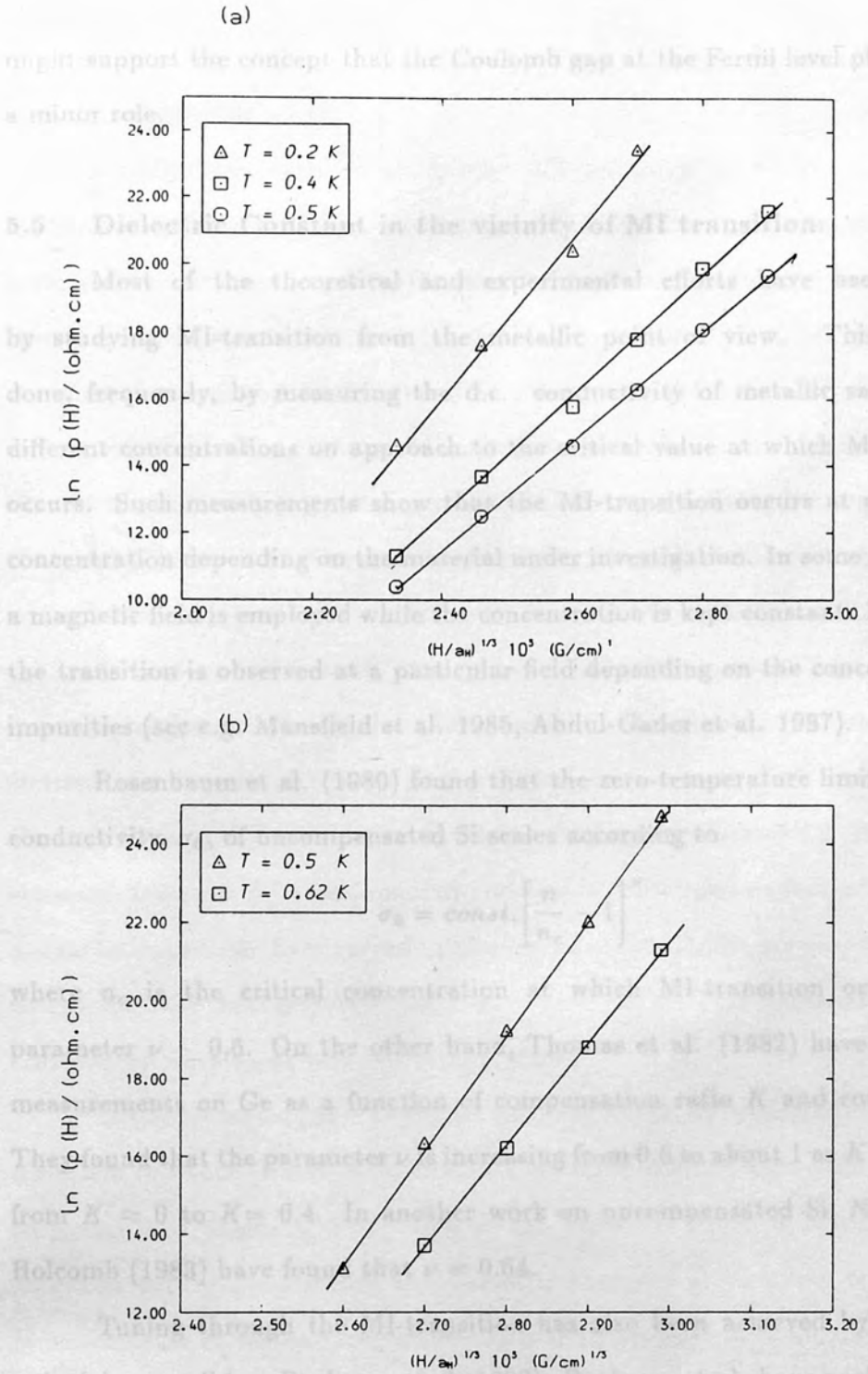

Figure 5.44

The d.c. resistivity as a function of $(H/a_H)^{1/3}$ of (a) Sample 9914 , (b) Sample 2015.

might support the concept that the Coulomb gap at the Fermi level plays at best a minor role.

5.5 Dielectric Constant in the vicinity of MI transition:

Most of the theoretical and experimental efforts have been confined by studying MI-transition from the metallic point of view. This has been done, frequently, by measuring the d.c. conductivity of metallic samples with different concentrations on approach to the critical value at which MI-transition occurs. Such measurements show that the MI-transition occurs at a particular concentration depending on the material under investigation. In some other cases, a magnetic field is employed while the concentration is kept constant. In this case, the transition is observed at a particular field depending on the concentration of impurities (see e.g. Mansfield et al. 1985, Abdul-Gader et al. 1987).

Rosenbaum et al. (1980) found that the zero-temperature limit of the d.c. conductivity, σ_0, of uncompensated Si scales according to

$$\sigma_0 = const.\left[\frac{n}{n_c} - 1\right]^{\nu} \tag{5.39}$$

where n_c is the critical concentration at which MI-transition occurs. The parameter $\nu \sim 0.6$. On the other hand, Thomas et al. (1982) have carried out measurements on Ge as a function of compensation ratio K and concentration. They found that the parameter ν is increasing from 0.6 to about 1 as K is increased from $K \approx 0$ to $K = 0.4$. In another work on uncompensated Si, Newman and Holcomb (1983) have found that $\nu = 0.64$.

Tuning through the MI-transition has also been achieved by applying a uniaxial stress S (see Paalanen et al. 1982). Paalanen et al. have performed their measurements on uncompensated Si at millikelvin temperatures down to about 3 mK, and they found that σ_0 obeys the relation

$$\sigma_0 \propto \left(S - S_c\right)^{\nu} \tag{5.40}$$

with $\nu \sim 0.5$, where S_c is a critical value of stress S. In a recent work, Mansfield et al. (1985) (see also Abdul-Gader et al. 1987) have studied the behaviour of σ_0

for compensated n-InSb as a function of a magnetic field. These authors found that the exponent ν =1.12.

Another approach to study the MI-transition is to invert the usual traditional technique of approaching the MI-transition from the metallic side. Instead, one can approach the MI-transition from the insulator side, a technique known as insulator-metal transition (IM). This, indeed, can be performed by studying the variation of the dielectric constant as a function of concentration or magnetic field. One of the problems which received a lot of investigations is the type of transition. It is generally accepted that the transition is a smooth rather than sharp transition. The smooth vanishing of an activation energy ε_3 as the critical concentration is approached is evidence of the smooth transition.

A semiconductor with a very small impurity content has a dielectric constant characteristic of the pure crystal. An increase in the impurity concentration causes a change in the dielectric constant. The study given by Castner et al. (1975) on doped Si shows that a large increase in the dielectric constant occurs as N^c is approached and this is considered as further evidence of a smooth transition. As observed by Castner et al (1975), the hopping contribution to conductivity becomes very large as $N_D \rightarrow N^c$. This contribution can be removed by working at very low temperatures.

In the present section we will be concerned with the variation of the relative dielectric constant (which is calculated from the measured capacitance) with the frequency and magnetic field. One of the problems which is of interest is the magnetic field dependence of the dielectric constant at very low temperatures. Measurements of the capacitive part of n-InSb samples were carried out in the same range of magnetic fields as described earlier. The variation of the capacitance with temperature, frequency and magnetic field is shown in Figures 5.45-5.54 for the three samples. One can distinguish three different regions;

(1) At very low temperatures, a temperature-independent behaviour is observed.

(2) There follows a gradual increase as the temperature is increased, and the capacitance becomes temperature dependent.

(3) At high temperatures, a sharp increase in the capacitance is observed. At high enough temperatures, depending on the magnetic field, the capacitance seems to decrease as the temperature is further increased. This can be seen clearly in Figures 5.48-5.54.

In what follows the magnetic field dependence of the relative dielectric constant which is calculated from the capacitive part will be discussed. Section 5.5.2 discuss the frequency and the temperature dependence of the dielectric constant.

5.5.1 Magnetic Field Dependence of the dielectric constant in the vicinity of IM-transition:

In order to analyse the data, the capacitance, C_0, due to the host crystal is subtracted from the the measured values. The relative dielectric constant due to donors, ϵ, is calculated from the relation

$$\epsilon = \frac{\ell}{\epsilon_0 d} C_{donors} \tag{5.41}$$

where ℓ and d are the thickness and area of the capacitor respectively and ϵ_0 is the free space dielectric constant $= 8.85 \times 10^{-12}$ Farad/meter. The lowest temperature values of the observed dielectric constant are obtained at different frequencies and magnetic fields. These values are plotted in Figures 5.55-5.57 as a function of the magnetic field H for the three samples respectively. The main feature of these graphs is the tendency of the dielectric constant to diverge as the field is reduced towards the critical value H_{cr}.

Capizzi et al. (1980) (see also Bhatt 1984) have carried out measurements on Si:P as a function of concentration and they have observed an enhancement in ϵ as N_D increases. These authors have discussed their results in terms of a scaling

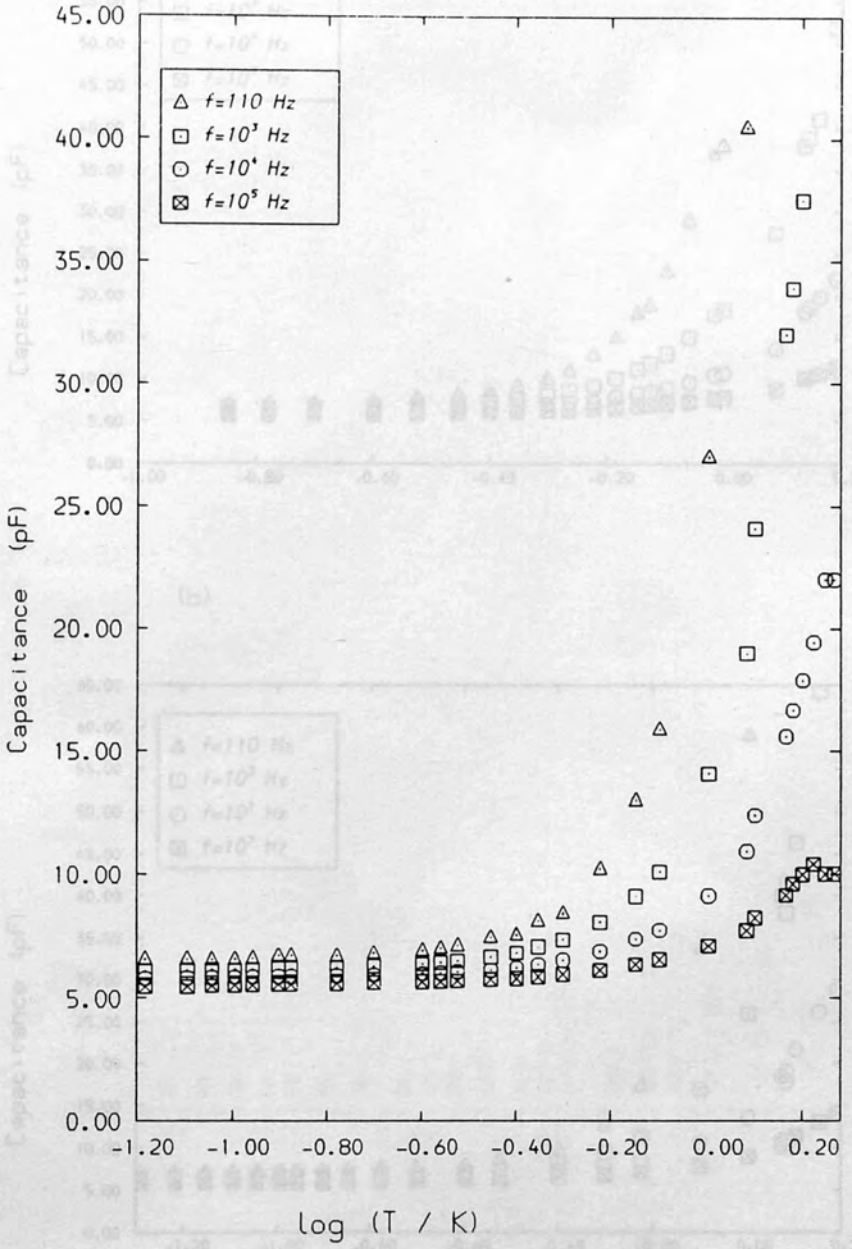

Figure 5.45

The capacitance of sample 5714 is plotted as a function of log T at H = 55 kG.

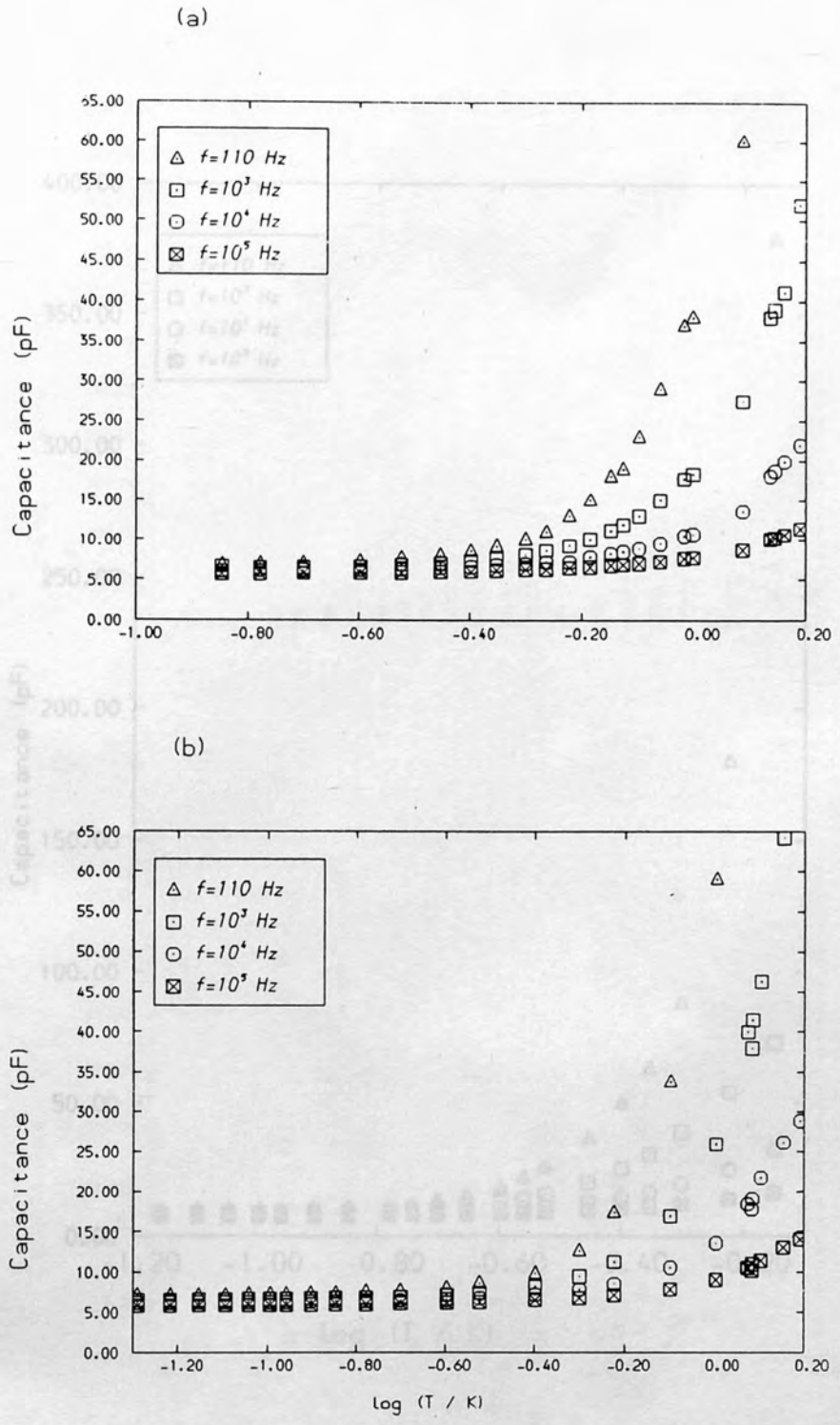

Figure 5.46

The capacitance of sample 5714 as a function of temperature T on a semi-log scale at magnetic fields (a) H=50 kG and (b) H= 45 kG.

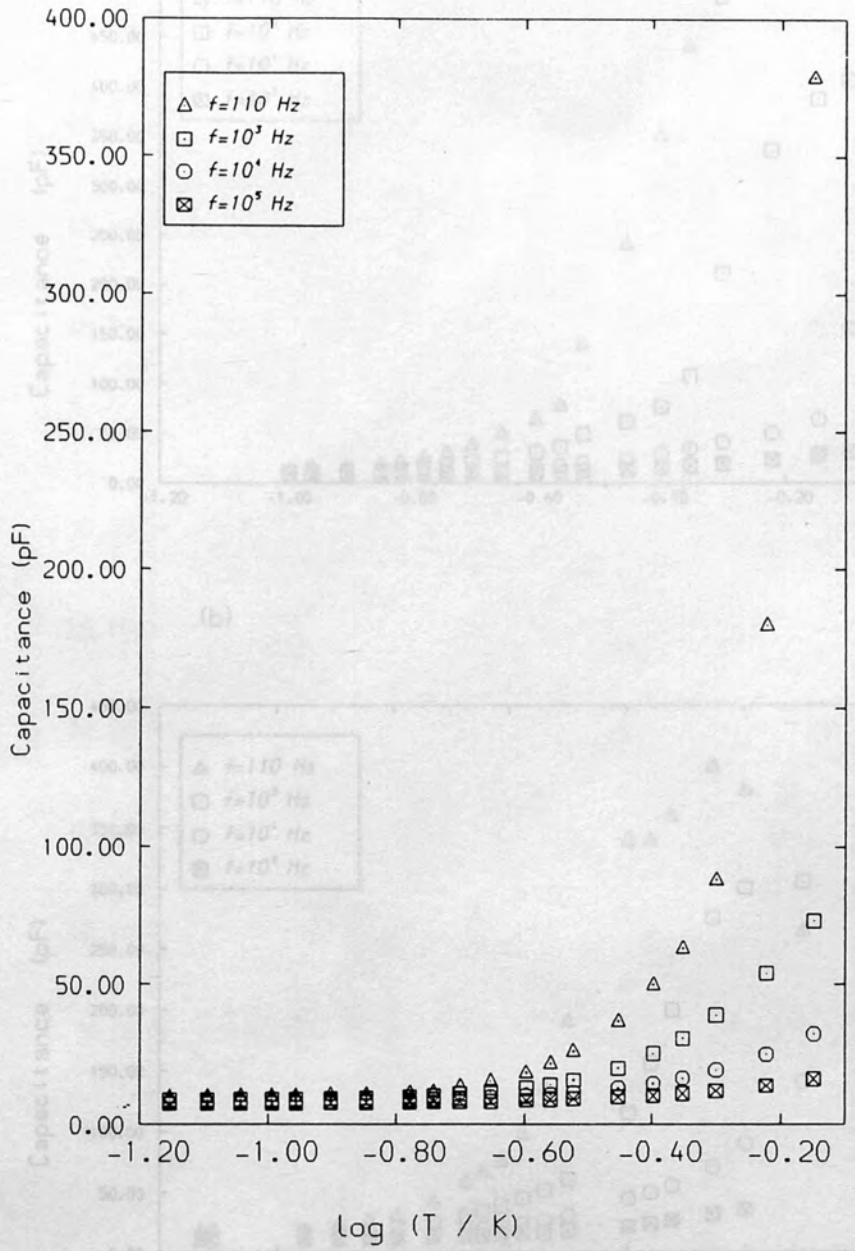

Figure 5.47

The capacitance of sample 5714 as a function of log T at H = 30 kG.

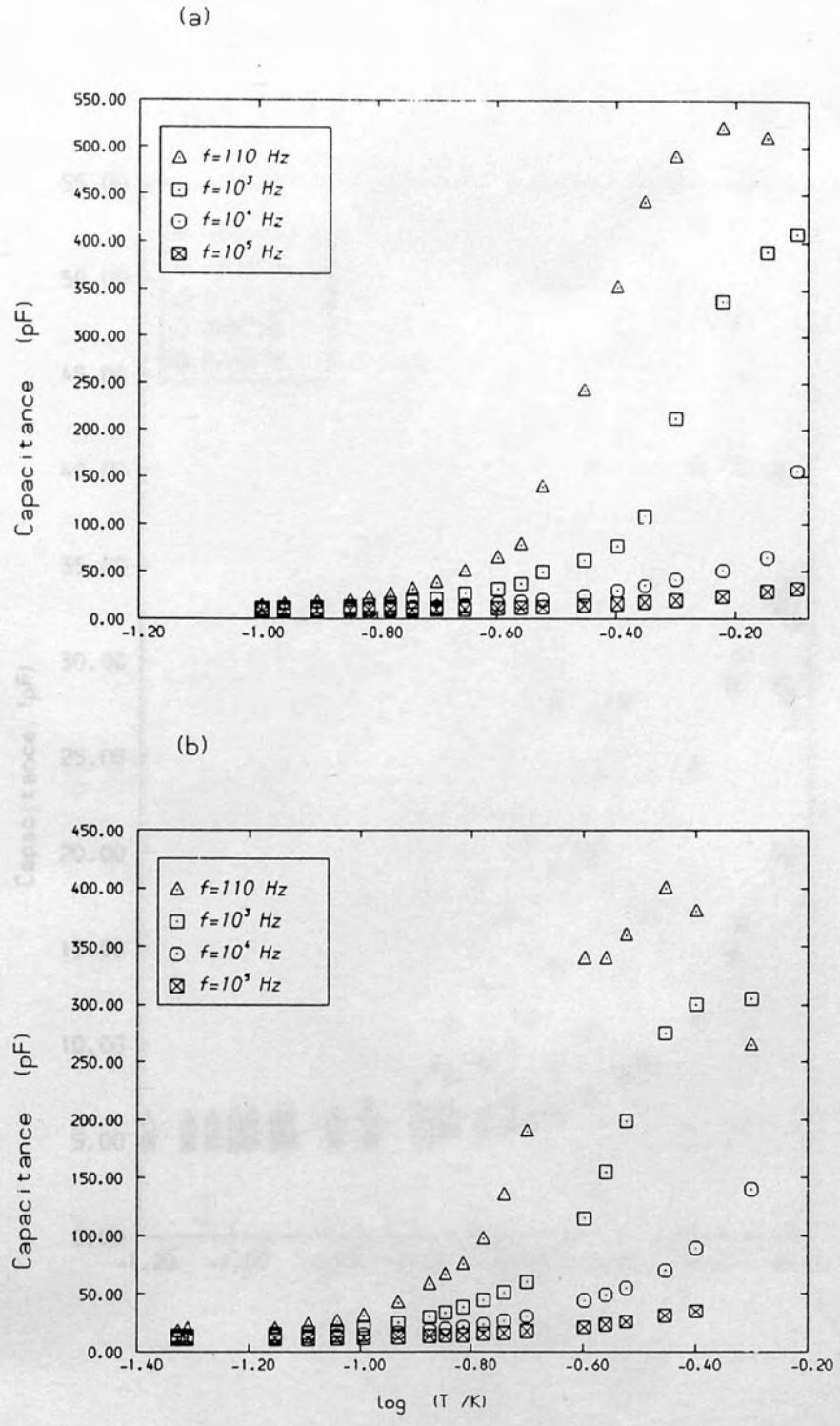

Figure 5.48

The capacitance of sample 5714 as a function of log T at (a) H= 25 kG, (b) H= 20 kG.

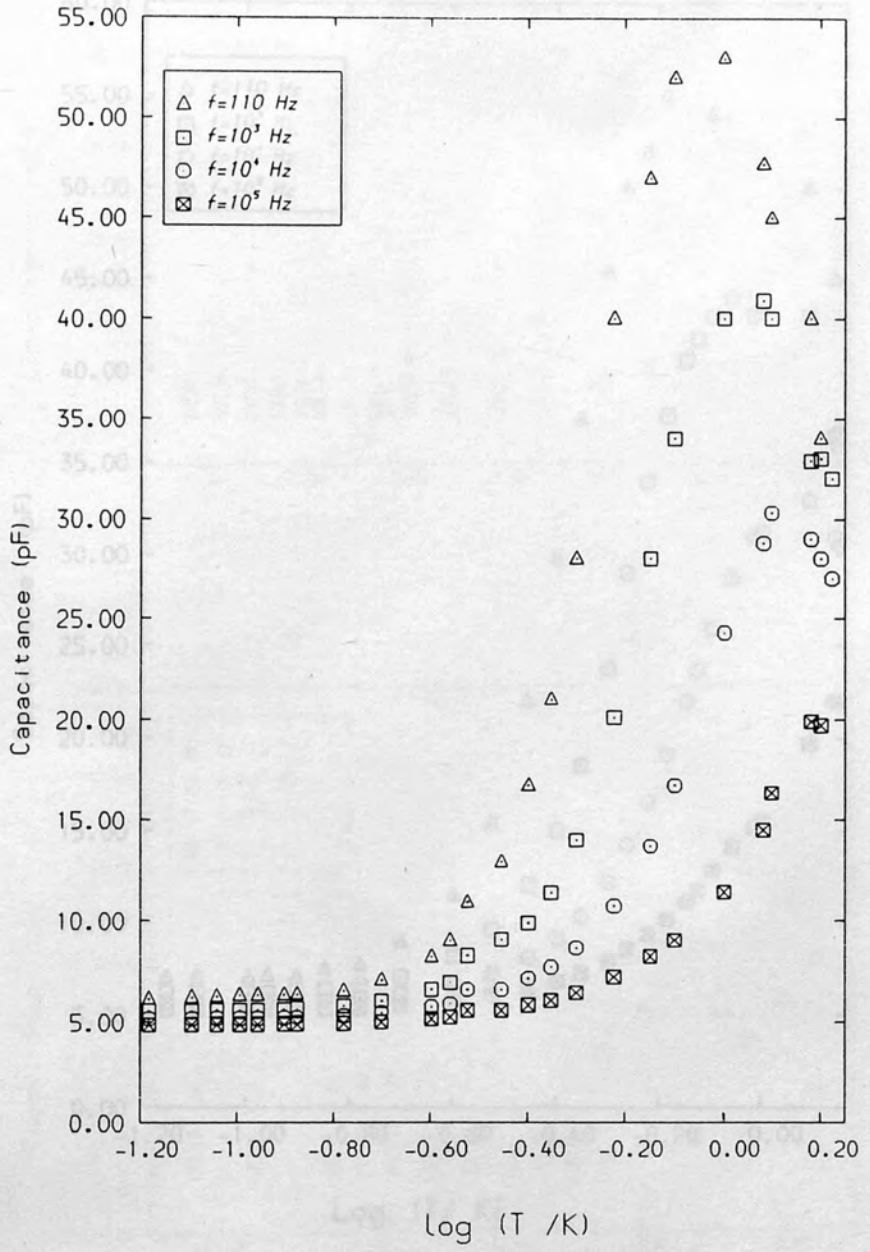

Figure 5.49

The capacitance of sample 9914 as a function of log T at a magnetic field H= 55 kG.

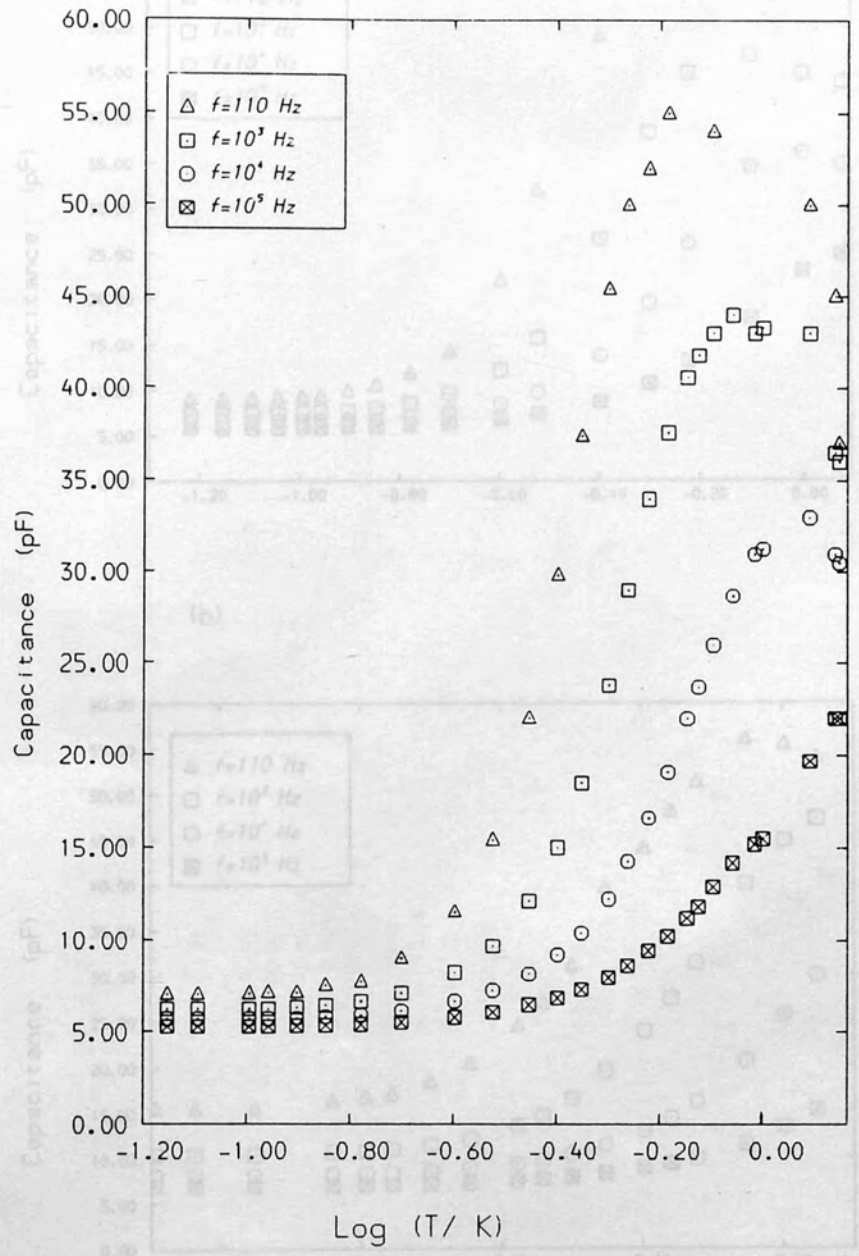

Figure 5.50

The capacitance of sample 9914 as a function of T at a magnetic field of 50 kG.

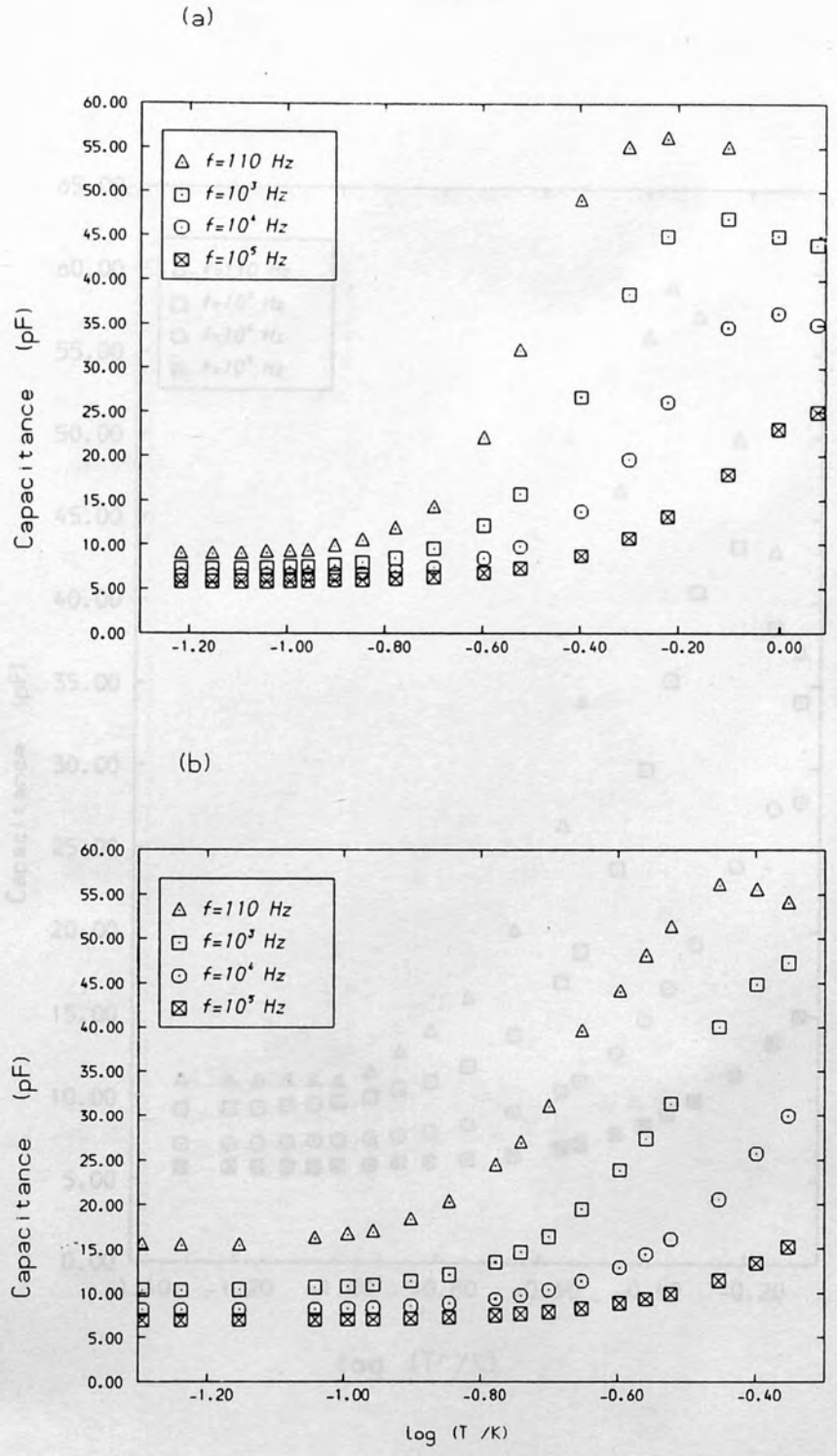

Figure 5.51

The capacitance of sample 9914 as a function of T at a magnetic field of (a) H = 45 kG, (b) H = 40 kG.

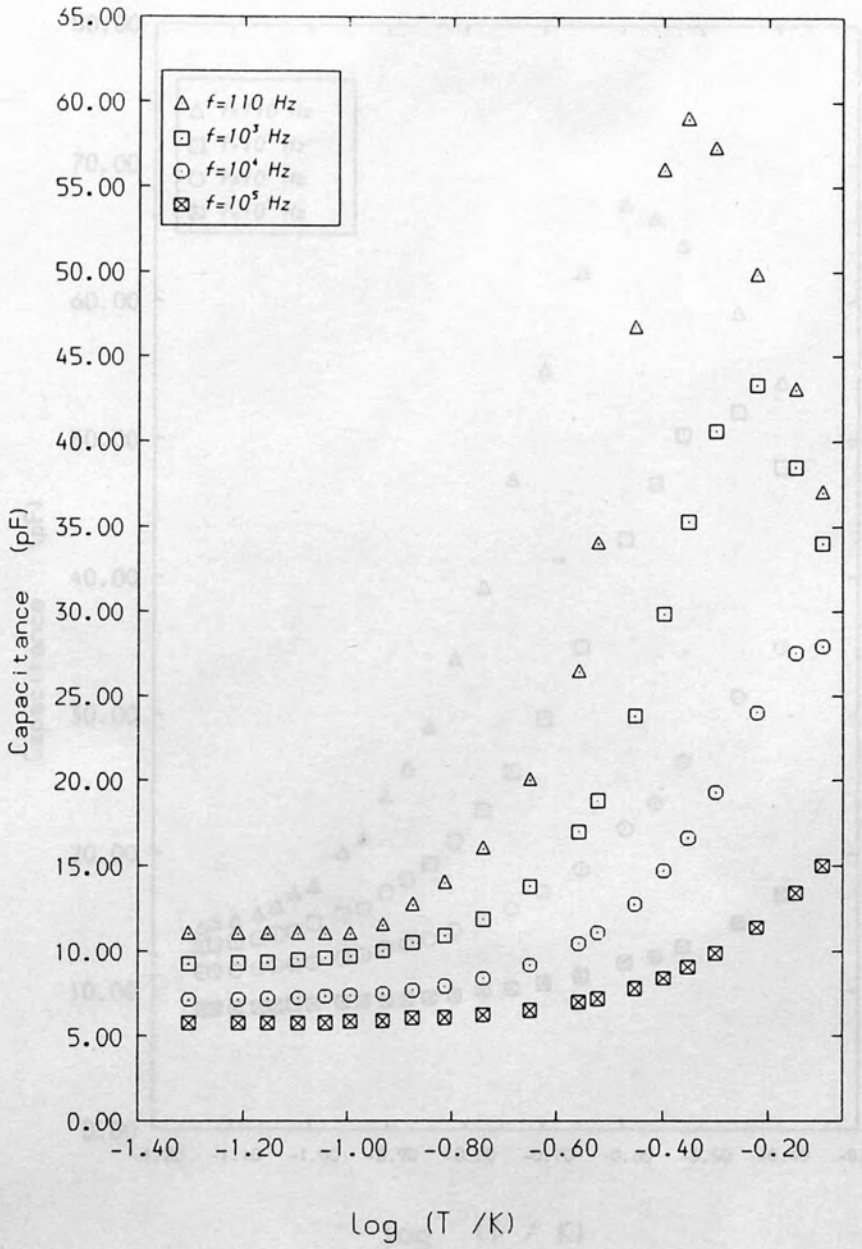

Figure 5.52

The capacitance of sample 2015 as a function of T at a magnetic field H= 65 kG.

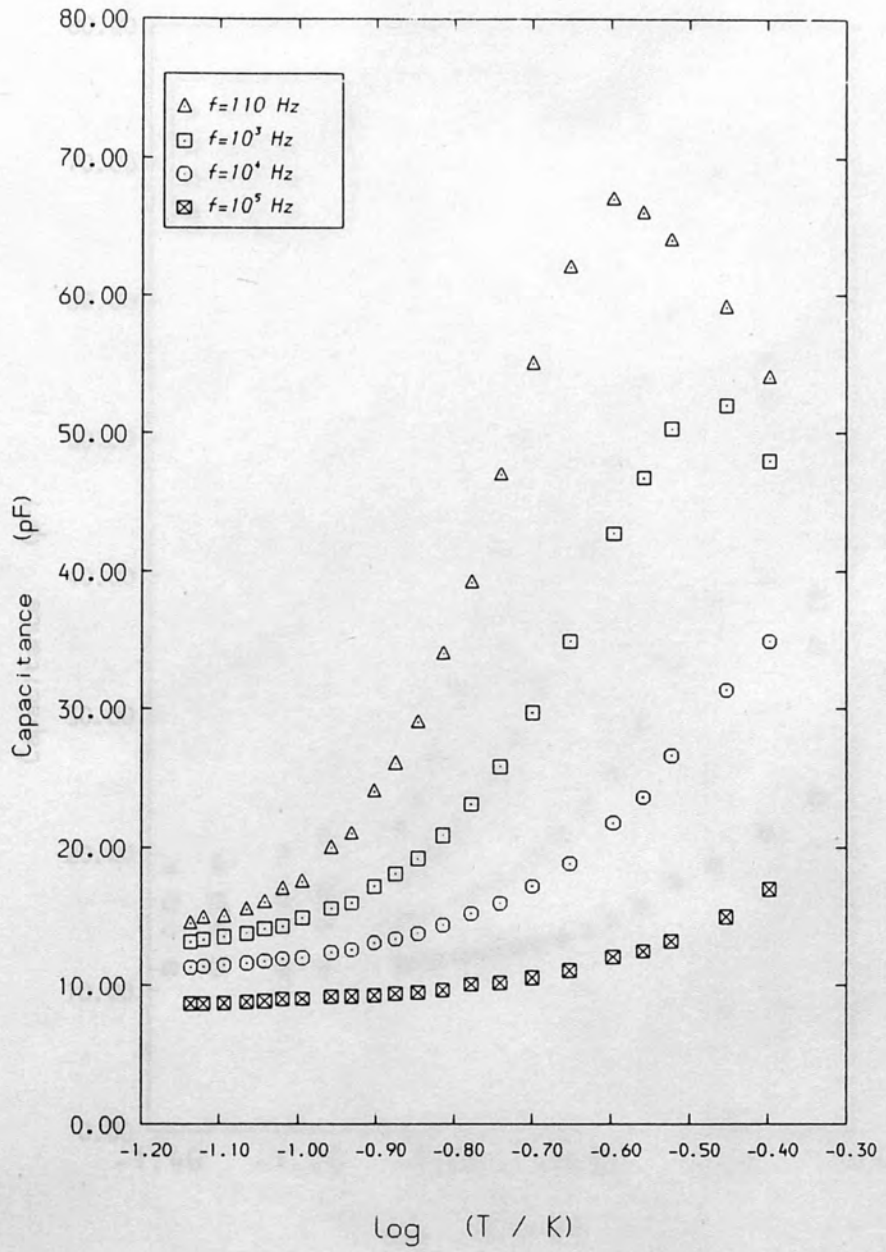

Figure 5.53

The capacitance of sample 2015 as a function of T at a magnetic field H = 55 kG.

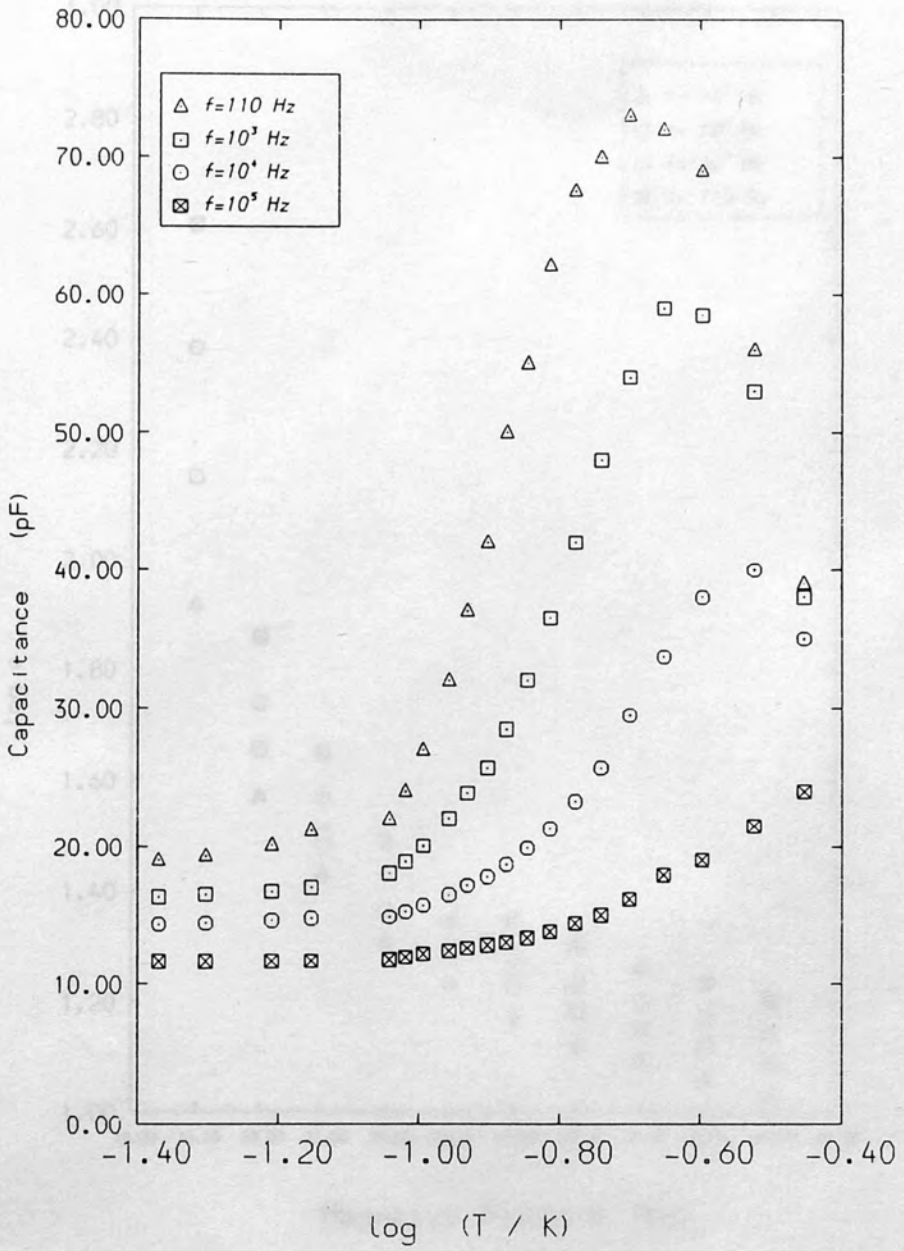

Figure 5.54

The capacitance of sample 2015 as a function of T at a magnetic field H = 50 kG.

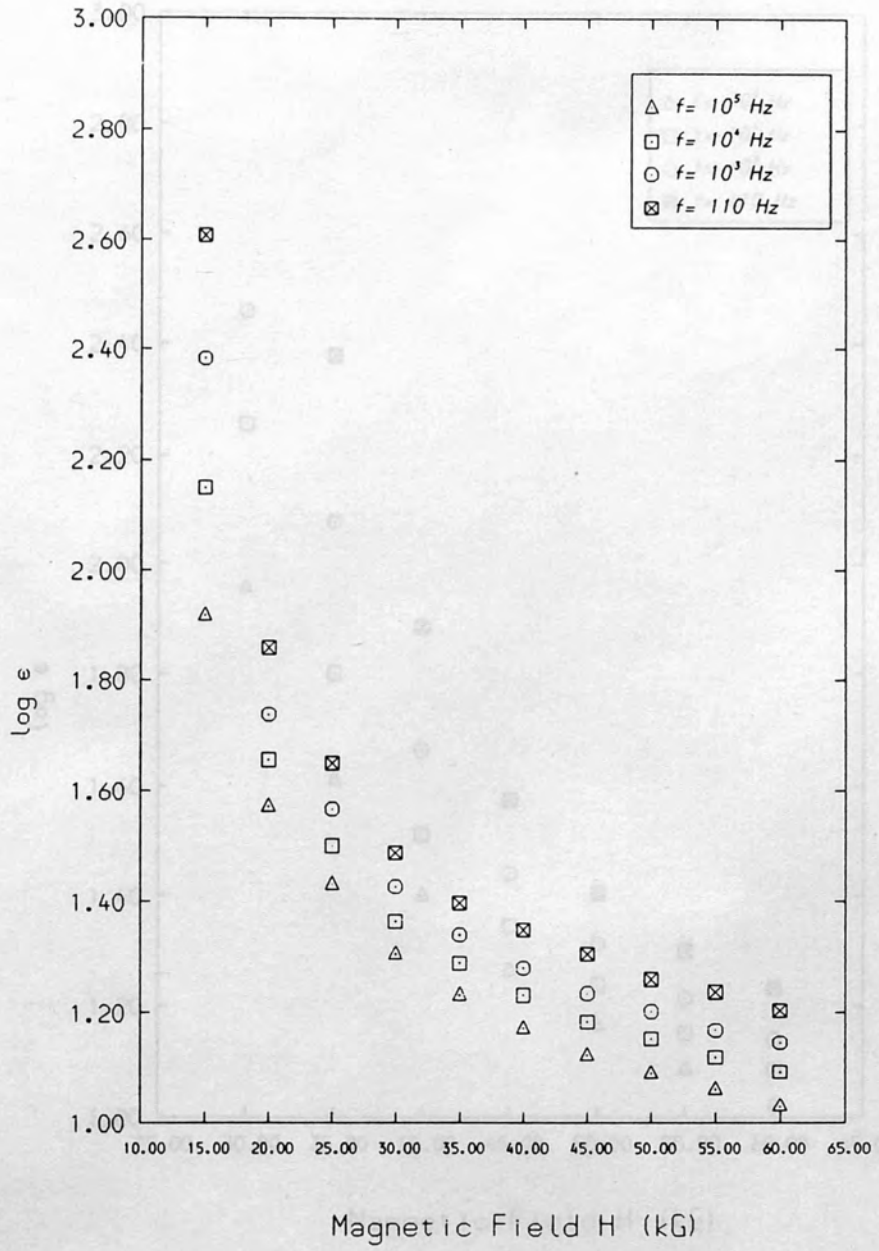

Figure 5.55

The relative dielectric constant of sample 5714 (obtained from the lowest temperature limit of the capacitance) as A function of the magnetic field H.

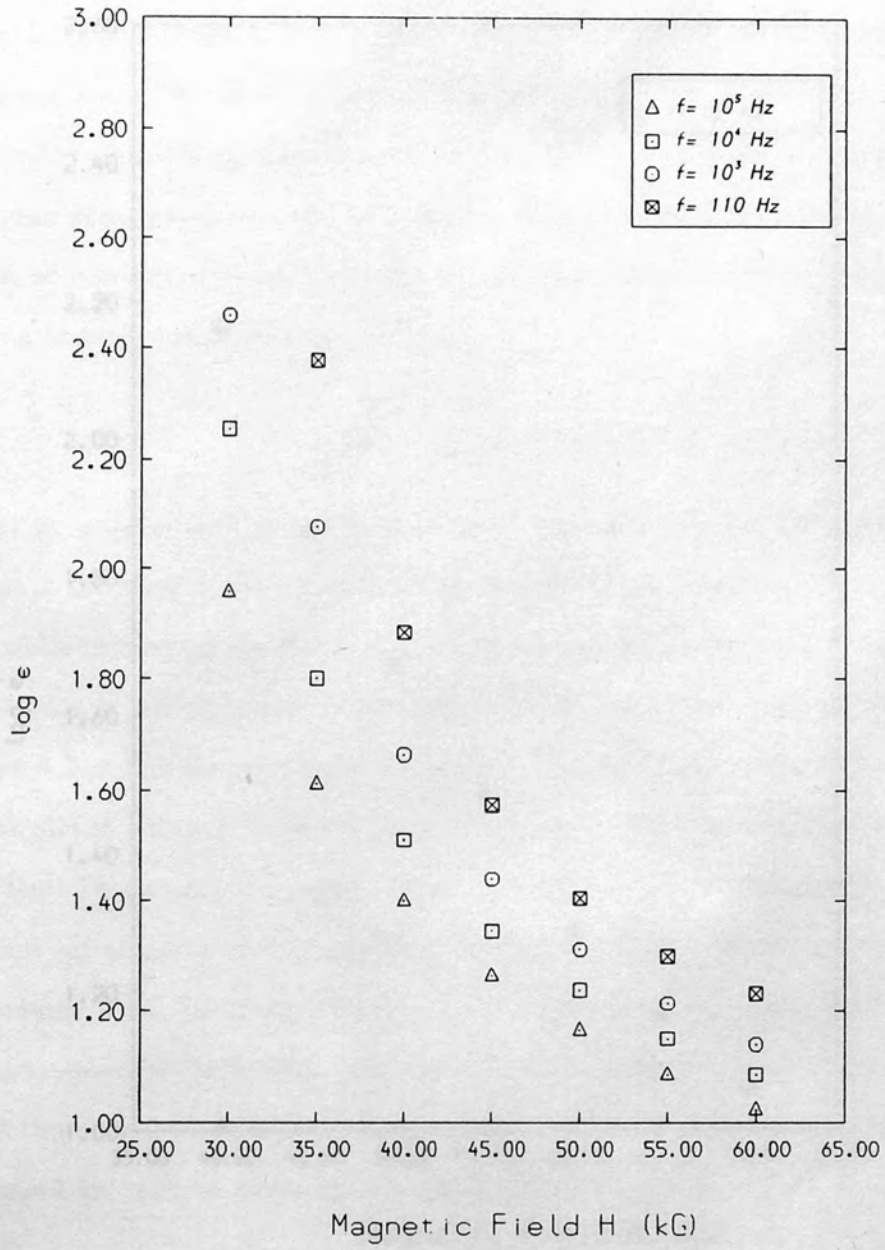

Figure 5.56

The relative dielectric constant of sample 9914 (obtained from the lowest temperature limit of the capacitance) as a function of the magnetic field H.

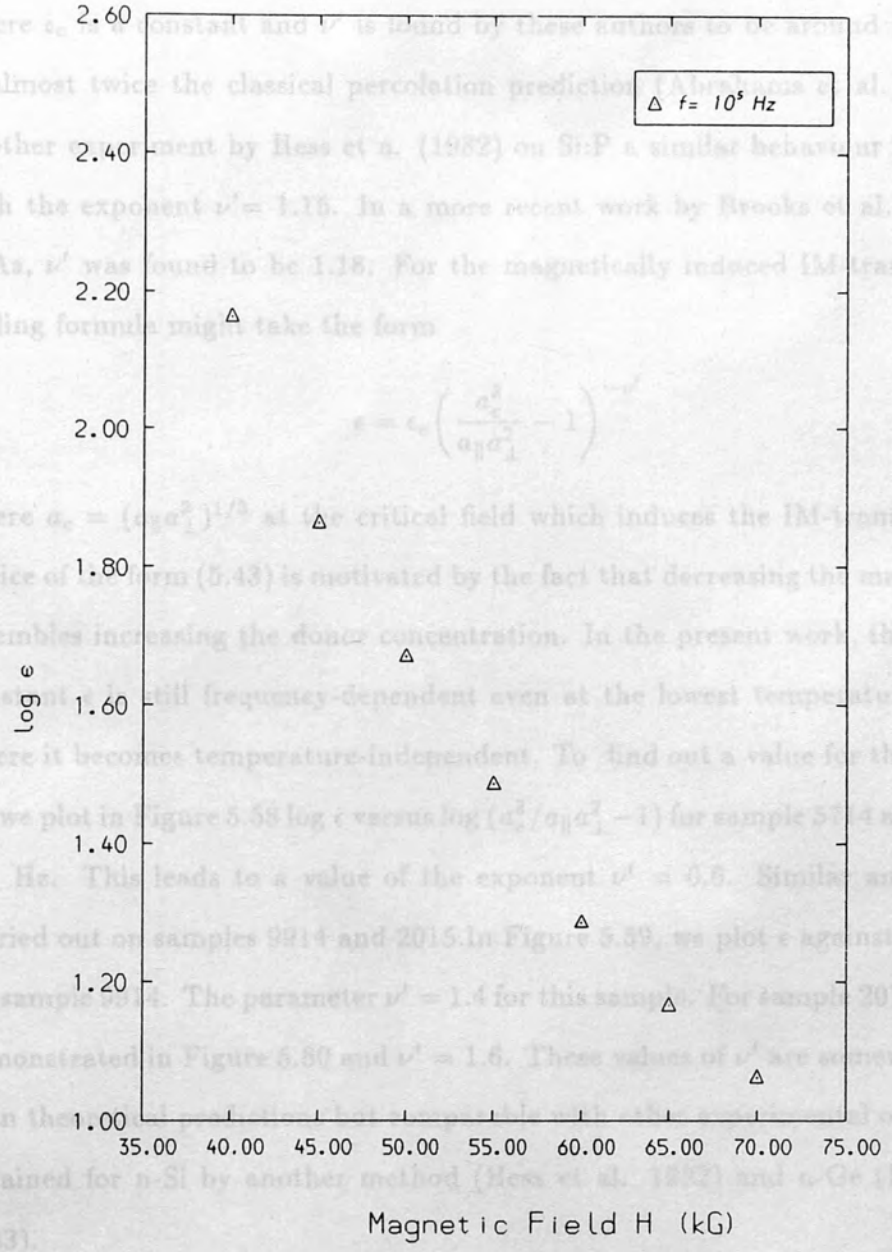

Figure 5.57

The relative dielectric constant of sample 2015 (obtained from the lowest temperature limit of the capacitance) as function of the magnetic field H.

theory of the form

$$\epsilon = \epsilon_c \left(\frac{N_c}{N_D} - 1 \right)^{-\nu'} \tag{5.42}$$

where ϵ_c is a constant and ν' is found by these authors to be around 1.09, which is almost twice the classical percolation prediction (Abrahams et al. 1975). In another experiment by Hess et a. (1982) on Si:P a similar behaviour is observed with the exponent ν'= 1.15. In a more recent work by Brooks et al. (1987) on Si:As, ν' was found to be 1.18. For the magnetically induced IM-transition, the scaling formula might take the form

$$\epsilon = \epsilon_c \left(\frac{a_c^3}{a_\parallel a_\perp^2} - 1 \right)^{-\nu'} \tag{5.43}$$

where $a_c = (a_\parallel a_\perp^2)^{1/3}$ at the critical field which induces the IM-transition. The choice of the form (5.43) is motivated by the fact that decreasing the magnetic field resembles increasing the donor concentration. In the present work, the dielectric constant ϵ is still frequency-dependent even at the lowest temperature achieved where it becomes temperature-independent. To find out a value for the exponent ν', we plot in Figure 5.58 $\log \epsilon$ versus $\log (a_c^3/a_\parallel a_\perp^2 - 1)$ for sample 5714 at frequency 10^5 Hz. This leads to a value of the exponent $\nu' = 0.6$. Similar analysis were carried out on samples 9914 and 2015.In Figure 5.59, we plot ϵ against $a_\parallel {a_\perp}^2/a_B^{*3}$ for sample 9914. The parameter $\nu' = 1.4$ for this sample. For sample 2015, data are demonstrated in Figure 5.60 and $\nu' = 1.6$. These values of ν' are somewhat higher than theoretical predictions but comparable with other experimental observations obtained for n-Si by another method (Hess et al. 1982) and n-Ge (Ionov et al. 1983).

Therefore, the scaling formula (5.43) seems to be applicable with the exponent ν' being higher than the theoretical prediction. This might suggest that the dielectric constant diverges with a critical exponent which could be related to the divergence of the localisation length as the IM-transition is approached from the insulator side. It is interesting to note that no common value of ν' can be inferred from the measurements, an increase in the doping level results in an increase in ν'. However measurements at lower fields close to the critical value and

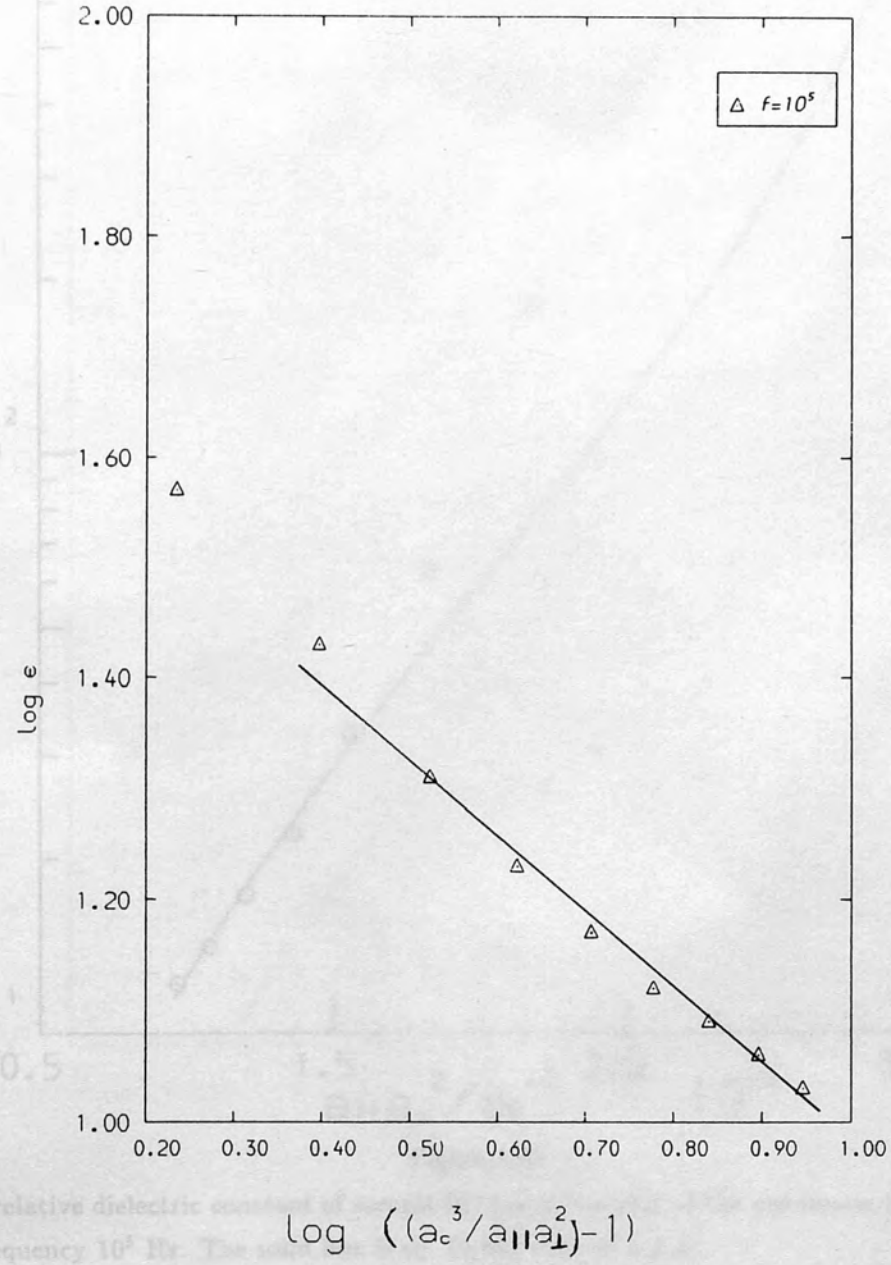

Figure 5.58

The relative dielectric constant of sample 5714 (obtained from the lowest temperature limit of the capacitance) as function of the parameter $((a_c^3/a_{\parallel}a_{\perp}^2) - 1)$. Where a_c is the critical value at which MI-transition occurs.

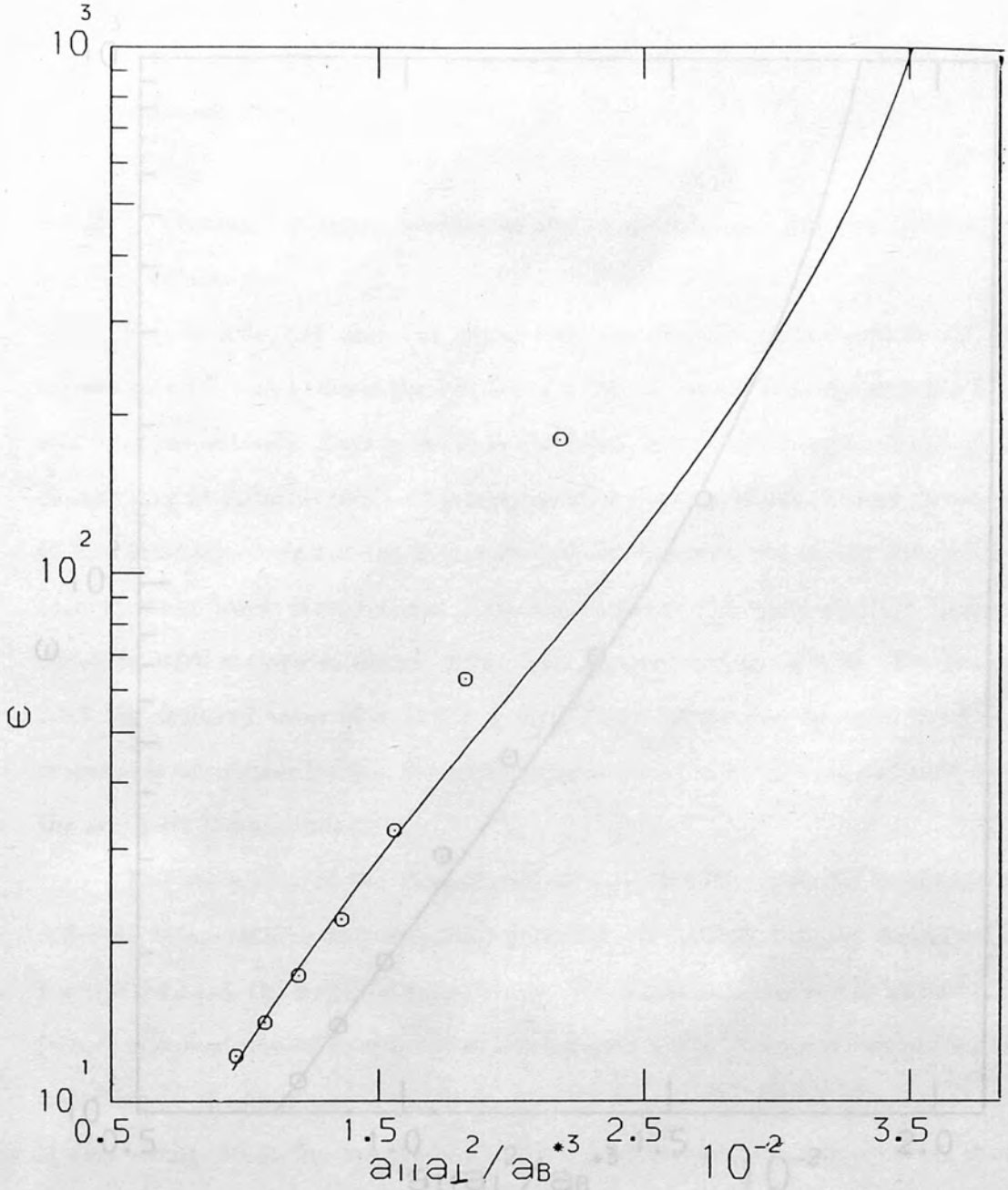

Figure 5.59

The relative dielectric constant of sample 9914 as a function of the parameter $(a_{\parallel}a_{\perp}^2/a_B^{3*})$ at frequency 10^5 Hz. The solid line is eq. (5.43) with $\nu l = 1.4$.

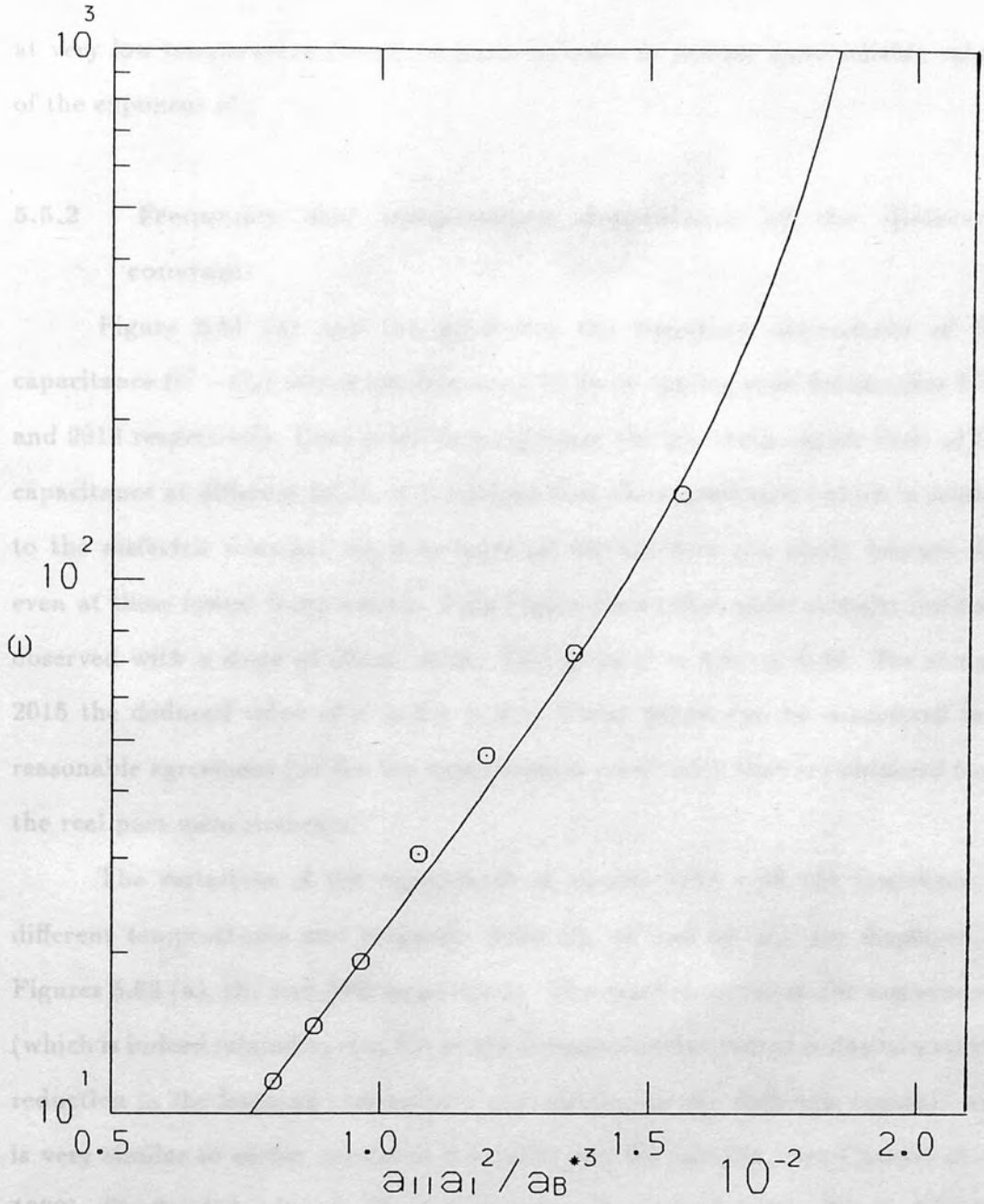

Figure 5.60

The relative dielectric constant of sample 2014 as a function of the parameter $(a_{\|}a_{\perp}^2/a_B^{*3})$ at frequency of 10^5 Hz. The solid line is eq. (5.43) with $\nu I = 1.6$.

at very low temperature should be made in order to deduce more reliable values of the exponent ν'.

5.5.2 Frequency and temperature dependence of the dielectric constant:

Figure 5.61 (a) and (b) illustrates the frequency dependence of the capacitance $(C - C_0)$ versus the frequency $\omega/2\pi$ on log-log scale for samples 5714 and 9914 respectively. Data given here represent the low-temperature limit of the capacitance at different fields. It is obvious that the capacitance (which is related to the dielectric constant via a geometrical factor) does not really become flat even at these lowest temperature. This Figure shows that quite straight lines are observed with a slope of about -0.06. This gives $s' = 0.94 \pm 0.08$. For sample 2015 the deduced value of s' is 0.9 ± 0.1. These values can be considered in a reasonable agreement (within the experimental error) with that (s) obtained from the real part measurements.

The variations of the capacitance of sample 5714 with the frequency at different temperatures and magnetic fields 60, 40 and 50 kG, are displayed in Figures 5.62 (a), (b) and 5.63 respectively. The rapid decrease in the capacitance (which is indeed related to $\epsilon(\omega, T)$) as the temperature is lowered is due to a strong reduction in the hopping conductivity contribution to the dielectric constant and is very similar to earlier results in n-type Si and Ge samples, (see Castner et al. 1980). Similar behaviour is observed for the other samples, (see Figure 5.64 (a) and (b)).

A comparison between the variation of the dielectric constant with frequency, (at H = 50 kG and T = 0.5 K), for samples 5714 and 9914 is shown in Figure 5.65 (a). It is obvious that the frequency dependence of the dielectric constant of sample 9914 is much stronger than that of sample 5714 and this is consistent with the fact that the donor concentration of sample 9914 is higher than that of sample 5714. Figure 5.65 (b) compares the temperature dependence of the dielectric constant of these samples at 10^4 Hz and 50 kG. The high-purity

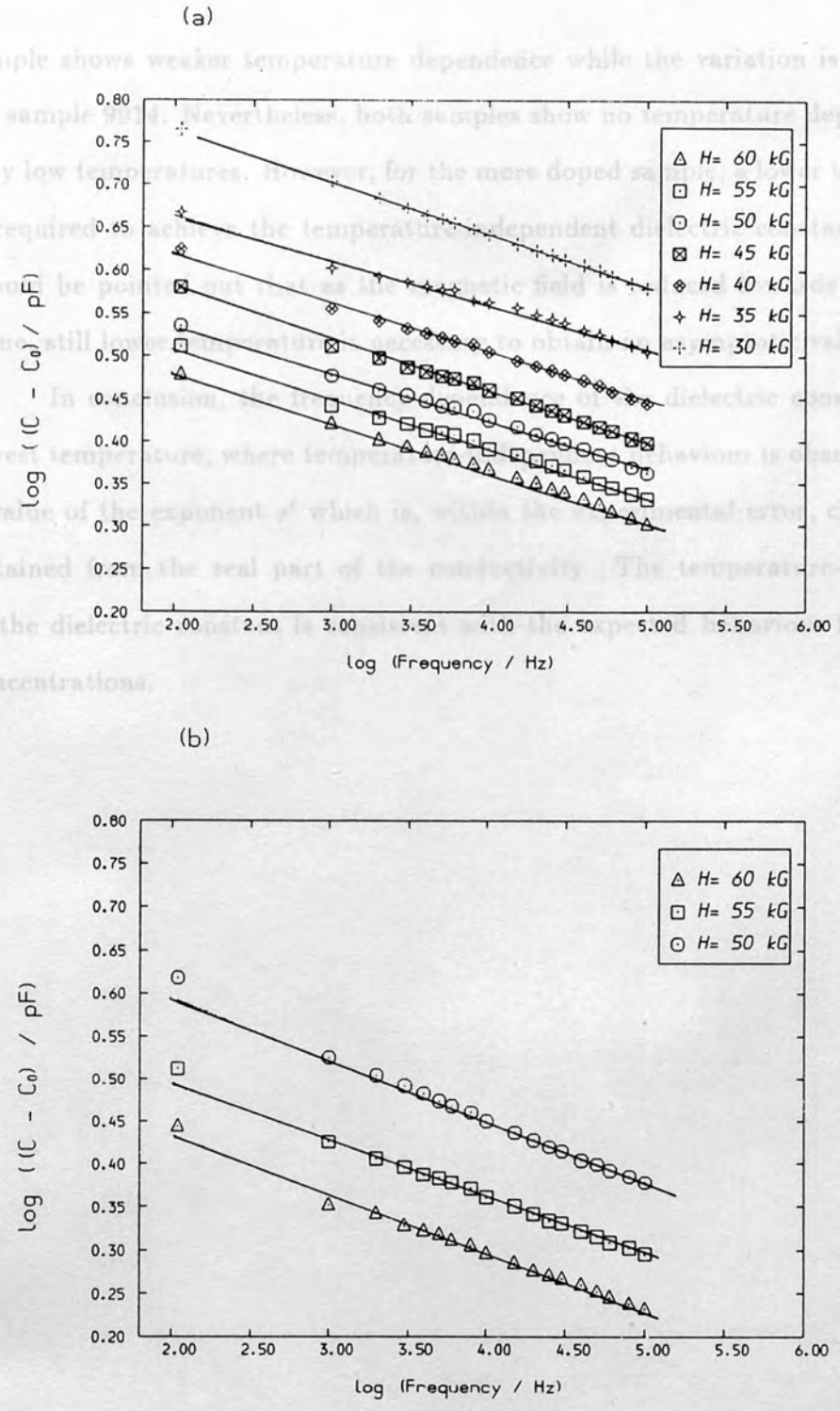

Figure 5.61

The frequency dependence of the low-temperature limit of the capacitance ($C - C_0$) at different magnetic fields for (a) Sample 5714 and (b) Sample 9914.

sample shows weaker temperature dependence while the variation is very sharp for sample 9914. Nevertheless, both samples show no temperature dependence at very low temperatures. However, for the more doped sample, a lower temperature is required to achieve the temperature-independent dielectric constant. Also, it should be pointed out that as the magnetic field is reduced towards the critical value, still lower temperature is necessary to obtain an asymptotic value of ϵ.

In conclusion, the frequency-dependence of the dielectric constant at the lowest temperature, where temperature-independent behaviour is observed, yields a value of the exponent s' which is, within the experimental error, close to that obtained from the real part of the conductivity. The temperature-dependence of the dielectric constant is consistent with the expected behaviour for different concentrations.

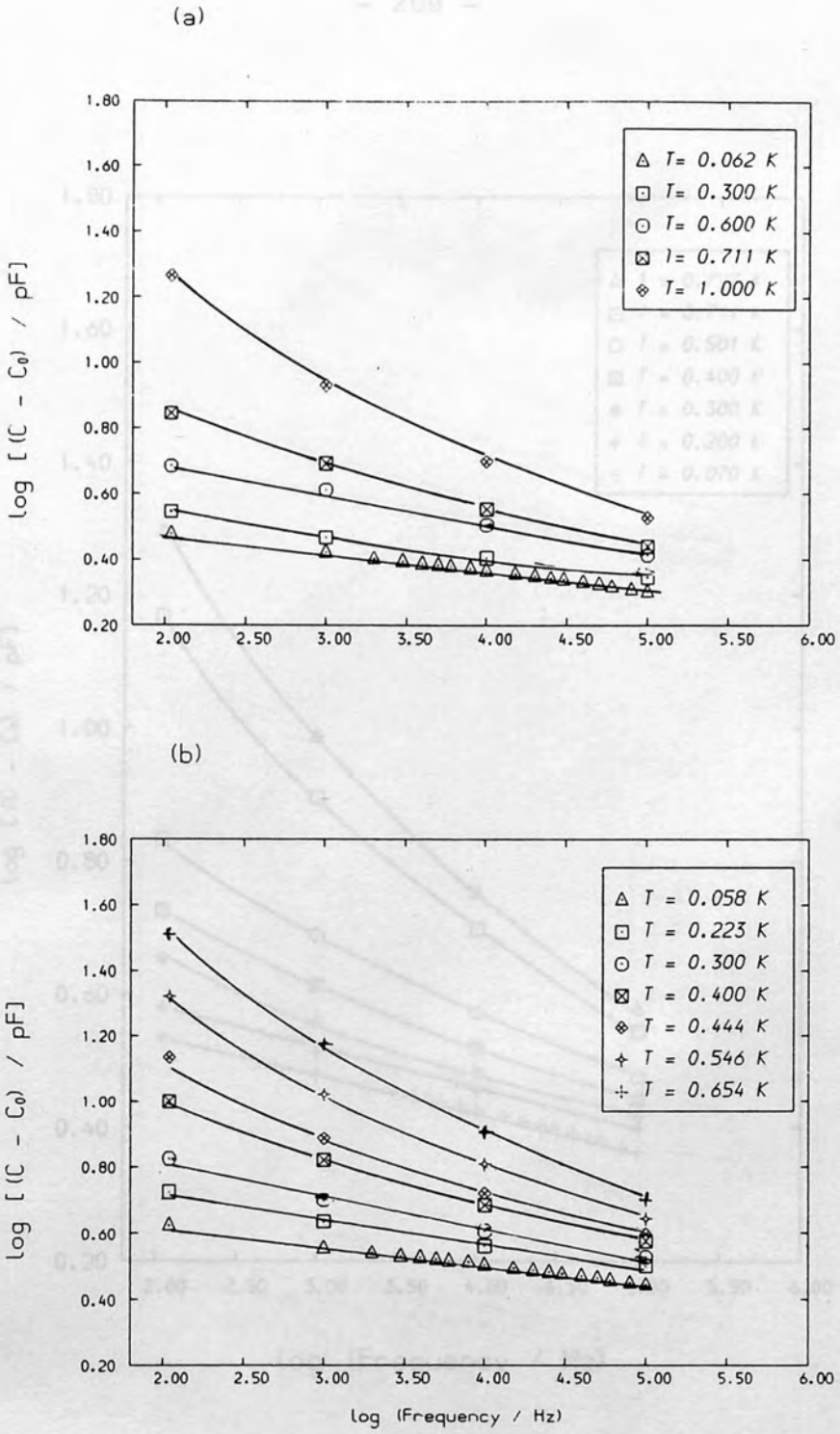

Figure 5.62

The frequency dependence of the capacitance $(C - C_0)$ of sample 5714 at magnetic fields (a) H = 60 kG and (b) H = 40 kG.

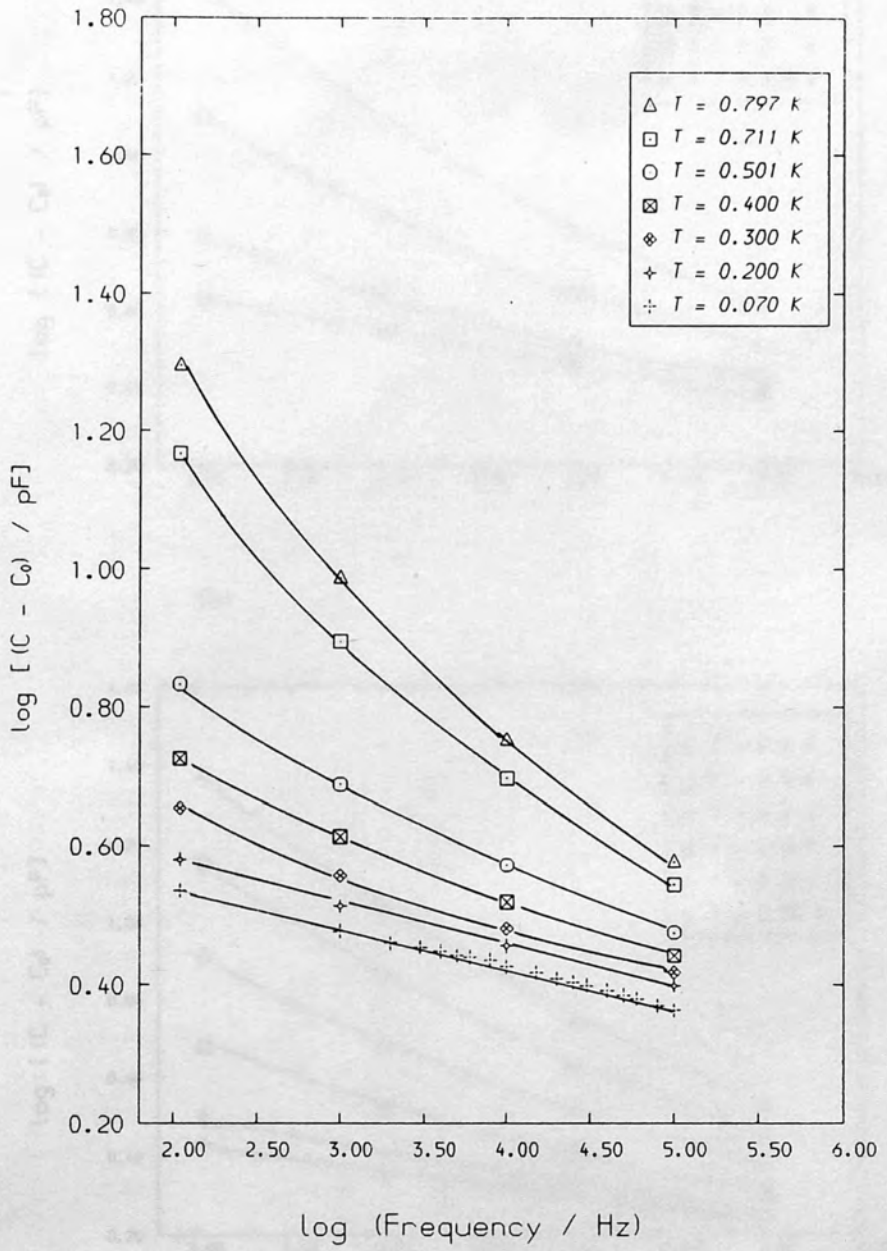

Figure 5.63

The frequency dependence of the the capacitance $(C - C_0)$ of sample 5714 at a magnetic field of 50 kG and at different temperatures.

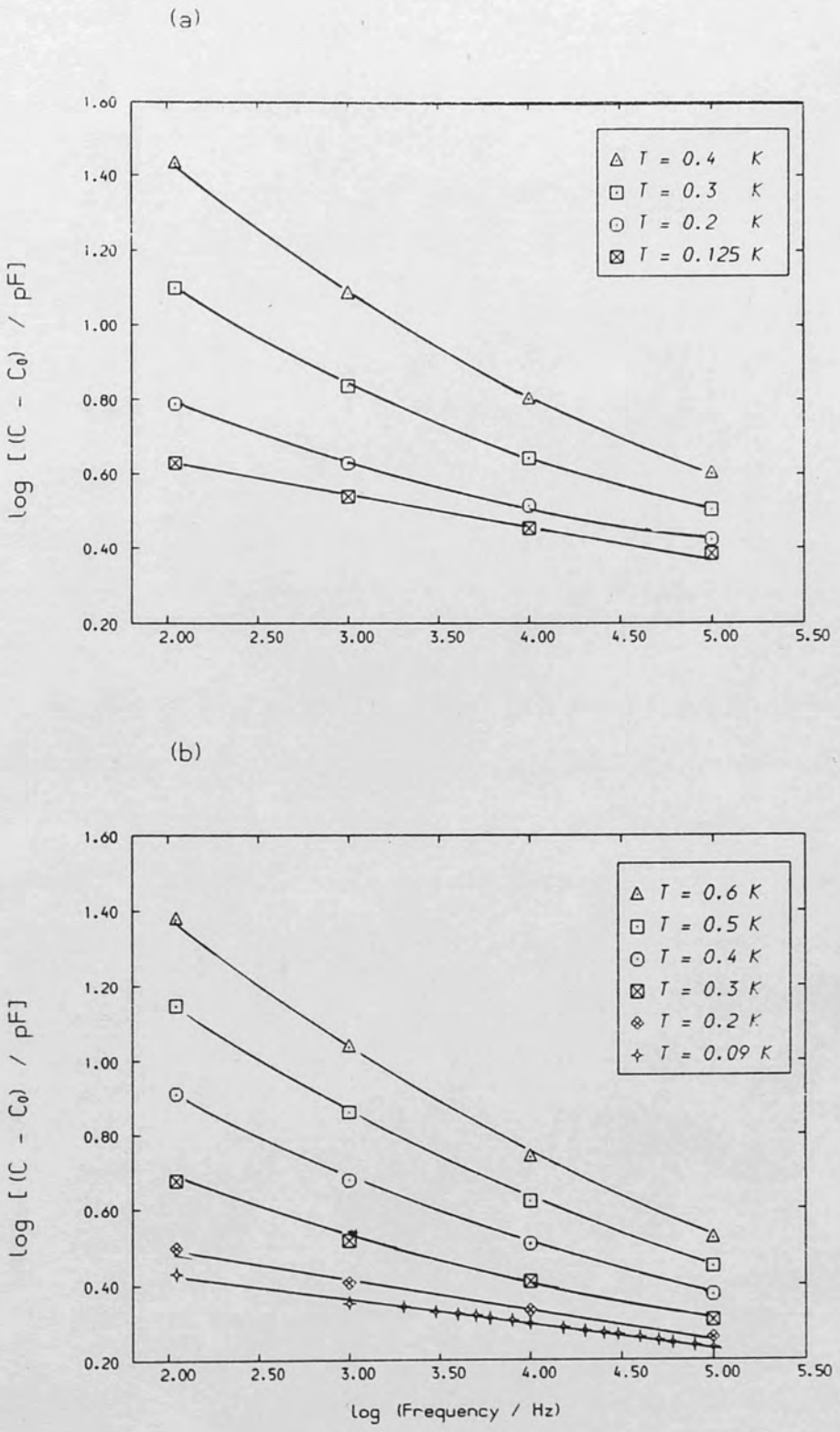

Figure 5.64

The frequency dependence of the capacitance $(C - C_0)$ of sample 9914 at different temperatures and at magnetic fields (a) H = 50 kG and (b) H = 60 kG.

(a)

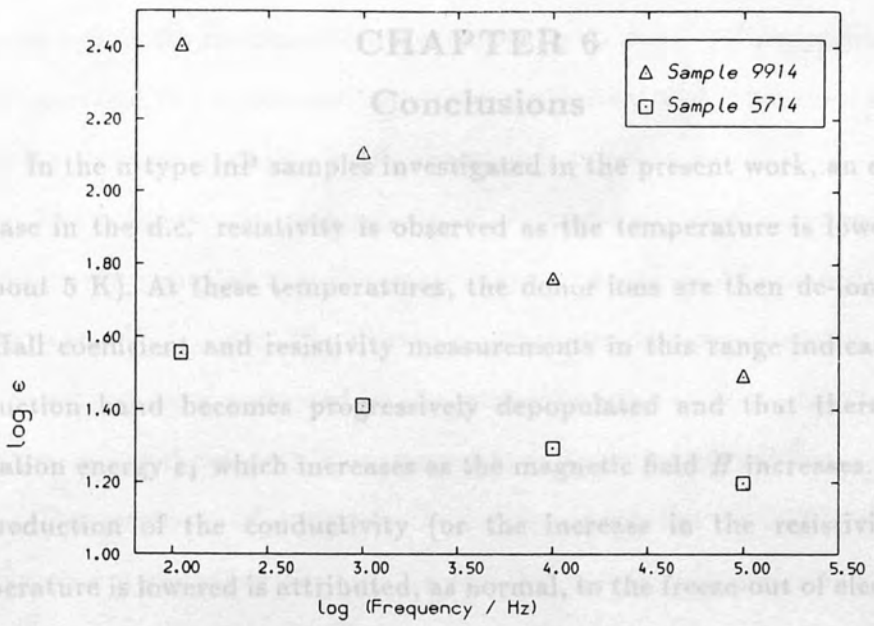

(b)

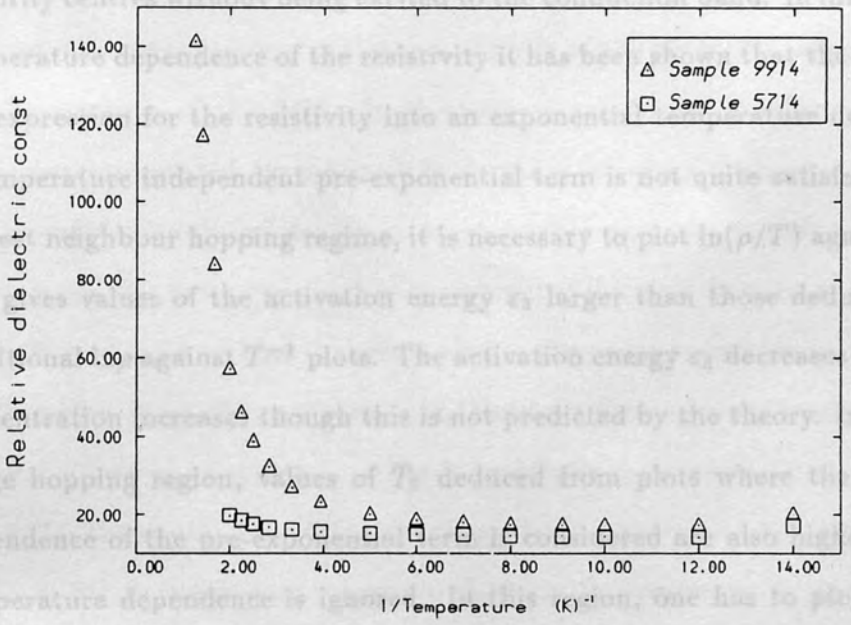

Figure 5.65

(a) A comparison between the frequency dependence of the relative dielectric constant of samples 5714 and 9914 at T= 0.5 K and H = 50 kG. (b) A comparison between the temperature dependence of the relative dielectric constant of samples 5714 and 9914 at a magnetic field H = 50 kG and frequency 10^4 Hz.

CHAPTER 6

Conclusions

In the n-type InP samples investigated in the present work, an exponential increase in the d.c. resistivity is observed as the temperature is lowered (down to about 5 K). At these temperatures, the donor ions are then de-ionized. Both the Hall coefficient and resistivity measurements in this range indicate that the conduction band becomes progressively depopulated and that there exists an activation energy ε_1 which increases as the magnetic field H increases. Therefore, the reduction of the conductivity (or the increase in the resistivity) as the temperature is lowered is attributed, as normal, to the freeze-out of electrons from the conduction band to donor sites. This freeze-out is followed by a situation in which the conduction is due to hopping mechanisms where electrons hop between impurity centres without being excited to the conduction band. In interpreting the temperature dependence of the resistivity it has been shown that the separation of the expression for the resistivity into an exponential temperature dependent and a temperature independent pre-exponential term is not quite satisfactory. In the nearest neighbour hopping regime, it is necessary to plot $\ln(\rho/T)$ against T^{-1} and this gives values of the activation energy ε_3 larger than those deduced from the traditional $\ln\rho$ against T^{-1} plots. The activation energy ε_3 decreases as the carrier concentration increases though this is not predicted by the theory. In the variable range hopping region, values of T_0 deduced from plots where the temperature dependence of the pre-exponential term is considered are also higher than if the temperature dependence is ignored. In this region, one has to plot $\ln(\rho/T^{1/2})$ versus $T^{-1/4}$ for a constant density of states at the Fermi level or $\ln(\rho/T)$ versus $T^{-1/2}$ for an arbitrary dependence of the density of states on the energy. The resistivity has been calculated over both regions, (nearest neighbour and variable range hopping regimes) assuming an enhanced dielectric constant having a value which is necessary to reduce ε_3 to its measured value. With no other adjustable parameters used in the calculations, the agreement between the experiment and

theory is good in the nearest neighbour hopping region. In the variable range hopping region, the results are more consistent with the $T^{-1/4}$ dependence than the $T^{-1/2}$ one, and the agreement between experimental and theoretical calculations using the same enhanced dielectric constant is satisfactory.

The concentration dependence of the resistivity in the nearest neighbour hopping regime showed that the parameter α_1 should be determined from the ln (ρ/T) versus T^{-1} plots. The discrepancy between the experimental finding and the theoretical value suggested by the percolation theory might also be related to enhancement in the dielectric constant due to the impurity centres.

The presence of magnetic field compresses the wave functions of the electrons located at impurity centres and this reduces the probability of electron jumps between these centres. As a result, the magnetic field produces a positive magnetoresistance. Observations of such positive magnetoresistance are in agreement with the theory put forward by Shklovskii. The theory predicts that the magnetic field dependence of the resistivity is of the form H^m, where m depends on the strength of the field. In the nearest neighbour hopping region, an H^2 dependence suggested for the weak field case is observed. Values of the numerical coefficient t were found to be in a reasonable agreement with the theoretical findings. In this case, one also has to use values deduced from $\ln(\rho/T)$ versus T^{-1} plots. It is also found that the anisotropy in the magnetoresistance is proportional to H^2 and is in good agreement with theory. It is interesting to observe that the activation energy ε_3 increases as the magnetic field increases.

In the weak field variable range hopping region, the resistivity ratio $(\rho(H)/\rho(0))$ in a constant magnetic field varies exponentially as $T^{-3/4}$, which is, indeed, appropriate for a constant density of states at the Fermi level. The same ratio varies as H^2 as also predicted by the theory. Values of the numerical coefficient t_1 of the $T^{-3/4}H^2$ term obtained from the experimental data range between 0.0044 to 0.0078, whereas theory gives t_1=0.0025. The discrepancy between experiment and theory is attributed to uncertainty in the value of T_0 which is difficult to determine accurately and which might be magnetic field dependent.

The a.c. measurements carried out on the n-InSb samples in presence of a magnetic field showed also freeze-out of electrons from the conduction band to donor sites at high temperatures. This is the well known magnetic freeze-out observed in these materials. In this region, the real part of the low frequency conductivity coincides with the d.c. limit. As the temperature is reduced, the d.c. conductivity becomes orders of magnitudes smaller than the a.c. one in the hopping region. Two regions are distinguished; a temperature-dependent (at intermediate temperatures) and a temperature-independent conductivity at lower temperatures. The temperature dependence of the real part of the conductivity, at the intermediate range of temperature, is stronger than the linear behaviour predicted by the pair approximation theory. On the other hand, the frequency dependence of σ follows the relation $\sigma \sim \omega^s$. The exponent s is temperature dependent. It, indeed, decreases as the temperature is increased and takes values even lower than (0.8) that suggested by the simple pair approximation. This temperature dependence of s is not predicted by the theory. The observed data are interpreted in terms of multiple hopping. In this case, the temperature dependence of the conductivity is assumed to vary as T^d. The exponent d was calculated as the best fit of ln $\sigma(\omega)$ against ln T and was found to be greater than unity. Its value depends on the particular frequency. Values deduced from low frequency behaviour are greater than those obtained at higher frequencies as expected since multiple hopping becomes more important at lower frequencies. The variation of the exponent s with temperature is also interpreted in terms of the multiple hopping mechanism.

In this temperature range, the a.c. conductivity was found to scale with the d.c. limit according to the scaling formula of Summerfield (1985); $\sigma(\omega, H, T)/\sigma(0, H, T) = f(Ae^2\omega\alpha/\sigma(0, H, T)k_BT)$. Data were found to follow the same pattern over a wide range of magnetic fields, temperatures and frequencies. With the coefficient A being the only adjustable parameter a good fit is obtained for the three samples. The observed values of the coefficient A are in the range of 2.8 to 3.2. These values are close to that calculated by Summerfield for the case

of constant density of states at the Fermi level.

At very low temperatures depending on the magnetic field, a temperature independent a.c. conductivity is observed. This is not predicted by a simple pair approximation theory. According to Efros (1981), this temperature independent conductivity arises when correlation effects become important at very low temperatures. Values of the exponent s were somewhat higher than Efros's prediction. The Pollak formula for a moderate concentration can be used to discuss these data, but one has to replace N_A by $N_A^{0.85}$ (Pollak and Geballe 1961).

In the variable range hopping regime, the d.c. resistivity behaviour with temperature and/or magnetic field cannot be represented solely by one common exponential dependence. Different theoretical approaches have been developed to account for this. It was found that the d.c. resistivity of the n-InSb samples can be interpreted reasonably in terms of $T^{-1/3}$ or $T^{-2/5}$ dependences. Analysis of the data in the light of Shklovskii's findings that the resistivity may follow $T^{-1/4}$ in a magnetic field for a constant density of states at the Fermi level or $T^{-1/2}$ when $g(\epsilon)$ is parabolic function of energy showed that $T^{-1/4}$ dependence is reasonably obeyed at lower fields than the $T^{-1/2}$ law.

Investigation of the magnetic field dependence of the d.c. resistivity of these samples showed that the $(H/a_H)^{1/3}$ dependence, appropriate for strong fields is obeyed. Values of g_0 calculated by this way were found to be about one order of magnitude less than the theoretical calculations from Shklovskii's estimation (1973).

Capacitance measurements of the n-InSb samples showed that a sharp decrease in the capacitance is observed at higher temperatures. There follows a gradual decrease as the temperature is reduced. At very low temperatures, however, a temperature-independent behaviour is observed. A scaling formula of the form $\epsilon = \epsilon_c(a_c^3/(a_\parallel a_\perp^2) - 1)^{-\nu'}$ is used to describe the change in the dielectric constant (deduced from the temperature independent behaviour of the capacitance) with the magnetic field. The choice of this form is motivated by the fact decreasing the magnetic field resembles increasing the donor concentration.

This formula is indeed similar to that used by Capizzi et al. (1980) and Hess et al. (1982) who have carried out measurements on Si:P with different concentrations. No common value of the exponent ν' is obtained, instead, values in the range of 0.6 to 1.6 are observed for the highest frequency used in the present measurements. More accurate experimental techniques to obtain accurate values would improve our understanding of the IM-transition and related phenomena.

The variation of the relative dielectric constant with the frequency at different temperatures and magnetic fields showed that a rapid decrease in $\epsilon(\omega, T)$ as the temperature is lowered and this is attributed to a strong reduction in the hopping conductivity contribution to the dielectric constant and is very similar to earlier work on other systems such as Si and Ge (Castner et al. 1980). Data also showed that the frequency dependence of ϵ is indeed concentration dependent. The dependence is much stronger for higher concentration. A comparison between the temperature dependence of ϵ at a fixed field and frequency for different concentrations showed that the high-purity sample shows a weaker temperature dependence than the more doped samples. Nevertheless, no temperature dependence is observed at lower temperatures.

REFERENCES

Abboudy, S., Fozooni, P., Mansfield, R. and Lea, M., 1988, Phil. Mag. letter, **57**, L277.

Abboudy, S., Mansfield, R. and Fozooni, P., 1987, Proceedings of the International Conference; Applications of High Magnetic Fields in Semiconductor Physics, Springer-Verlag Series in Solid State Science, Ed. Landwehr, G., **71**, 518.

Abdul-Gader, M.M., 1984, Ph.D. Thesis, London University.

Abdul-Gader, M., Mansfield, R. and Fozooni, P., 1987, Pr oceedings of the International Conference; Applications of High Magnetic Fields in Semiconductor Physics, Springer-Verlag Series in Solid State Science, Ed. Landwehr, G. **71**, 381.

Abrahams, E., Anderson, P. W., Licciardello D. C. and Ramakrishnan T. V., 1979, Phys. Rev. Letters, **42**, 673.

Abrams, R.A., Childs, G.N. and Saunderson, P.A., 1984, J. Phys. C: Solid State Phys., **17**, 6105.

Allen, F.R. and Adkins, C.J., Phil. Mag., 1972, **26**, 1027.

Ambegaokar, V., Halperin, B.I. and Langer, J.S.,1971, Phys. Rev. B **4**, 2612.

Austin, I.G. and Mott, N.F., 1969, Adv. Phys., **18**, 41.

Averous, M., Galas, J., Fau, C. and Bonnafe, J., 1976, J. Physique, **37**,89.

Balkan, N., Butcher, P.N, Hogg, W.R., Long, A.R. and Summerfield, S., 1985, Phil. Mag. Lett., **51**, L7.

Baranovskii, S. D. and Uzakov, A. A., 1980, Solid State Commun., **36**, 829.

Baranovskii, S. D. and Uzakov, A. A., 1981, Sov. Phys.-Semiond., **15**, 533.

Benzaquen, M., Mazuruk, K., Walsh, D. and di Forte-Poisson, M.A., 1985, J. Phys. C: Solid State Phys., **18**, L1007.

Benzaquen, M. and Walsh, D., 1984, Phys.. Rev. B, **30**, 7287

Bhatt, R. N. , 1984, Phil. Mag. B, **50**, 189.

Biskupski, G. Dubois, H., Laborde, O. and Zotos, X., 1980, Phil. Mag. B, **42**, 19.

Biskupski, G. and Dubois, H., 1982, (see Biskupski G., 1982 Thesis, Lille).

Biskupski, G. Dubois, H., Wojkiewicz, J. L., Briggs, A. and Remenyi, G., 1984, J. Phys. C: Solid State Phys., **17**, L411.

Blakemore, J.S., 1974, *Solid State Physics*,(W. Saunders; London Toronto).

Bötteger, H. and Bryksin, V.V, 1976, Phys Stat. Sol. (b), **78**, 415.

Bötteger, H. and Bryksin, V.V, 1985, *Hopping Conduction in Solids*, (GDR: VCH publishers).

Brandt, N.B. and Chudinov, S.M., 1975, *Electrical Structure of Metals*, (Moscow: Mir Publishers).

Brooks, J.S., Symko, O.G. and Castner, T.G., 1987, Proc. 18th Int. Conf. on Low Temperature Physics, Japanese J... of Applied Physics, **26**, 721.

Butcher, P.N., 1980, Phil. Mag. B, **42**, 799.

Butcher, P.N. and Hayden, K.J., 1977, Proc. 7th Int.Conf. on Amorphous and Liquid Semiconductors, Ed. by W.E. Spear (CICL, Univ. of Edinburgh), 234.

Butcher, P.N. and Summerfield, S., 1981, J. Phys. C : Solid State Phys. **14**, L1099.

Capizzi, M., Thomas,G. A., DeRosa, F., Bhatt, R. N. and Rice,T. M., 1980, Phys. Rev. Letters, **44**, 1019.

Castner, T. G., Lee, N. K., Cieloszyk, G. S. and Salinger, G. L., 1975, Phys. Rev. Letters, **34**, 1627.

Castner, T. G., Lee, N. K. and Tan, H. S., 1980, J. low Temp. Phys., **38**, 447.

Chroboczek, J.A., Eaves, L., Guimares, P.S.S., Main, P.C., Roche, I.P., Mitter, H., Portal, J.C., Butcher, P.N., Ketkar, M.S. and Summerfield, S., 1985, Proceedings of the 17th International Conference on the Physics of Semiconductors (Springer Verlag) 697.

Dallacasa, V., Paracchini, C. and De Stabile, S., 1988, J. Phys. C, **21**, L567.

Deri, R.J. and Castner, T.G., 1986, Phys Rev. Letters, **57**, 134.

Eddols, D.V., 1966, Phys. Stat. Sol., **17**, 67.

Edwards, P.P. and Sienko, M.J., 1978, Phys Rev. B, **17**, 2575.

Efros, A.L., 1976, J. Phys. C, **9**, 2021.

Efros, A.L., 1981, Phil. Mag. B, **43**, 829.

Efros, A.L., Lien, N. and Shklovskii, B.I., 1979, J. Phys. C: Solid State Phys., **12**, 1869.

Efros, A.L. and Shklovskii, B.I., 1975, J. Phys. C: Solid State Phys., **8**, L49.

Efros, A. L. and Shklovskii, B.I. 1985, *Electron – Electron interactions in Disordered*

systems (Ed: A.L. Efros and M. Pollak; Elsevier Science Publishers B.V.) 409).

Efros, A. L., Shklovskii, B.I. and Yanchev, I. Ya., 1972, Phys. Status Solidi (b), **50**, 45.

Elizavov, A.I. and Ivanov, V.I., 1981, Sov. Phys.-Semicond., **15**, 531.

Elliott, S.R., 1987, Adv. in Phys., **36**, 135.

Emel'yanenko, O.V., Lagunova, T.S., Nasledov, D.N., Nedeoglo, D.D and Timchenko, I.N., 1974, Sov. Phys.-Semicond., **7**, 1280.

Emel'yanenko, O.V., Masagutov, K.G., Nasledov, D.N. and Timchenko, I.N., 1975, Sov. Phys.-Semicond., **9**, 330.

Emel'yanenko, O.V., Nasledov D.N., Nikulin, E.I. and Timchenko, I.N., 1973, Sov. Phys.-Semicond., **6**, 1926.

Fenton, E.W. and Haering, R.R., 1967, Phys. Rev., **159**, 593.

Ferre, D., Dubois, H. and Biskupski, G., 1975, Phys. State Sol. (b), **70**, 81.

Finlayson, D.M. and Mason, P.J., 1986, J. Phys. C: Solid State Phys., **19**, L299.

Fritzsche, H., 1962, Phys. Rev., **125**, 1552.

Gadzhiev, A.R. and Shlimak, I.S., 1973, Sov. Phys.-Semicond., **6**, 1364.

Golin, S., 1963, Phys. Rev., **132**, 178.

Hasegawa, H. and Howard, R.F., 1961, J. Phys. Chem. Solids, **21**, 1791.

Hauser, J.J., Pasteur, G.A. and Staudinger, A., 1981, Phys. Rev. B, **24**, 5844.

Hess, H.F., Deconde, K., Rosenbaum, T.F. and Thomas, G.A., 1982, Phys Rev. B, **25**, 5578.

Hill, R.M., 1976, Phys. Stat. Sol. (a), **35**, K29.

Hirsch, M.J. and Holcomb, D.F., 1987, Proceeding of the 18th Inter. Conf. Phys. Semiconductors, Stockholm,, Ed. by O. Engström, (World Scientific Publishing Co. Pte Ltd.), 1241.

Ionov, A.N., Shlimak, I.S. and Matveev, M.N., 1983, Solid State Commun., **47**, 763.

Ishida, S. and Otsuka, E., 1977, J. Phys. Soc. Japan **43**, 124.

Ishida, S. and Otsuka, E., 1979, J. Phys. Soc. Japan, **46**, 1207.

Jonscher, A.K., 1972, J. Non-Crystalline Solids **8-10**, 293.

Jonscher, A.K., 1983, *Dielectric Relaxation in Solids*, (London: Chelsea Dielectric Press).

Kahlert, H., Landwehr, G., Schlachetzhi, A. and Salow, H., 1976, Z. Phys. B, **24**, 361.

Kaufman, L.A. and Neuringer, L.J., 1970, Phys. Rev. B, **2**, 1840.

Klyatskina, I.V. and Shlimak, I.S., 1978, Sov. Phys.-Semicond., **20**, 76.

Knotek, M.L., 1977, Phys. Rev., **16**, 2629.

Knotek, M.L. and Pollak, M., 1972, J.Non-Crystal. Solids, **8-10**, 505.

Knotek, M.L. and Pollak, M., 1974, Phys. Rev. B, **9**, 662.

Lemoine, D., Pelletier, C., Rolland, S. and Ganger, G., 1976, Phys. lett., **A56**, 493.

Long, A.R., 1982, Adv. Phys., **31**, 553.

Long, A.R. and Balkan, N.: Proceedings of the International Conference on Amorphous and Liquid Semiconductors, 1979, Cambridge, Mass., edited by W. Paul and M. Kastner (Amsterdam: North Holland) pp 415-420.

Long, A.R. and Balkan, N., 1980, J. Non-Crystal. Solids, **35** & **36**, 415.

Long, A.P. and Pepper, M., 1984, J. Phys. C: Solid State Phys., **17**, 3391.

Long, A.P. and Pepper, M., 1985, Solid-State Elect., **28**, 61.

Lounasmaa, O.V., 1974, *Experimental Principles and Methods Below* 1 K, (London; Academic Press.).

Loweny, J.R., 1986, J. Applied Phys., **60**, 2858.

Madelung, O., 1978, "*Introduction to Solid State theory*", 2nd ed., vol. 2, (Berlin: Springer-Verlag).

Mansfield, R., Abboudy, S. and Fozooni, P., 1988, Phil. Mag. B, **57**, 777.

Mansfield, R., Abdul-Gader, M. and Fozooni, P., 1985, Solid State Elect. **28**, 109.

Mansfield, R. and Kusztelan, L., 1978, J. Phys. C: Solid State Phys., **11**, 4157.

Mansfield, R. and Tokumoto, H., 1983, Phil. Mag. B, **48**, L1.

Manukyan, A.L. and Andreev, A.A., 1976, Sov. Phys. Solid State, **18**, 2108.

Mikoshiba, N., 1963, Phys. Rev., **127**, 1962.

Miller, A. and Abrahams, E., 1960, Phys. Rev. **120**, 745.

Mott, N.F., 1949, Proc. Phys. Soc. A, **62**, 416.

Mott, N.F., 1967, Adv. Phys., **16**, 49.

Mott, N.F., 1968, J. Non-Crystal. Solids, **1**, 1.

Mott, N.F., 1969, Phil. Mag., **19**, 835.

Mott, N.F., 1974, *Metal Insulator Transition*, (London: Taylor and Francis Limited).

Mott, N.F., 1981, Phil. Mag. B, **44**, 265.

Mott, N.F., 1982, Proc. R. Soc. London. A, **382**, 1.

Mott, N.F. and Davis, E.A., 1979, "*Electronic processes in non−crystalline materials*", 2nd ed. (Oxford: Clarendon Press).

Mott, N.F., Davis, E.A. and Street, R.A., 1975, Phil. Mag., **32**, 961.

Mott, N.F. and Twose, W.D., 1961, Adv. Phys., **10**, 107.

Narasimhan, K.L., Guha, S. and Agarwal, 1976, Solid State Commun., **20**, 573.

Newman, P.F. and Holcomb, D.F., 1983, Phys. Rev. B, **28**, 638.

Nishimura, H., 1965, Phys. Rev., **138**, A815.

Owen, A.E. and Robertson, J.M., 1970, J. Non-Cryst. Solids, **2**, 40.

Paalanen, M.A., Rosenbaum, T.F., Thomas, G.A., and Bhatt, R.N., 1982, Phys. Rev. Lett., **48**, 1284.

Pike, G.E., 1972, Phys. Rev. B, **6**, 1572.

Pike, G.E. and Seager, C.H., 1974, Phys. Rev. B, **10**, 1421.

Pollak, M., 1964, Phys. Rev. A, **133**, 564.

Pollak, M., 1965, Phys. Rev. A, **138**, 1822.

Pollak, M., 1970, Disc. Faraday Soc., **50**, 13.

Pollak, M., 1971, Phil. Mag., **23**, 519.

Pollak, M., 1972, J. Non-Crystal. Solids, **11**, 1.

Pollak, M. and Geballe, T.H., 1961, Phys. Rev. **122**, 1742.

Pollak, M. and Watt, D.H., 1965, Phys. Rev., **140**, A87.

Powell, J.L. and Crasemann, B., 1965, "*Quantum Mechanics*", (Addison-Wesley).

Putley, E.H., 1966, *Physics of* III-V *compounds*: Semiconductors and Semimetals, (ed: R.K. Willardson and A.C. Beer), p. 289.

Putley, E.H., 1968, "*The Hall effect and Semiconductor Physics*", (New York Dover).

Robert, J.L., Reymond, A., Aulombard, R.L. and Bousquet, C., 1980, Phil. Mag. B, **42**, 1003.

Rosenbaum, T.F., Andres, K., Thomas, G.A. and Bhatt, R.N., 1980, Phys Rev. Letters, **45**, 1723.

Rosenbaum, T.F., Milligan, R.F., Paalanen, M.A., Thomas, G.A., Bhatt, R.N. and Lin, W., 1983, Phys Rev. B, **27**, 7509.

Sasaki, W., 1985, Phil. Mag. B, **52**, 427.

Shklovskii, B.I., 1972, Sov. Phys.-Semicond., **34**, 1084.

Shklovskii, B.I., 1973, Sov. Phys.-Semicond., **6**, 1053.

Shklovskii, B.I., 1974, Sov. Phys.-Semicond., **8**, 268.

Shklovskii, B.I., 1977, Sov. Phys.-Semicond., **11**, 1253.

Shklovskii, B.I., 1982, JETP Letters, **36**, 51.

Shklovskii, B.I. and Efros, A.L., 1970, Sov. Phys. JETP, **33**, 468.

Shklovskii, B.I. and Efros, A.L., 1971, Sov. Phys. JETP, **33**, 468.

Shklovskii, B.I. and Efros, A.L., 1984, *Electronic Properties of Doped Semiconductors*, (Ed: M. Cardona, Berlin: Springer Verlag.)

Shklovskii, B.I. and Shlimak, I.S., 1972, Sov. Phys.-Semicond., **6**, 104.

Summerfield, S., 1985, Phil. Mag. B **52**, 9.

Summerfield, S. and Butcher, P.N., 1982, J. Phys. C : Solid State Phys. **15**, 7003.

Summerfield, S. and Butcher, P.N., 1983, J. Phys. C : Solid State Phys. **16**, 295.

Summerfield, S. and Chroboczek, J.A., 1984, Solid-St. Commun., **53**, 129.
Suprapto, B.B. and Butcher, P.N., 1975, J. Phys. C, **8**, L517.

Thomas, G.A., 1983, Physica, **117B & 118B**, 81.

Thomas, G.A., Ootuka, Y., Katsumoto, S., Kobayashi, S, and Sasaki, W., 1982,, Phys. Rev. B, **26**, 2113.

Tokumoto, H., Mansfield, R. and Lea, M., 1980, Solid State Commun., **35**, 941.

Tokumoto, H., Mansfield, R. and Lea, M., 1982, Phil. Mag. B, **46**, 93.

Walton, A.K. and Dutt, J.C., 1977, J. Phys. C: Solid State Phys., **10**, L29.

Wieder, H.H., 1979, "Laboratory Notes on Electrical and Galvanomagnetic Measurements": Material Science Monographs 2 (Elsevier Scientific Publishing company; Oxford and New York.

Yafet, Y., Keyes, R.W. and Adams, E.N., 1956, J. Chem. Solids **1**, 37.

Yamanouchi, C., 1965, J. Soci. Japan, **20**, 1029.

Yushida, A. and Arizumi, T., 1976, Proc. 6th Int. Conf. on Amorphous and Liquid Semicond.; (Nauka, Leningrad) 231.

Zabrodskii, A.G., 1977, Sov. Phys.-Semicond., **11**, 345.

Ziman, J.M., 1972, "*Principles of the theory of Solids*", 2nd ed. (Cambridge: University Press).